# NUMERICAL BENCHMARKING OF A COARSE-MESH TRANSPORT (COMET) METHOD FOR MEDICAL PHYSICS APPLICATIONS

A Dissertation
Presented to
The Academic Faculty

by

Megan Satterfield Blackburn

In Partial Fulfillment
of the Requirements for the Degree
Doctor of Philosophy in the
School of Mechanical Engineering

Georgia Institute of Technology
August 2009

**COPYRIGHT 2009 BY MEGAN S. BLACKBURN**

# NUMERICAL BENCHMARKING OF A COARSE-MESH TRANSPORT (COMET) METHOD FOR MEDICAL PHYSICS APPLICATIONS

Approved by:

Dr. Farzad Rahnema, Advisor
School of Mechanical Engineering
*Georgia Institute of Technology*

Dr. Eric Elder, Co-Advisor
School of Mechanical Engineering
*Georgia Institute of Technology*

Dr. C.-K. Chris Wang
School of Mechanical Engineering
*Georgia Institute of Technology*

Dr. Sang Cho
School of Mechanical Engineering
*Georgia Institute of Technology*

Dr. Rebecca Howell
Department of Radiation Physics
*University of Texas at M.D. Anderson Cancer Center*

Date Approved: June 24, 2009

For Pop,

who always asked if graduate school had a retirement plan since it appeared to him I would be here forever.

I wish you were here to see me finish.

# ACKNOWLEDGEMENTS

I wish to thank many people who have helped me throughout graduate school. First thank you to my graduate advisor throughout this journey – Dr. Farzad Rahnema. I appreciate all you have done for me throughout the past 5 years. I would also like to thank my co-advisor from Emory University Department of Radiation Oncology, Dr. Eric Elder. Thank you for all the time and effort you have put in to helping me get whatever data I needed. Sincere appreciation is also extended to Dr. Chris Wang, Dr. Sang Cho, and Dr. Rebecca Howell for serving on my committee. Dr. Dingkang Zhang also offered extensive help throughout this entire project. I truly appreciate all he has done. I would like to thank my office mates and friends from Neely, especially Zach Friis and Justin Pounders. A big thanks also goes to Shauna Boyd and Glenda Johnson for always being so helpful with all of my questions on paperwork in the ME department. I thank my family for supporting me through this long educational endeavor. Thanks to my mom and dad for being my biggest supporters. Thank you to my friends, especially Julie, for all the advice on life along the way. Mostly thanks to my husband, David, for always being there when I needed anything at all.

# TABLE OF CONTENTS

# LIST OF TABLES

## LIST OF FIGURES

# SUMMARY


Radiation therapy has become a very import method for treating cancer patients. Thus, it is extremely important to accurately determine the location of energy deposition during these treatments, maximizing dose to the tumor region and minimizing it to healthy tissue. A Coarse-Mesh Transport Method (COMET) has been developed at the Georgia Institute of Technology in the Computational Reactor and Medical Physics Group for use very successfully with neutron transport to analyze whole-core criticality. COMET works by decomposing a large, heterogeneous system into a set of smaller fixed source problems. For each unique local problem that exists, a solution is obtained that we call a response function. These response functions are pre-computed and stored in a library for future use. The overall solution to the global problem can then be found by a linear superposition of these local problems. This method has now been extended to the transport of photons and electrons for use in medical physics problems to determine energy deposition from radiation therapy treatments.

The main goal of this work was to develop benchmarks for testing in order to evaluate the COMET code to determine its strengths and weaknesses for these medical physics applications. For response function calculations, legendre polynomial expansions are necessary for space, angle, polar angle, and azimuthal angle. An initial sensitivity study was done to determine the best orders for future testing. After the expansion orders were found, three simple benchmarks were tested: a water phantom, a simplified lung phantom, and a non-clinical slab phantom. Each of these benchmarks was decomposed into 1cm x 1cm and 0.5cm x 0.5cm coarse meshes. Three more

clinically relevant problems were developed from patient CT scans. These benchmarks modeled a lung patient, a prostate patient, and a beam re-entry situation. As before, the problems were divided into 1cm x 1cm, 0.5cm x 0.5cm, and 0.25cm x 0.25cm coarse mesh cases. Multiple beam energies were also tested for each case. The COMET solutions for each case were compared to a reference solution obtained by pure Monte Carlo results from EGSnrc. When comparing the COMET results to the reference cases, a pattern of differences appeared in each phantom case. It was found that better results were obtained for lower energy incident photon beams as well as for larger mesh sizes. Possible changes may need to be made with the expansion orders used for energy and angle to better model high energy secondary electrons. Heterogeneity also did not pose a problem for the COMET methodology. Heterogeneous results were found in a comparable amount of time to the homogeneous water phantom. The COMET results were typically found in minutes to hours of computational time, whereas the reference cases typically required hundreds or thousands of hours.

A second sensitivity study was also performed on a more stringent problem and with smaller coarse meshes. Previously, the same expansion order was used for each incident photon beam energy so better comparisons could be made. From this second study, it was found that it is optimal to have different expansion orders based on the incident beam energy.

Recommendations for future work with this method include more testing on higher expansion orders or possible code modification to better handle secondary electrons. The method also needs to handle more clinically relevant beam descriptions with an energy and angular distribution associated with it.

# CHAPTER 1

# INTRODUCTION

## 1.1 Objectives

In the Computational Reactor/Medical Physics (CRMP) Group at the Georgia Institute of Technology, a Coarse-Mesh Transport Method (COMET) has been developed. It has very successfully been applied to neutron transport in purely nuclear engineering related problems.[1,2] The method was recently extended to the transport of photons and electrons in medical physics applications to calculate the dose received during radiation therapy treatment. The main goal of this work is to fully evaluate the COMET code to determine its strengths and weaknesses for medical physics applications. In order to conduct this evaluation, appropriate numerical benchmarks were developed and tested. These benchmarks have varying degrees of heterogeneity within them in order to test the methodology completely. After testing each of the benchmark cases, recommendations were made for further alterations.

## 1.2 Motivation

In today's world, cancer affects everyone in some way, whether it affects you direct, a family member, or a friend. At times it can be quite manageable, and at others it can be very destructive. The treatment of cancer has become of utmost importance to society as a whole. One of the main treatments in use today is radiation therapy. The current dose calculation algorithms integrated into the radiation therapy treatment planning software is much improved from the past. Many of the past and present algorithms will be described in the literature review section. Any improvement in the calculation algorithms may have a significant impact in cancer treatment. In modern radiation therapy planning, the accuracy of dose calculations by treatment planning systems is of utmost importance. The quality of the treatment the patient receives can be traced back to the accuracy of the dose calculations.[3] Reduced uncertainty may mean better tumor coverage and less dose to critical structures.

The main goal of radiation therapy is for ionizing radiation to deposit its energy within the tumor cells and killing them. While at the same time, the radiation needs to deposit a minimum amount of energy within healthy cells. Thus, radiation therapy is a matter of balance. With a large amount of energy deposition, the cancer cells may all be dead; however, too many healthy cells may die as well resulting in unwanted side effects. If treatment is too conservative, the tumor cells may not all be killed. This could in turn result in cancer spread.

For a majority of radiation therapy treatments, a linear accelerator (LINAC) is used. This machine accelerates electrons through a tube by using high-frequency electromagnetic waves. At times, these electrons are used for treatment in cases when the tumors lie close to the surface of the patient. Most times however, tumors deeper within the bodies must be treated. In order for the radiation to reach these regions, the electrons must be accelerated onto a high Z target material. One material in use is tungsten. This interaction produces bremsstrahlung x-rays that can then be used for patient treatment. These gamma rays can travel farther into the body. The beam is typically altered by additional methods in order to obtain the correct energy distribution as well as physical shape.[4]

Radiation therapy includes many areas of uncertainties that may affect the actual dose a patient receives. According to the International Commission on Radiation Units and Measurements (ICRU) Report 24, the uncertainty associated with the dose delivered to the tumor region should be within 5%.[5] The uncertainty stems from many different areas during image acquisition, treatment planning, and the actual treatment itself. Uncertainty can be introduced at any step in the treatment process. Dose calculation algorithms produce uncertainties themselves. This is the area that this research is trying to improve upon. Because there are so many areas during the treatment process that add to the uncertainty, a smaller uncertainty should be associated with the dose calculation algorithm than the 5% stated earlier. The accuracy of the dose calculation should be around 2 -3% in order to keep the overall uncertainty under 5%.[6]

The Monte Carlo method is considered the gold standard for particle transport. Monte Carlo simulations model this transport using an in-depth description of the particle physics and the interactions that occur. Thus, it is considered to be the most accurate methodology for describing dose deposition.[7-9] At this time, Monte Carlo methods still require too much calculation time to be implemented clinically. Thus many methods have been implemented over the years to approximate the transport of particles in a heterogeneous media.

A few of the most notable approximation methods used for inhomogeneity corrections are the tissue-air ratio (TAR) method[4], the power-law tissue-air ratio method[10-12], the equivalent tissue-air ratio (ETAR) method[13], and the differential scatter-air ratio (dSAR) method.[14] These methods only account for the transport of photons, and it is assumed that if a charged particle is liberated, the energy is immediately deposited. More advanced dose calculation algorithms have been developed in order to consider the tranport of electrons within the media. These methods include convolution superposition[15], collapsed cone convolution[16], pencil beam[17], and most recently the analytical anisotropic algorithm.[18-19]

Since the use of pure Monte Carlo is not yet a reality, improving upon the current dose calculation algorithms prove to be quite valuable to radiation therapy treatment planning. It is the hope that the coarse-mesh transport method (COMET) tested in this work can improve upon the current methodologies. COMET decomposes a large heterogeneous global problem into a set of smaller fixed source local problems. Detailed solutions, or rather response functions, are obtained for these small problems. These can all be pre-computed and stored in a library based on material definition, mesh size, and incident energy. These response functions can then be coupled together to determine a final dose deposition within the larger global problem.

In order to determine the usefulness of COMET in medical physics applications, a number of benchmark problems have been developed for testing. From these problems, the next steps can be taken to develop COMET such that is moves closer toward becoming completely clinically applicable. The main goal of COMET is to decrease this uncertainty associated with dose calculation and produce a result in a fast amount of time.

# CHAPTER 2

# LITERATURE REVIEW

## 2.1 Dose Calculation Algorithms

In order to treat a patient using radiation therapy methods, a treatment plan must be prepared to estimate the amount of radiation dose a patient will actually receive during treatment. Different dose calculation algorithms may perform these estimations.

### Correction Based Algorithms

When using correction-based algorithms to calculate patient dose, the results are based mostly on measured data found by irradiating a homogeneous water or water-equivalent phantom. The measured data that is typically used is in the form of percent depth doses as well as cross-beam profiles. As the name implies, corrections are usually made to compensate any differences from the water phantom and the patient body of interest. Corrections must be performed based on the shape of the actual patient. Corrections are also performed to account for the scattering that occurs within the volume. Other corrections may also be necessary if any beam modification is done using wedges or blocks. Finally attenuation corrections must also be made for patient heterogeneities.[3] Many correction methods have been developed. A few of the most prominent have been described here.

Contour Irregularities Correction Methods

*Tissue-Air Ratio (TAR) Method*

The Tissue-Air Ratio Ratio (TAR) Method is based on the tissue-air ratio, which can be seen below in Equation 2.1. The tissue-air ratio, $TAR(d,r_d)$, was used because it was independent of the distance from the source, thus making it more useful for clinical application.[4]

$$TAR(d,r_d) = \frac{D_d}{D_{fs}} \qquad \text{Equation 2.1}$$

where

d = depth within the phantom at which the measurement is taken

$r_d$ = size of the radiation field at the depth d

$D_d$ = Dose at a given depth d within the phantom

$D_{fs}$ = Dose in free space at the same point

The TAR method was used to correct for contour irregularities. When taking measurements from a water phantom, the radiation beam hit directly perpendicular to the perfectly flat phantom surface. The human body is however rarely flat, thus corrections must be made for these irregularities. A source to surface distance (SSD) is defined at a certain point on the patient; however, the surface is actually higher in some locations and deficient in others. A correction factor can be found by taking the Ratio of TAR's at two distances seen in Equation 2.2. This correction factor can then be used to correct the percentage dose deposition (PDD) to account for the air gap region.

$$CF = \frac{TAR(d,r_d)}{TAR(d+h,r_d)} \qquad \text{Equation 2.2}$$

where

CF = correction factor

$TAR(d,r_d)$ = TAR at depth d where the tissue deficiency is

$TAR(d+h,r_d)$ = TAR at depth d+h

h = distance between the surface used to define the SSD and the surface at the location of the deficiency.

Other methodologies have been used to correct for contour irregularities. These include Effective Source-to-Surface Distance Method and Isodose Shift Method.[4]

Tissue Inhomogeneities Corrections

As stated earlier, the phantoms typically used to gather data are one material – water. This is used as a material equivalent to tissue; however, the human body is not composed of only water. Thus, correction methods were designed to help take into account these inhomogeneities.

*Tissue-Air Ratio (TAR) Method*

As earlier, a correction factor, CF, is found using ratios of TAR's. This can be seen below in Equation 2.3.

$$CF = \frac{TAR(d', r_d)}{TAR(d, r_d)} \qquad \text{Equation 2.3}$$

where $d' = d_1 + \rho_e d_2 + d_3$

$d_1$= distance from the surface to the heterogeneity

$d_2$=distance from the top to bottom of the heterogeneity

$\rho_e$=electron density of the heterogeneity relative to that of water

$d_3$=distance from the bottom of the heterogeneity to the point of calculation

*Batho Method*

The Batho Method, or the Power Law Tissue-Air Ratio Method, becomes slightly more complicated by using a ratio of TAR's raised to a power.[10,11] The correction factor is shown in Equation 2.4.

$$CF = \left[ \frac{TAR(d_2 + d_3, r_d)}{TAR(d_3, r_d)} \right]^{\rho_e - 1} \qquad \text{Equation 2.4}$$

In this case, the correction factor does depend on the location of the heterogeneity with relation to the point of calculation; however, it does not rely on the distance from the surface. This methodology only assumes Compton interactions, and it cannot be applied to calculation points that lie within the heterogeneity and within the build-up region.

A modification was made to the Batho method in order to allow the dose calculations to be made to points that are within the heterogeneity.[12]

$$CF = \frac{TAR(d_3, r_d)^{\rho_3 - \rho_2}}{TAR(d_2 + d_3)^{1-\rho_2}} \quad \text{Equation 2.5}$$

where $\rho_3$=density of the material in which the calculation point lies

$d_3$ = depth of the calculation point within the material

$\rho_2$= density of the material overlying the heterogeneous region

*Equivalent Tissue-Air Ratio (ETAR) Method*

The TAR Method described by Equation 2.3 to correct for heterogeneities appropriately takes into account the primary dose deposition. It does not however, correctly model the dose that is due to scattered particles due to the geometric make up of the heterogeneity. In order to correct this, the field size parameter was scaled, thus an “equivalent” tissue-air ratio is used.[13] The ETAR method was also extended to calculate dose due to scattered particles separately from that of primary dose. This method is known as the differential scatter-air ratio (dSAR) method.[14,20]

These correction based methods are typically only used in two dimensional situations. The accuracy is not high enough to apply for treatment planning situations in which there is a three dimensional treatment volume with great heterogeneity.

$$P_{corrected} = P'' \cdot CF$$

**Convolution Superposition**

Previously, dose calculation algorithms assumed all energy was locally deposited. Thus, if a charged particle was liberated, the energy was immediately deposited rather than following the particle. The next step in dose calculation was to follow these charged particles and determine where the energy was actually deposited. Mackie et. al presented this new method for determining dose deposition.[15] This new methodology rigorously tracked the lateral spread of the charged particles set in motion by incident photons. The data necessary for this method is generated by Monte Carlo techniques. Monte Carlo is used to map the spatial distribution of charged particles away from the primary photon interaction site. This produces a primary dose spread array, a spatial energy deposition distribution of both electrons and positrons due to the interaction of a primary photon in a specific interaction voxel. The values obtained in the array are the primary energy deposited in that specific voxel normalized to the total energy released.

The method described also separates scatter dose from primary dose. Monte Carlo methods are also used to follow first-scatter photons. The first-scatter photons that deposit dose relatively close to the primary interaction voxel are stored in a separate dose spread array. Some first-scatter photons along with multiple-scatter photons deposit their dose relatively far from the interaction site. These are stored in yet another dose spread array.

These dose spread arrays are essentially the response of all voxels in a phantom to a single photon interaction occurring in a single voxel. It is not possible to determine these from measurements because individual photons cannot be forced to interact in a specific voxel. In a homogeneous phantom, the dose spread arrays are convolved with the relative fluence to determine the dose deposition. The dose, D(r), at the point r obtained from a convolution superposition is shown below in Equation 2.6.

$$D(r) = \int \frac{\mu}{\rho} \Psi_p(r') A(r - r') d^3 r' = \int T_p(r') A(r - r') d^3 r' \qquad \text{Equation 2.6}$$

where $\frac{\mu}{\rho}$ is the mass attenuation coefficient

$\Psi_p(r')$ is the primary photon energy fluence

$A(r - r')$ is the convolution kernel

$T_p(r')$ is the TERMA (total energy released per unit mass)

In the case of heterogeneous media, large numbers of primary dose spread arrays would have to be generated in order to account for all the possible combinations of voxel configurations. O’Connor’s theorem is used in order to extend this method for use in heterogeneous materials. For the heterogeneous media of interest, an average density value is found between the interaction site and all the dose deposition sites. Using the average density values and the specified resolution (voxel size), interpolation can be used to determine the correct dose spread array values from those obtained from homogeneous phantoms.

Mackie, et. al's paper was the starting point to many improvements to the method in order to make it more clinically relevant. Many improvements were made including extension to a polyenergetic spectra [21] as well as increased speed of the method by faster ray-tracing[22] or fast fourier transform (FFT) calculations.[23]

**Collapsed Cone Convolution**

Ahnesjo describes a new convolution method called collapsed cone convolution to calculate the dose a person receives.[16] It was found that convolution superposition could require a large amount of time to perform the numerous integrations. It was also found that large sampling errors occurred in convolution superposition because of the very steep gradient that occurs within the electron range. This collapsed cone convolution helps to solve these problems. It begins by discretizing the problem into spherical coordinates. The voxels are thus defined as conical shell segments that occur in a solid angle of $\Omega_m$. Energy from volume elements is released into these coaxial cones. This energy is rectilinearly transported; it then becomes attenuated and deposited along the axis into specific elemental volumes. These convolution kernels are scaled implicitly to account for tissue heterogeneities.

A Cartesian coordinate system is then placed over the spherical system. Close to a scattering location, one Cartesian voxel may cover more than one cone, thus no accuracy is lost. However, further from the scattering event, multiple Cartesian voxels occur within one conical segment. Errors may be introduced here because some voxels will have too much energy deposition, while others will have none. It was found that this method was very accurate when charged particle equilibrium was present. In this model, the charged particle transport is not modeled exactly; however, the general behavior is correctly predicted.

**Pencil Beam**

Ahnesjo, et. al describes another convolution method for photon dose calculation.[17] The main difference is the use of empirical polyenergetic pencil beam kernels. The method is point oriented, thus it is actually faster than a full 3-D convolution algorithm. These kernels are described as the sum of two exponentials given below. This equation was found by fitting the data to Monte Carlo results. The first term represents the primary dose, while the second results from scatter dose.

$$\frac{p}{\rho}(r,z) = \frac{A_z e^{-a_z r}}{r} + \frac{B_z e^{-b_z r}}{r} \qquad \text{Equation 2.7}$$

where r is the cylindrical radius from pencil beam axis

$A_z$, $a_z$, $B_z$, and $b_z$ fitting parameters at a depth of z

$\frac{p}{\rho}$ is the energy fraction deposited per unit mass.

Other specific kernels are obtained from the previous one for specific situations such as accounting for the pnumbra region, charged particle contamination, and photon contamination. In order to obtain the dose, the pencil beam distribution is convolved with the incident energy fluence distribution.

**Analytical Anisotropic Algorithm (AAA)**

The Analytical Anisotropic Algorithm (AAA) is a three dimensional pencil beam convolution superposition dose calculation algorithm. It separately models primary photons, scattered photons, and electrons. This methodology better handles the complex heterogeneities that occur within a patient volume.

The AAA Model is separated into two components. The first is the configuration algorithm, which determines the basic physical parameters of the fluence and energy spectra of the clinical beam. It also takes into account the scattering properties of the beam in a water equivalent phantom. The second component is the actual dose calculation algorithm. Separate convolution models are used for the primary photons, contaminating electrons, and scattered photons. The photon dose is calculated by a 3-D convolution of scatter kernals which have been precalculated using Monte Carlo methods and scaled according to an electron density matrix.[18,19]

**Monte Carlo**

The Monte Carlo method is a computer code that simulates particle transport. Using the laws of physics, probability distributions are determined for specific particle interactions. A specific number of particles are simulated, and they are followed. Each particles fate is determined from their interaction probability distribution. This is used in medical physics to determine the amount of dose deposited in specific regions. The accuracy of the dose deposition is dependant on the number of particles that are followed. With more particles comes greater accuracy. The problem with this is that the computational time required to obtain acceptable statistics can be quite long. This is not a feasible method to use for treatment planning since typically results are needed within a few days or possibly even a few hours. Monte Carlo is considered the gold standard for calculating dose distributions. It is considered to be the most accurate methodology for describing dose deposition, and most computational methods today are compared to Monte Carlo results to determine their accuracy.[7-9,24]

## 2.2 Clinical Use

As seen previously, dose calculation algorithms began very simply by determining dose within a homogenous phantom. This however, is not clinically applicable because the human body has much heterogeneity located within it. There are basically two types of heterogeneities that occur within the body. There are those that are lower density than human tissue or water, which is typically representative of a lung heterogeneity. The other is high Z materials, such as bone. Most studies have only looked into lung heterogeneities, while only a handful have studied heterogeneities of bone.[19] This is actually quite surprising because according to the American Association of Physicists in Medicine (AAPM) Report Number 85, bones are the main heterogeneity located within the body; however, a small number of papers have addressed this heterogeneity specifically.[3]

According to Carrasco et. al in 2004, every dose calculation algorithm implemented in commercial treatment planning systems that used invariant kernels obtained from water phantom measurements for their convolutions, overpredicted the dose inside low density materials when a high energy x-ray beam was used.[25] These treatment planning systems only took into account the lower density material resulting in increased transmission of the particles; however, it did not correctly model the decrease in the interaction coefficient inside the lung region. The exact opposite is true for higher density materials. The dose is underpredicted inside these regions, such as bone, for high-energy x-ray beams. The cause of this is accounting only for the decreased transmission but not the increase in the interaction coefficient.[26]

Convolution-superposition algorithms have been implemented in most treatment planning systems in use today; however, they have not been extensively tested in phantoms with bone-equivalent material.[26] In Carrasco's work, a recommendation is made to include a test with heterogeneities for quality assurance because the different algorithms available within the same treatment planning system behaved differently. The new Analytical Anisotropic Algorithm being implemented by Varian has been shown to improve the accuracy of dose calculations. It was shown that for heterogeneous materials, the improvements were quite large when compared to the pencil beam algorithm. The more accurate results will likely result in a change in clinical practice because of the lower doses that will be shown in the lower density regions when AAA is used. Thus, clinicians must be careful to not try to increase the dose unnecessarily to try to obtain the same dose histogram that was obtained with the pencil beam algorithm. Sub optimal results however were still obtained at the interface of heterogeneities.[18]

The dose calculation algorithms are improving; however, any improvement to the current state of knowledge is considered valuable. Monte Carlo calculations will be the eventual answer to the problem; however, at this time, they are still much too time consuming to be used in clinical practice.

# CHAPTER 3

# COMET BACKGROUND

In the Computational Reactor/Medical Physics Group at the Georgia Institute of Technology, a heterogeneous **co**arse-**me**sh **t**ransport method (COMET) has been developed. In this work, the method is now being applied to the transport of photons and electrons in medical physics type applications. The general method for obtaining the solution to large heterogeneous problems is described. This methodology is described in depth by Mosher and Rahnema[2] as well as Forget and Rahnema.[1]

## 3.1 General Description and Notation

Beginning with a large heterogeneous system, the composition is well known and can be easily characterized. COMET begins with the particle transport equation in its typical form as seen in Equation 3.1.

$$\hat{\Omega}.\nabla\psi\left(\vec{r},\hat{\Omega},E\right)+\sigma_t\left(\vec{r},E\right)\psi\left(\vec{r},\hat{\Omega},E\right)= \\ Q\left(\vec{r},\hat{\Omega},E\right)+\int_0^\infty dE'\int_{4\pi}d\Omega'\,\sigma_s\left(\vec{r},\hat{\Omega}',E'\to\hat{\Omega},E\right)\psi\left(\vec{r},\hat{\Omega}',E'\right) \qquad \text{Equation 3.1}$$

The boundary condition is given below.

$$\psi\left(\vec{r}_b,\hat{\Omega},E\right)=B\psi\left(\vec{r}_b,\hat{\Omega}',E'\right) \quad \text{with} \quad \vec{n}.\hat{\Omega}<0,\ \vec{n}.\hat{\Omega}'>0,\ \vec{r}_b\in\partial V \qquad \text{Equation 3.2}$$

The variables $\psi$, Q, and B represent the angular flux distribution, the source term, and the boundary condition operator, respectively. The external boundary of the system is denoted by $\partial V$, and the outward normal vector $\vec{n}$ is given with respect to this external boundary. The phase-space variables can be seen in parenthesis above as $\vec{r},\hat{\Omega},E$, where $\vec{r}$ represents the spatial variable, $\hat{\Omega}$ describes the angle, and $E$ defines the energy.

The system is then decomposed into a set of $N$ non-overlapping regions $V_i$ with each of these regions composing a single coarse-mesh. The transport equation and boundary condition then can be represented by Equations 3.3 and 3.4 respectively below.

$$\hat{\Omega}.\nabla\psi_i\left(\vec{r},\hat{\Omega},E\right)+\sigma_t\left(\vec{r},E\right)\psi_i\left(\vec{r},\hat{\Omega},E\right)= Q_i\left(\vec{r},\hat{\Omega},E\right)+\int_0^\infty dE'\int_{4\pi}d\Omega'\,\sigma_s\left(\vec{r},\hat{\Omega}',E'\rightarrow\hat{\Omega},E\right)\psi_i\left(\vec{r},\hat{\Omega}',E'\right) \quad \text{Equation 3.3}$$

$$\psi_i^-\left(\vec{r}_{ij},\hat{\Omega},E\right)=\psi_j^+\left(\vec{r}_{ij},\hat{\Omega},E\right)\ \ with\ \vec{r}_{ij}\in\left\{V_i\cap V_j\right\},\ V_j\,bounds\ V_i \quad \text{Equation 3.4}$$

Note that $\left|\vec{n}_i\cdot\hat{\Omega}_i\right|=\left|\vec{n}_j\cdot\hat{\Omega}_j\right|$ with $\vec{n}_i.\hat{\Omega}_i<0$ and $\vec{n}_j.\hat{\Omega}_j>0$. In the equations given above, $\psi_i$ defines the angular flux within the volume $V_i$. The volumes represented by $V_j$ share a boundary with the volume $V_i$. The angular flux values $\psi_i^-$ and $\psi_i^+$ represent the angular flux in the incoming and outgoing direction respectively.[1,2] In the instance where $V_i$ shares a boundary with the global system, the specific boundary condition for this situation can be seen below in Equation 3.5.

$$\psi_i^-\left(\vec{r}_{ib},\hat{\Omega},E\right)=B\psi_i^+\left(\vec{r}_{ib},\hat{\Omega},E\right)\ \ with\ \vec{r}_{ib}\in\left\{V_i\cap\partial V\right\} \quad \text{Equation 3.5}$$

After this decomposition, N local fixed source problems remain in place of the larger global problem that they make up. These N problems can now be solved on their own. Each of these smaller local fixed source problems can be solved by Monte Carlo methods. The Monte Carlo code EGSnrc was used for each of the response function calculations. Monte Carlo algorithms are extremely accurate when enough histories are followed to allow for excellent statistics; however, this typically requires huge amounts of computational time. Because of this, Monte Carlo methods cannot be used on the global problem itself; however, since the local problems are much smaller in size, it is an excellent method to obtain the solution to each unique local problem in an efficient manner. Once the solutions to the local problems have been obtained, they are then coupled together using an iterative scheme. The surface angular fluxes are compared to the previous iteration value to determine if the pre-defined convergence parameter, $\varepsilon_\psi$, has been met. This is seen below in Equation 3.6

$$\left|\frac{\psi^l}{\psi^{l-1}} - 1\right| < \varepsilon_\psi \qquad \text{Equation 3.6}$$

The value *l* represents the iteration number. In addition to the surface angular fluxes, convergence may also be calculated on any other quantity. In this work, energy deposition was used.

### 3.2 Response Function Generation

Each unique coarse-mesh ($V_i$) is solved by assuming a unit current entering on one face. The outgoing currents are then obtained through conventional Monte Carlo methods. In this case, EGSnrc was used to obtain these responses to the incoming unit current. Other quantities in addition to the outgoing currents may be tallied in this response such as energy deposition which is of utmost importance in the medical physics applications. These outgoing currents then provide the incoming current to its neighbor volumes. This solution to the coarse-mesh is known as the response function.

The COMET method makes the assumption that the surface angular flux distribution in angle, space, and energy is known exactly. Because this never occurs, an approximation of this value must be used. The fixed source equation presented in Equation 3.1 is solved using a new boundary condition below in Equation 3.7.

$$\psi_i\left(\vec{r}_{is}, \hat{\Omega}, E\right) = \begin{cases} \Gamma^m\left(\vec{r}_{is}, \hat{\Omega}, E\right) & \text{where } r_{is} \in \{V_i \cap \partial V_s\} \\ 0 & \text{elsewhere} \end{cases} \qquad \text{Equation 3.7}$$

In this equation $\partial V_S$ is the sub-region of a boundary of coarse-mesh $V_j$ that shares a boundary with $V_i$. $\Gamma^m$ is defined as the $m^{th}$ member of a set of orthogonal functions. In this case, Legendre Polynomials were used. The equation for N non-overlapping sub regions found in Equation 3.4 is solved using the boundary condition given above.

After obtaining the solution for an individual unique coarse-mesh with the specified boundary condition, the response function, $R_{is}^{m}\left(\vec{r},\hat{\Omega},E\right)$, is obtained. This response provides us with the angular flux solution of the coarse-mesh with the boundary condition given by $\Gamma^{m}$. It is shown in Equation 3.8 as a linear superposition.

$$\psi_i(\vec{r},\hat{\Omega},E)=\sum_{m=0}^{\infty}\sum_{s}c_{is}^{m}R_{is}^{m}(\vec{r},\hat{\Omega},E), \qquad \text{Equation 3.8}$$

with $c_{is}^{m}=\iiint\psi_i^{-}\left(\vec{r}_{is},\hat{\Omega},E\right)\Gamma^{m}d\vec{r}_{is}d\hat{\Omega}dE$

The variable $\vec{r}_{is}$ is the spatial variable defined along the boundary between $V_i$ and $\partial V_S$.

For practical application, the response function expansion is truncated at an arbitrary low order. The expansion order is determined based on the desired accuracy. These response functions are all pre-computed and stored in a library based on their unique coarse-mesh definition and boundary conditions.

### 3.3 Summary of Method

A response function library is generated based on mesh size, energy, and material definition. These response functions are all precomputed and can be reused for many different problems. To begin solving a large, global problem, it must be decomposed into meshes. Our COMET code then couples the response functions together based on the definitions of each mesh. The output obtained is the energy deposition obtained within each mesh. The COMET solution is compared against a pure Monte Carlo Method.

# CHAPTER 4

# SENSITIVITY STUDY

As described in Chapter 3, the COMET Code requires Legendre polynomial expansions for energy, space, polar angle, and azimuthal angle. A higher expansion order typically will provide better results than a lower order; however, at times the lower expansion order may be "good enough" for a predefined (desired) accuracy. Higher expansion orders will produce larger response function libraries because of the increased information they provide, and this does in turn result in longer COMET run times. This basic sensitivity study was performed in order to determine which combination of orders is best in regards to timing and statistical results for use in more difficult benchmark problems. Please note that for every reference calculation obtained in this entire work, EGSnrc was the Monte Carlo code used.[27] For more detailed information regarding each of the benchmarks and the parameters used in EGSnrc, see Appendix B.

## 4.1 Problem Definitions

Two simple benchmark problems were defined for testing. The first was a 30 cm x 20 cm box composed entirely of water. The second was a phantom meant to depict a simplified lung description, also of size 30 cm x 20 cm. In both cases, the third dimension is assumed to extend to infinity in both directions. This was meant to be a very course portrayal of two lungs and a spinal column. These benchmarks were composed of 1 cm x 1 cm meshes. These benchmarks are shown below in Figure 4.1.1 and Figure 4.1.2. These benchmark problems were studied in my previous Master's thesis work, which focused on photon only transport with larges mesh sizes.[28] They were chosen as the beginning point before more difficult phantoms were studied. Reference calculations were performed using EGSnrc for comparison with our COMET Solutions.

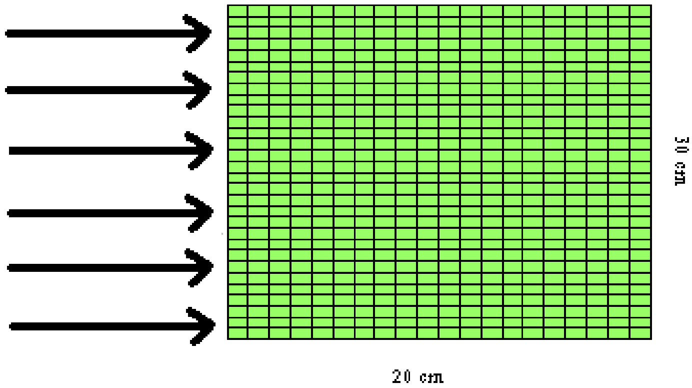


Figure 4.1.1: Water Phantom
Green: Water

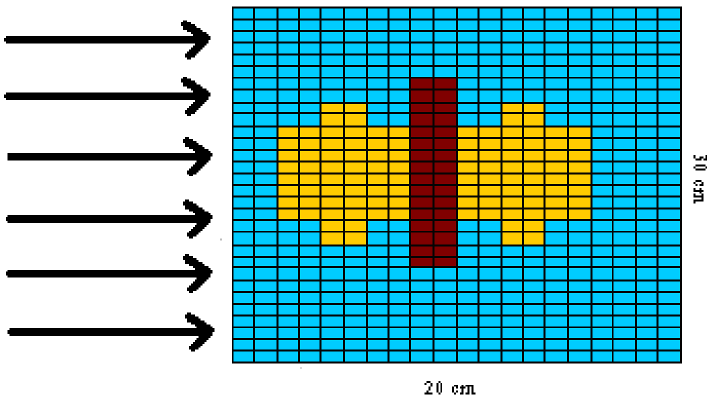


Figure 4.1.2: Simplified Lung Phantom
Blue: Tissue/Water
Red: Bone
Yellow: Lung Tissue

The incident beam on each of these problems runs the entire length of the 30 cm face. Currently COMET can only handle incident beams that are composed of mono-energetic and mono-directional photons. Obviously radiation therapy treatment does not use mono-energetic photon beams, so for the testing in this work, multiple different energies were selected for benchmarking.

Two typical poly-energetic spectrums used for treatment at Emory University are 18 MV and 6 MV.[29] For testing these benchmark methods, three incident photon beam energies were chosen: 2 MeV, 6 MeV, and 18 MeV. The 18 MeV energy was chosen because it is the typically the maximum energy associated with the 18 MV beam, and 6

MeV is approximately the average energy of the same poly-energetic beam. The average is approximately one third of the maximum energy.[29] The same logic was applied to the 6 MV beam – thus it has an associated maximum 6 MeV energy and an average 2 MeV energy. From this, the three mono-energetic energies, 2 MeV, 6 Mev, and 18 MeV, were chosen for testing in this sensitivity study and all of the following benchmark problems.

To begin, response function libraries were obtained using EGSnrc in order to determine the best expansion order for each variable (energy, space, polar and azimuthal angle). Response functions were obtained up to 5$^{th}$ order in each variable. Using this one response function library, every combination up to the 5$^{th}$ order can be obtained for COMET calculations. For the sensitivity study, three of the variables were set to 5$^{th}$ order while the fourth variable was altered from 1$^{st}$ to 5$^{th}$. For each of these combinations, a COMET solution was obtained. Each of the COMET solutions was compared to the EGSnrc reference solution. These comparisons could then be used to determine the best expansion to be used for future COMET calculations.

For all of the cases in the benchmark study, twenty million particle histories were followed for each response function library that was generated. A new response function must be generated for each new energy, material definition, and size of the coarse mesh. For the reference calculation in EGSnrc, ten billion particles were used.

## 4.2 Benchmark Problems

### Water Phantom

A water phantom was chosen because of its simplicity and its use within the clinic. A single response function library with 5$^{th}$ order in energy, space, and angle was produced for each energy. For this water benchmark, three libraries were created. Each material definition was for that of water; however, one was required for each of the incident energies: 2 MeV, 6 MeV, and 18 MeV. The results for the water phantom simulation are shown below for each of the three energies. For each expansion order and beam energy, the maximum percent difference and average percent difference between the COMET solution and the reference solution is shown along with a COMET calculation time.  Please see Appendix A for further information on the statistical values calculated.

Table 4.2.1: Sensitivity Study Results for Water Phantom with 1cm x 1cm Coarse-Meshes – The four numbers in the expansion order column represent the energy, space, polar angle, and azimuthal angle expansion orders.

| | 2 MeV Incident Beam | | | 6 MeV Incident Beam | | | 18 MeV Incident Beam | | |
|---|---|---|---|---|---|---|---|---|---|
| **Exp Order** | **Max % Diff** | **Avg % Diff** | **Calc Time (min)** | **Max % Diff** | **Avg % Diff** | **Calc Time (min)** | **Max % Diff** | **Avg % Diff** | **Calc Time (min)** |
| **1555** | 1.945% | 1.265% | 13.6 | 5.935% | 3.461% | 10.9 | 15.186% | 8.214% | 14.0 |
| **2555** | 0.467% | 0.250% | 66.1 | 2.530% | 1.025 % | 43.6 | 9.904% | 2.688% | 43.8 |
| **3555** | 0.486% | 0.169% | 110.2 | 1.640% | 0.624 % | 109.1 | 7.897% | 1.401% | 111.9 |
| **4555** | 0.486% | 0.161% | 207.9 | 1.506% | 0.525 % | 206.2 | 6.520% | 1.089% | 206.4 |
| **5555** | 0.445% | 0.151% | 311.8 | 1.582% | 0.540 % | 305.3 | 5.626% | 0.869% | 304.9 |
| | | | | | | | | | |
| **5155** | 0.527% | 0.154% | 10.8 | 1.675% | 0.533% | 11.1 | 5.554% | 0.902% | 11.1 |
| **5255** | 0.463% | 0.153% | 42.8 | 1.580% | 0.535% | 43.2 | 5.676% | 0.868% | 44.0 |
| **5355** | 0.461% | 0.153% | 112.0 | 1.586% | 0.539% | 111.6 | 5.634% | 0.869% | 107.2 |
| **5455** | 0.451% | 0.151% | 212.7 | 1.583% | 0.539% | 228.7 | 5.646% | 0.870% | 201.7 |
| **5555** | 0.445% | 0.151% | 311.8 | 1.582% | 0.540 % | 305.3 | 5.626% | 0.869% | 304.9 |
| | | | | | | | | | |
| **5515** | 7.256% | 5.234% | 13.9 | 10.265% | 4.169% | 11.2 | 30.336% | 7.632% | 10.8 |
| **5525** | 1.055% | 0.658% | 109.2 | 2.661% | 0.894% | 111.7 | 13.799% | 2.414% | 108.3 |
| **5535** | 1.055% | 0.658% | 109.7 | 2.661% | 0.894% | 112.9 | 13.799% | 2.414% | 108.1 |
| **5545** | 0.445% | 0.151% | 316.9 | 1.582% | 0.540% | 327.2 | 5.626% | 0.869% | 303.4 |
| **5555** | 0.445% | 0.151% | 311.8 | 1.582% | 0.540 % | 305.3 | 5.626% | 0.869% | 304.9 |
| | | | | | | | | | |
| **5551** | 2.603% | 0.513% | 11.1 | 7.699% | 1.039% | 11.5 | 30.006% | 5.047% | 10.8 |
| **5552** | 1.340% | 0.304% | 43.7 | 3.486% | 0.610% | 43.2 | 24.516% | 2.508% | 59.2 |
| **5553** | 0.872% | 0.190% | 109.1 | 1.322% | 0.523% | 111.8 | 6.211% | 0.771% | 113.7 |
| **5554** | 0.800% | 0.205% | 227.9 | 1.564% | 0.510% | 206.4 | 7.993% | 0.896% | 211.4 |
| **5555** | 0.445% | 0.151% | 311.8 | 1.582% | 0.540 % | 305.3 | 5.626% | 0.869% | 304.9 |

For each energy case, the response function library required around 240 hours of computational time to run.  It should be once again noted that this is completely pre-computational, and these response functions can be re-used.  The reference calculations for the water case required 202 hours for a 2 MeV beam, 300 hours for a 6 MeV beam, and 440 hours for an 18 MeV beam.

The highlighted values represent those that provided the best results with an adequate amount of timing.  In some instances the maximum percent difference may have been slightly higher; however, the average percent difference was actually lower.  This did occur in the 2MeV case for expansion order 2555.  The minimum value for maximum percent difference was found here; however, it the average percent difference was still larger than that of a higher expansion order. Fifth order expansions were not chosen here because the time required for this is much higher. The best expansion order between all three energies was chosen to be 4$^{th}$ in Energy, 2$^{nd}$ in Space, 4$^{th}$ in Polar Angle, and 3rd in Azimuthal Angle. With the same expansion order for each energy being used, better comparisons can be made.

**Simplified Lung Phantom**

A simplified lung phantom was developed in order to add heterogeneity into the system. A lung definition and bone definition are used in order to test how the COMET methodology handles both higher and lower density regions within the phantom. As with the water phantom, a single response function library with 5$^{th}$ order in energy, space, and angle was produced for each energy and each material definition in this case. For this simplified lung benchmark, nine libraries were created. For each of the three materials – lung, water, and bone – a library was generated for each of the three incident energies, 2 MeV, 6 MeV, and 18 MeV. The results for the simplified lung phantom simulation are shown below for each of the three energies.

Table 4.2.2: Sensitivity Study Results for Simplified Lung Phantom with 1cm x 1cm Coarse-Meshes- The four numbers in the expansion order column represent the energy, space, polar angle, and azimuthal angle expansion orders.

| | 2 MeV Incident Beam | | | 6 MeV Incident Beam | | | 18 MeV Incident Beam | | |
|---|---|---|---|---|---|---|---|---|---|
| **Exp Order** | **Max % Diff** | **Avg % Diff** | **Calc Time (min)** | **Max % Diff** | **Avg% Diff** | **Calc Time (min)** | **Max % Diff** | **Avg % Diff** | **Calc Time (min)** |
| **1555** | 2.368 % | 1.339% | 14.6 | 6.494% | 3.610% | 13.8 | 15.652% | 9.092% | 14.3 |
| **2555** | 0.454% | 0.226% | 65.4 | 2.610% | 1.046% | 44.2 | 10.620% | 2.988% | 46.3 |
| **3555** | 0.503% | 0.169% | 117.2 | 1.685% | 0.627% | 118.1 | 8.559% | 1.603% | 114.1 |
| **4555** | 0.521% | 0.156% | 281.6 | 1.465% | 0.465% | 221.8 | 6.641% | 1.183% | 208.8 |
| **5555** | 0.485% | 0.158% | 415.0 | 1.624% | 0.506% | 331.7 | 5.816% | 0.970% | 316.1 |
| | | | | | | | | | |
| **5155** | 0.529% | 0.158% | 14.8 | 1.718% | 0.497% | 10.9 | 5.740% | 1.002% | 11.2 |
| **5255** | 0.513% | 0.160% | 55.1 | 1.622% | 0.500% | 44.6 | 5.864% | 0.968% | 43.2 |
| **5355** | 0.509% | 0.160% | 148.2 | 1.627% | 0.504% | 124.5 | 5.824% | 0.969% | 112.3 |
| **5455** | 0.498% | 0.158% | 285.9 | 1.625% | 0.505% | 228.4 | 5.836% | 0.970% | 218.6 |
| **5555** | 0.485% | 0.158% | 415.0 | 1.624% | 0.506% | 331.7 | 5.816% | 0.970% | 316.1 |
| | | | | | | | | | |
| **5515** | 7.701% | 5.258% | 13.6 | 10.320% | 4.290% | 11.0 | 30.381% | 8.148% | 11.2 |
| **5525** | 1.195% | 0.652% | 138.8 | 2.655% | 0.930% | 126.5 | 13.690% | 2.438% | 111.8 |
| **5535** | 1.195% | 0.652% | 139.2 | 2.655% | 0.930% | 121.2 | 13.690% | 2.438% | 111.9 |
| **5545** | 0.485% | 0.158% | 400.2 | 1.624% | 0.506% | 291.0 | 5.816% | 0.970% | 328.8 |
| **5555** | 0.485% | 0.158% | 415.0 | 1.624% | 0.506% | 331.7 | 5.816% | 0.970% | 316.1 |
| | | | | | | | | | |
| **5551** | 2.647% | 0.547% | 13.8 | 7.695% | 1.055% | 10.8 | 29.927% | 5.165% | 10.9 |
| **5552** | 1.341% | 0.294% | 55.6 | 3.521% | 0.579% | 45.9 | 24.735% | 2.624% | 58.1 |
| **5553** | 0.838% | 0.203% | 139.5 | 1.360% | 0.493% | 116.9 | 6.258% | 0.880% | 124.6 |
| **5554** | 0.749% | 0.204% | 285.5 | 1.608% | 0.482% | 217.1 | 8.177% | 1.007% | 206.6 |
| **5555** | 0.485% | 0.158% | 415.0 | 1.624% | 0.506% | 331.7 | 5.816% | 0.970% | 316.1 |

For each energy, the three pre-computed response function libraries combined required around 720 hours of computational time. The reference calculations for the water case required 280 hours for a 2 MeV beam, 480 hours for a 6 MeV beam, and 770 hours for an 18 MeV beam. The same conclusions for expansion order, 4243, for the all the energies combined were found for the more strenuous lung case. Again, some expansion orders were chosen that had a higher maximum percent error; however, the average for the entire system was found to be lower for this expansion order. Overall, it handled the entire problem better as a whole.

### 4.3 Conclusions

Based on the data presented in the tables, it was found that the best expansion orders to be used were 4$^{th}$ order in energy, 2$^{nd}$ order in space, 4$^{th}$ order in polar angle, and

$3^{rd}$ order in azimuthal angle. COMET solutions for both the water and simplified lung phantom were now obtained for this optimal expansion order. The results are shown below in Table 4.3.1. For the each of the incident beam energy cases, the results obtained for the water phantom and the lung phantom produce results that are quite similar in terms of percent differences and COMET calculation time.

Table 4.3.1: Optimized Expansion Order Results

| 2 MeV Incident Beam | | | | |
|---|---|---|---|---|
| | Max % Diff | Avg % Diff | COMET Calc Time | Ref Calc Time |
| Water Phantom - 4243 | 0.89 % | 0.19 % | 8.4 min | 202 hours |
| Lung Phantom - 4243 | 0.78% | 0.20% | 10.6 min | 280 hours |

| 6 MeV Incident Beam | | | | |
|---|---|---|---|---|
| | Max % Diff | Avg % Diff | COMET Calc Time | Ref Calc Time |
| Water Phantom - 4243 | 1.26% | 0.50% | 8.4 min | 300 hours |
| Lung Phantom - 4243 | 1.22 % | 0.45 % | 8.3 min | 480 hours |

| 18 MeV Incident Beam | | | | |
|---|---|---|---|---|
| | Max % Diff | Avg % Diff | COMET Calc Time | Ref. Calc Time |
| Water Phantom - 4243 | 7.24% | 0.90% | 8.4 min | 440 hours |
| Lung Phantom - 4243 | 7.34% | 1.03% | 8.2 min | 770 hours |

When comparing the values in Table 4.3.1 to that of the previous sensitivity study tables for the 2 MeV beam, it can be seen that some of the values obtained in the optimized expansion order for the maximum percent difference are slightly higher in some cases than that from the sensitivity study; however, the values obtained for the average percent difference are typically right around the values from the sensitivity study or better. The main point is that for this optimal expansion order which produced similar results to those obtained for the best expansions in the sensitivity study, the time required to run the COMET calculation was smaller than all of the COMET times during the sensitivity study. The optimized COMET calculations ran between 1400 and 5600 times faster than the reference calculations.

# CHAPTER 5

# SIMPLE BENCHMARK PROBLEMS

## 5.1 Problem Definitions

For my Master's thesis work, initial studies were performed on simplified phantoms of large mesh size and for photon transport only. These phantoms are two-dimensional phantoms with the third dimension extended to infinity in both directions. Two of these were a water phantom and a simplified lung phantom. These are the same phantoms described previously in the Chapter 4 sensitivity study; however, the coarse meshes used during my Master's work were of size 2 cm x 2 cm.[28] This very large size was acceptable for the initial comparison; however, for further investigations, it was determined that the study would continue with benchmarks composed of smaller meshes that are closer to those that are used clinically. A third simple benchmark problem was also studied in my Master's thesis work. It was a slab phantom composed of three materials: water, lung material, and aluminum. This problem was not meant to be clinically relevant; however, it had been developed by Mohan and Rogers to put stress on dose calculation algorithms.[30] In previous testing, this benchmark was also composed of 2 cm x 2 cm meshes.

These three benchmark problems were restudied here with smaller mesh sizes of 1 cm x 1 cm and 0.5 cm x 0.5 cm, and with the inclusion of photon and electron transport. As stated previously, each mono-energetic incident photon beam impinges normally on the face of the phantom. The three energies described in Chapter 4 were studied for each of these simplified phantom cases as well: 2 MeV, 6 MeV, and 18 MeV. The expansion orders found in the previous sensitivity study are used here: 4$^{th}$ in Energy, 2$^{nd}$ in space, 4$^{th}$ in polar angle, and 3$^{rd}$ in azimuthal angle.

For each reference calculation performed, ten billion particle histories were followed using the pure Monte Carlo code EGSnrc. For the response function generation, twenty million particles were followed for each library generation. The response function libraries were re-calculated for the optimal expansion order using more particles than previously with the sensitivity study. For more detailed information regarding each of the benchmarks and the parameters used in EGSnrc, see Appendix B. Also, additional plots regarding dose deposition can be found in Appendix C. For more information on the statistical values calculated, please see Appendix A.

## 5.2 Simple Benchmark Problem Results

**Water Phantom**

<u>Mesh Size: 1 cm x 1 cm</u>

The water phantom composed of 1 cm x 1 cm meshes is shown below in Figure 5.2.1. It can be seen that the incident photon beam is incident perpendicular on the left face of the phantom. Three response function libraries were needed – one for each incident beam energy. Each of these response function libraries required around 42 hours to calculate.

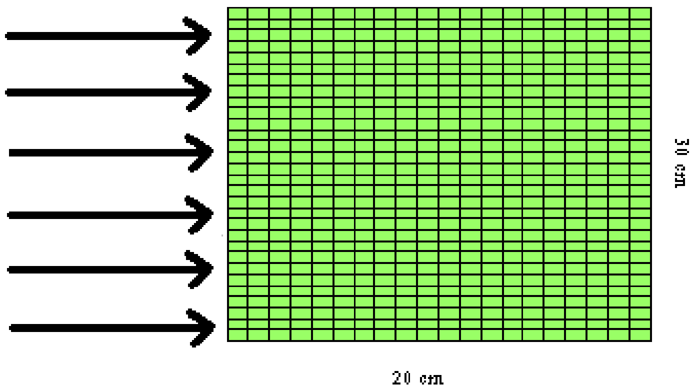


Figure 5.2.1: Water Phantom
Green: Water

The energy deposition determined from the EGSnrc reference solution for the 2 MeV, 6 MeV, and 18 MeV incident photon beam are shown below in Figures 5.2.2, 5.2.3, and 5.2.4 respectively. The energy deposition figures show that as the incident beam energy increases, the location for maximum energy deposition occurs deeper within the phantom, while the surface receives less dose as expected.

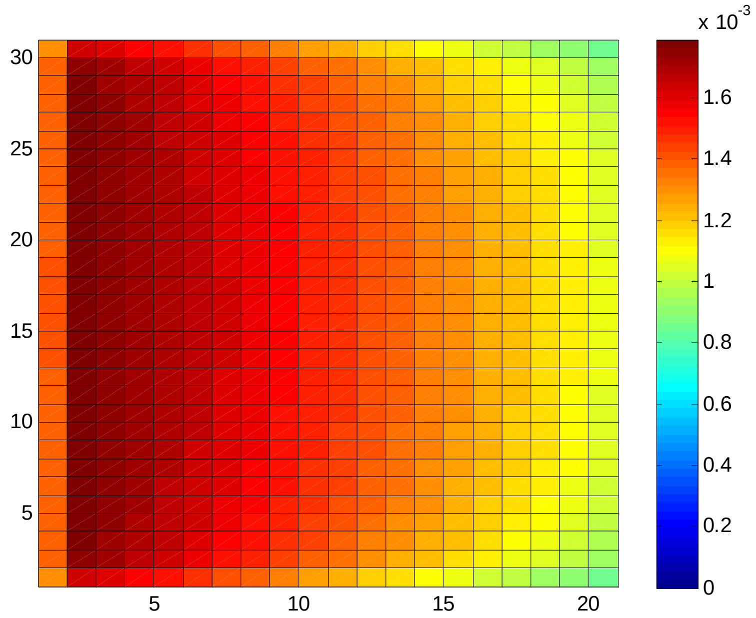


Figure 5.2.2: Energy Deposition Map (MeV) for Water Phantom with 1cm x 1cm coarse meshes for Incident Beam of 2 MeV

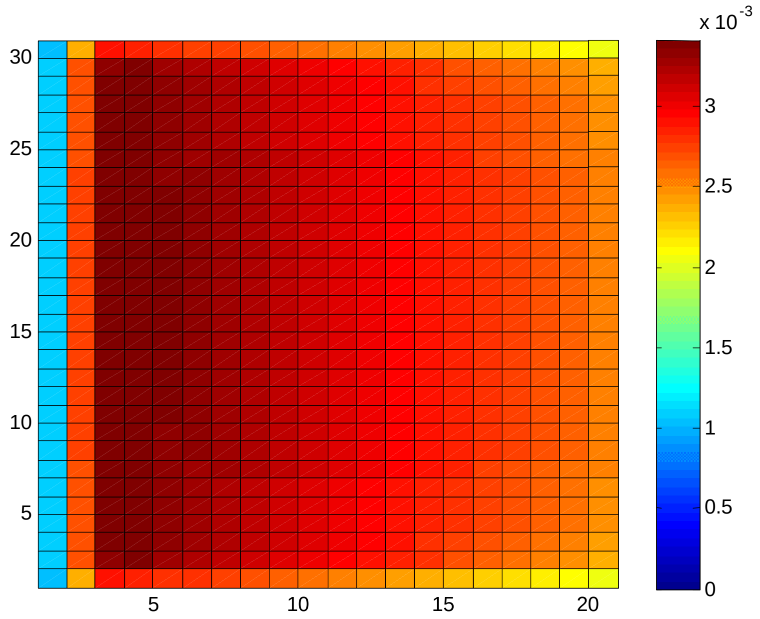


Figure 5.2.3: Energy Deposition Map (MeV) for Water Phantom with 1cm x 1cm coarse meshes for Incident Beam of 6 MeV

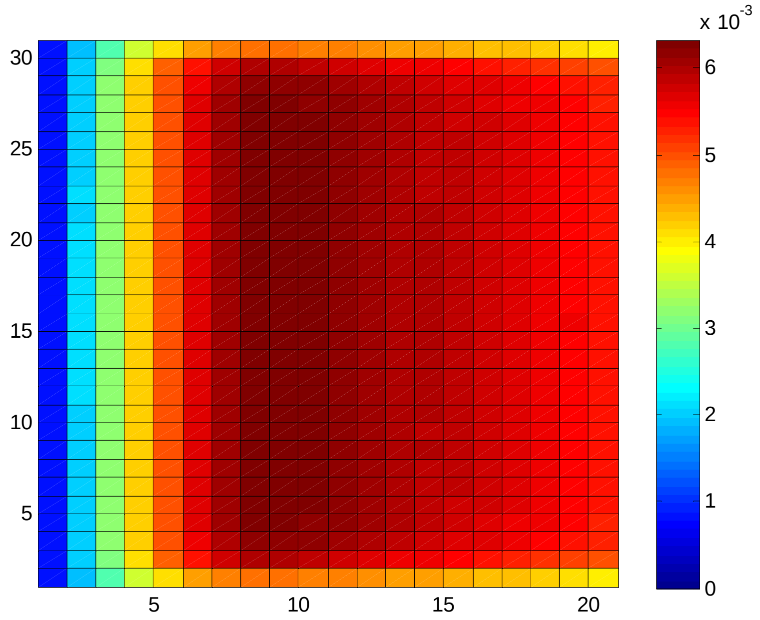


Figure 5.2.4: Energy Deposition Map (MeV) for Water Phantom with 1cm x 1cm coarse meshes for Incident Beam of 18 MeV

The comparison of the COMET solution and reference solution for each energy beam is shown below in Table 5.1.1. The statistics for the COMET solutions and the reference solutions themselves along with the computational times are shown in Table 5.1.2. It can be seen that the maximum percent difference and the average percent difference are best for the lower energy beams. The results are actually quite good for the 2 MeV and the 6 MeV beams. The maximum for the 2 MeV lies below 1 % and the average is 0.19 %. The RMS value was found to be 0.23 %. For the 6 MeV case, the maximum percent difference is only 1.26 %, while the average is still quite low at 0.50%. For this case, the RMS value was 0.54%. The values obtained for the 18 MeV case are not quite as good with a maximum percent difference of 7.24 %, an average percent difference of 0.9 %, and an RMS value of 1.76%. When comparing computational time, the COMET solutions for all three energies required around 8.4 minutes, while the EGSnrc reference solutions required around 202 hours for the 2 MeV case, 300 hours for the 6 MeV case, and 440 hours for the 18 MeV case. The COMET solution is substantially faster than the pure Monte Carlo results.

Table 5.2.1: Comparison Chart for Water Phantom with 1cm x 1cm Coarse Meshes

| | COMPARISON For 2 MeV Incident Beam | COMPARISON For 6 MeV Incident Beam | COMPARISON For 18 MeV Incident Beam |
|---|---|---|---|
| Max % Difference | 0.89 % | 1.26 % | 7.24 % |
| St. Dev. Of Max % Diff | 0.11 % | 0.19 % | 0.18 % |
| Avg % Difference | 0.19 % | 0.50 % | 0.90 % |
| St. Dev. Of Avg % Diff | 0.14 % | 0.20 % | 1.51 % |
| RMS | 0.23 % | 0.54 % | 1.76 % |

Table 5.2.2: Reference and COMET Solution Statistics and Computational Times for Water Phantom with 1cm x 1cm Coarse Meshes\

| | 2 MeV Incident Beam | | 6 MeV Incident Beam | | 18 MeV Incident Beam | |
|---|---|---|---|---|---|---|
| | Reference Solution | COMET Solution | Reference Solution | COMET Solution | Reference Solution | COMET Solution |
| Max Rel Std. Dev. | 0.034 % | 0.12 % | 0.040 % | 0.19 % | 0.049 % | 0.29 % |
| Avg Rel Std. Dev. | 0.026 % | 0.10 % | 0.026 % | 0.09 % | 0.022 % | 0.11 % |
| Comp Time | 202 hours | 8.4 min | 300 hours | 8.4 min | 440 hours | 8.4 min |

In Figure 5.2.5, the percent difference is shown for the 2 MeV incident energy case. It can be seen that the maximum percent error occurs at the end furthest from the incident photon beam in the corners. If we look back at the energy deposition plot for this energy in Figure 5.2.2, it can be seen that this is the region with the smallest energy deposition. Thus, it is more understandable that our difference will be higher since when obtaining our percent difference, the absolute difference between the COMET and reference solution energy depositions is divided by the reference solution's value for energy deposition. Thus, in this location, there is a division by a small number, which results in a higher value.

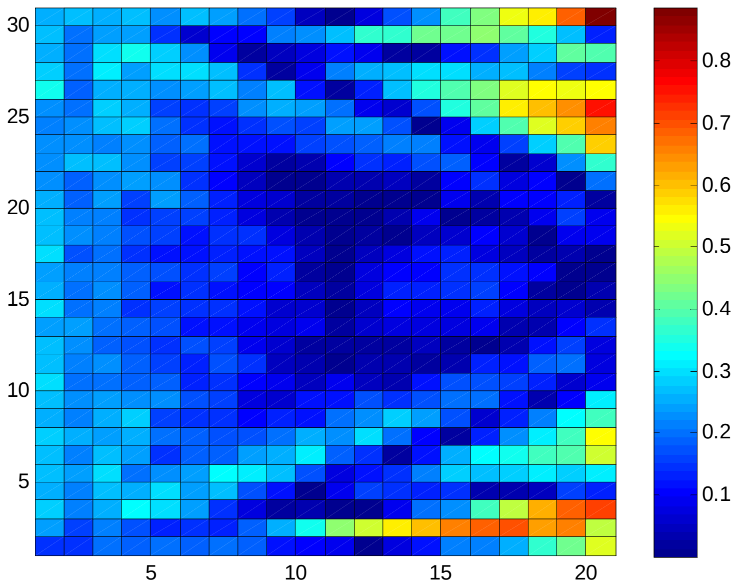


Figure 5.2.5: Percent Difference Between COMET and Reference Solutions for Water Phantom with 1cm x 1cm coarse meshes for Incident Beam of 2 MeV

Below in Figure 5.2.6, the percent difference for the incident 6 MeV beam is shown. You can see that the highest percent difference occurs at the surface of the phantom closest to the incident beam. As with the 2 MeV case, this largest error does occur in the region with the lowest energy deposition.

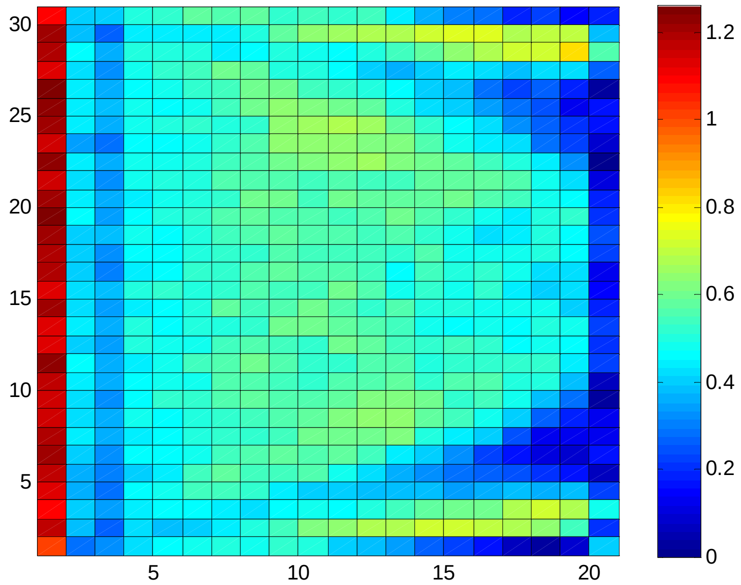


Figure 5.2.6: Percent Difference Between COMET and Reference Solutions for Water Phantom with 1cm x 1cm coarse meshes for Incident Beam of 6 MeV

Below in Figure 5.2.7, the percent difference for the incident 18 MeV beam is plotted. The difference plot here looks slightly different from what is expected. As with the 6 MeV beam, the maximum error occurred in the region with the least amount of energy deposition. Here the maximum error occurs between one and two cm from the surface source rather than directly on the surface source. The problem most likely results from the secondary electrons produced by the high-energy photons. The angle and energy of these electrons is extremely correlated, thus the low expansion coefficients are not accurately describing this situation.

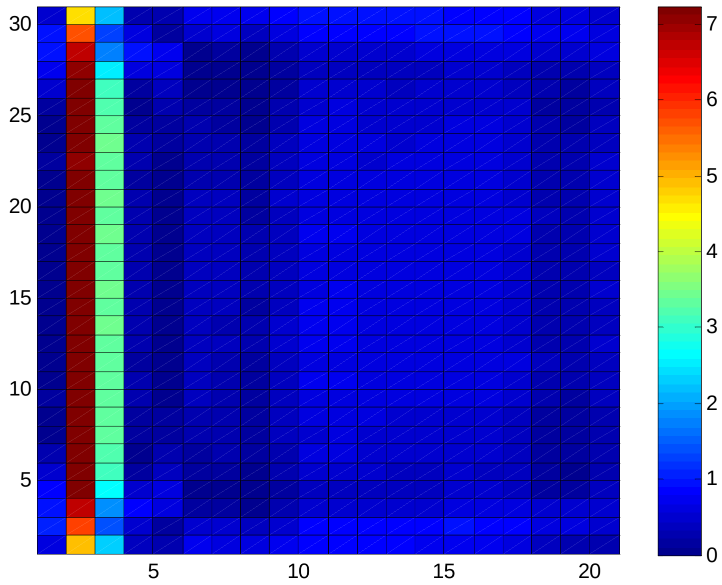


Figure 5.2.7: Percent Difference Between COMET and Reference Solutions for Water Phantom with 1cm x 1cm coarse meshes for Incident Beam of 18 MeV

<u>Mesh Size: 0.5 cm x 0.5 cm</u>

The water phantom composed of 0.5 cm x 0.5 cm meshes is shown below in Figure 5.2.8. Three response function libraries were needed – one for each incident beam energy. Each of these response functions required around 42 hours to calculate.

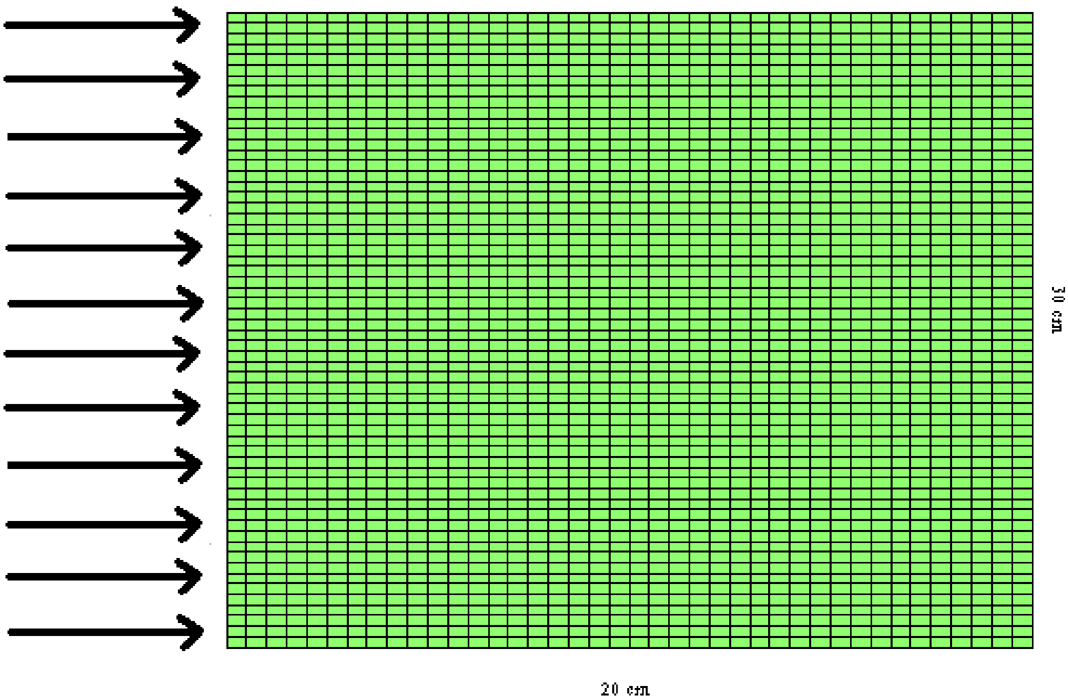


Figure 5.2.8: Water Phantom with 0.5cm x 0.5cm Coarse-Meshes
Green: Water

For each of the incident beam energies, the energy deposition plots are shown below in Figures 5.2.9, 5.2.10, and 5.2.11 for the 2 MeV, 6 MeV, and 18 MeV beam respectively. The pattern of energy deposition follows what was shown earlier for the same benchmark with mesh sizes 1cm x 1cm. As the incident beam energy increases, the location of maximum energy deposition occurs deeper within the phantom.

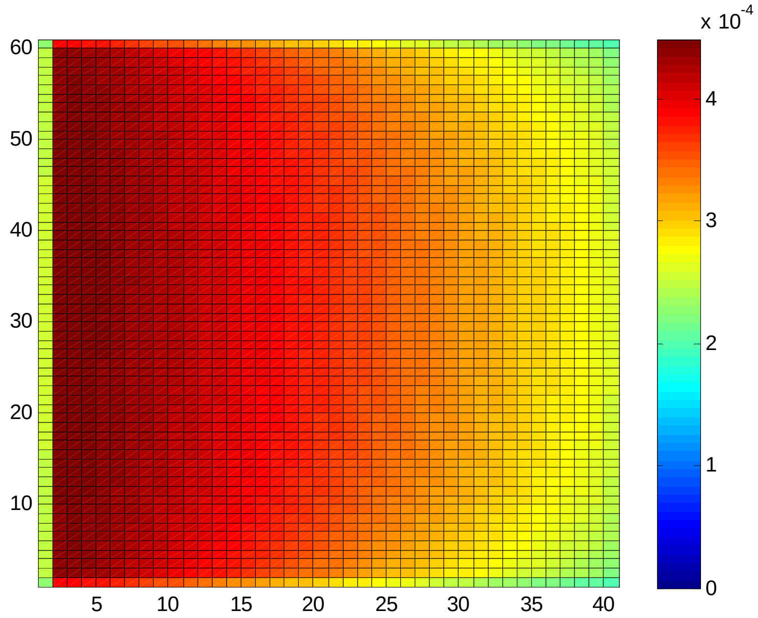


Figure 5.2.9: Energy Deposition Map (MeV) for Water Phantom with 0.5cm x 0.5cm coarse meshes for Incident Beam of 2 MeV

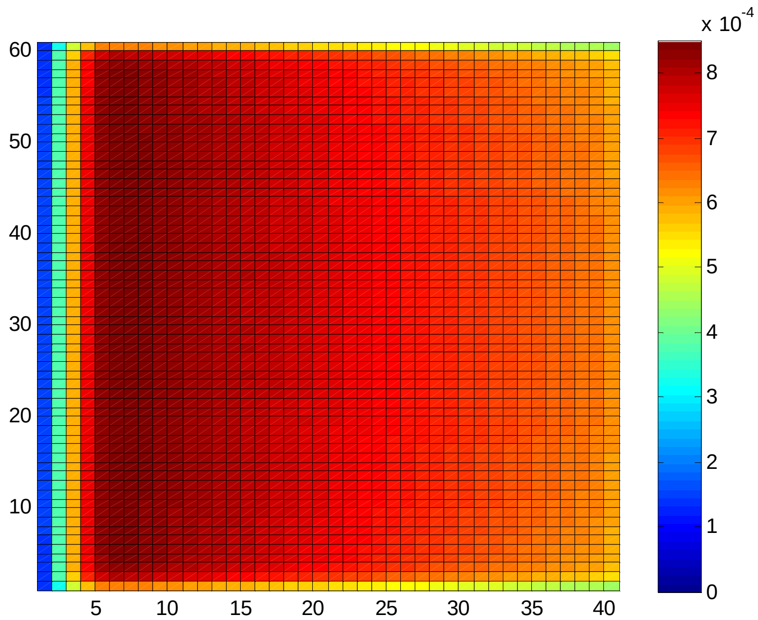


Figure 5.2.10: Energy Deposition Map (MeV) for Water Phantom with 0.5cm x 0.5cm coarse meshes for Incident Beam of 6 MeV

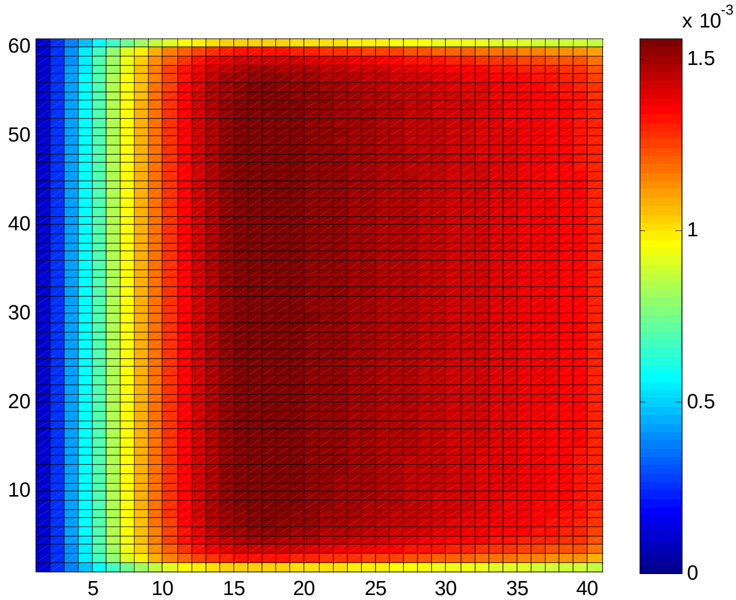


Figure 5.2.11: Energy Deposition Map (MeV) for Water Phantom with 0.5cm x 0.5cm coarse meshes for Incident Beam of 18 MeV

The comparison of the COMET solution and reference solution for each energy beam is shown below in Table 5.1.3. The statistics for the COMET solutions and the reference solutions themselves along with the computational times are shown in Table 5.1.4. It can be seen that the maximum percent difference and the average percent difference are best for the lower energy beams. These values are however not quite as good as those obtained for the 1cm x 1cm mesh case presented earlier. For the 2 MeV case, the maximum percent difference is around 1.23 %, while the average percent difference and RMS were 0.23 % and 0.30% respectively. For the 6 MeV case, the maximum percent difference and the average percent difference was found to be 3.13 % and 0.59 % respectively. The RMS value was found to be 0.72 %. The values are once again not nearly as good for the 18 MeV case. The maximum percent difference obtained was 13.16 %, and the average percent difference was 1.60 %. The RMS value was higher at 3.30 %. When comparing computational time, the COMET solutions for all three energies required between 34 and 44 minutes, while the EGSnrc reference solutions required around 385 hours for the 2 MeV case, 556 hours for the 6 MeV case, and 804 hours for the 18 MeV case. The COMET solution is substantially faster than the pure Monte Carlo results.

Table 5.2.3: Comparison Chart for Water Phantom with 0.5cm x 0.5cm Coarse Meshes

| | COMPARISON For 2 MeV Incident Beam | COMPARISON For 6 MeV Incident Beam | COMPARISON For 18 MeV Incident Beam |
|---|---|---|---|
| Max % Difference | 1.23 % | 3.13 % | 13.16 % |
| St. Dev. Of Max % Difference | 0.14 % | 0.29 % | 0.25 % |
| Avg % Difference | 0.23 % | 0.59 % | 1.60 % |
| St. Dev. Of Avg % Diff | 0.19 % | 0.43 % | 2.89 % |
| RMS | 0.30 % | 0.72 % | 3.30 % |

Table 5.2.4: Reference and COMET Solution Statistics and Computational Times for Water Phantom with 0.5cm x 0.5cm Coarse Meshes

| | 2 MeV Incident Beam | | 6 MeV Incident Beam | | 18 MeV Incident Beam | |
|---|---|---|---|---|---|---|
| | Reference Solution | COMET Solution | Reference Solution | COMET Solution | Reference Solution | COMET Solution |
| Max Rel Std. Dev. | 0.063 % | 0.17 % | 0.079 % | 0.28 % | 0.098 % | 0.42 % |
| Avg Rel Std. Dev. | 0.047 % | 0.12 % | 0.039 % | 0.091 % | 0.032 % | 0.12 % |
| Comp Time | 385 hours | 34.5min | 556 hours | 44.1min | 808 hours | 41.1 min |

Once again to determine the actual location of the error, the plots of the percent difference for each energy are shown below. As with the previous cases with the 1cm x 1cm meshes, it can be seen that the error plots follow the same patterns for each energy case. Here however, the values are larger than before. Even though a smaller size mesh reveals more detailed results, in this case it is the cause for the higher error. With smaller meshes, electrons may travel through the mesh entirely, depositing energy along the way. Because of this, the energy expansion coefficient may not be correctly modeling this.

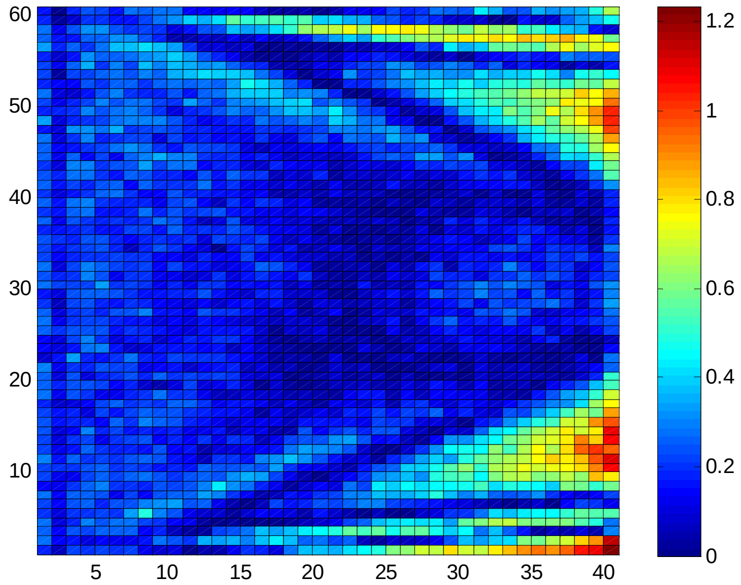


Figure 5.2.12: Percent Difference Between COMET and Reference Solutions for Water Phantom with 0.5cm x 0.5cm coarse meshes for Incident Beam of 2 MeV

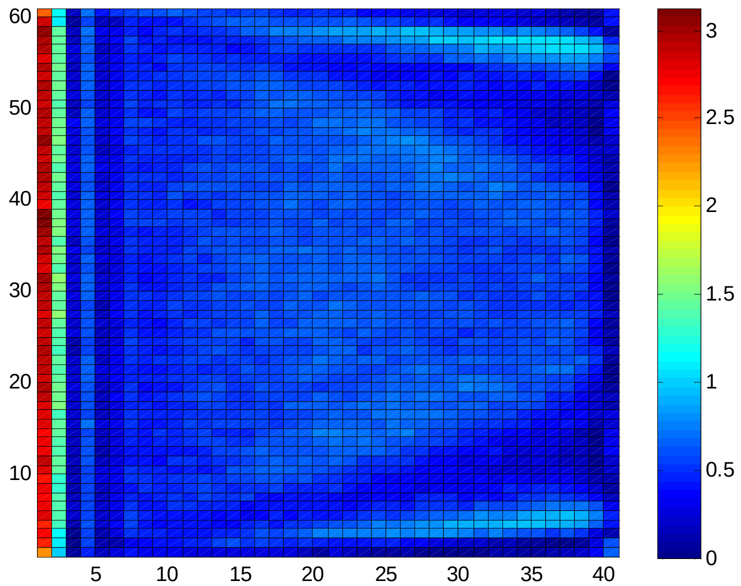


Figure 5.2.13: Percent Difference Between COMET and Reference Solutions for Water Phantom with 0.5cm x 0.5cm coarse meshes for Incident Beam of 6 MeV

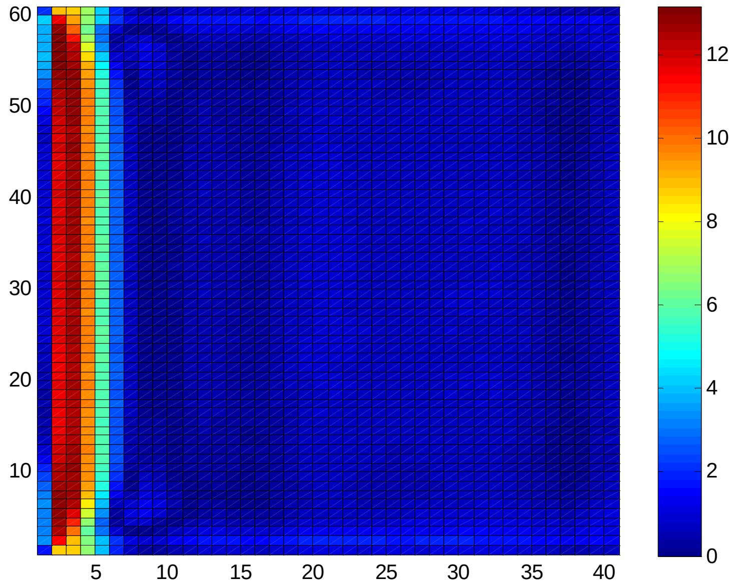


Figure 5.2.14: Percent Difference Between COMET and Reference Solutions for Water Phantom with 0.5cm x 0.5cm coarse meshes for Incident Beam of 18 MeV

**Simplified Lung Phantom**

Mesh Size: 1 cm x 1 cm

A simplified lung phantom composed of 1 cm x 1 cm meshes was used for testing the methodology. It was composed of three materials – tissue, bone, and lung. It is shown below in Figure 5.2.15. Nine response function libraries were needed – one for each of the three material definitions with each of the three incident energies. Each of these response functions required around 42 hours to calculate. So for each incident energy case, 126 hours was needed to calculate the response function library for that energy and the three materials.

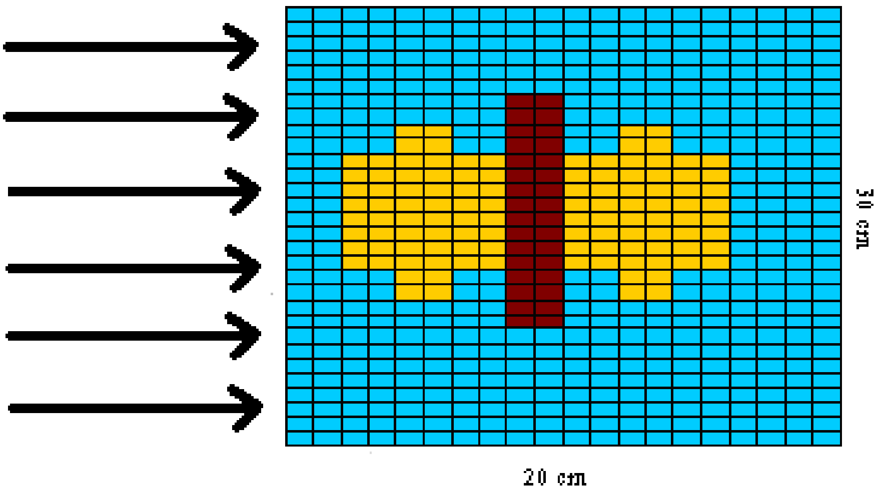


Figure 5.2.15: Simplified Lung Phantom with 1cm x 1cm Coarse-Meshes
Blue: Tissue/Water
Red: Bone
Yellow: Lung Tissue

The energy deposition for each incident beam energy is shown in the next three figures. The energy deposition plots look quite similar to those obtained for just the water phantom except the higher energy deposition in the spinal column region. The energy deposition within the lung tissue is similar to that of tissue/water since a lung tissue definition was used rather than inflated lung.

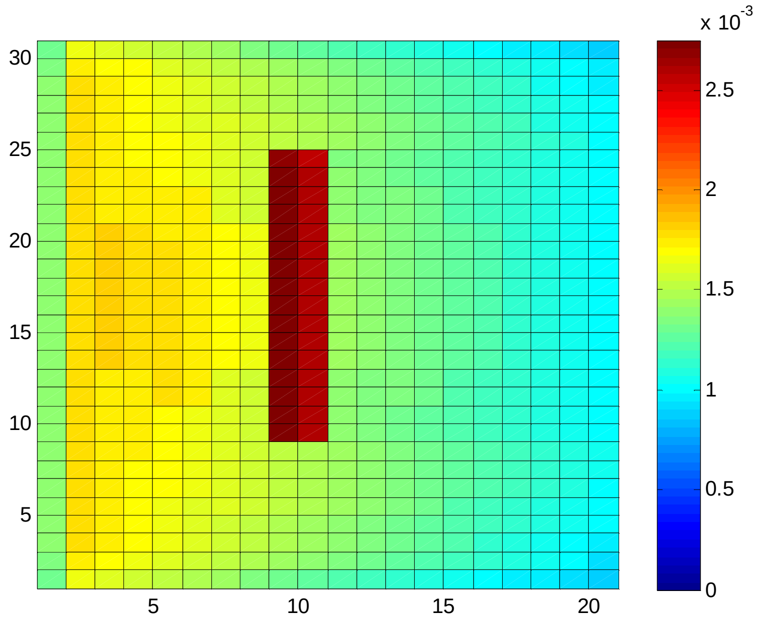


Figure 5.2.16: Energy Deposition (MeV) for Simplified Lung Phantom with 1cm x 1cm coarse meshes for Incident Beam of 2 MeV

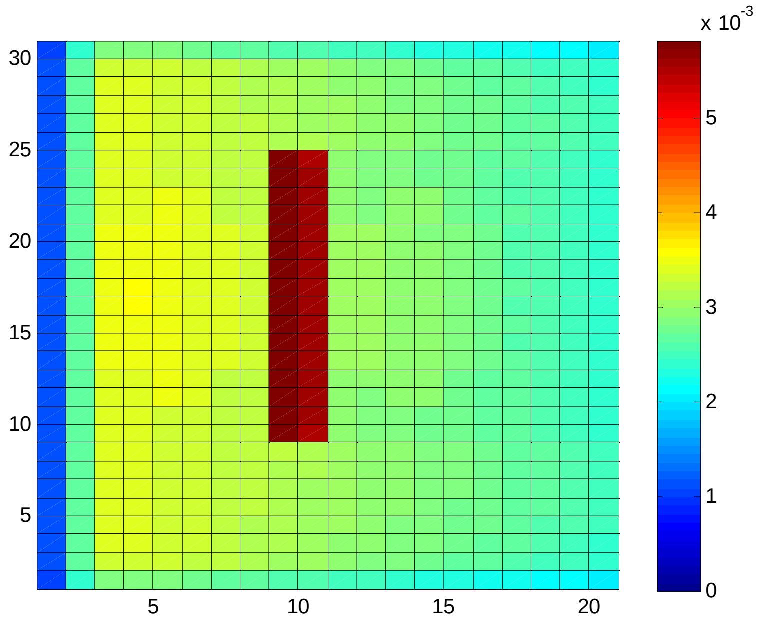


Figure 5.2.17: Energy Deposition (MeV) for Simplified Lung Phantom with 1cm x 1cm coarse meshes for Incident Beam of 6 MeV

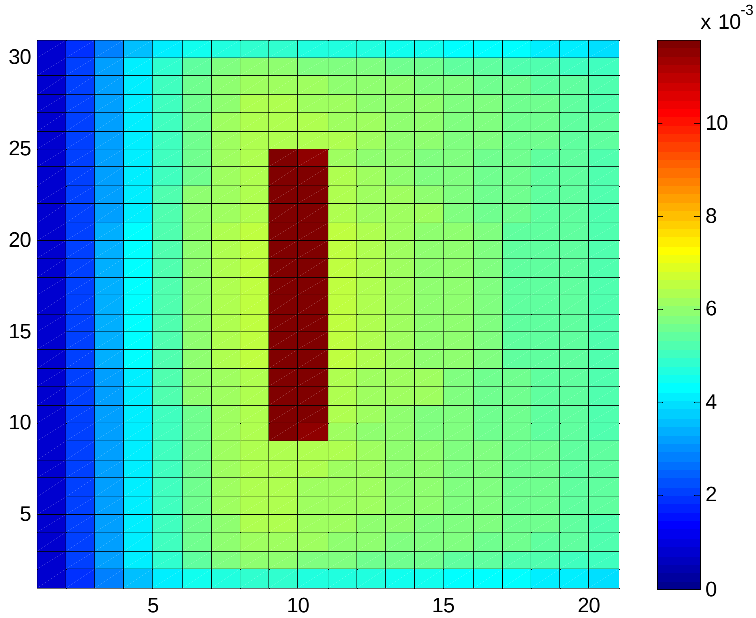


Figure 5.2.18: Energy Deposition (MeV) for Simplified Lung Phantom with 1cm x 1cm coarse meshes for Incident Beam of 18 MeV

As before, the results obtained are better for the lower energy incident beams. For the 2 MeV beam, a maximum percent difference of 0.78 %, an average percent difference of 0.20 % difference, and an 0.24 % RMS value was found. The COMET solution required 10.6 minutes, while the reference solution found using pure Monte Carlo solutions required around 280 minutes. For the 6 MeV incident beam case, the maximum goes up to 1.22 % and the average value is 0.45 %. The RMS value for this case was 0.49%. The COMET solution required only 8.2 minutes, while the EGSnrc reference case required 480 hours. The heterogeneous case produced results similar to the homogeneous water phantom. As for the 18 MeV case, the maximum percent difference obtained was 7.34 % and an average percent difference was found to be 1.03%. The RMS value obtained for the 18 MeV case was 1.83%. Again, COMET only required just over 8 minutes, while in this case EGSnrc took around 770 hours.

Table 5.2.5: Comparison Chart for Simplified Lung Phantom with 1cm x 1cm Coarse Meshes

| | COMPARISON For 2 MeV Incident Beam | COMPARISON For 6 MeV Incident Beam | COMPARISON For 18 MeV Incident Beam |
|---|---|---|---|
| Max % Difference | 0.78 % | 1.22 % | 7.34 % |
| St. Dev. Of Max % Diff | 0.11 % | 0.19 % | 0.18 % |
| Avg % Difference | 0.20 % | 0.45 % | 1.03 % |
| St. Dev. Of Avg % Diff | 0.14 % | 0.21 % | 1.52 % |
| RMS | 0.24 % | 0.49 % | 1.83 % |

Table 5.2.6: Reference and COMET Solution Statistics and Computational Times for Simplified Lung Phantom with 1cm x 1cm Coarse Meshes

| | 2 MeV Incident Beam | | 6 MeV Incident Beam | | 18 MeV Incident Beam | |
|---|---|---|---|---|---|---|
| | Reference Solution | COMET Solution | Reference Solution | COMET Solution | Reference Solution | COMET Solution |
| Max Rel Std. Dev. | 0.034 % | 0.12 % | 0.040 % | 0.19 % | 0.049 % | 0.30 % |
| Avg Rel Std. Dev. | 0.026 % | 0.098 % | 0.026 % | 0.096 % | 0.022 % | 0.11 % |
| CompTime | 280 hours | 10.6min | 480 hours | 8.2 min | 770 hours | 8.3 min |

The plots for percent difference are shown below in the next three figures. The results are quite similar as those obtained for the water phantom. In Figure 5.2.19, the outline of the lungs and spinal column can be seen. These locations were actually some of the areas that were handled the most correctly by the method. There was very little discrepancy between the COMET and reference solution. For this energy level, the maximum percent difference occurs in the corners furthest from the incident beam just as with the water phantom.

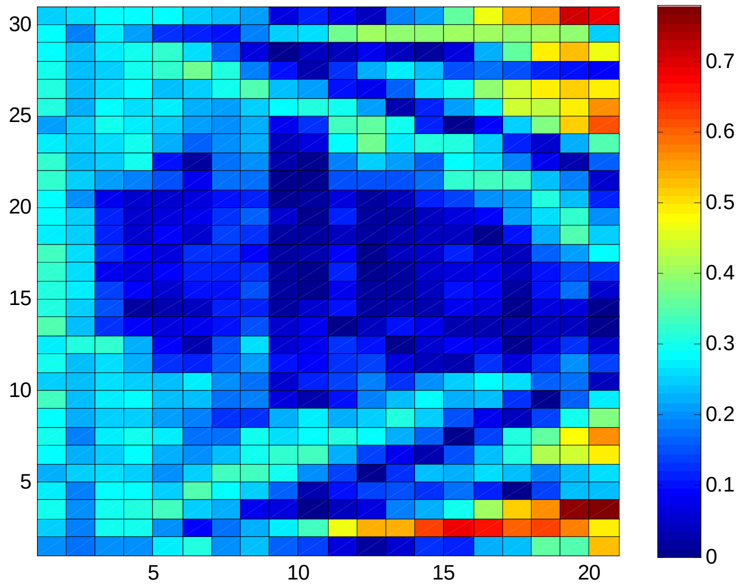


Figure 5.2.19: Percent Difference Between COMET and Reference Solutions for Simplified Lung Phantom with 1cm x 1cm coarse meshes for Incident Beam of 6 MeV

For the 6 MeV percent difference plot, yet again the plot looks very similar to that of the 1cm x 1cm water plot. The maximal discrepancy occurs at the surface where the beam is incident. Again, the outline of the lungs and spine can be made out in the image below. It can be seen that the relative error in these regions is still very low.

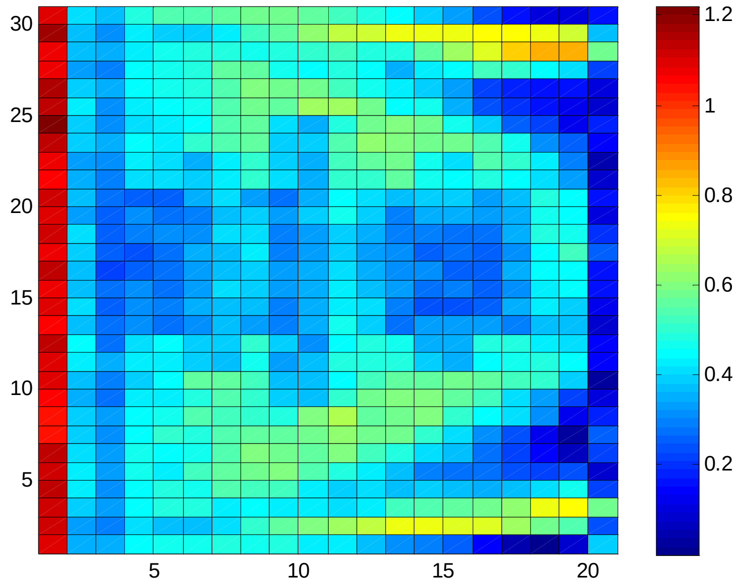


Figure 5.2.20: Percent Difference Between COMET and Reference Solutions for Simplified Lung Phantom with 1cm x 1cm coarse meshes for Incident Beam of 6 MeV

For the 18 MeV incident beam case, the results are yet again similar to those of the water phantom. The maximal error occurs around the 1 cm mark within the phantom, while the region directly adjacent to the surface source is much lower. In this case as well, the discrepancy between the COMET and reference solution is slightly larger in the spinal cord region. The error that occurs closer to the surface is only again due to the inability to correctly model the secondary electrons.

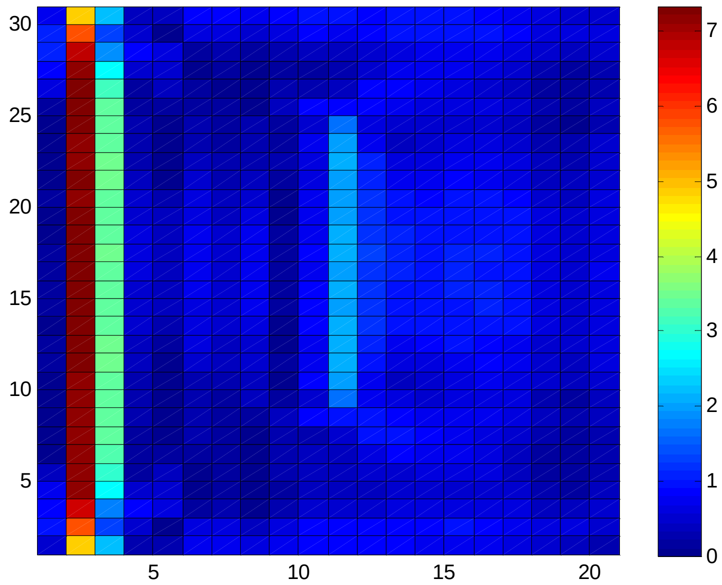


Figure 5.2.21: Percent Difference Between COMET and Reference Solutions for Simplified Lung Phantom with 1cm x 1cm coarse meshes for Incident Beam of 18 MeV

Mesh Size: 0.5 cm x 0.5 cm

As before with the water phantom, the lung phantom was further divided into smaller mesh sizes. Again, three material definitions were used – tissue, bone, and lung. In Figure 5.1.22, the new lung phantom composed of 0.5cm x 0.5cm coarse meshes is shown. Nine response function libraries were needed – one for each of the three material definitions with each of the three incident energies. Each of these response functions required around 42 hours to calculate. So for each incident energy case, 126 hours was needed to calculate the response function library for that energy and the three materials.

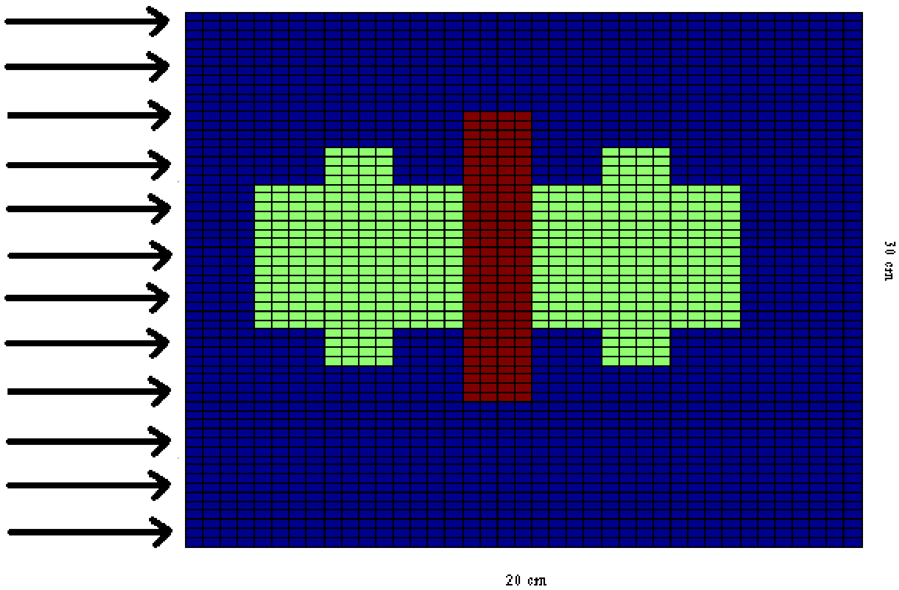


Figure 5.2.22: Simplified Lung Phantom of 0.5cm x 0.5cm coarse meshes
Blue: Tissue/Water
Red: Bone
Green: Lung

The plots of the energy deposition for the three incident photon energies are shown below in the next three figures. They again show the same pattern of energy deposition as with the lung phantom with meshes of 1cm x 1cm size. With a smaller mesh size, more detail can be obtained for the energy deposition map.

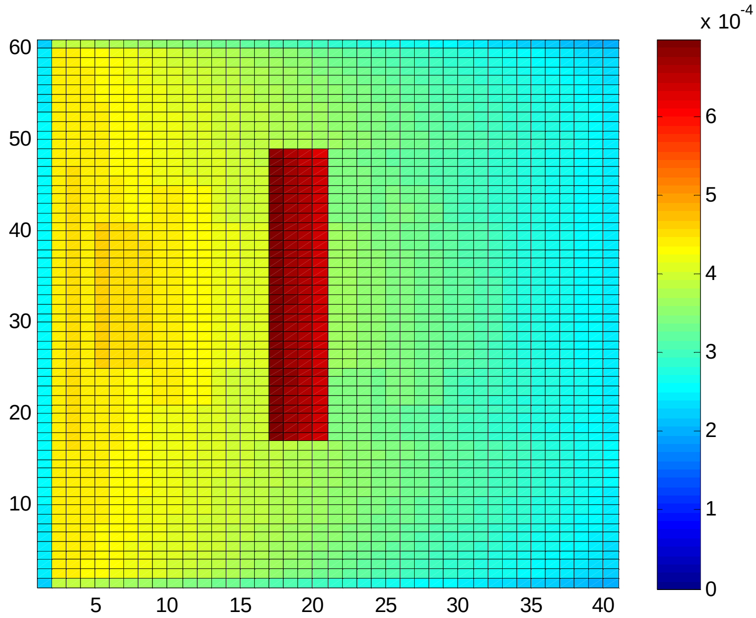


Figure 5.2.23: Energy Deposition Map (MeV) for Simplified Lung Phantom with 0.5cm x 0.5cm coarse meshes for Incident Beam of 2 MeV

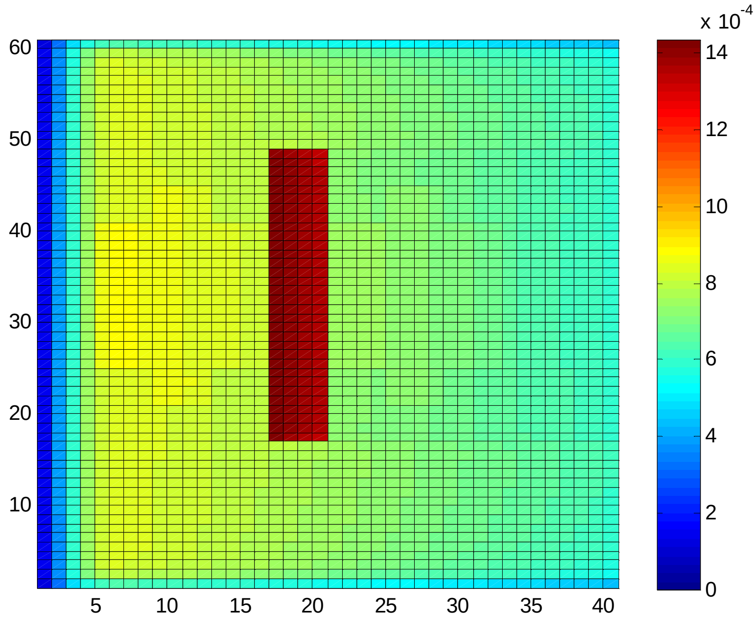


Figure 5.2.24: Energy Deposition Map (MeV) for Simplified Lung Phantom with 0.5cm x 0.5cm coarse meshes for Incident Beam of 6 MeV

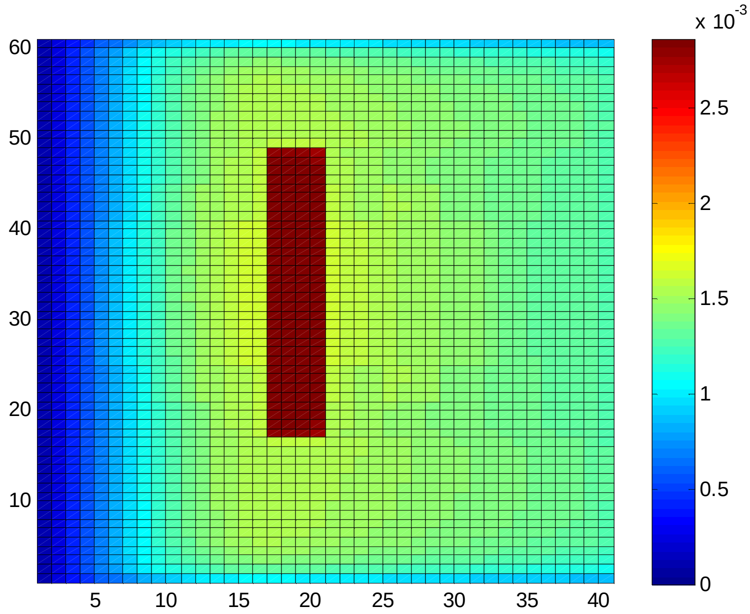


Figure 5.2.25: Energy Deposition Map (MeV) for Simplified Lung Phantom with 0.5cm x 0.5cm coarse meshes for Incident Beam of 18 MeV

Below in Table 5.1.7 and 5.1.8, the comparison and statistical data for the smaller mesh simplified lung phantom is shown. The values obtained are very similar to those found for the water only phantom. The inclusion of heterogeneities does not seem to have much influence on this problem. For the 2 MeV beam, the maximum percent difference was found to be around 1.49 % with an average percent difference of 0.22 % and an RMS value of 0.30%. The values for the 6 MeV case increase as was seen with the previous examples. The maximum percent difference was found to be 3.21 % and the average percent difference was 0.56 %. A value of 0.71% was found for the RMS value. Once again, the 18 MeV incident beam resulted in the highest percent differences. For the maximal value, 13.13% was calculated, and 1.60 % for the average percent difference was found. A value of 3.31% was obtained for the RMS value. For the smaller mesh size, both the COMET and reference calculations required more time. For the 2 MeV case, COMET required 34 minutes as compared to 480 hours for the reference case. For the 6 MeV incident energy, 42.5 minutes were required for the COMET solution and 721 hours for the reference calculation. Lastly, for the 18 MeV case, 32.4 minutes of computational time was required for the COMET solution and 812 hours for the reference solution.

Table 5.2.7: Comparison Chart for Simplified Lung Phantom with 0.5cm x 0.5cm Coarse Meshes

| | COMPARISON For 2 MeV Incident Beam | COMPARISON For 6 MeV Incident Beam | COMPARISON For 18 MeV Incident Beam |
|---|---|---|---|
| Max % Difference | 1.49 % | 3.21 % | 13.13 % |
| St. Dev. Of Max % Diff | 0.14 % | 0.28 % | 0.26 % |
| Avg % Difference | 0.22 % | 0.56 % | 1.60 % |
| St. Dev. Of Avg % Diff | 0.20 % | 0.44 % | 2.90 % |
| RMS | 0.30 % | 0.71 % | 3.31 % |

Table 5.2.8: Reference and COMET Solution Statistics and Computational Times for Simplified Lung Phantom with 0.5cm x 0.5cm Coarse Meshes

| | 2 MeV Incident Beam | | 6 MeV Incident Beam | | 18 MeV Incident Beam | |
|---|---|---|---|---|---|---|
| | Reference Solution | COMET Solution | Reference Solution | COMET Solution | Reference Solution | COMET Solution |
| Max RelStd. Dev. | 0.063 % | 0.17 % | 0.079 % | 0.28 % | 0.10 % | 0.43 % |
| Avg Rel Std. Dev. | 0.047 % | 0.12 % | 0.039 % | 0.092 % | 0.032 % | 0.12 % |
| Comp Time | 480 hours | 34.0min | 721 hours | 42.5min | 812 hours | 32.4min |

Below in the next three figures, the percent difference plots are shown for each of the three incident energies. The same pattern of discrepancy between the reference and COMET solutions is seen here as with the simplified lung phantom with the 1cm x 1cm coarse meshes. The errors are once again higher for the smaller coarse mesh phantoms due to the partial deposition of energy within each coarse mesh and the expansion order incorrectly handling this.

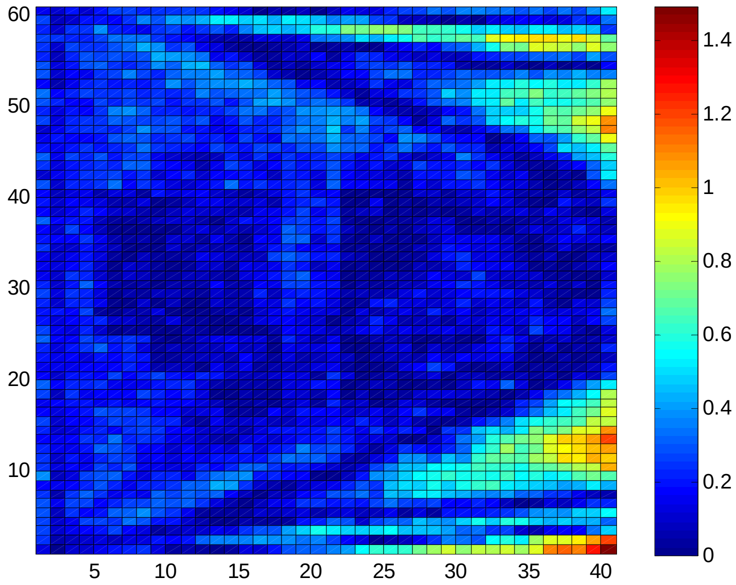


Figure 5.2.26: Percent Difference Between COMET and Reference Solutions for Simplified Lung Phantom with 0.5cm x 0.5cm coarse meshes for Incident Beam of 2 MeV

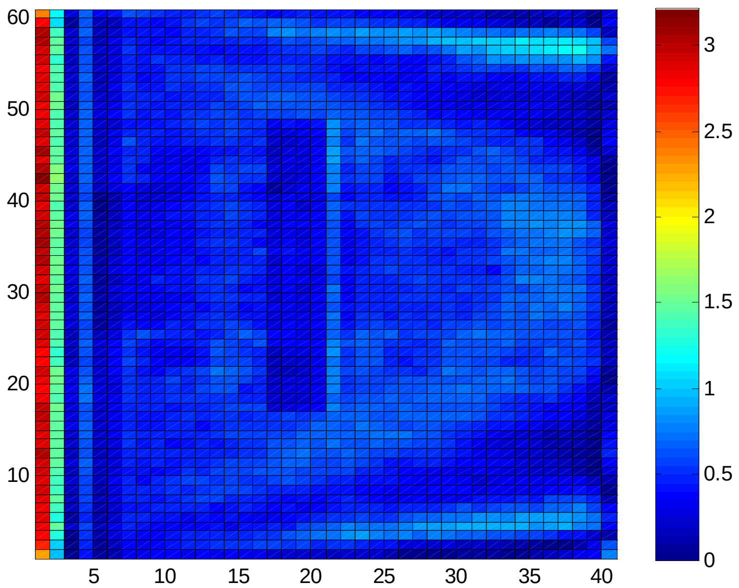


Figure 5.2.27: Percent Difference Between COMET and Reference Solutions for Simplified Lung Phantom with 0.5cm x 0.5cm coarse meshes for Incident Beam of 6 MeV

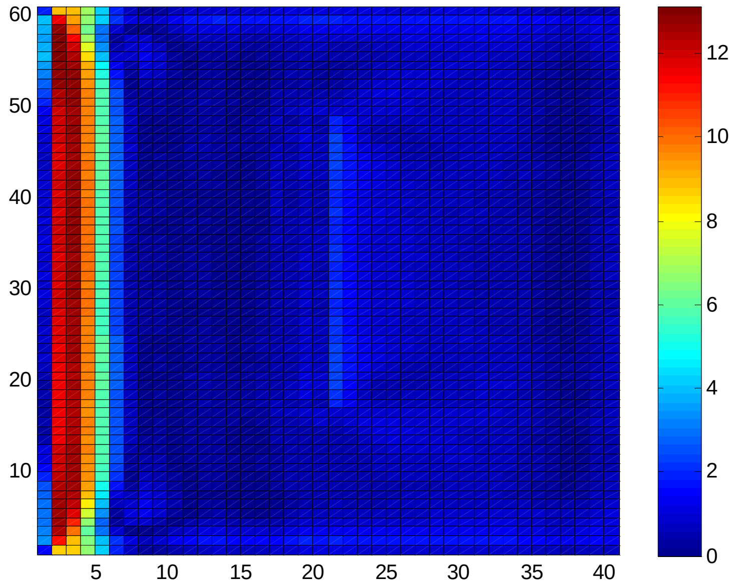


Figure 5.2.28: Percent Difference Between COMET and Reference Solutions for Simplified Lung Phantom with 0.5cm x 0.5cm coarse meshes for Incident Beam of 18 MeV

**Non-Clinical Slab Phantom**

This non-clinical slab phantom originally described by Rogers and Mohan is composed of three materials – water, lung tissue and aluminum.[30] This phantom is not meant to represent any portion of the body, but it is however meant to place stress on the system. For this case, there is a 3 cm portion of water followed by a 2 cm slab region of aluminum. Next is a 5 cm portion of lung tissue followed finally by a 20 cm region of water.

**Mesh Size: 1 cm x 1 cm**

The non-clinical slab phantom composed of 1 cm x 1 cm meshes is shown below in Figure 5.2.29. This phantom is composed of regions of lung tissue, water, and aluminum. Three incident beam energies are once again tested- 2 MeV, 6 MeV, and 18

MeV.  Since three material definitions were used, around 126 hours of pre-computational time was necessary for the response function library generation for each incident energy.

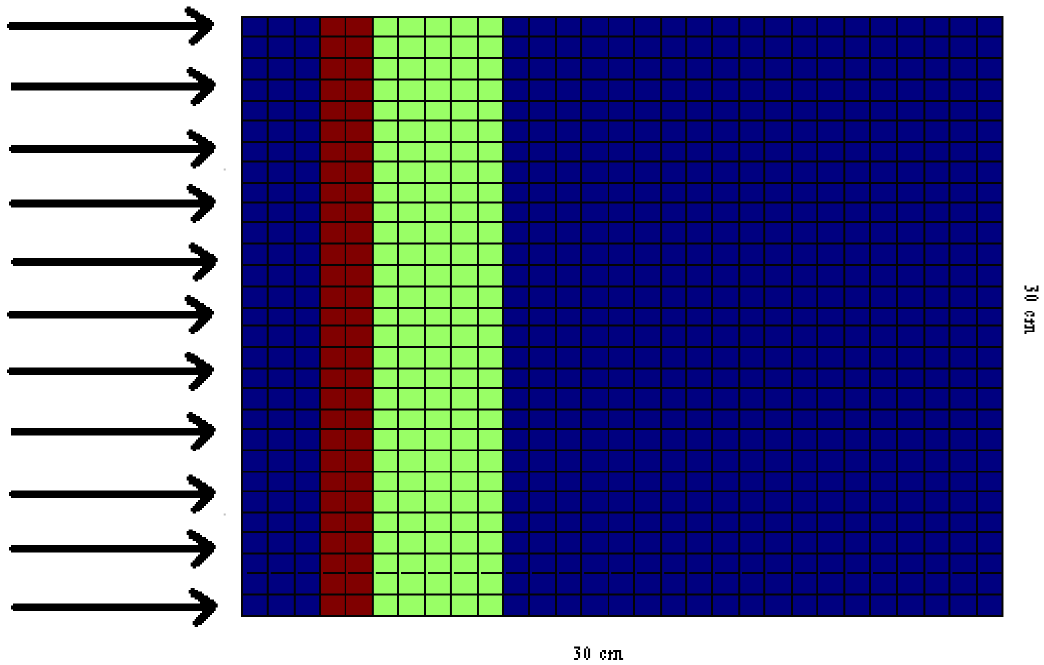


Figure 5.2.29:  Non-Clinical Slab Phantom with 1cm x 1cm Coarse-Meshes
Dark Blue:  Water
Dark Red: Aluminum
Green: Lung

Below in the following three figures, the energy deposition plots are shown for the three incident beam energies tested.  The energy plots show the expected results.  For the 2 MeV case, the least amount of energy is deposited furthest from the incident beam, while the maximum energy deposition occurs within the aluminum region.  For the 6 MeV case, minimal energy deposition occurs in the region closest to the source since the higher energy photons travel deeper within the phantom before interacting and liberating electrons.  The highest energy deposition once again occurs in the aluminum region.  For the 18 MeV case, the minimum energy deposition occurs in a larger portion of the phantom close to the incident photon beam.  Once again, this is due to the higher energy photons traveling further into the phantom before interacting.

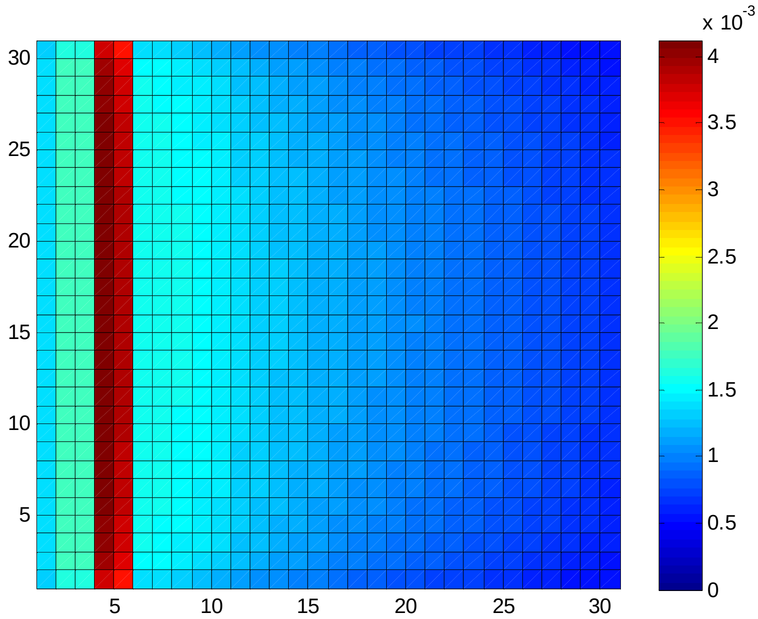


Figure 5.2.30: Energy Deposition (MeV) for Slab Phantom with 1cm x 1cm coarse meshes for Incident Beam of 2 MeV

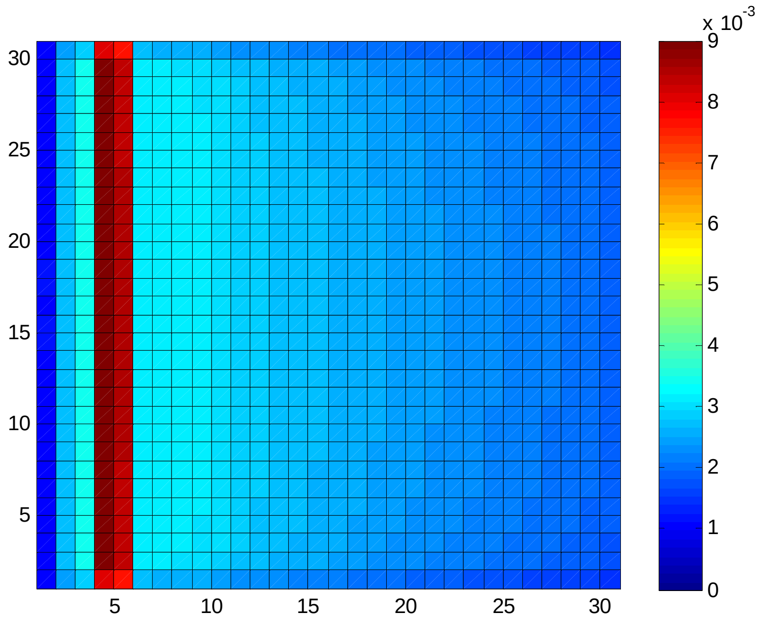


Figure 5.2.31: Energy Deposition (MeV) for Slab Phantom with 1cm x 1cm coarse meshes for Incident Beam of 6 MeV

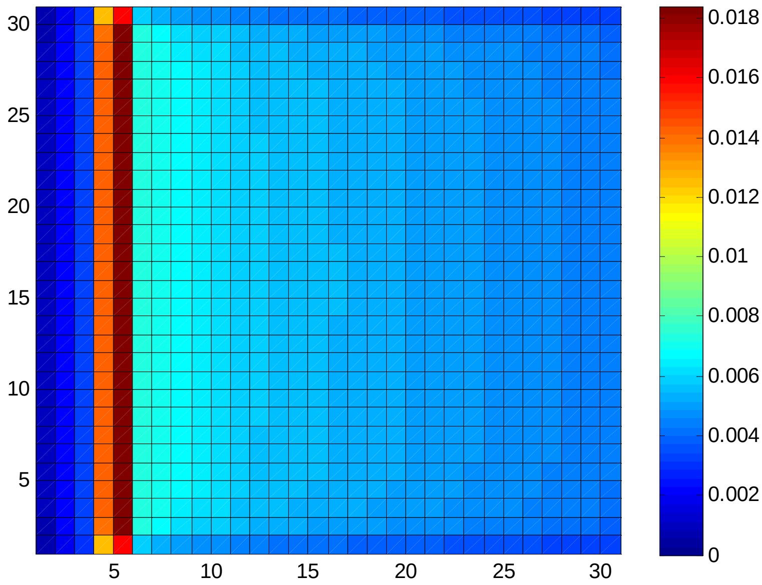


Figure 5.2.32: Energy Deposition (MeV) for Slab Phantom with 1cm x 1cm coarse meshes for Incident Beam of 18 MeV

Below in Tables 5.2.9 and 5.2.10, the results for comparing COMET and the reference solutions are shown. For the 2 MeV and 6 MeV cases, the maximum percent difference is quite good at 1.64% and 1.14% respectively. The average percent differences are also below half a percent for both cases with 0.34% for the 2 MeV case and 0.42% for the 6 MeV case. The RMS values for the 2 MeV and 6 MeV cases were found to be 0.45 % and 0.48 % respectively. The 18 MeV incident beam case produced higher errors with maximum percent difference of 6.68% and an average percent difference of 1.07%. The RMS value was found to be 1.59 %. The computational time required for these COMET calculations was between 10.3 and 14 minutes, while the reference solutions were calculated using EGSnrc in 488 hours for the 2 MeV case, 925 hours for the 6 MeV case, and 1720 hours for the 18 MeV case.

Table 5.2.9: Comparison Chart for Slab Phantom with 1cm x 1cm Coarse Meshes

| | COMPARISON For 2 MeV Incident Beam | COMPARISON For 6 MeV Incident Beam | COMPARISON For 18 MeV Incident Beam |
|---|---|---|---|
| Max % Difference | 1.64 % | 1.14 % | 6.68 % |
| St. Dev. Of Max % Diff | 0.13 % | 0.20 % | 0.20 % |
| Avg % Difference | 0.34 % | 0.42 % | 1.07 % |
| St. Dev. Of Avg % Diff | 0.30 % | 0.24 % | 1.17 % |
| RMS | 0.45 % | 0.48 % | 1.59 % |

Table 5.2.10: Reference and COMET Solution Statistics and Computational Times for Slab Phantom with 1cm x 1cm Coarse Meshes

| | 2 MeV Incident Beam | | 6 MeV Incident Beam | | 18 MeV Incident Beam | |
|---|---|---|---|---|---|---|
| | Reference Solution | COMET Solution | Reference Solution | COMET Solution | Reference Solution | COMET Solution |
| Max Rel Std. Dev. | 0.042 % | 0.13 % | 0.040 % | 0.21 % | 0.049 % | 0.38 % |
| Avg Rel Std. Dev. | 0.028 % | 0.11 % | 0.027 % | 0.11 % | 0.021 % | 0.13 % |
| CompTime | 488 hours | 14.0min | 925 hours | 13.3min | 1720 hours | 10.3min |

Below in Figures 5.2.33, 5.2.34, and 5.2.35, the percent difference plots are shown for each of the three incident beam cases. The error plot shown for the 2 MeV case shows the same pattern as that for the simple water phantom. Maximum percent difference occurs at the region furthest from the incident beam in the corners. This shows that the heterogeneity introduced into the system did not hinder the COMET methodology. For the 6 MeV case, the plot also looks quite similar to that for the water phantom. In this case, it appears that the COMET method actually handled the energy deposition located within the aluminum better than some regions of the pure water phantom. The percent difference plot for the 18 MeV incident beam energy also shows the same type error as with the water phantom. The maximum percent error occurs just past the region directly adjacent to the incident beam as with the previous cases. Again, this is most likely due to the inability of the expansion orders to accurately describe the electrons exiting the mesh surface because of the high correlation between energy and angle.

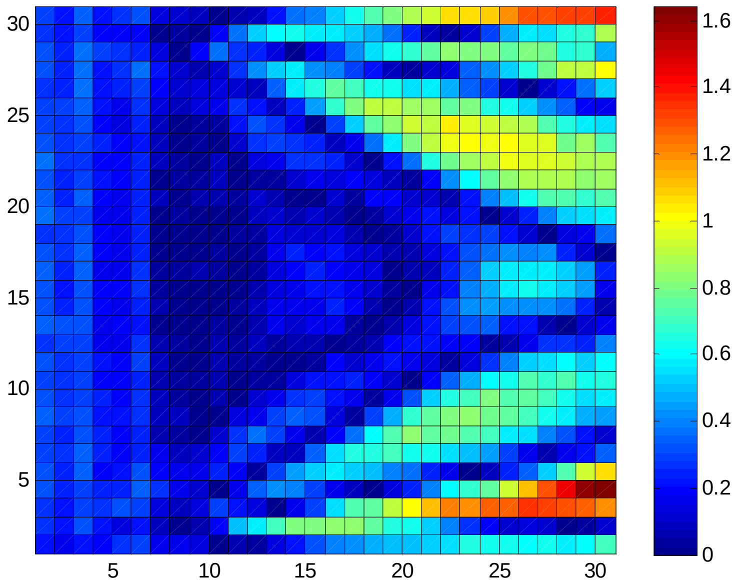


Figure 5.2.33: Percent Difference Between COMET and Reference Solutions for Slab Phantom with 1cm x 1cm coarse meshes for Incident Beam of 2 MeV

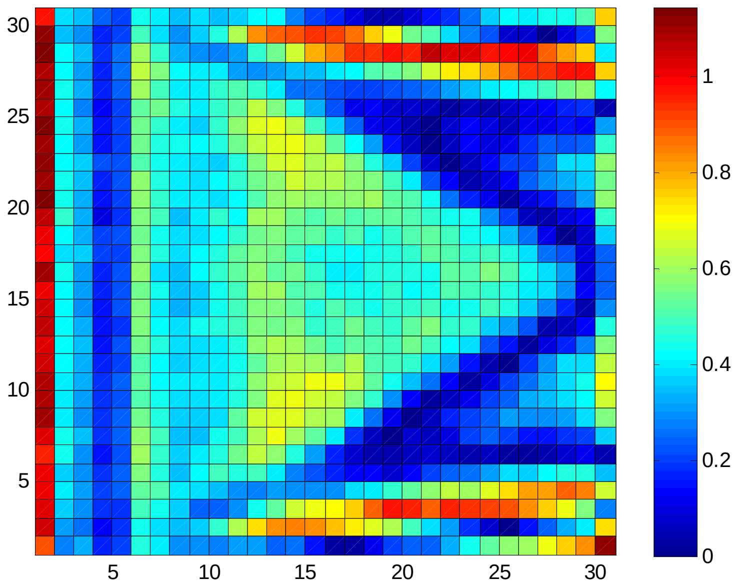


Figure 5.2.34: Percent Difference Between COMET and Reference Solutions for Slab Phantom with 1cm x 1cm coarse meshes for Incident Beam of 6 MeV

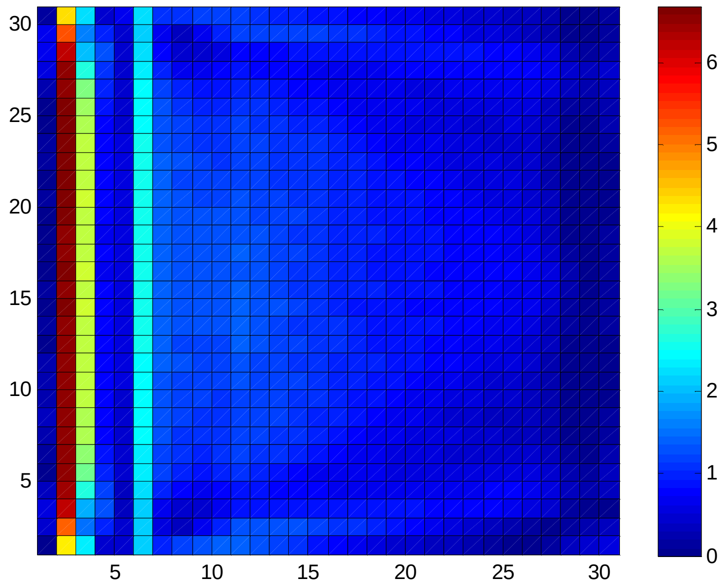


Figure 5.2.35: Percent Difference Between COMET and Reference Solutions for Water Phantom with 1cm x 1cm coarse meshes for Incident Beam of 18 MeV

### Mesh Size: 0.5 cm x 0.5 cm

The non-clinical slab phantom composed of 0.5 cm x 0.5 cm meshes is shown below in Figure 5.2.35. The composition of the phantom is the same as that described for the 1cm x 1cm case. Again three material definitions were used, and around 126 hours of pre-computational time was needed to obtain the response function library for each incident energy.

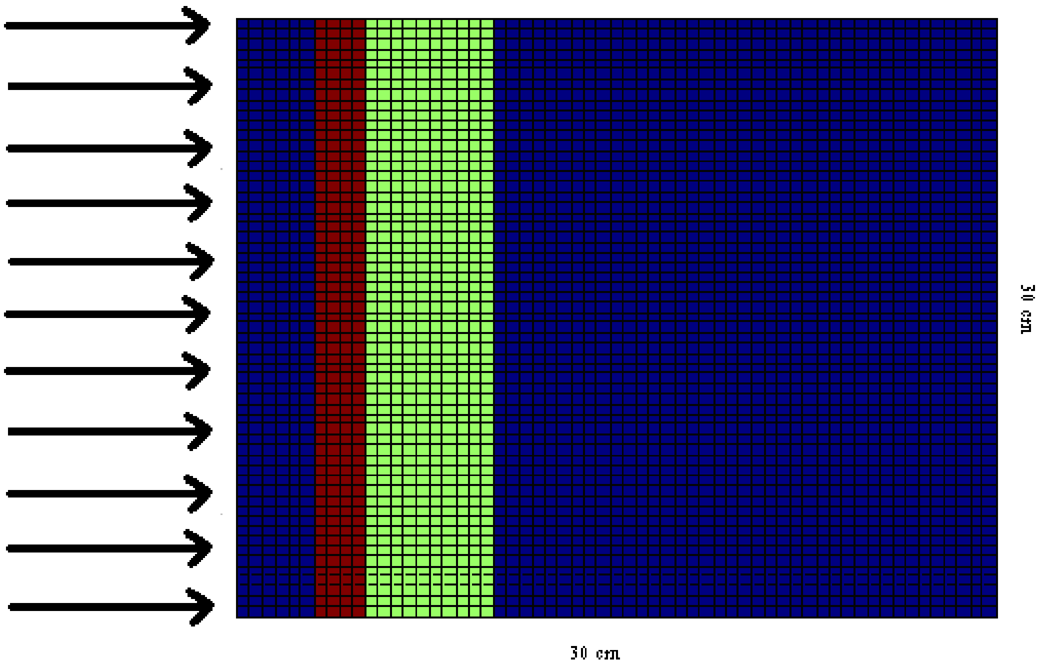


Figure 5.2.36: Non-Clinical Slab Phantom with 0.5cm x 0.5cm Meshes
Dark Blue: Water
Dark Red: Aluminum
Green: Lung

Below in the following three figures, the energy deposition plots are once again shown. The results are the same as with the larger mesh cases. The minimal energy deposition occurs furthest from the beam for the 2 MeV case. For the 6 MeV and 18 MeV cases, the minimum energy deposition occurs closest to the surface upon which the beam was incident due to the higher energy photons traveling deeper within the phantom. For all cases, the maximum energy deposition occurs within the aluminum region.

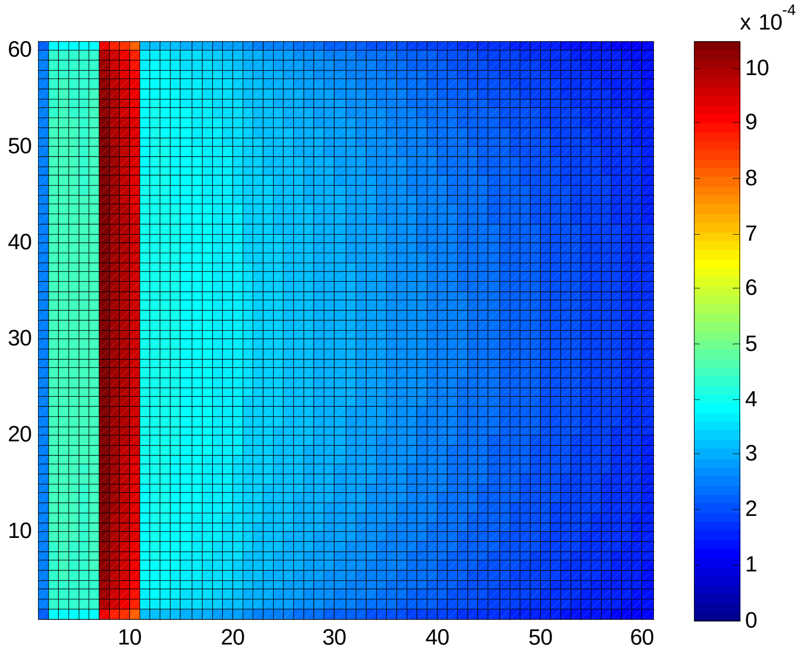


Figure 5.2.37: Energy Deposition (MeV) for Slab Phantom with 0.5cm x 0.5cm coarse meshes for Incident Beam of 2 MeV

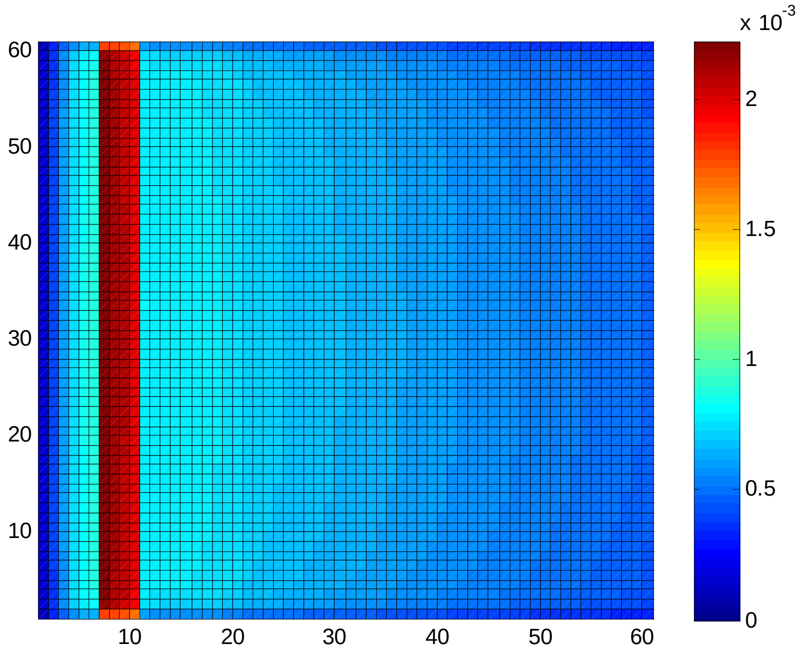


Figure 5.2.38: Energy Deposition (MeV) for Slab Phantom with 0.5cm x 0.5cm coarse meshes for Incident Beam of 6 MeV

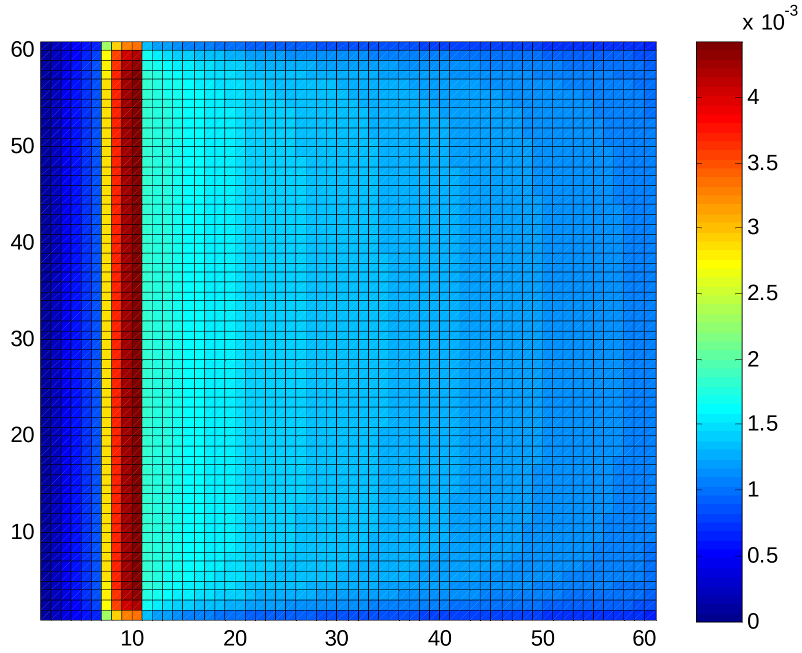


Figure 5.2.39: Energy Deposition (MeV) for Slab Phantom with 0.5cm x 0.5cm coarse meshes for Incident Beam of 18 MeV

The comparison results shown in the two tables below are not as good as with the larger size meshes. For the 2 MeV case, the maximum percent difference was found to be 2.13% with an average percent difference of just under half a percent at 0.45%. An RMS value of 0.64% was also found. The 6 MeV case produced a larger maximum percent difference with 3.18% and an average percent difference of 0.62%. Here, a value of 0.76% was obtained for the RMS value. The 18 MeV case produced results that were much worse than the other two energies with 12.87% maximum difference and 1.59% average difference. The RMS value was found to be 2.77 %. Since many more meshes were used, the COMET calculations did require more time between 51 and 56 minutes for all three cases. The reference calculations however also required much more time with 690 hours, 1240 hours, and 2125 hours necessary for the 2 MeV, 6 MeV, and 18 MeV cases respectively.

Table 5.2.11: Comparison Chart for Simplified Lung Phantom with 0.5cm x 0.5cm Coarse Meshes

| | COMPARISON For 2 MeV Incident Beam | COMPARISON For 6 MeV Incident Beam | COMPARISON For 18 MeV Incident Beam |
|---|---|---|---|
| Max % Difference | 2.13 % | 3.18 % | 12.87 % |
| St. Dev. Of Max % Diff | 0.16 % | 0.29 % | 0.28 % |
| Avg % Difference | 0.46 % | 0.62 % | 1.59 % |
| St. Dev. Of Avg % Diff | 0.45 % | 0.44 % | 2.27 % |
| RMS | 0.64 % | 0.76 % | 2.77 % |

Table 5.2.12: Reference and COMET Solution Statistics and Computational Times for Slab Phantom with 0.5cm x 0.5cm Coarse Meshes

| | 2 MeV Incident Beam | | 6 MeV Incident Beam | | 18 MeV Incident Beam | |
|---|---|---|---|---|---|---|
| | Reference Solution | COMET Solution | Reference Solution | COMET Solution | Reference Solution | COMET Solution |
| Max Rel Std. Dev. | 0.079 % | 0.17 % | 0.078 % | 0.31 % | 0.097 % | 0.55 % |
| Avg Rel Std. Dev. | 0.051 % | 0.13 % | 0.041 % | 0.10 % | 0.032 % | 0.12 % |
| CompTime | 690 hours | 54.5min | 1240 hours | 51.8min | 2125 hours | 55.7min |

The percent difference plots below are shown below. The patterns are the same as with the larger mesh sizes presented previously. For the 2 MeV case, maximum error occurs in a region of lower energy deposition furthest from the source. With regard to the 6 MeV case, maximum error occurs directly adjacent to the surface upon which the incident beam strikes due to once again smaller energy deposition. The 18 MeV case still produces results that show the region directly adjacent to the surface is calculated sufficiently, while the next few regions are the location of the highest errors. This is once again due to the expansion order not adequately describing the liberated electrons traveling within the phantom. The percent differences are also higher for each energy case than those obtained for its corresponding larger mesh case. This is also due to inadequate expansion orders. As with the previous water and lung phantoms, liberated electrons deposit portions of their energy within these smaller meshes, thus a larger energy expansion order is needed to handle this.

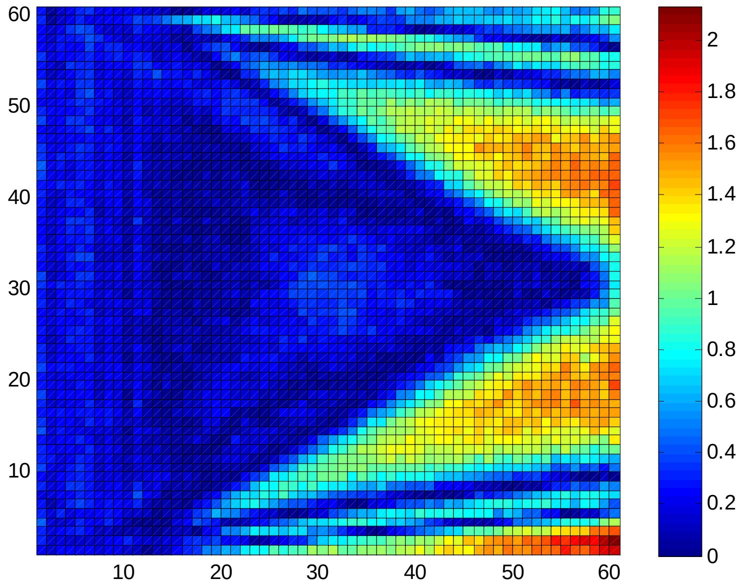


Figure 5.2.40: Percent Difference Between COMET and Reference Solutions for Slab Phantom with 0.5cm x 0.5cm coarse meshes for Incident Beam of 2 MeV

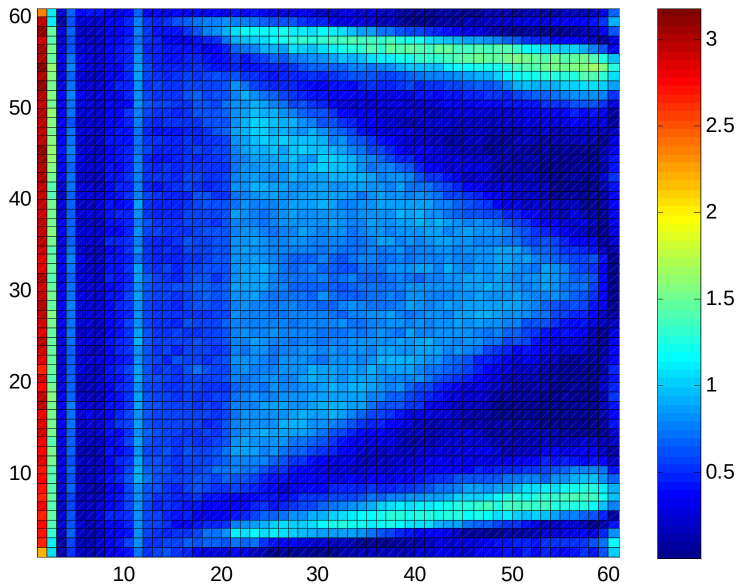


Figure 5.2.41: Percent Difference Between COMET and Reference Solutions for Slab Phantom with 0.5cm x 0.5cm coarse meshes for Incident Beam of 6 MeV

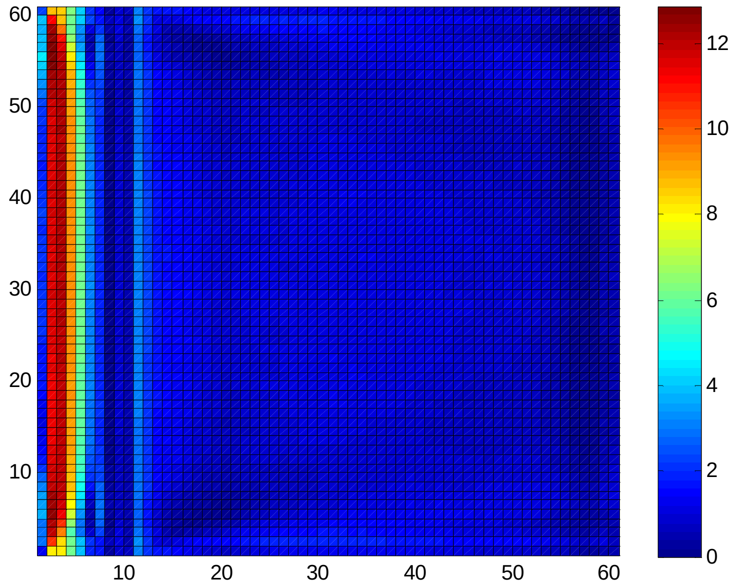


Figure 5.2.42: Percent Difference Between COMET and Reference Solutions for Slab Phantom with 0.5cm x 0.5cm coarse meshes for Incident Beam of 18 MeV

## 5.3 Conclusions

The water phantom, simplified lung phantom, and the non-clinical slab phantom together provide very useful information regarding COMET. Errors occurred in all situations; however, they occurred at the same locations and the same intensity for same incident energy and coarse mesh size. Thus, heterogeneity introduced into the system does not have an effect on the accuracy or timing of the COMET method.

The agreement was quite good for the 2 MeV and the 6 MeV situations with maximal errors occurring around or below 3%; however, the cases with the 18 MeV incident beam produced percent differences that were too high to be accepted clinically. Looking back at the sensitivity study described in the preceding chapter, the results for the 18 MeV cases, none of the expansion orders used produced clinically acceptable values. Most likely higher expansion orders in energy and angle than were studied here will be needed to produce better results for these situations in order to handle the liberated electrons crossing mesh boundaries due to the high correlation between energy and angle.

Also results were not as good for smaller mesh sizes. Higher percent difference was associated with the smaller mesh sizes than with that of the larger. This is due to liberating electrons depositing a portion of their energy within these smaller meshes and continuing to the next region. The current expansion order cannot adequately describe this situation, and higher expansion orders in energy and angle may be needed to improve upon this.

The timing for each of these situations should also be noted. Each of the COMET solutions ran in tens of minutes up to around an hour for larger cases shown here, while the COMET solution required hundreds of hours of computational time. It should again be stated that the response function library generation does require a fair amount of time; however, this is completely pre-computational. These response functions can be put together as building blocks and reused over and over again for many different situations.

# CHAPTER 6

# COMPUTED TOMOGRAPHY (CT) SCAN COMPARISONS

## 6.1 CT Scan Benchmark Development

The next step in testing the COMET methodology was to develop more intricate, clinically relevant benchmark problems composed of more material definitions. These benchmark problems were developed using CT Scans obtained from Emory University. For each benchmark problem, a single slice from a DICOM data set was obtained. The slice was used as an input into the program SCAN2MCNP to transform the data into a useful format for EGSnrc.[31]

For each scan, the image was segmented into 4-6 material definitions based on a range of CT numbers defined for each CT image. At this point, the mesh size was determined by the user, and the program SCAN2MCNP combined CT pixels based on this information to obtain the designated mesh size. The SCAN2MCNP program actually outputs an MCNP[32] data file as is evident from the name; however, for this work, EGSnrc was the Monte Carlo program used. From the SCAN2MCNP output file, the material definition and the new mesh location can be extracted and subsequently used in the input to the EGSnrc program.

The first scan studied was obtained from a transverse lung scan. The second scan was obtained from a transverse prostate scan slice, while the third scan was developed to model a beam re-entry situation in a transverse slice of the arm and chest wall. For each scan multiple mesh sizes were studied: 1 cm x 1 cm, 0.5 cm x 0.5 cm, 0.25 cm x 0.25 cm. As previously stated, my Master's work focused on very large mesh sizes of 2 cm x 2 cm, which do not accurately capture the curvature of the body and organs. Thus, smaller mesh sizes were studied. In the previous two chapters, the mesh sizes chosen were 1 cm x 1 cm and 0.5 cm x 0.5 cm. It was decided that a third level was necessary at 0.25 cm x 0.25cm. In the validation done by A. Fogliata et al. on the AAA algorithm, this grid size was also tested.[19] Also for each mesh size, multiple incident beam energies were studied:  2 MeV, 6 MeV, 18 MeV.   For each reference case, ten billion particle histories were followed, and for each response function calculation, one hundred thousand particles were used.

For more detailed information regarding each of the benchmarks and the parameters used in EGSnrc, see Appendix B.  Also, additional plots regarding dose deposition can be found in Appendix C.  Statistical calculations are also explained in Appendix A.

## 6.2 Lung Benchmark

Many studies have looked into the dose deposition in materials with lower densities than those for tissue.  Typically a lung equivalent material was used for testing.[26]  This heterogeneity is studied so often because a miscalculation of the dose to the lung can result in injury to the lung at doses beginning at 20 Gy.[33]  Because of this, it was thought a necessity to include a lung benchmark in this study.

The actual CT slice is shown below in Figure 6.2.1.  The image was then segmented in the program SCAN2MCNP.  This segmentation is shown in Figure 6.2.2. After the image was segmented into specific materials, the pixels were combined to form coarser meshes.   A separate lung benchmark was created for each coarse mesh size:  1cm x 1cm,  0.5cm x 0.5cm, and 0.25cm x 0.25cm.  For each mesh size, three incident beam energies are studied – 2MeV, 6MeV, 18MeV – which run the entire length of one side of the phantom.

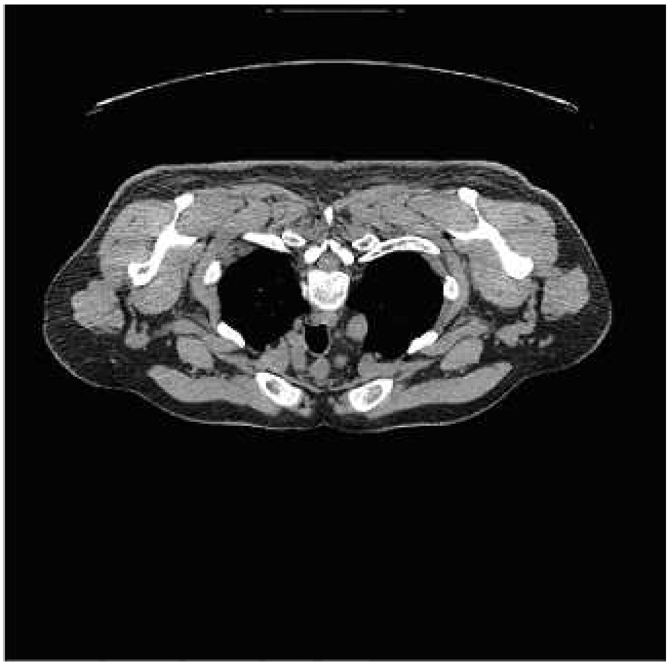

Figure 6.2.1: Lung CT Scan

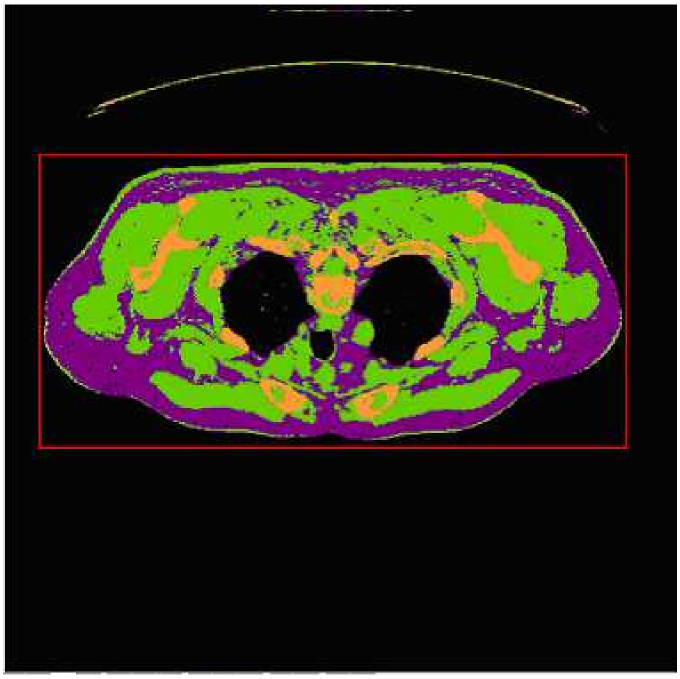

Figure 6.2.2: Segmented Lung CT Scan

**1cm x 1cm Mesh Size**

To begin, the 1cm x 1cm coarse mesh size was chosen. The lung benchmark for this size can be seen below in Figure 6.2.3. It measures 29 cm x 56 cm. The third dimension is said to extend to infinity in both directions for these calculations. As it can be seen in the figure, the incident photon beam impinges perpendicularly on the left face along the entire length of the phantom. For this case, there are five unique material definitions. For each incident beam energy, 420 hours of pre-computational time was necessary to calculate the necessary response function libraries.

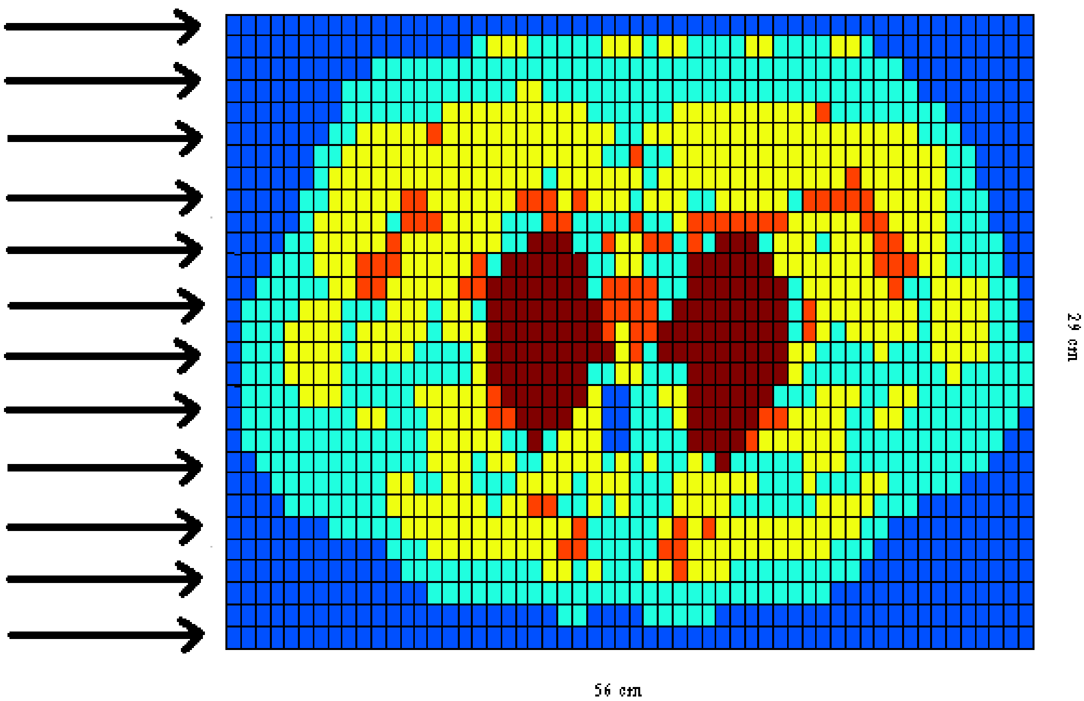


Figure 6.2.3: Lung Phantom Description with 1cm x 1cm Meshes
Dark Blue: Air
Light Blue: Adipose Tissue
Yellow: Muscle
Orange: Skeleton
Dark Red: Inflated Lung Tissue

In the next three figures, the energy deposition plots are shown for each incident energy beam. These plots show that the energy deposition for each case is as to be expected. As the incident energy increases, the location of maximal dose occurs deeper within the tissue. The lung and esophageal region both receive little dose since they have a very low density.

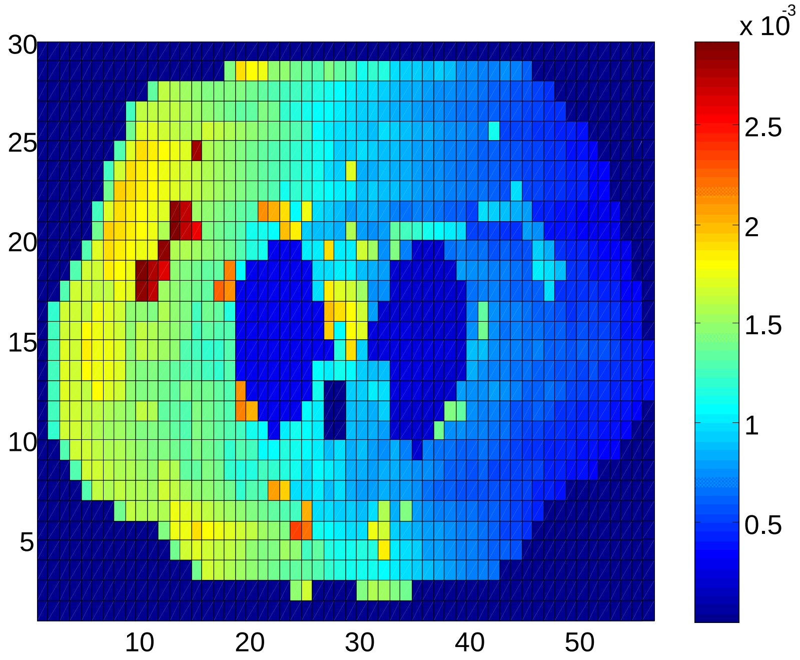


Figure 6.2.4: Energy Deposition Map (MeV) for Lung Phantom with 1cm x 1cm Meshes with 2 MeV Incident Photon Beam

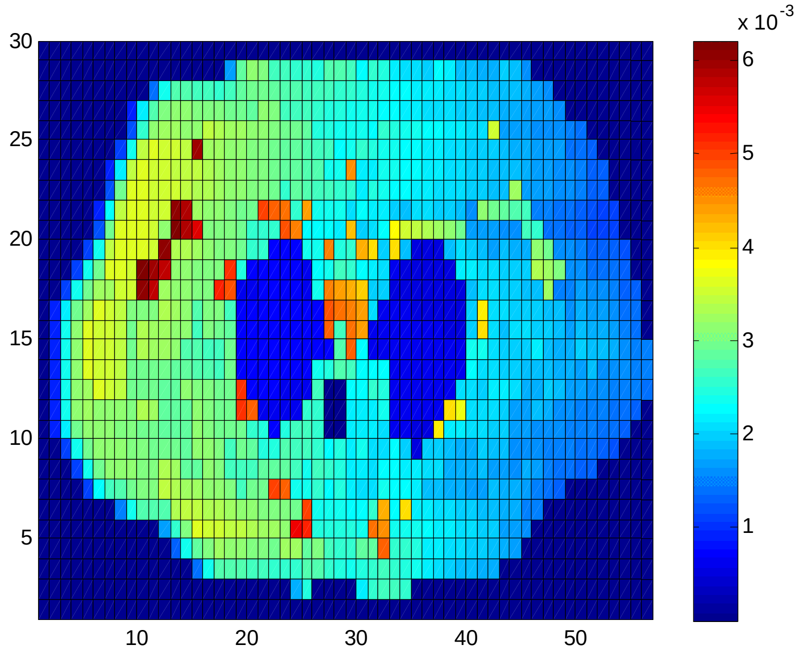


Figure 6.2.5: Energy Deposition Map (MeV) for Lung Phantom with 1cm x 1cm Meshes with 6 MeV Incident Photon Beam

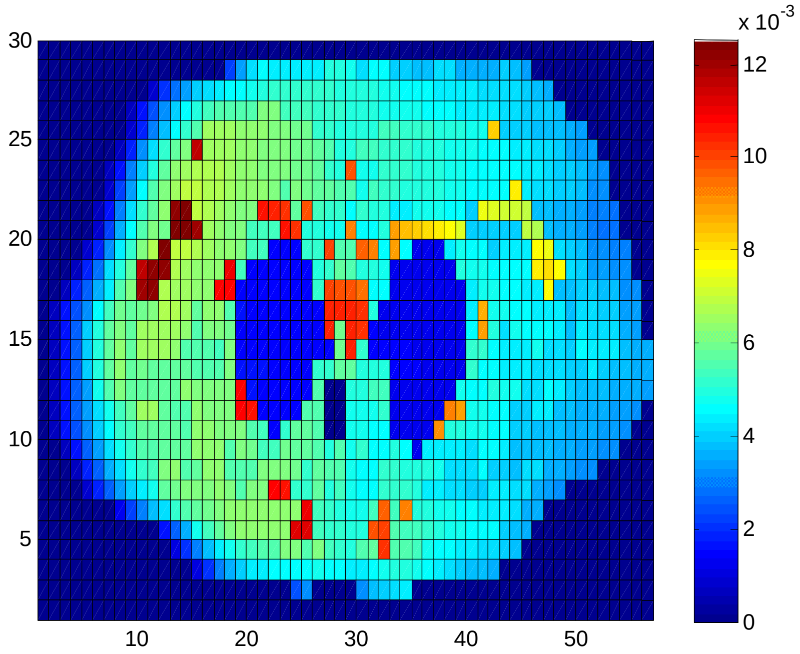


Figure 6.2.6: Energy Deposition Map (MeV) for Lung Phantom with 1cm x 1cm Meshes with 2 MeV Incident Photon Beam

Below the results for comparing the EGSnrc reference solution to the COMET solutions are shown in Table 6.2.1. Results are shown for the entire benchmark region, which includes the air surrounding the patient body as well as results for the patient body only. Any air regions inside the patient body were included in the latter comparison as well. The results for the 2 MeV and 6 MeV cases are quite good. The maximum percent difference does not exceed three percent, and the average percent difference is around 0.35 % for both. The RMS values for both cases are also around 0.45% The 18 MeV case produces results with a fairly large percent difference. The maximal value of 17.34% is quite large; however, it does appear near the surface of the patient. This is the problem region described during the sensitivity study. The average percent difference is still less than 1.5%, and the RMS value is 2.21%.

Additional data is shown in Table 6.2.2. Statistics associated directly with the COMET and reference solutions as well as timing required to run each case. The timing difference obtained between the EGSnrc reference calculation and the COMET solution is quite large. For the 2 MeV case, the reference case required around 339 hours, while the COMET solution ran in only 25.4 minutes. The difference in timing widens as the incident energy beam increases. For the 6 MeV beam, 25.9 minutes and 640 hours were needed for the COMET and reference solutions respectively. Lastly, the 18 MeV case required even more time for the reference solution at around 1062 hours, while the time required for the COMET case increased only slightly from the previous cases to 34.9 minutes total.

Table 6.2.1: Comparison of COMET and Reference Solutions for Lung Phantom with 1cm x 1cm Meshes

| | 2 MeV Beam | 6 MeV Beam | 18 MeV Beam |
|---|---|---|---|
| | Comparison without air | Comparison without air | Comparison without air |
| Max % Difference | 2.31 % | 2.81 % | 17.34 % |
| St. Dev. Of Max % Diff. | 0.15 % | 0.085 % | 0.14 % |
| Avg % Difference | 0.36 % | 0.34 % | 1.26 % |
| St. Dev. Of Avg % Diff | 0.30 % | 0.30 % | 1.81 % |
| RMS | 0.46 % | 0.45% | 2.21 % |

Table 6.2.2: Uncertainty Associated with COMET and Reference Solutions and Running Time Comparison for Lung Phantom with 1cm x 1cm Meshes

| | 2 MeV Beam | | 6 MeV Beam | | 18 MeV Beam | |
|---|---|---|---|---|---|---|
| | Ref Sol w/o air | COMET Sol w/o air | Ref Sol w/o air | COMET Sol w/o air | Ref Sol w/o air | COMET Sol w/o air |
| Max Rel Std. Dev. | 0.12 % | 0.095 % | 0.092 % | 0.061 % | 0.052 % | 0.14 % |
| Avg Rel Std. Dev. | 0.033% | 0.052 % | 0.048 % | 0.028 % | 0.022 % | 0.056 % |
| Comp Time | 339 hrs | 25.4 min | 640 hrs | 25.9 min | 1062 hrs | 34.9 min |

The percent difference plots for the three energies are shown below in Figure 6.2.7, 6.2.8, and 6.2.9. For the 2 MeV case, the maximal error occurs in the air cavity representing the esophagus as well as the portion of the body furthest from the incident beam. This is to be expected because this is the region of smallest energy deposition. For the 6 MeV case, the maximal error also occurs in the esophageal air cavity as with the 2 MeV case. The surface of the body closest to the incident beam also is an area where difference occurs. This is also due to a small energy deposition occurring here. The 18 MeV case resulted in high errors occurring near the surface of the body closest to the incident beam as well; however, the errors extended deeper within the body. This results not from the minimal energy deposition but from problems with the expansion order being too low to handle the liberated electrons crossing the mesh boundaries due to the high correlation between energy and angle.

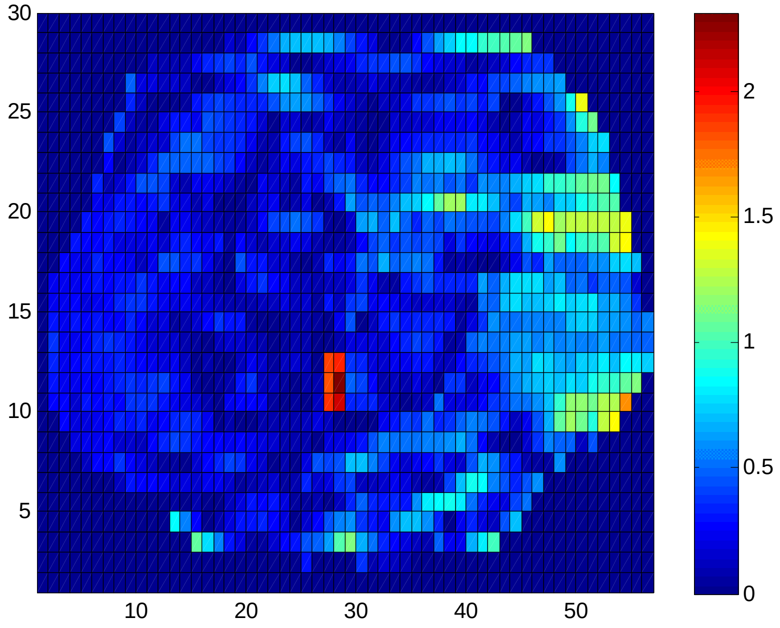


Figure 6.2.7: Percent Difference in Energy Deposition Estimate between COMET and Reference Calculations for Lung Phantom with 1cm x 1cm Meshes with 2 MeV Incident Photon Beam

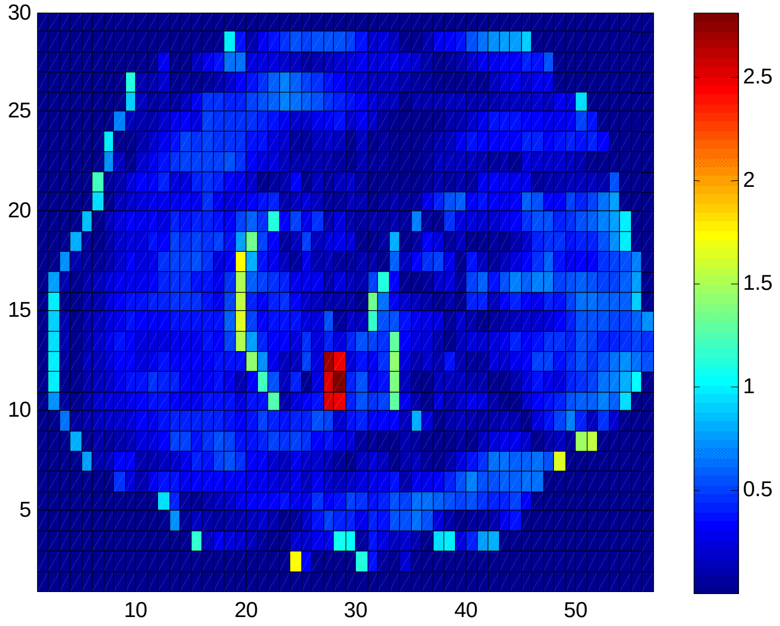


Figure 6.2.8: Percent Difference in Energy Deposition Estimate between COMET and Reference Calculations for Lung Phantom with 1cm x 1cm Meshes with 6 MeV Incident Photon Beam

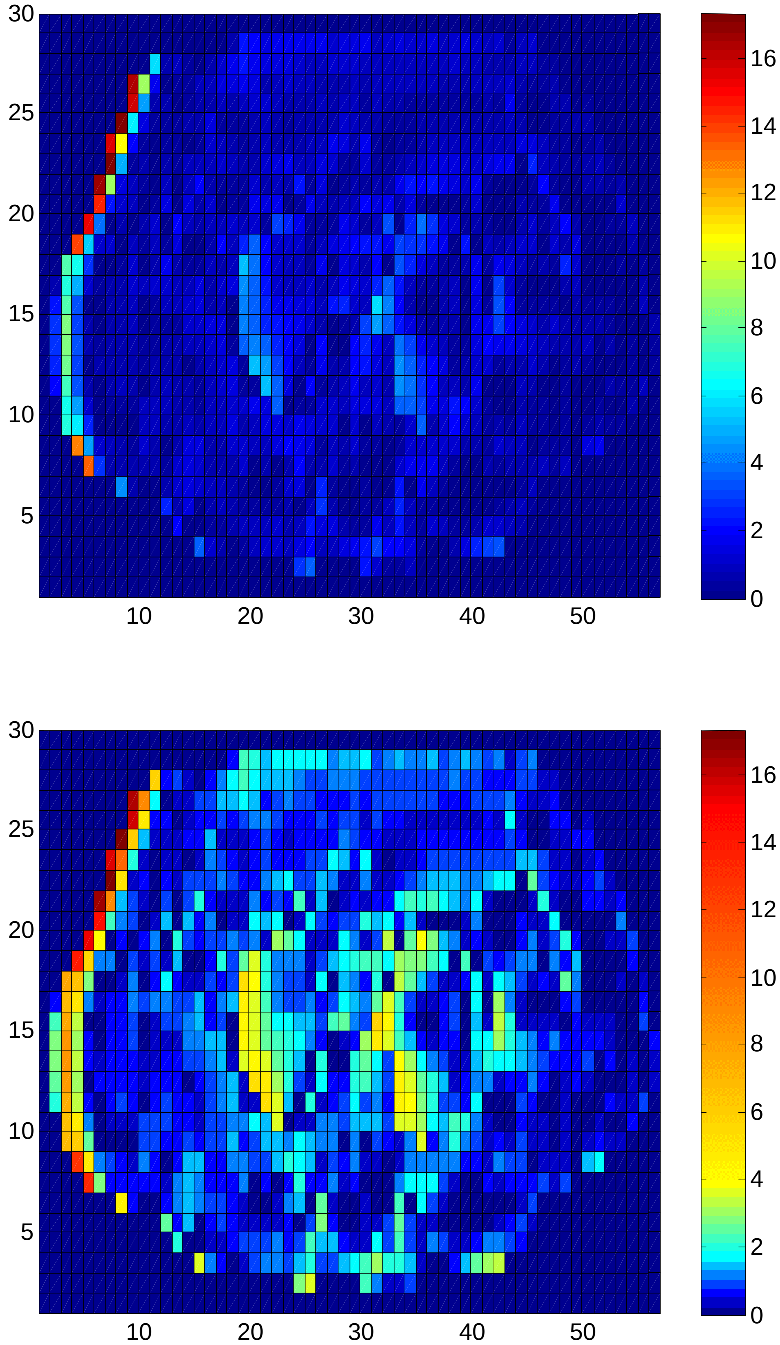


Figure 6.2.9: Percent Difference in Energy Deposition Estimate between COMET and Reference Calculations for Lung Phantom with 1cm x 1cm Meshes with 18 MeV Incident Photon Beam – The bottom figure has had the colormap altered to better highlight the energy deposition in the lower percentage range.

**Mesh Size:  0.5 cm x 0.5 cm**

The second mesh size chosen was 0.5cm x 0.5cm with total dimensions of 28 cm x 55.5 cm.  This benchmark problem can be seen below in Figure 6.2.10.  Again, five material definitions are used for this problem.  For each of the three incident energy beams, response function libraries were calculated in 420 hours.  It should be noted again that this is completely pre-computational.

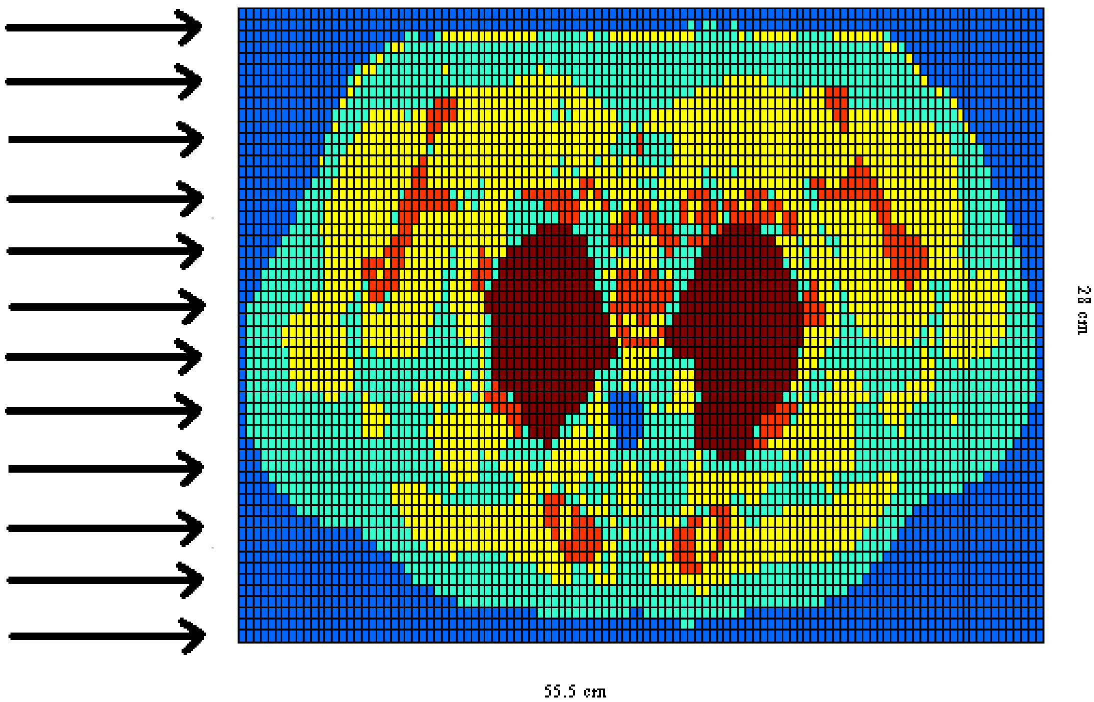


Figure 6.2.10:  Lung Phantom Description with 0.5cm x 0.5cm Meshes
Dark Blue:  Air
Light Blue:  Adipose Tissue
Yellow:  Muscle
Orange:  Skeleton
Dark Red:  Inflated Lung Tissue

As before, the next three figures show the energy deposition for the 2 MeV, 6 MeV, and 18 MeV cases.  As before, it is as we expected.  As the photon energy increases, the location of maximal dose occurs deeper in the body rather than at the surface.

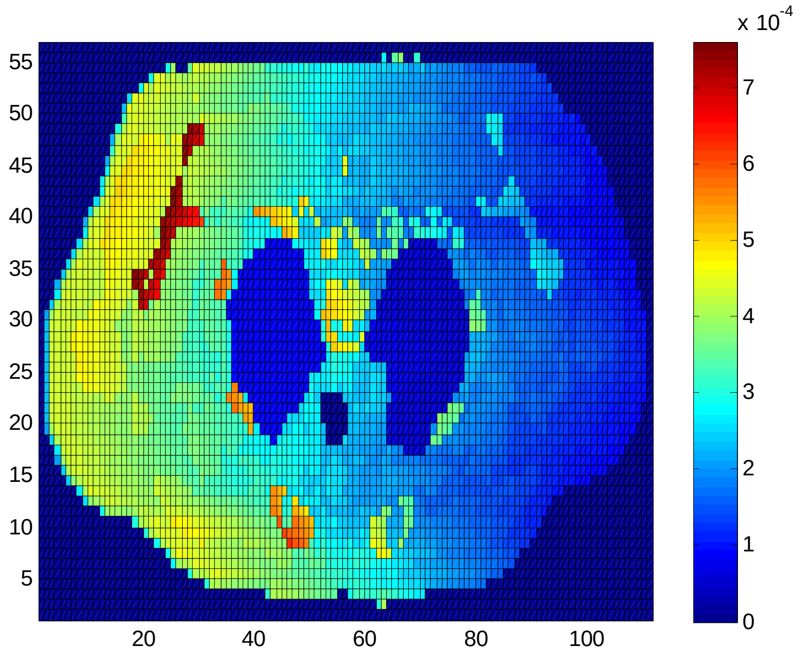


Figure 6.2.11: Energy Deposition (MeV) Map for Lung Phantom with 0.5cm x 0.5cm Meshes with 2 MeV Incident Beam

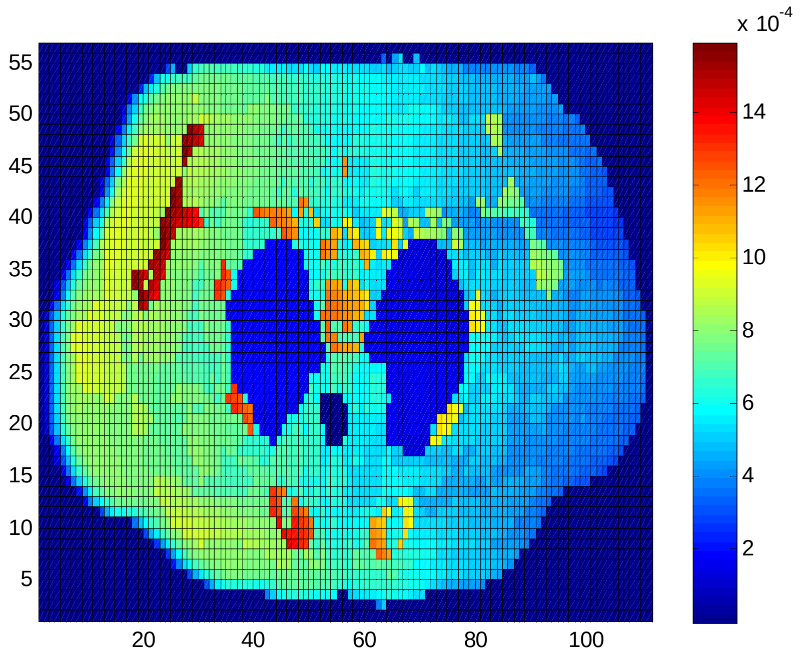


Figure 6.2.12: Energy Deposition Map (MeV) for Lung Phantom with 0.5cm x 0.5cm Meshes with 6 MeV Incident Photon Beam

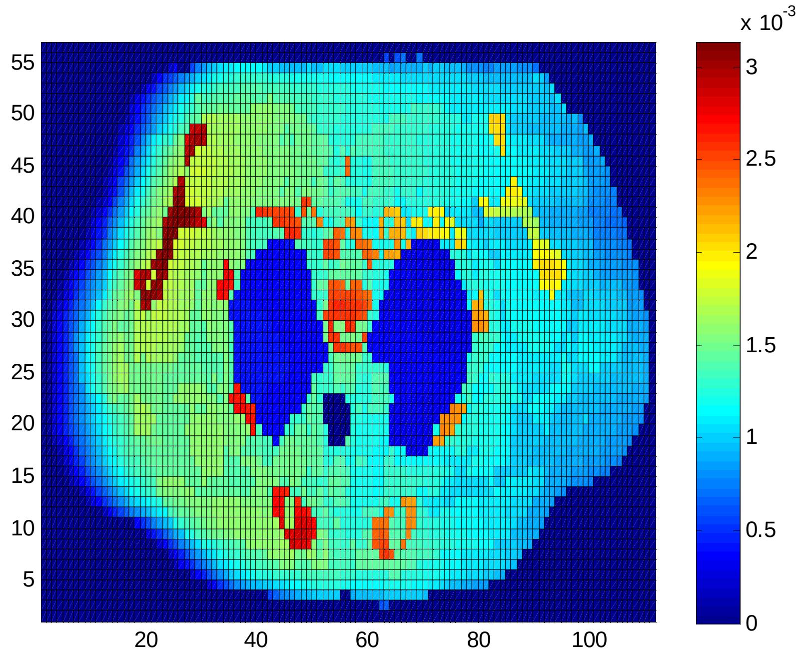


Figure 6.2.13: Energy Deposition Map (MeV) for Lung Phantom with 0.5cm x 0.5cm Meshes with 18 MeV Incident Photon Beam

The comparison results are shown in Tables 6.2.3 and 6.2.4. As before, as the incident energy increases, the maximal and average percent difference increases as well. The results for the smaller mesh are not as good as those obtained for the 1cm x 1cm mesh size. The maximal difference for the 2 MeV beam is 2.93 % with an average percent difference of around 0.41 %. The RMS value was found to be 0.55%. The 6 MeV case still has a relatively low average percent difference around 0.43 %, but the maximal value is too high at 7.41%. A value of 0.61% was obtained for the RMS value. Again, the 18 MeV case produces a very large maximal value of 46.29 % with an average percent difference and RMS of 1.46 % and 3.78 % respectively.

Also, the timing results still show that the COMET solutions required much less time than the reference cases. For the 2 MeV case, almost 2 hours was required for the COMET solution, while the reference solution was calculated in 722 hours. The 6 MeV COMET solution was obtained in 115 minutes, but the reference solution took much longer at 1124 hours. Lastly the 18 MeV reference case ran in 1808 hours, while the COMET solution only required 163.5 minutes.

Table 6.2.3: Comparison of COMET and Reference Solutions for Lung Phantom with 0.5cm x 0.5cm Meshes

| | 2 MeV Beam | 6 MeV Beam | 18 MeV Beam |
|---|---|---|---|
| | Comparison without air | Comparison without air | Comparison without air |
| Max % Difference | 2.93 % | 7.41 % | 46.29 % |
| St. Dev. Of Max % Diff. | 0.11 % | 0.078 % | 0.18 % |
| Avg % Difference | 0.41 % | 0.43 % | 1.46 % |
| St. Dev. Of Avg % Diff | 0.36 % | 0.43 % | 3.49 % |
| RMS | 0.55 % | 0.61 % | 3.78 % |

Table 6.2.4: Uncertainty Associated with COMET and Reference Solutions and Running Time Comparison for Lung Phantom with 0.5cm x 0.5cm Meshes

| | 2 MeV Beam | | 6 MeV Beam | | 18 MeV Beam | |
|---|---|---|---|---|---|---|
| | Ref Sol w/o air | COMET Sol w/o air | Ref Sol w/o air | COMET Sol w/o air | Ref Sol w/o air | COMET Sol w/o air |
| Max Rel Std. Dev. | 0.21 % | 0.099% | 0.11 % | 0.13 % | 0.10 % | 0.21 % |
| Avg Re Std. Dev. | 0.06 % | 0.061 % | 0.042 % | 0.045 % | 0.031 % | 0.05 % |
| Comp Time | 722 hrs | 115.1 min | 1124 hrs | 115 min | 1808 hrs | 163.5 min |

The next three figures plot the difference between the COMET and reference solutions. The pattern seen is the same as with the 1 cm x 1 cm case. Maximal error occurs at the body surface farthest from the incident beam for the photon case. For the 6 MeV case, errors occur at the surface of the body closest to the incident beam because of the minimal energy deposition here. The same problems result with the 18 MeV case with this mesh size as with the previous 1 cm x 1 cm case. Errors result close to the surface because of the inability of the expansion coefficients to accurately depict the forward peaking electrons liberated. The errors are however higher here for all cases compared to the 1 cm x 1 cm case. This results from liberated electrons depositing their energy partially in the smaller meshes. Thus a larger energy expansion is most likely needed to take care of this.

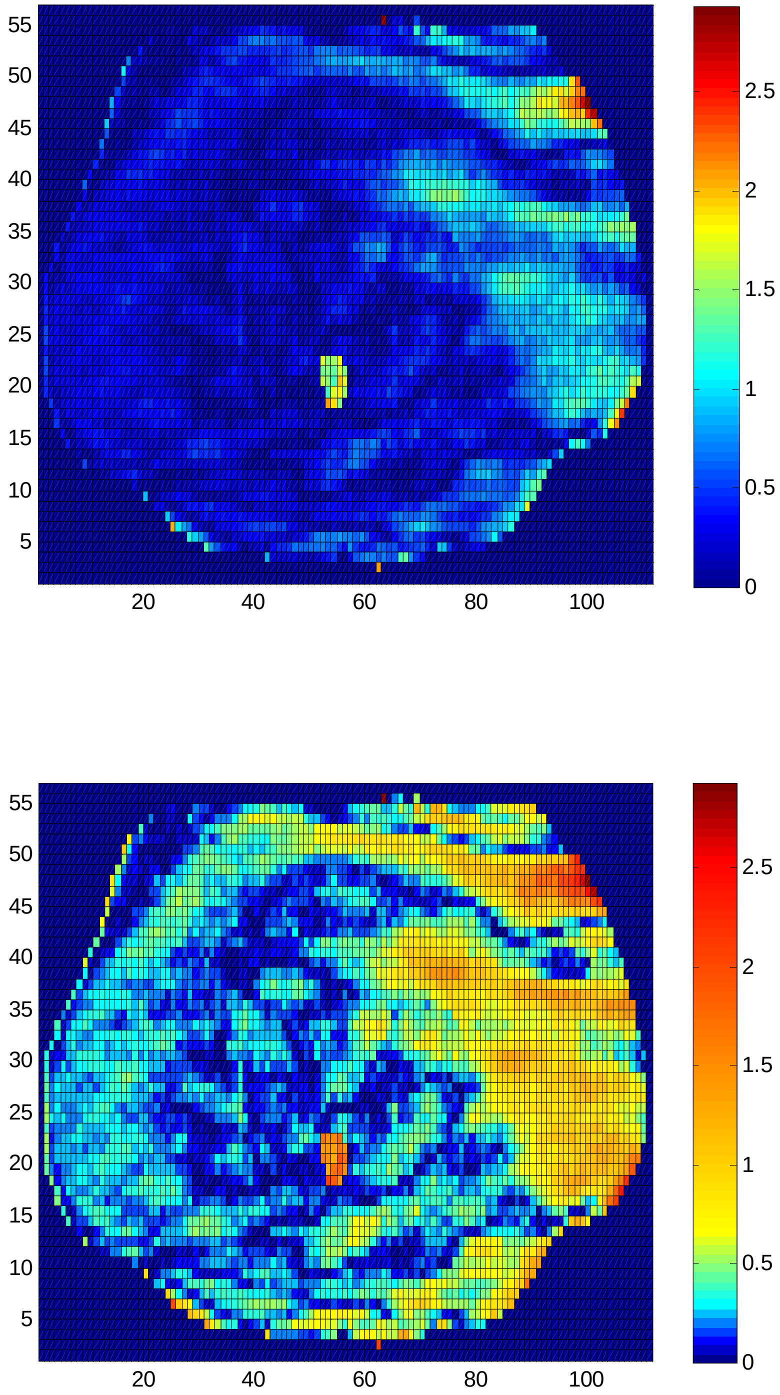


Figure 6.2.14: Percent Difference in Energy Deposition Estimate between COMET and Reference Calculations for Lung Phantom with 0.5cm x 0.5cm Meshes with 2 MeV Incident Photon Beam – The bottom figure has had the colormap altered to better highlight the energy deposition in the lower percentage range.

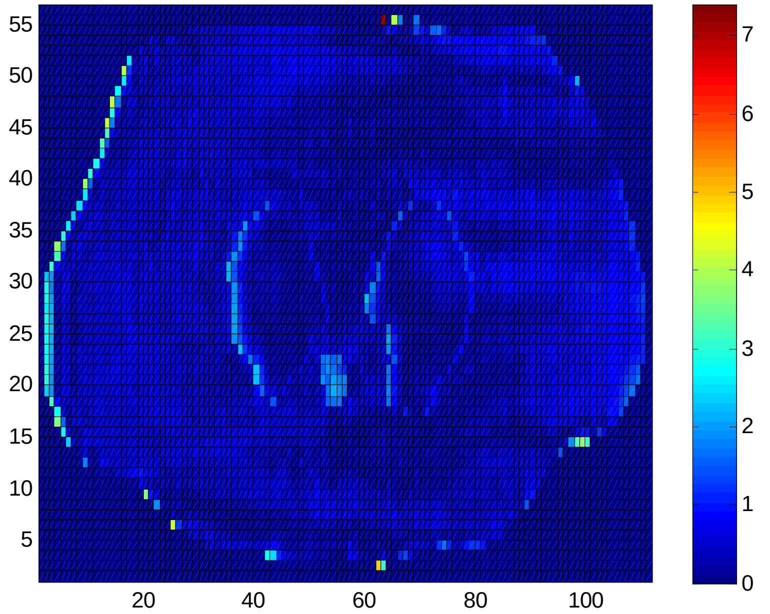


Figure 6.2.15: Percent Difference in Energy Deposition Estimate between COMET and Reference Calculations for Lung Phantom with 0.5cm x 0.5cm Meshes with 6 MeV Incident Photon Beam

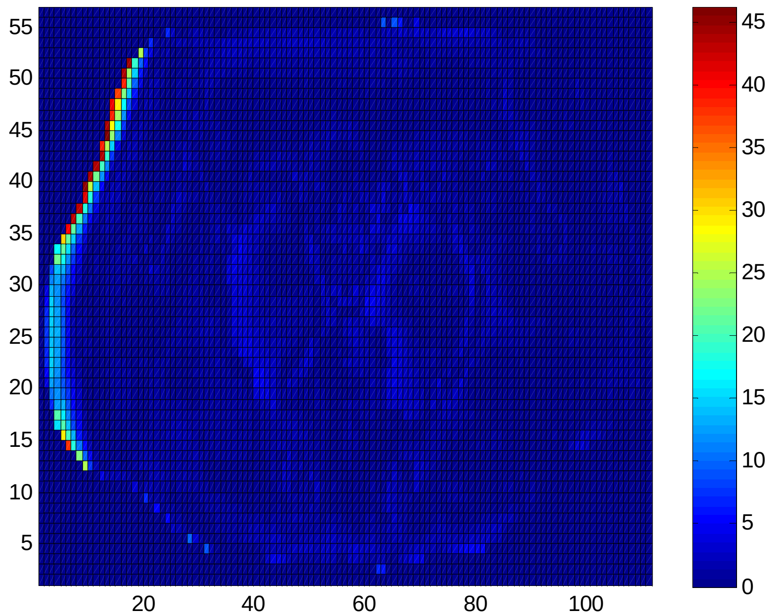


Figure 6.2.16: Percent Difference in Energy Deposition Estimate between COMET and Reference Calculations for Lung Phantom with 0.5cm x 0.5cm Meshes with 18 MeV Incident Photon Beam

**Mesh Size:  0.25 cm x 0.25 cm**

A third coarse mesh size was chosen at 0.25cm x 0.25cm.  This coarse mesh decomposition of the lung phantom is shown below in Figure 2.6.17.  The overall dimensions of the phantom are 27.5 cm x 55.5 cm with the third dimension extending to infinity in both directions.  As before, the incident photon beam impinges normally along the 27.5 cm surface.  Again five materials definitions were defined, and 420 hours of pre-computational time for each incident energy was necessary for the response function library generation.

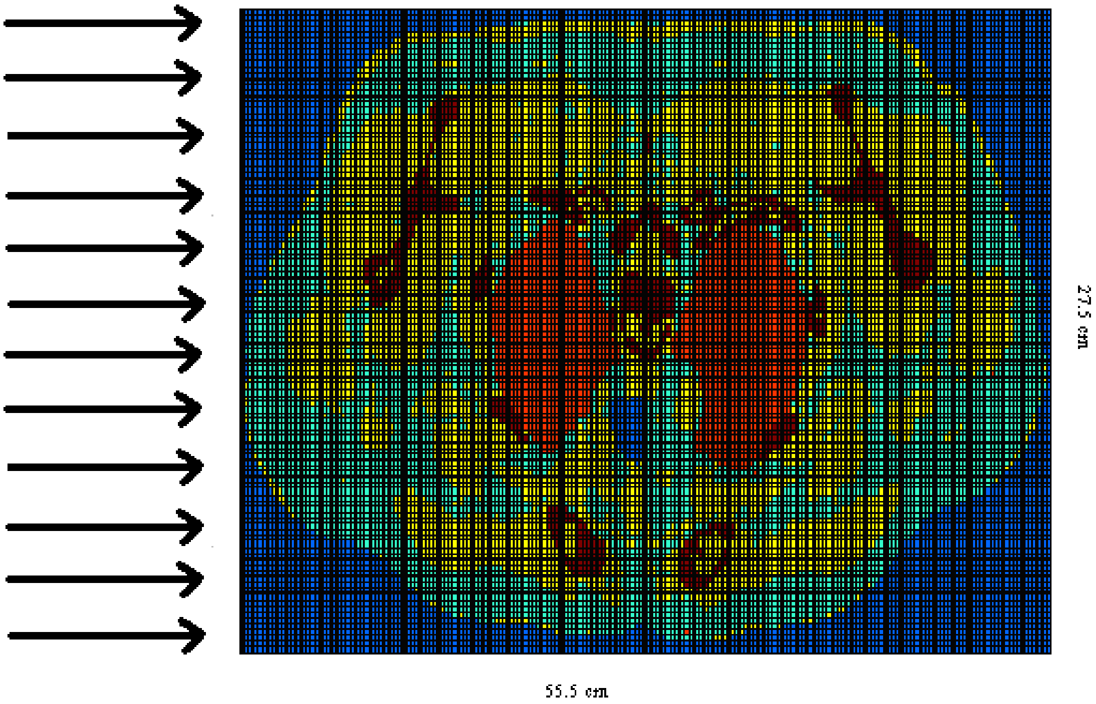


Figure 6.2.17:  Lung Phantom Description with 0.25cm x 0.25cm Meshes
Dark Blue:  Air
Light Blue:  Adipose Tissue
Yellow:  Muscle
Orange:  Skeleton
Dark Red:  Inflated Lung Tissue

Below in the next three figures, the energy deposition plots for the three incident beam energies of 2 MeV, 6 MeV, and 18 MeV are shown.  As has been seen before, the energy deposition is what is to be expected with the location of maximal energy dose occurring deeper within the phantom as the impinging photon energy increases. More dose is deposited within the bone and less within the inflated lung region.

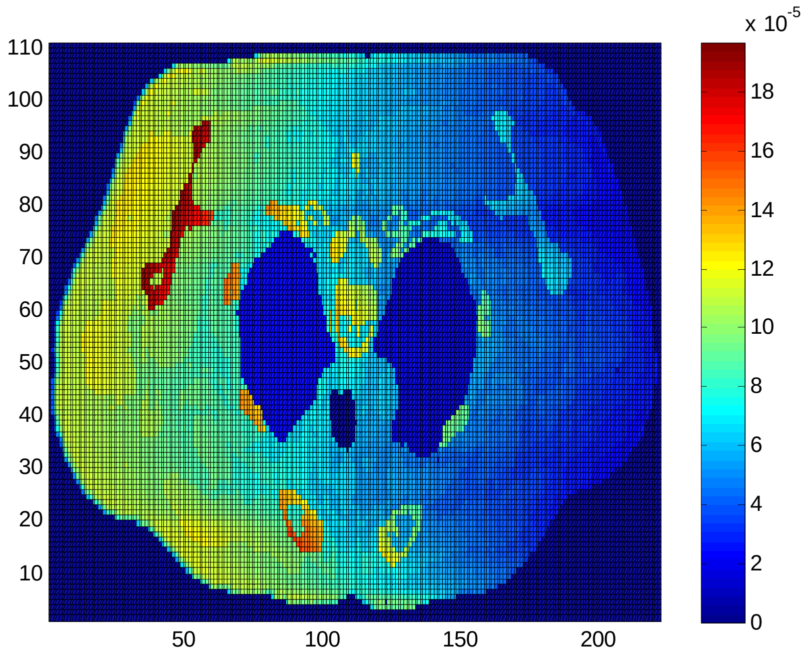


Figure 6.2.18: Energy Deposition Map (MeV) for Lung Phantom with 0.25cm x 0.25cm Meshes with 2 MeV Incident Photon Beam

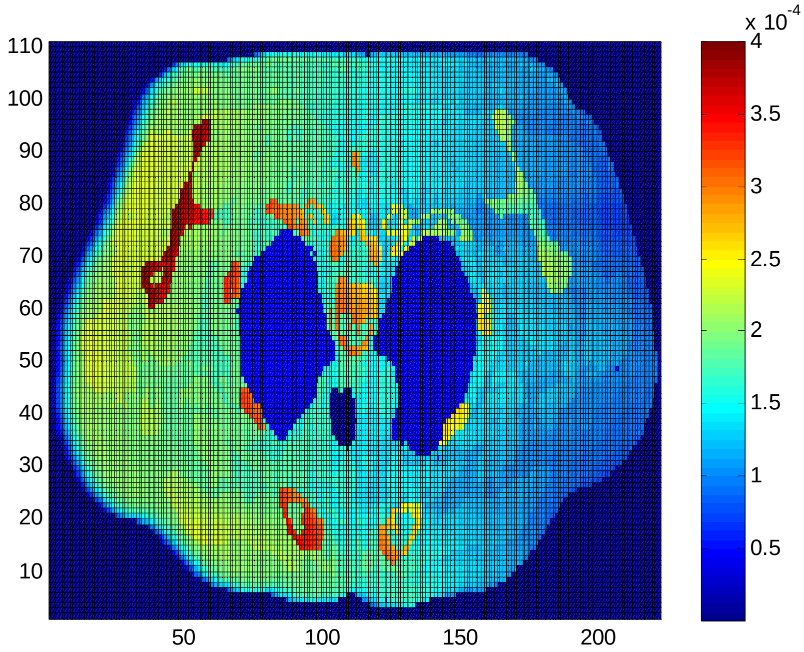


Figure 6.2.19: Energy Deposition Map (MeV) for Lung Phantom with 0.25cm x 0.25cm Meshes with 6 MeV Incident Photon Beam

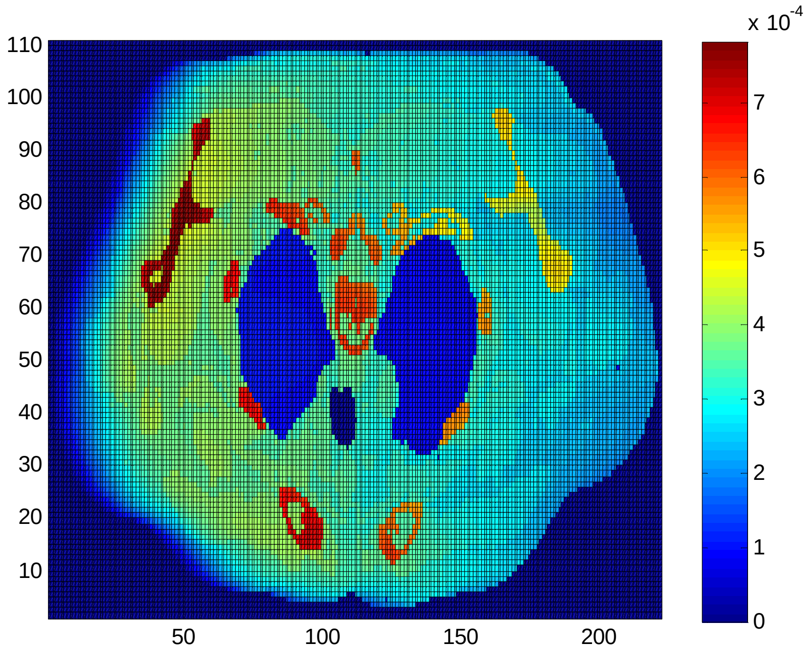


Figure 6.2.20: Energy Deposition Map (MeV) for Lung Phantom with 0.25cm x 0.25cm Meshes with 18 MeV Incident Photon Beam

As before, the comparison results are shown below in the following two tables. The percent difference increases as the photon beam energy increases. For the 2 MeV case, the maximal percent difference is slightly high around 3.62 %; however, the average percent difference is just over half a percent, and the RMS value was 0.70 %. The 6 MeV beam has a high maximum percent difference of 11.33 %, while the average percent difference is only slightly higher than that found for the 2 MeV case at 0.61 %. The RMS value was found to be 0.95 %. The 18 MeV case produces a very high maximum percent difference of 107.3% with an average percent difference of 1.88 %. The RMS value for this case was 6.09 %. The COMET calculations required around 8.5 hours for the 2 MeV and 6 MeV cases and around 9.5 hours for the 18 MeV instance. The reference calculations required around 4 months for the 2 MeV and 6 MeV incident beam energies. For the 18 MeV case, around 4.25 months was needed on a single processor.

Table 6.2.5: Comparison of COMET and Reference Solutions for Lung Phantom with 0.25cm x 0.25cm Meshes

| | 2 MeV Beam | 6 MeV Beam | 18 MeV Beam |
|---|---|---|---|
| | Comparison without air | Comparison without air | Comparison without air |
| Max % Difference | 3.62 % | 11.33 % | 107.30 % |
| St. Dev. Of Max % Diff. | 0.16 % | 0.21 % | 0.24 % |
| Avg % Difference | 0.51 % | 0.61 % | 1.88 % |
| St. Dev. Of Avg % Diff | 0.47 % | 0.73 % | 5.79 % |
| RMS | 0.70 % | 0.95 % | 6.09 % |

Table 6.2.6: Uncertainty Associated with COMET and Reference Solutions and Running Time Comparison for Lung Phantom with 0.25cm x 0.25cm Meshes

| | 2 MeV Beam | | 6 MeV Beam | | 18 MeV Beam | |
|---|---|---|---|---|---|---|
| | Ref Sol w/o air | COMET Sol w/o air | Ref Sol w/o air | COMET Sol w/o air | Ref Sol w/o air | COMET Sol w/o air |
| Max Rel Std. Dev. | 0.39 % | 0.12 % | 0.20 % | 0.18 % | 0.20 % | 0.28 % |
| Avg Re Std. Dev. | 0.094 % | 0.061 % | 0.06 % | 0.04 % | 0.045 % | 0.52 % |
| Comp Time | 6816 hrs | 515.0 min | 7059 hrs | 515.1 min | 7652 hrs | 579.3 min |

The following three figures depict the percent difference for each of the three incidences. The pattern of the results is similar to what has been seen for larger mesh sizes; however, the errors are much higher in some cases. For the 2 MeV case, the maximal error occurs inside the phantom at the surface furthest from the incident beam at the location of minimal dose deposition. For the 6 MeV, the highest errors for each occur close the surface of the body closest to the incident beam, which corresponds to lower dosages. The 18 MeV case once again produces larger errors because of the inability of the expansion orders to accurately depict the energy and directionality of the liberated electrons. The smaller mesh size here continues to produce worse results than the 0.5 cm x 0.5 cm case. The same reasoning applies here that the electron only deposit a portion of their energy within these smaller meshes. Thus, the energy expansion coefficient cannot correctly model this.

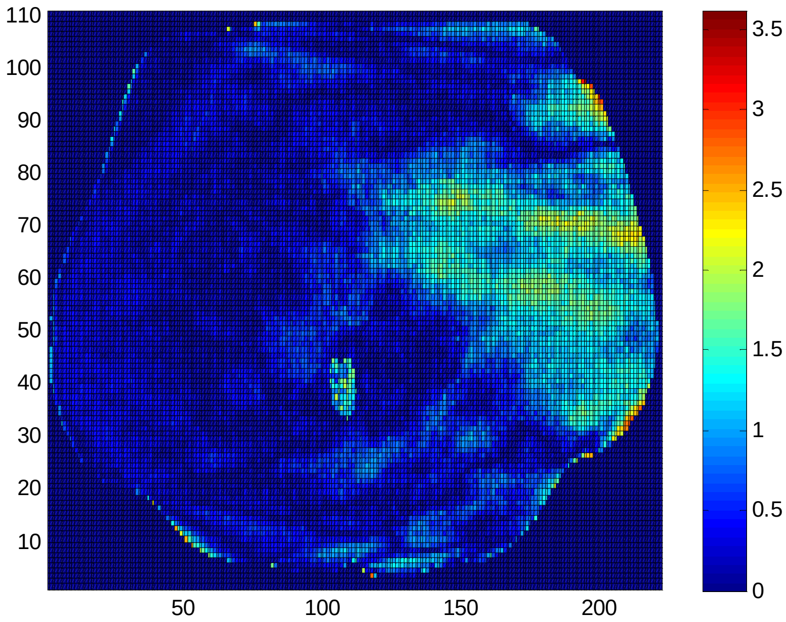


Figure 6.2.21: Percent Difference in Energy Deposition Estimate between COMET and Reference Calculations for Lung Phantom with 0.25cm x 0.25cm Meshes with 2 MeV Incident Photon Beam

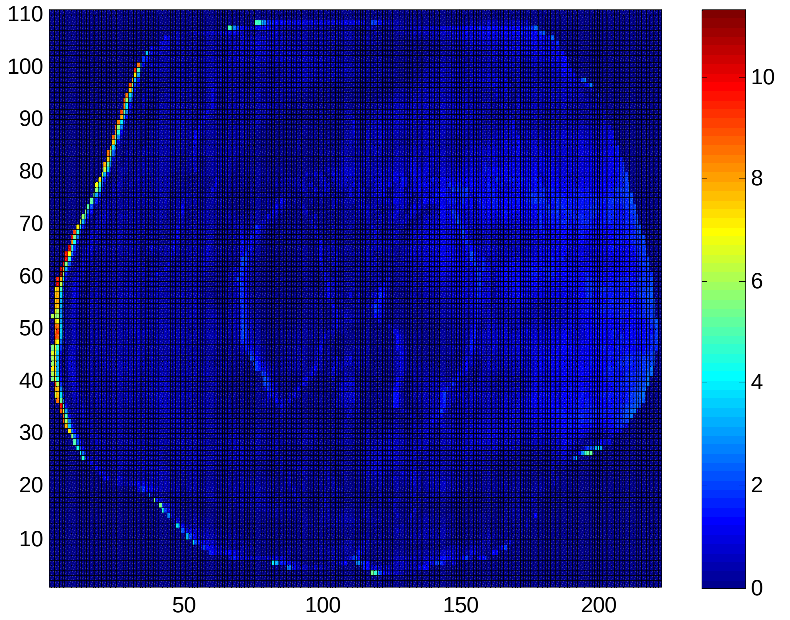


Figure 6.2.22: Percent Difference in Energy Deposition Estimate between COMET and Reference Calculations for Lung Phantom with 0.25cm x 0.25cm Meshes with 6 MeV Incident Photon Beam

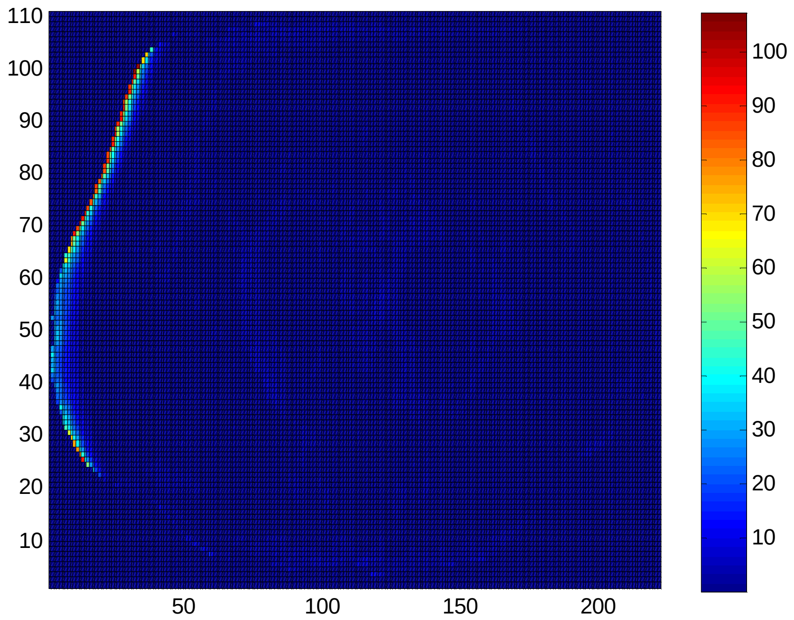


Figure 6.2.23: Percent Difference in Energy Deposition Estimate between COMET and Reference Calculations for Lung Phantom with 0.25cm x 0.25cm Meshes with 18 MeV Incident Photon Beam

## 6.3 Prostate Benchmark

The main heterogeneity located within the human body is bone; however, the AAPM Report Number 85 has found that there are few papers that address this specific heterogeneity when testing dose calculation algorithms.[3] Earlier, it was stated that the lung heterogeneity is typically tested because of the high likelihood of patient injury if an overdosing occurs in this region. Injury to the bone requires a much higher dosage around 50-65 Gy to cause injury to occur.[34-35] Thus an error to the bone is not as detrimental as one to the lung may be. Even though these errors may not result in an injury, it is felt that a benchmark with a large amount of bone should be tested. In this case, a prostate patient was chosen. Within this phantom, there is quite a large amount of bone within the chosen scan. As before, the image was segmented using the SCAN2MCNP program.[31] Below in Figure 6.3.1 is the original CT scan, while the segmented CT scan is shown in Figure 6.3.2. As before, three coarse mesh sizes were studied – 1cm x 1cm, 0.5cm x 0.5cm, and 0.25cm x 0.25cm – and three beam energies for each mesh size – 2 MeV, 6 MeV, and 18 MeV.

Figure 6.3.1: Prostate CT Scan

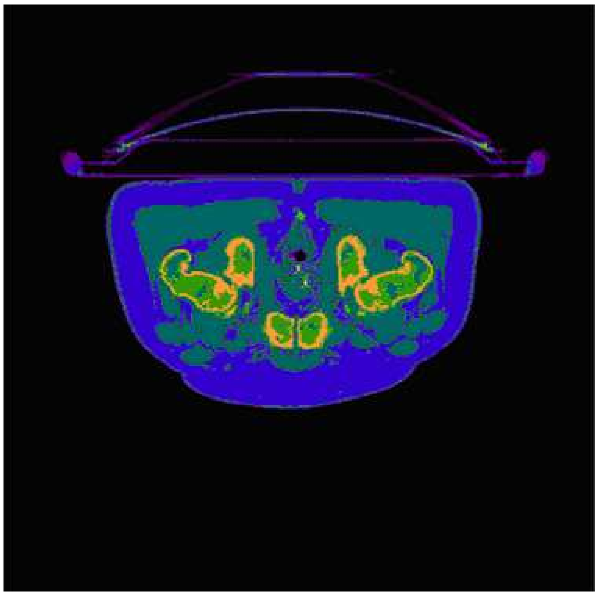

Figure 6.3.2: Segmented Prostate CT Scan

**1 cm x 1 cm Mesh Size**

The prostate benchmark problem decomposed into 1cm x 1cm coarse meshes is shown below in Figure 6.3.3. It measures 27 cm x 43 cm with the third dimension extending to infinity in both the positive and negative directions. The photon beam impinges perpendicularly on the surface on the phantom as seen below. Five material definitions were used. For each of the three incident photon beams tested, response function libraries required around 420 hours of pre-computational time.

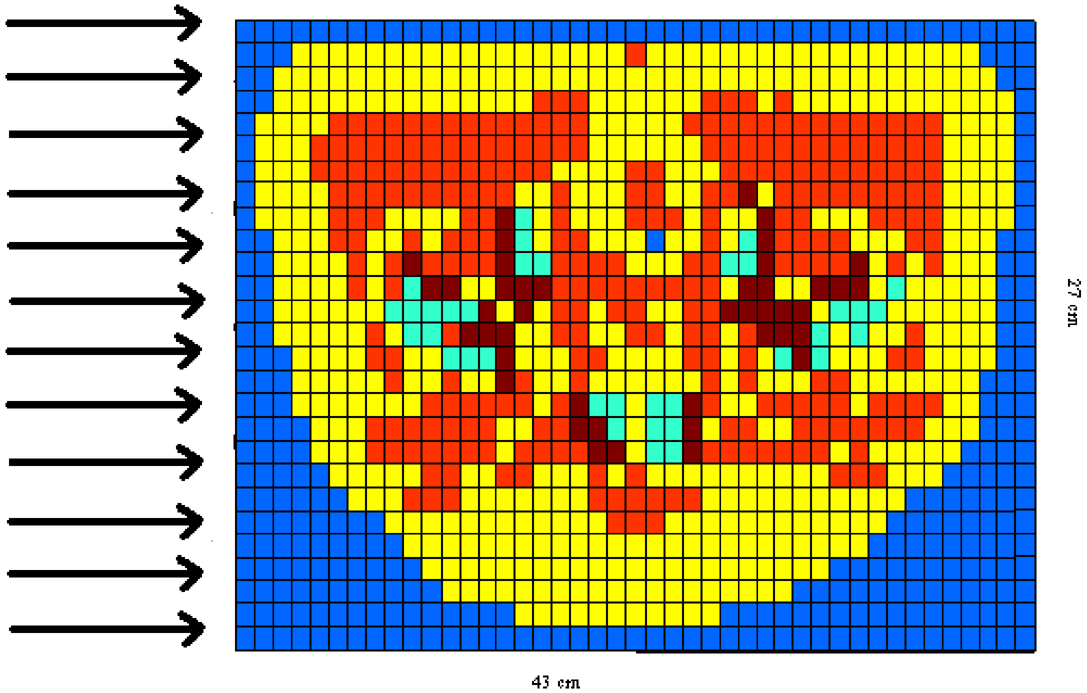


Figure 6.3.3: Prostate Phantom Description with 1cm x 1cm Meshes
Dark Blue: Air
Light Blue: Bone Marrow
Yellow: Adipose Tissue
Orange: Muscle
Dark Red: Skeleton

The next three plots show the energy deposition for each of the three incident energy beam. The energy deposition follows the pattern that is to be expected as with all the other. The location of maximum dose occurs further from the incident beam with an increase in incident energy. The bones closest to the incident beam also receive a higher dose.

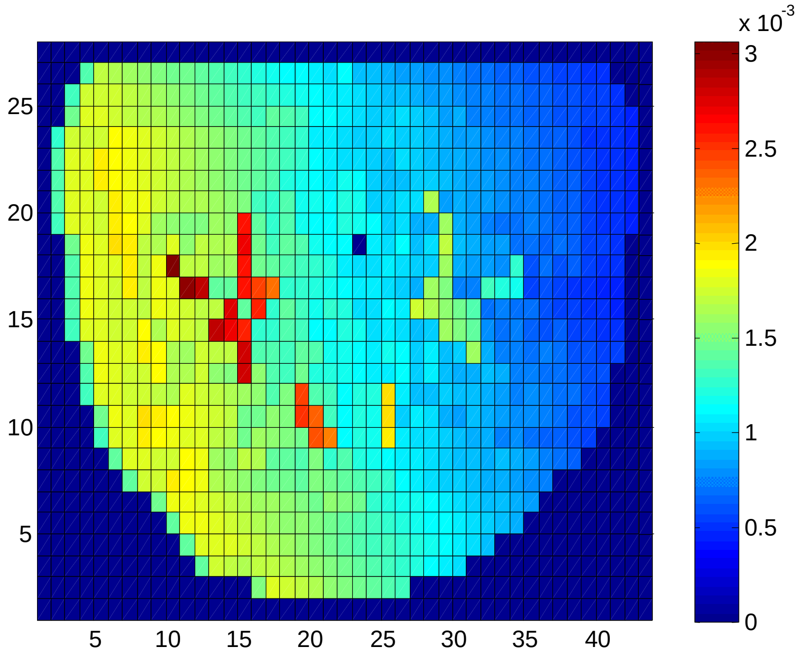


Figure 6.3.4: Energy Deposition Map (MeV) for Prostate Phantom with 1cm x 1cm Meshes with 2 MeV Incident Photon Beam

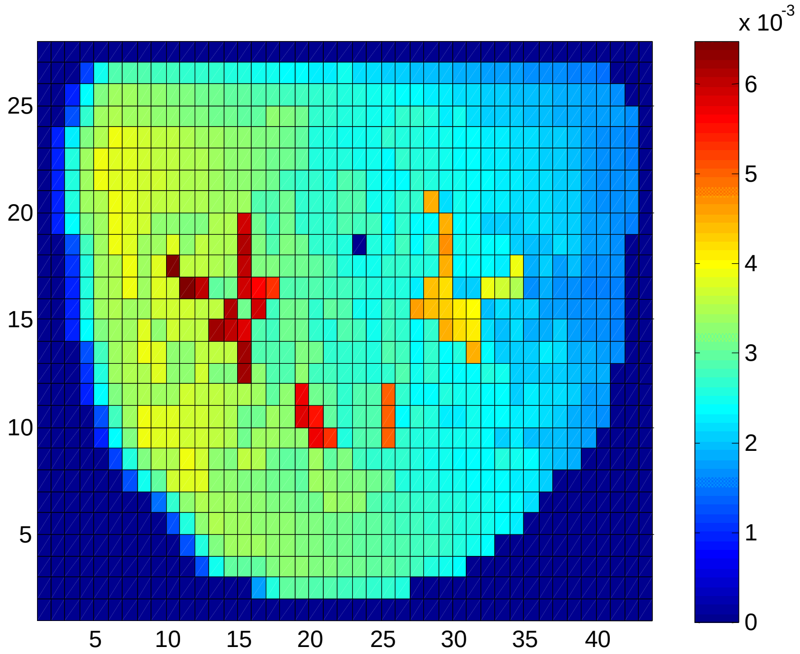


Figure 6.3.5: Energy Deposition Map (MeV) for Prostate Phantom with 1cm x 1cm Meshes with 6 MeV Incident Photon Beam

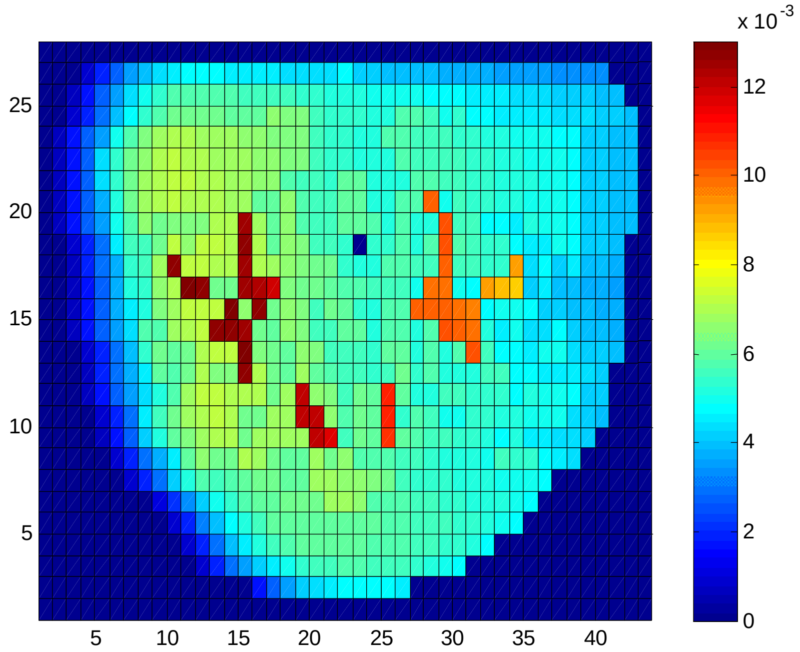


Figure 6.3.6: Energy Deposition Map (MeV) for Prostate Phantom with 1cm x 1cm Meshes with 18 MeV Incident Photon Beam

Below in Tables 6.3.1 and 6.3.2, the results for comparing the EGSnrc reference solution to the COMET solutions are shown. The maximum percent difference for the 2 MeV case is 1.44 % with an average percent difference of 0.32 %, while the maximum percent difference for the 6 MeV incident beam is 2.39 % and an average percent difference of 0.31 %. For the 2 MeV and 6 MeV cases, the RMS values were found to be 0.41 % and 0.38 % respectively. The results for the 18 MeV case show that the maximum percent different is higher than 15 %, while the average is slightly over one percent at 1.15%; however, data was still useful inside the body region where no errors had occurred. The RMS value for this case was 2.04 %.

The timing data in Table 6.3.2 shows that the COMET solution for the 2 MeV case required just over 18 minutes, while the EGSnrc reference solution required 340 hours. For the 6 MeV incident beam, the amount of computational time required for the COMET solution was again just over 18 minutes, while the reference solution took even longer at 540 hours. The 18 MeV incident beam problem required 33.2 minutes for the COMET solution to be obtained and 880 hours to calculate the EGSnrc reference solution. The COMET solution is obviously obtained much faster than the reference calculations. Minutes are required rather than weeks or months on a single processor.

Table 6.3.1: Comparison of COMET and Reference Solutions for Prostate Phantom with 1cm x 1cm Meshes

| | 2 MeV Beam | 6 MeV Beam | 18 MeV Beam |
|---|---|---|---|
| | Comparison without air | Comparison without air | Comparison without air |
| Max % Difference | 1.44 % | 2.39 % | 15.21 % |
| St. Dev. Of Max % Diff. | 0.15 % | 0.084 % | 0.14 % |
| Avg % Difference | 0.32 % | 0.31 % | 1.15 % |
| St. Dev. Of Avg % Diff | 0.26 % | 0.22 % | 1.68 % |
| RMS | 0.41 % | 0.38 % | 2.04 % |

Table 6.3.2: Uncertainty Associated with COMET and Reference Solutions and Running Time Comparison for Prostate Phantom with 1cm x 1cm Meshes

| | 2 MeV Beam | | 6 MeV Beam | | 18 MeV Beam | |
|---|---|---|---|---|---|---|
| | Ref Sol w/o air | COMET Sol w/o air | Ref Sol w/o air | COMET Sol w/o air | Ref Sol w/o air | COMET Sol w/o air |
| Max Rel Std. Dev. | 0.098 % | 0.11% | 0.058 % | 0.092 % | 0.050 % | 0.15 % |
| Avg Re Std. Dev. | 0.049 % | 0.029 % | 0.026 % | 0.047 % | 0.021 % | 0.055 % |
| Comp Time | 340 hrs | 18.2 min | 540 hrs | 18.1 min | 880 hrs | 33.2 min |

Below in the following three figures shows the percent difference for each of the three energy cases. For the 2 MeV case, the maximal percent difference occurs furthest from the beam where minimal energy deposition occurs. For the 6 MeV case, minimal energy deposition occurs near the surface, and this again is where the maximal percent difference can be seen. Lastly, for the 18 MeV case, the maximal percent difference is also close to the surface. As with the lung phantom, the 18 MeV case produces higher errors because of the inability of the energy and angular expansion coefficients to accurately describe the liberated electrons.

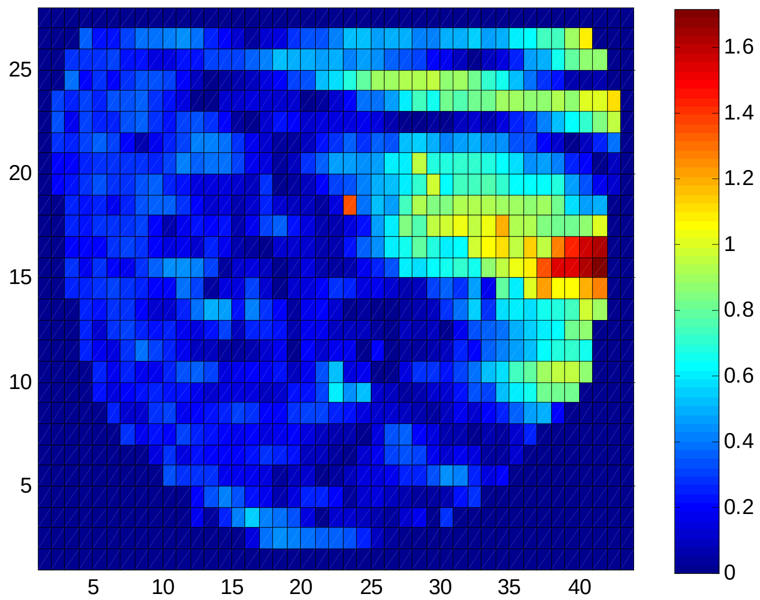


Figure 6.3.7: Percent Difference in Energy Deposition Estimate between COMET and Reference Calculations for Prostate Phantom with 1cm x 1cm Meshes with 2 MeV Incident Photon Beam

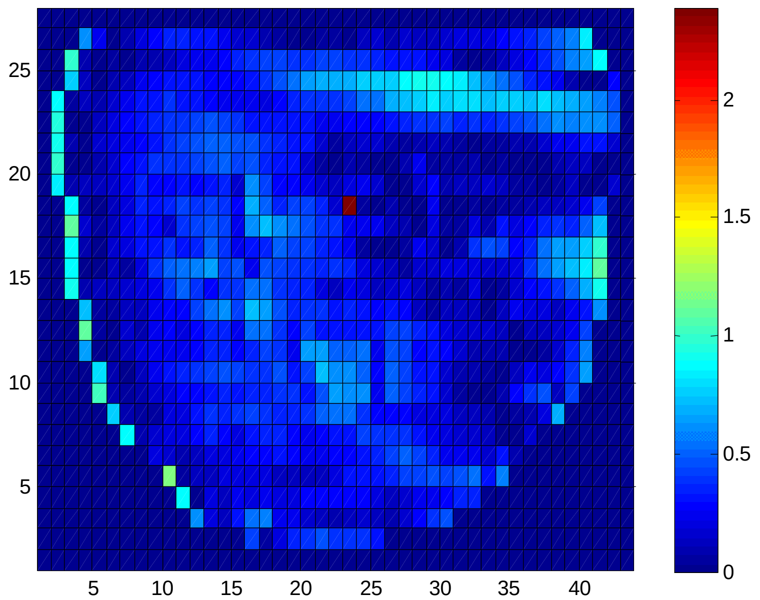


Figure 6.3.8: Percent Difference in Energy Deposition Estimate between COMET and Reference Calculations for Prostate Phantom with 1cm x 1cm Meshes with 6 MeV Incident Photon Beam

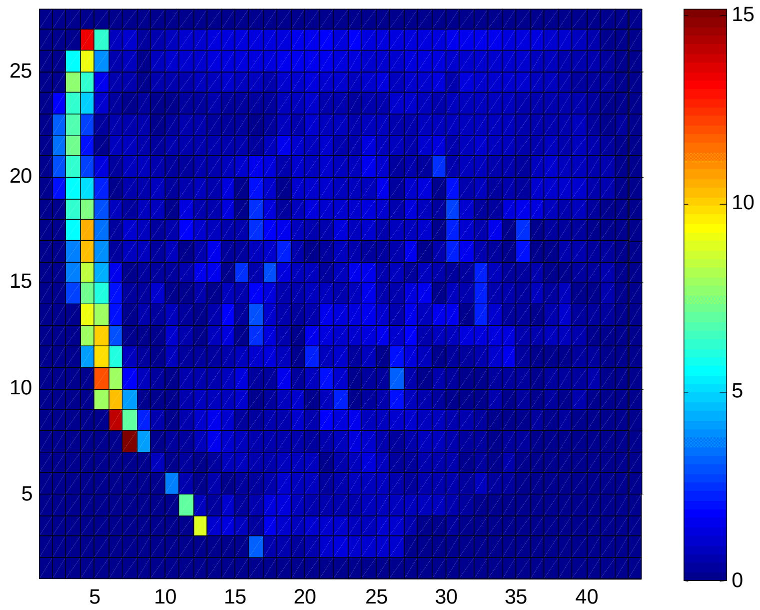


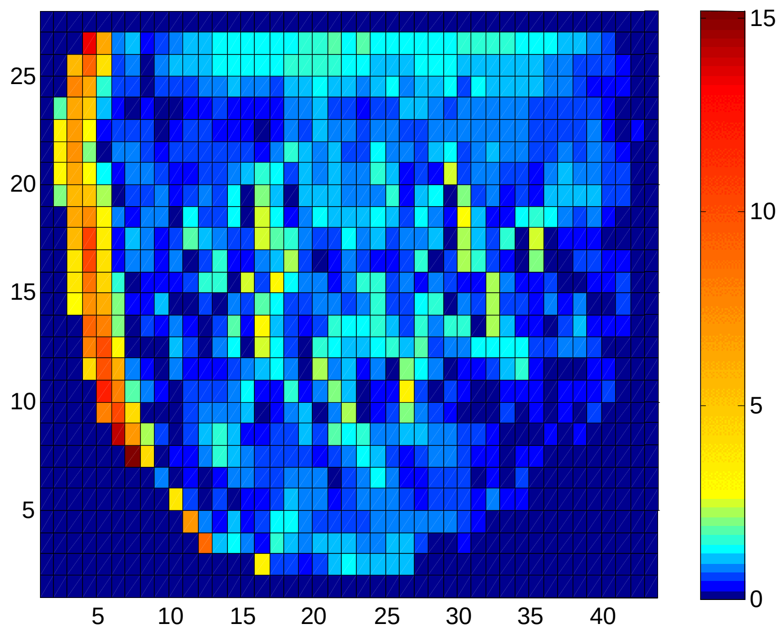


Figure 6.3.9: Percent Difference in Energy Deposition Estimate between COMET and Reference Calculations for Prostate Phantom with 1cm x 1cm Meshes with 18 MeV Incident Photon Beam – The bottom figure has had the colormap altered to better highlight the energy deposition in the lower percentage range.

**Mesh Size: 0.5 cm x 0.5 cm**

The prostate benchmark was then decomposed into 0.5 cm x 0.5 cm meshes. The dimensions of the benchmark are 26 cm x 42 cm. This benchmark problem is shown below in Figure 6.3.9. The same incident beam definitions apply here. Five material definitions were also used here. As before, for each incident beam definition, response function libraries were generated in around 420 hours for all the material definitions.

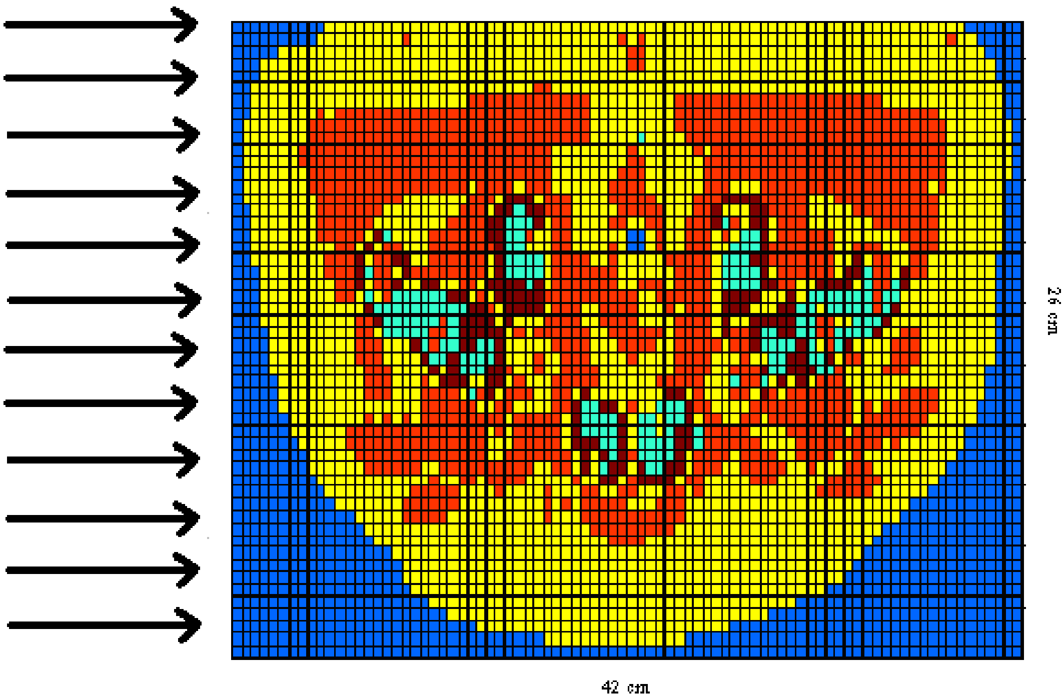


Figure 6.3.10: Prostate Phantom Description with 0.5cm x 0.5cm Meshes
Dark Blue: Air
Light Blue: Bone Marrow
Yellow: Adipose Tissue
Orange: Muscle
Dark Red: Skeleton

Below in Figures 6.3.11, 6.3.12, and 6.3.13, the energy deposition plots for the 2 MeV, 6 MeV, and 18 MeV cases are shown respectively. As before, these energy deposition plots depict what is expected. As photon energy increases, the location of maximal dose occurs deeper within the patient body.

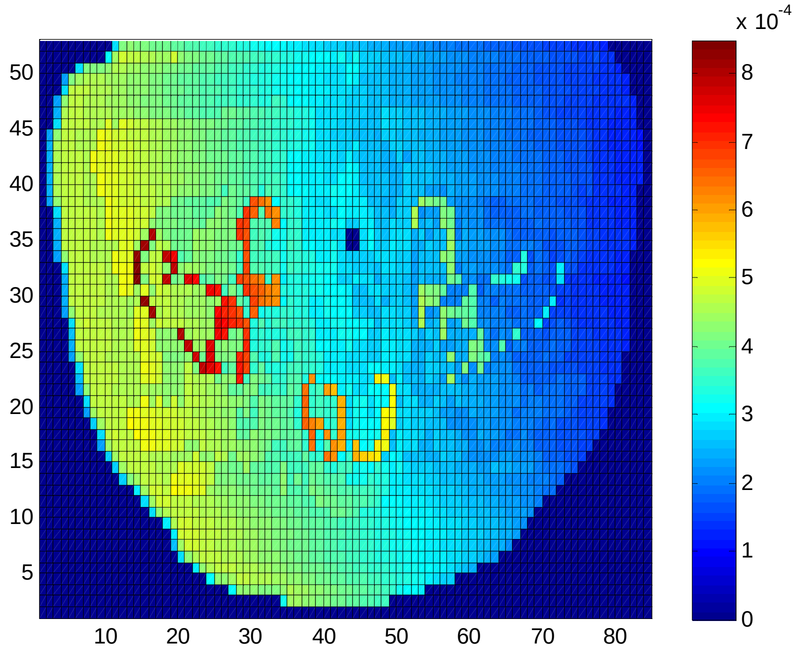


Figure 6.3.11: Energy Deposition Map (MeV) for Prostate Phantom with 0.5cm x 0.5cm Meshes with 2 MeV Incident Photon Beam

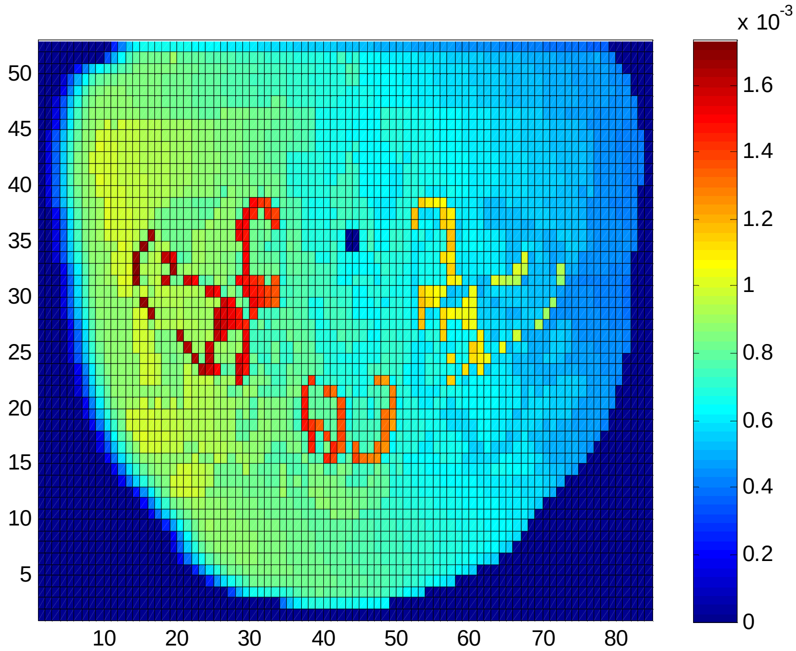


Figure 6.3.12: Energy Deposition Map (MeV) for Prostate Phantom with 0.5cm x 0.5cm Meshes with 6 MeV Incident Photon Beam

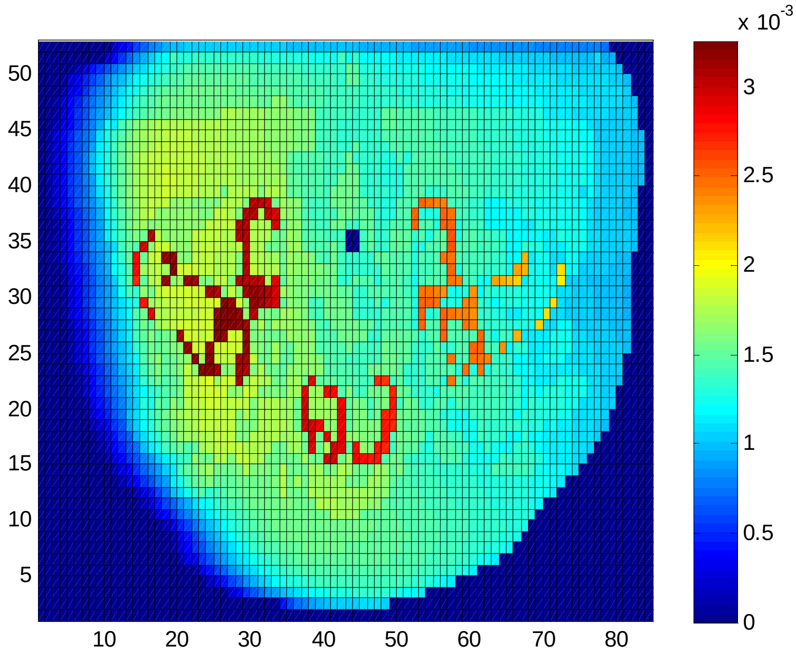


Figure 6.3.13: Energy Deposition Map (MeV) for Prostate Phantom with 0.5cm x 0.5cm Meshes with 18 MeV Incident Photon Beam

The data for comparison of the reference solutions and the COMET solutions are shown below in Tables 6.3.3 and 6.3.4. As has been seen before, as the incident energy increases, the maximal and average percent difference increases as well. For the 2 MeV case, the maximum percent difference is 1.75 %, while the average percent difference is still quite low at 0.31 % with an RMS value of 0.28 %. For the 6 MeV case, the maximum percent difference jumps to 4.14 %, and the average percent difference is still quite low at 0.41 %. The RMS value found for this case is 0.56 %. At 18 MeV, the maximum percent difference becomes quite large at 43.54 %. Compared to the maximum, the average percent difference is still quite small at 1.48 % and an RMS value of 3.24 %. The time required for the COMET solutions for the 2 MeV and 6 MeV cases are both around 80 minutes, while the reference solutions required 1434 hours and 1104 hours respectively of computational time for the reference calculations. The 18 MeV COMET solution took longer at around 114 minutes with a reference solution calculation time of 1622 hours.

Table 6.3.3: Comparison of COMET and Reference Solutions for Prostate Phantom with 0.5cm x 0.5cm Meshes

| | 2 MeV Beam | 6 MeV Beam | 18 MeV Beam |
|---|---|---|---|
| | Comparison without air | Comparison without air | Comparison without air |
| Max % Difference | 1.75 % | 4.14 % | 43.54 % |
| St. Dev. Of Max % Diff. | 0.10 % | 0.14 % | 0.18 % |
| Avg % Difference | 0.31 % | 0.41 % | 1.48 % |
| St. Dev. Of Avg % Diff | 0.28 % | 0.38 % | 3.24 % |
| RMS | 0.42 % | 0.56 % | 3.56 % |

Table 6.3.4: Uncertainty Associated with COMET and Reference Solutions and Running Time Comparison for Prostate Phantom with 0.5cm x 0.5cm

| | 2 MeV Beam | | 6 MeV Beam | | 18 MeV Beam | |
|---|---|---|---|---|---|---|
| | Ref Sol w/o air | COMET Sol w/o air | Ref Sol w/o air | COMET Sol w/o air | Ref Sol w/o air | COMET Sol w/o air |
| Max Rel Std. Dev. | 0.19 % | 0.33 % | 0.10 % | 0.13 % | 0.097 % | 0.21 % |
| Avg Re Std. Dev. | 0.050 % | 0.074 % | 0.039 % | 0.045 % | 0.030 % | 0.05 % |
| Comp Time | 1434 hrs | 79.7 min | 1104 hrs | 79.5 min | 1622 hrs | 114.3 min |

Below in the following figures are the percent difference plots for each of the incident beam energies. For the 2 MeV case, the maximum percent error occurs in the region furthest from the beam in the area of least energy deposition. For the 6 MeV beam, the largest error occurs in the region of the phantom closest to the surface on which the beam is incident, where the lowest energy deposition occurs. For the 18 MeV case, this error continues as the beam enters further inside the patient. Once again, this is due to the electrons liberated in this area and the high correlation between their energy and angle. The Legendre polynomial expansions may not be high enough to accurately describe this situation. As with the lung case, the smaller the mesh size results in a higher the percent difference.

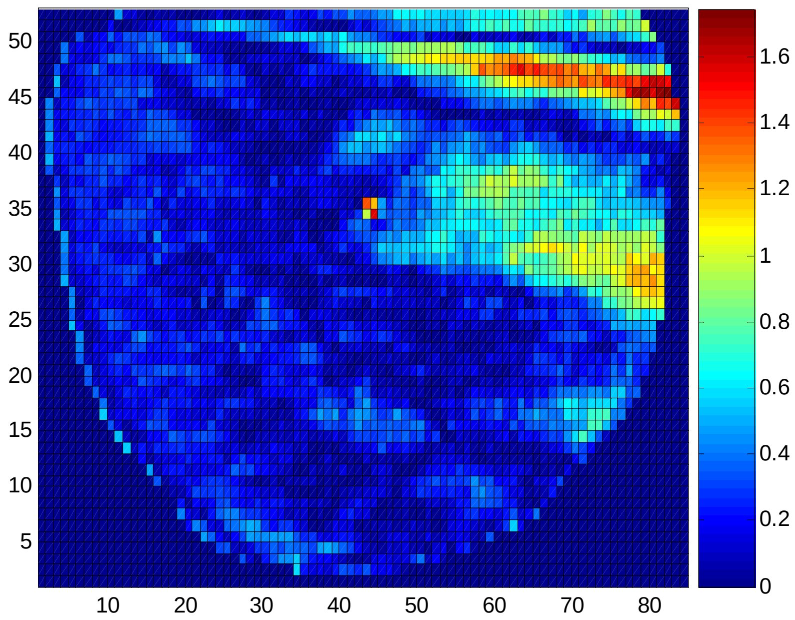


Figure 6.3.14: Percent Difference in Energy Deposition Estimate between COMET and Reference Calculations for Prostate Phantom with 0.5cm x 0.5cm Meshes with 2 MeV Incident Photon Beam

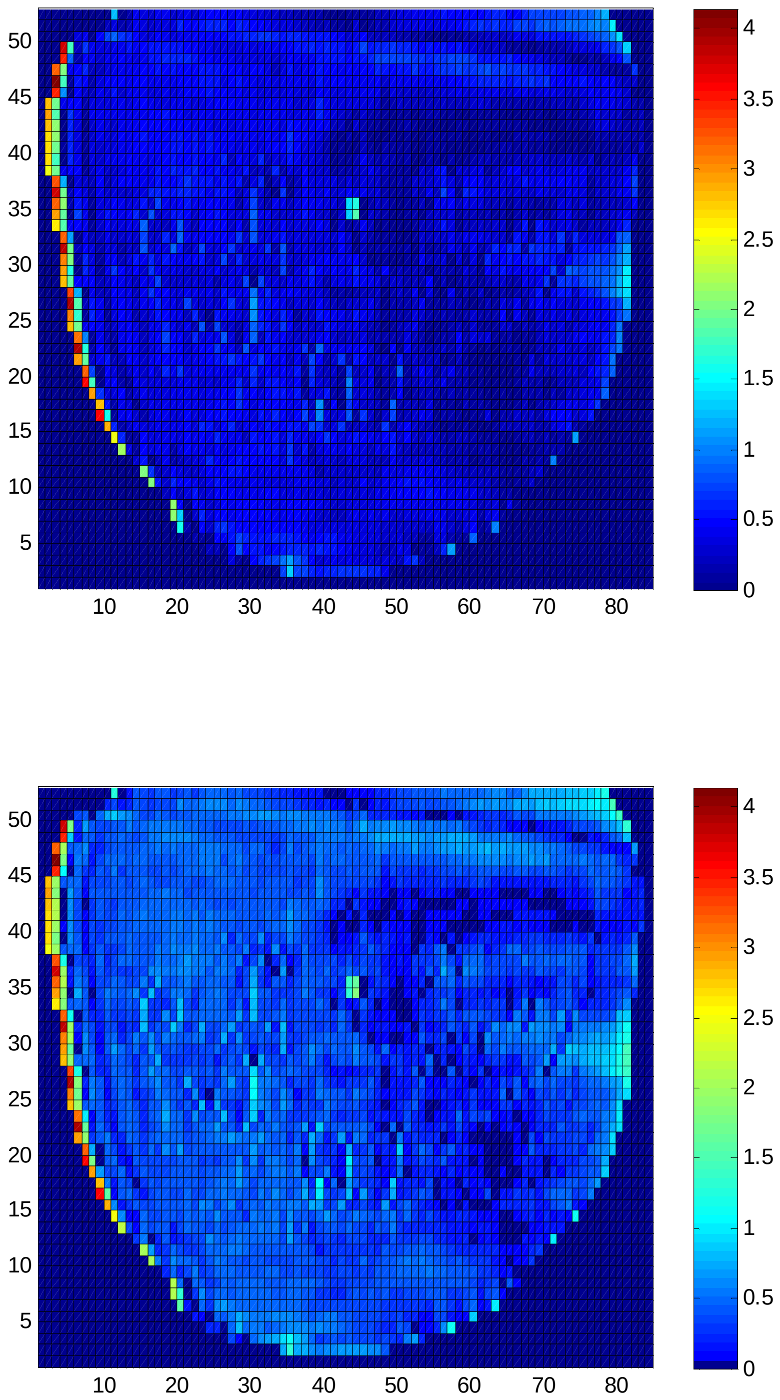


Figure 6.3.15: Percent Difference in Energy Deposition Estimate between COMET and Reference Calculations for Prostate Phantom with 0.5cm x 0.5cm Meshes with 6 MeV Incident Photon Beam – The bottom figure has had the colormap altered to better highlight the energy deposition in the lower percentage range.

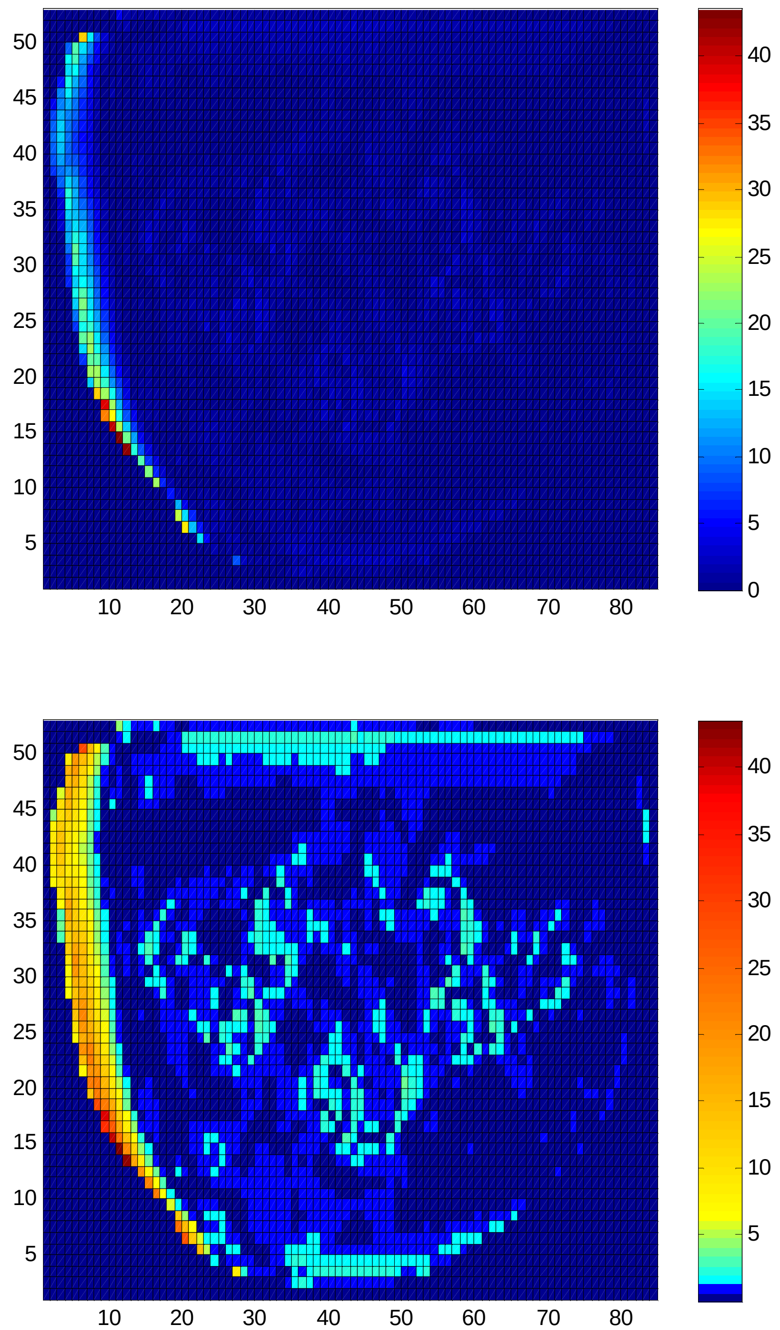


Figure 6.3.16: Percent Difference in Energy Deposition Estimate between COMET and Reference Calculations for Prostate Phantom with 0.5cm x 0.5cm Meshes with 18 MeV Incident Photon Beam – The bottom figure has had the colormap altered to better highlight the energy deposition in the lower percentage range.

**Mesh Size: 0.25 cm x 0.25 cm**

A third mesh size of 0.25 cm x 0.25 cm was also tested here. It can be seen below in Figure 6.3.12. This smaller mesh size captures much more detail than the larger meshes seen earlier. The dimensions of the entire phantom are 25.5 cm x 41.5 cm. Again, the incident photon beam of energies 2 MeV, 6 MeV, or 18 MeV are incident on the left face along the entire length of the phantom. The third dimension extends to infinity in both directions. Five material definitions were used. Response function libraries were pre-computed for each incident beam energy. For each energy, all of the material response function libraries were generated in around 420 hours.

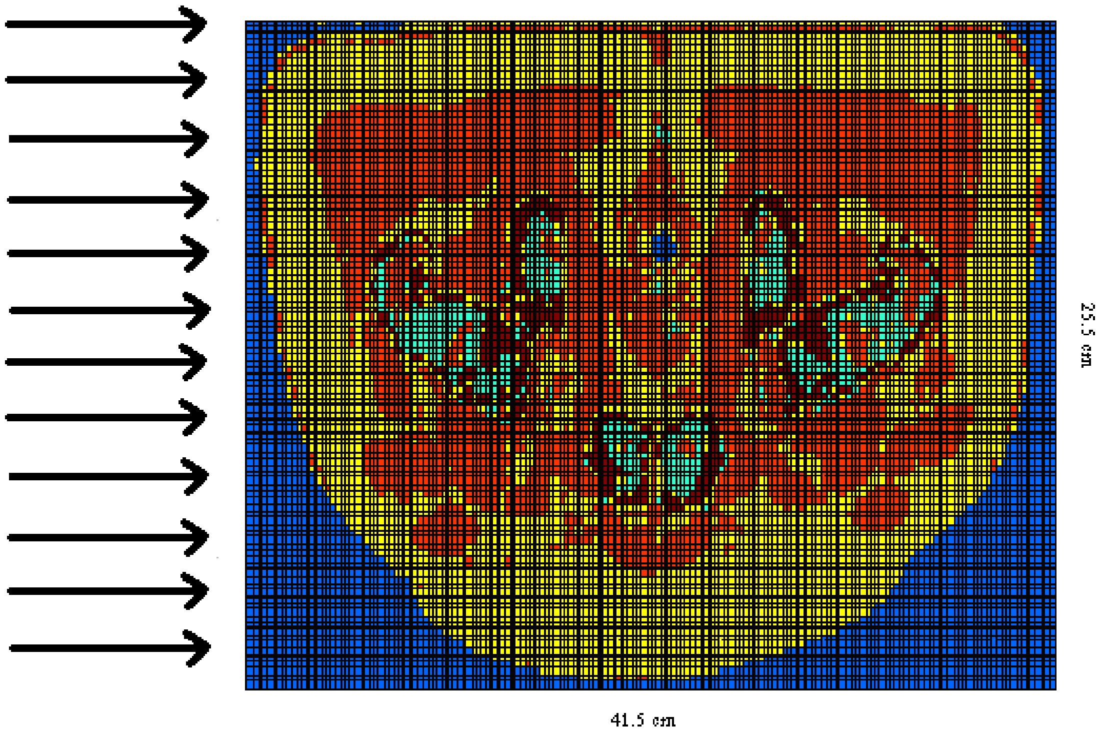


Figure 6.3.17: Prostate Phantom Description with 0.25cm x 0.25cm Meshes
Dark Blue: Air
Light Blue: Bone Marrow
Yellow: Adipose Tissue
Orange: Muscle
Dark Red: Skeleton

The energy deposition plots for this mesh size can be seen below in the following figures. Once again, this does show the results that one would expect with maximal energy deposition occurring deeper within the phantom with increasing photon energy.

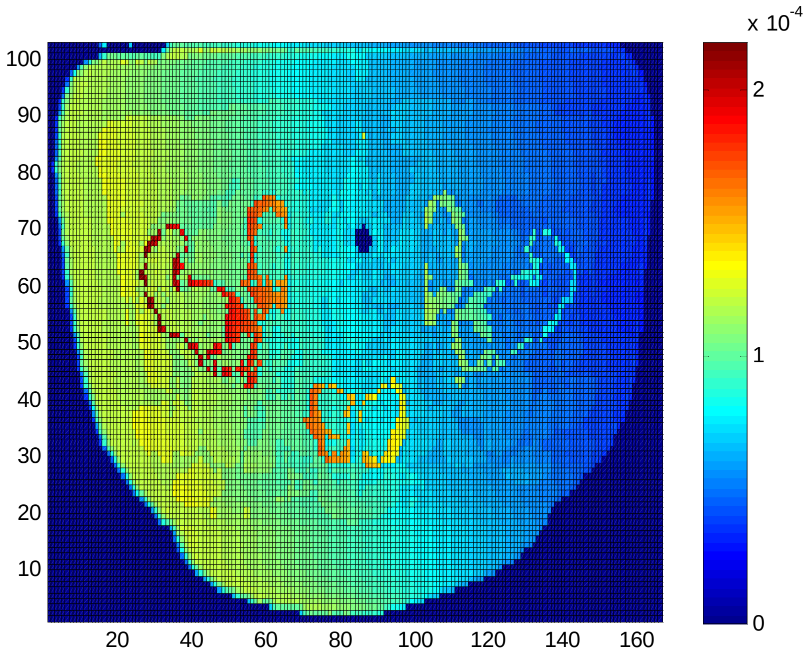


Figure 6.3.18: Energy Deposition Map (MeV) for Prostate Phantom with 0.25cm x 0.25cm Meshes with 2 MeV Incident Photon Beam

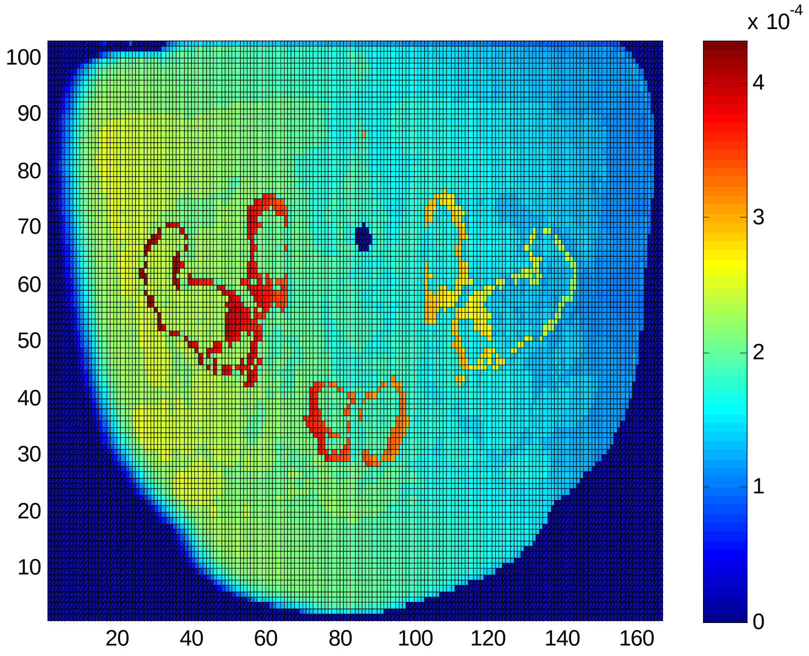


Figure 6.3.19: Energy Deposition Map (MeV) for Prostate Phantom with 0.25cm x 0.25cm Meshes with 6 MeV Incident Photon Beam

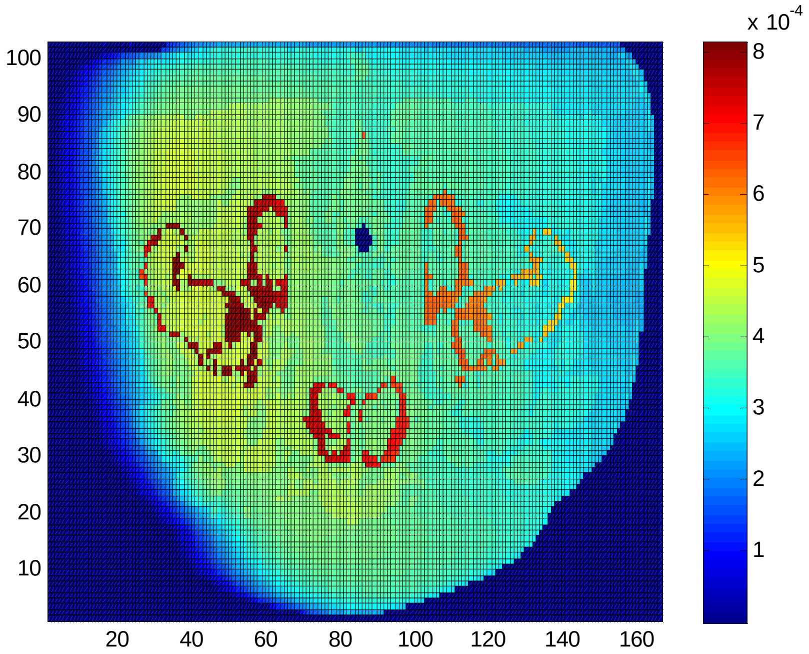


Figure 6.3.20: Energy Deposition Map (MeV) for Prostate Phantom with 0.25cm x 0.25cm Meshes with 18 MeV Incident Photon Beam

In Table 6.3.5 and 6.3.6, the comparison results are shown. For this scenario, the maximum and average percent difference for the 2 MeV incident beam is actually higher than that for the 6 MeV incident beam. For the 2 MeV case, the maximum percent difference is 21.21%, while the average percent difference is 0.94 %. The RMS value for this case was found to be 0.30 %. The 6 MeV case produces a maximum percent difference of 10.24 % and an average percent difference of just over half a percent at 0.56 % with an RMS value of 1.00 %. The values become much larger for the 18 MeV case. The maximum percent difference is 101.90 %, while the average percent difference is 2.06 %. A value of 6.25 % was found for the 18 MeV incident beam case.

The computation time required for COMET does increase as the mesh size increases; however, the reference calculation increases as well. For the 2 MeV case, the COMET solution required around 400 minutes, while the reference calculation took 3223 hours, which is close to 2 months. The 6 MeV reference case required 3156 hours, whiel the COMET solution was found in 311 minutes. Lastly, the 18 MeV case took around 3380 hours to successfully compute; however, the COMET solution only took 400 minutes.

Table 6.3.5: Comparison of COMET and Reference Solutions for Prostate Phantom with 0.25cm x 0.25cm Meshes

| | 2 MeV Beam | 6 MeV Beam | 18 MeV Beam |
|---|---|---|---|
| | Comparison without air | Comparison without air | Comparison without air |
| Max % Difference | 2.00 % | 10.24 % | 101.90 % |
| St. Dev. Of Max % Diff. | 0.37 % | 0.22 % | 0.24 % |
| Avg % Difference | 0.24 % | 0.56 % | 2.06 % |
| St. Dev. Of Avg % Diff | 0.18 % | 0.83 % | 5.91 % |
| RMS | 0.30 % | 1.00 % | 6.25 % |

Table 6.3.6: Uncertainty Associated with COMET and Reference Solutions and Running Time Comparison for Prostate Phantom with 0.25cm x 0.25cm

| | 2 MeV Beam | | 6 MeV Beam | | 18 MeV Beam | |
|---|---|---|---|---|---|---|
| | Ref Sol w/o air | COMET Sol w/o air | Ref Sol w/o air | COMET Sol w/o air | Ref Sol w/o air | COMET Sol w/o air |
| Max Rel Std. Dev. | 0.35 % | 0.37% | 0.19 % | 0.18 % | 0.19 % | 0.27 % |
| Avg Re Std. Dev. | 0.081 % | 0.079% | 0.057 % | 0.04 % | 0.043 % | 0.053 % |
| Comp Time | 3223 hrs | 400.5 min | 3156 hrs | 311.4 min | 3380 hrs | 400.3 min |

Below in the next three figures, the percent differences are plotted. For the 2 MeV case, the maximum percent difference occurs in the region furthest from the beam as with all the previous cases. As before, the maximum percent dose for the 6 MeV case occurs closer to the surface, where smaller amounts of energy are deposited. This percent difference does continue to be a factor for the 18 MeV case for the first few centimeters within the phantom body for each of the reasons presented earlier. Higher expansion orders in angle are needed to better model the liberated electrons for the high-energy photon beam. Higher expansion orders are needed for all incident beam energies since the mesh size has been made so small. The current expansion order cannot correctly handle the liberated electrons depositing portions of their energy within a coarse-mesh.

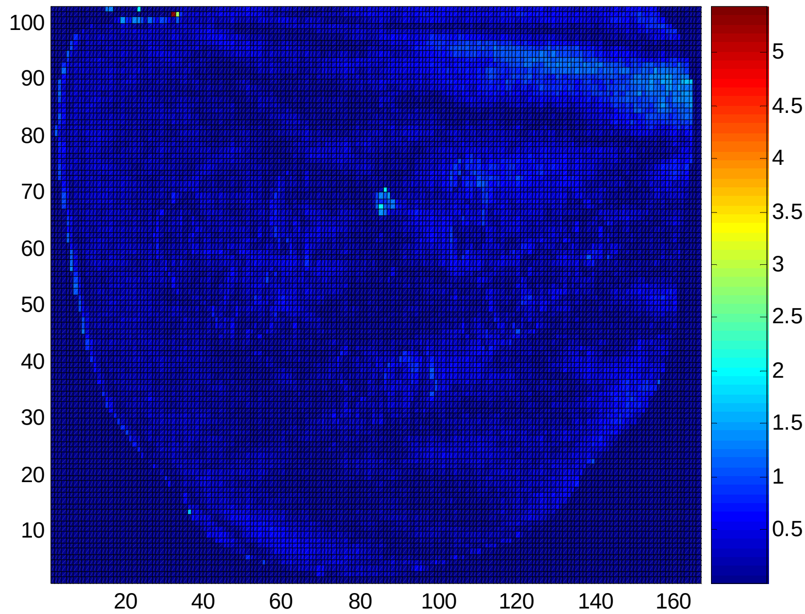


Figure 6.3.21: Percent Difference in Energy Deposition Estimate between COMET and Reference Calculations for Prostate Phantom with 0.25cm x 0.25cm Meshes with 2 MeV Incident Photon Beam

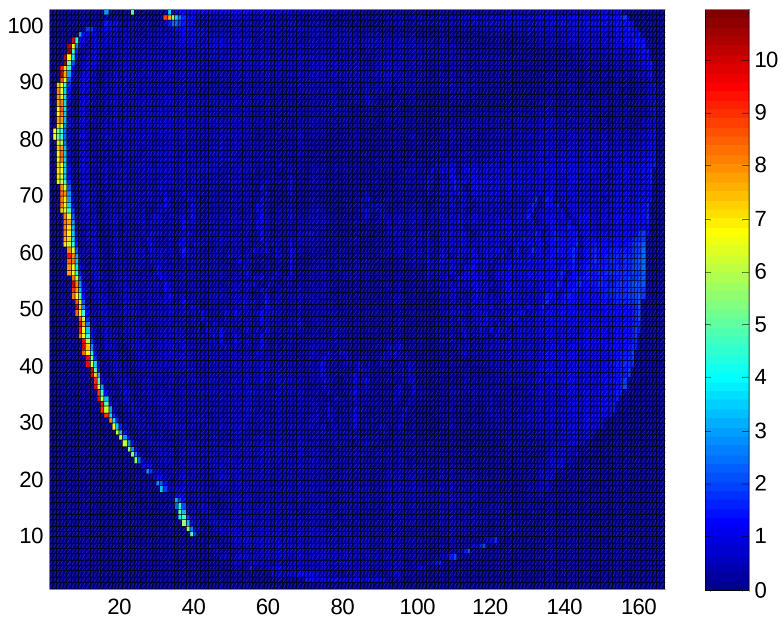


Figure 6.3.22: Percent Difference in Energy Deposition Estimate between COMET and Reference Calculations for Prostate Phantom with 0.25cm x 0.25cm Meshes with 6 MeV Incident Photon Beam

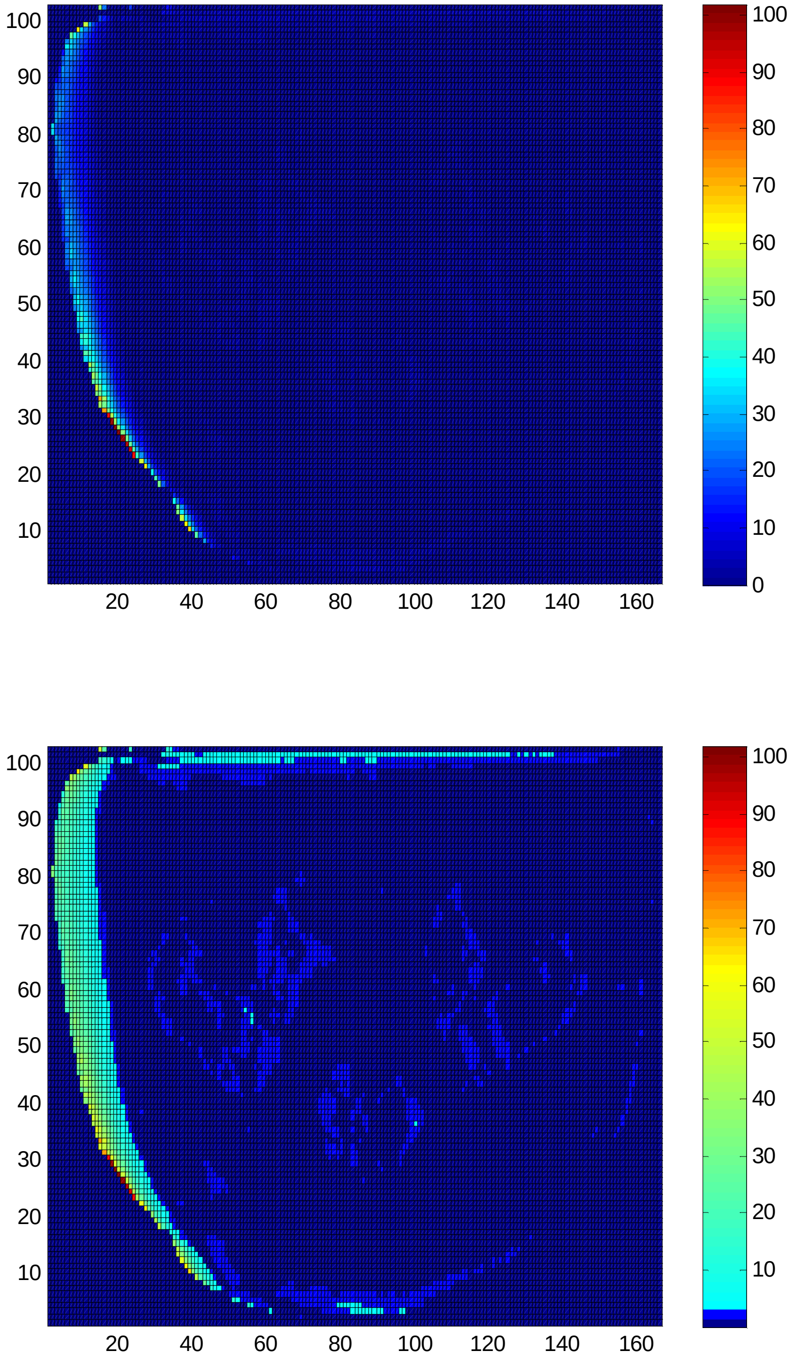


Figure 6.3.23: Percent Difference in Energy Deposition Estimate between COMET and Reference Calculations for Prostate Phantom with 0.25cm x 0.25cm Meshes with 18 MeV Incident Photon Beam – The bottom figure has had the colormap altered to better highlight the energy deposition in the lower percentage range.

## 6.4 Beam Re-Entry Benchmark

Previously all of the benchmark problems have been very regular in shape. The simple phantoms were all rectangular in shape, and the prostate and lung scans were quite oval. In this case, a scan was chosen that had a very irregular boarder to determine how well the methodology would handle this situation. The final CT scan benchmark was developed from the scan shown in Figure 6.4.1. The image shows a patient being cradled by a piece of Plexiglas to keep them positioned correctly during treatment. In this situation, the beam may exit a region of the arm and re-enter a portion of the neck/torso. This re-entry can sometimes cause radiation burns at the site of re-entry, thus it is important to correctly identify the amount of energy deposited in this region to avoid these unwanted side effects if possible.[4] As with the two previous CT benchmarks, the beam re-entry case was segmented using the program SCAN2MCNP.[31] The segmentation can be seen in Figure 6.4.2. The segmented image was then combined to form benchmark problems with differing mesh sizes of 1cm x 1cm, 0.5cm x 0.5cm, and 0.25cm x 0.25cm, and three incident beam energies of 2 MeV, 6 MeV, and 18 MeV were studied as before.

Figure 6.4.1: Beam Re-Entry CT Scan

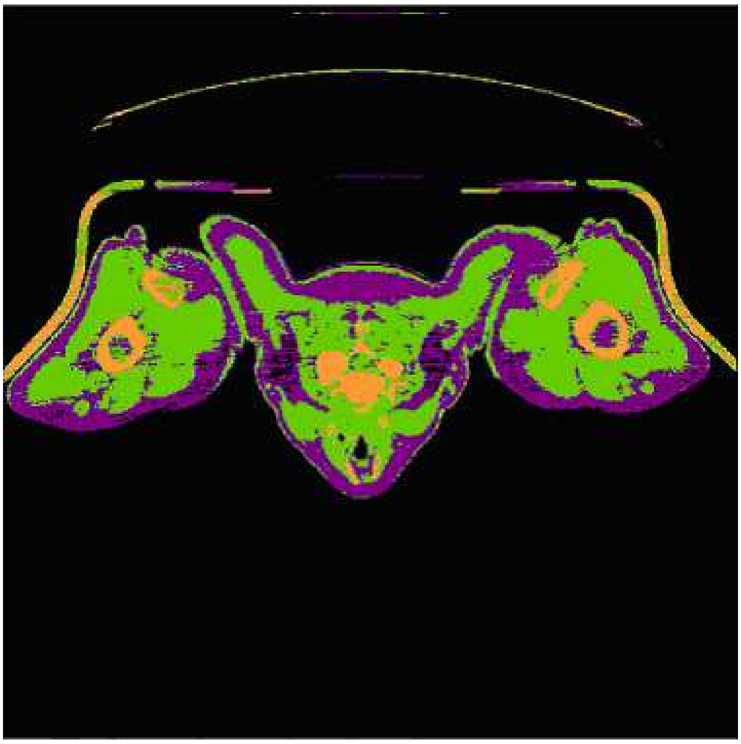

Figure 6.4.2: Segmented Beam Re-Entry CT Scan

**Mesh Size:  1 cm x 1 cm**

Below in Figure 6.4.2, the segmented CT scan was combined to form 1cm x 1cm coarse meshes.  Only a portion of the CT scan was chosen in order to focus attention on one area where beam re-entry occurs.  The phantom measures 27 cm x 39 cm with the third dimension extending to infinity in both directions.   As with all the previous cases, the incident photon beam impinges perpendicularly along the left face along the entire length of the phantom.  Five material definitions were defined in this case.  For each beam energy, response function libraries were pre-computed in around 420 hours for all of the material definitions.

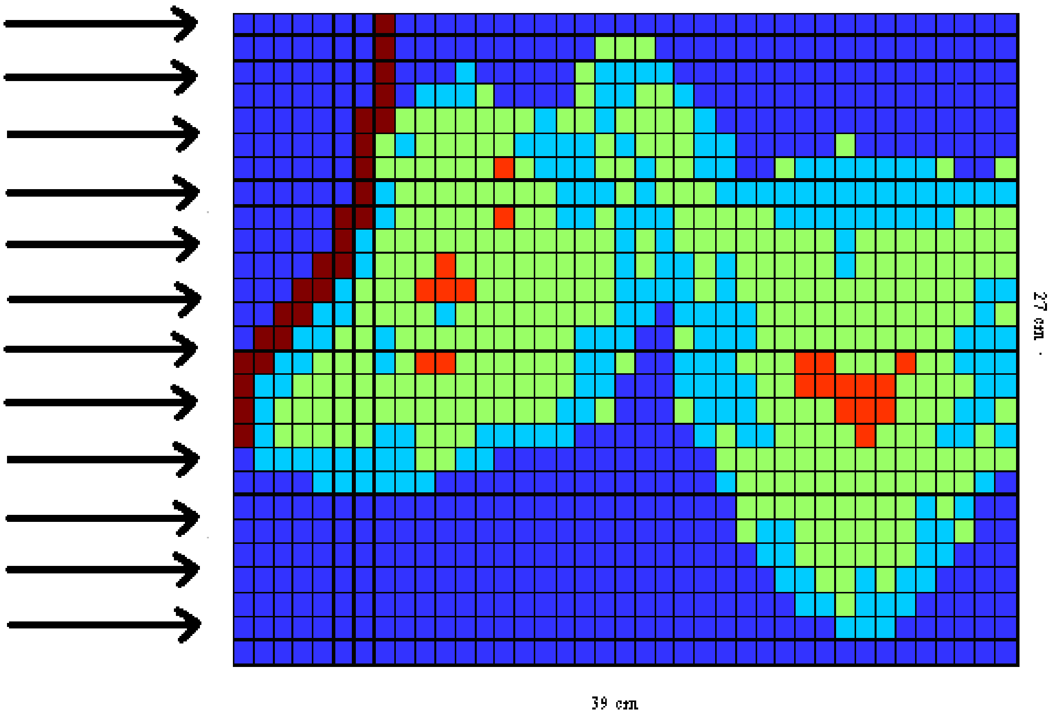


Figure 6.4.3:  Beam Re-Entry  Phantom Description with 1cm x 1cm Meshes
Dark Blue:  Air
Light Blue:  Adipose Tissue
Green:  Muscle
Orange:  Skeleton
Dark Red:  Plexiglas

The next three figures show the energy deposition for each incident beam energy – 2 MeV, 6 MeV, and 18 MeV. These plots show that the energy deposition for each case is as to be expected. As the incident energy increases, the location of maximal dose occurs deeper within the tissue. The bone region closest to the incident beam does receive a higher amount of energy deposition.

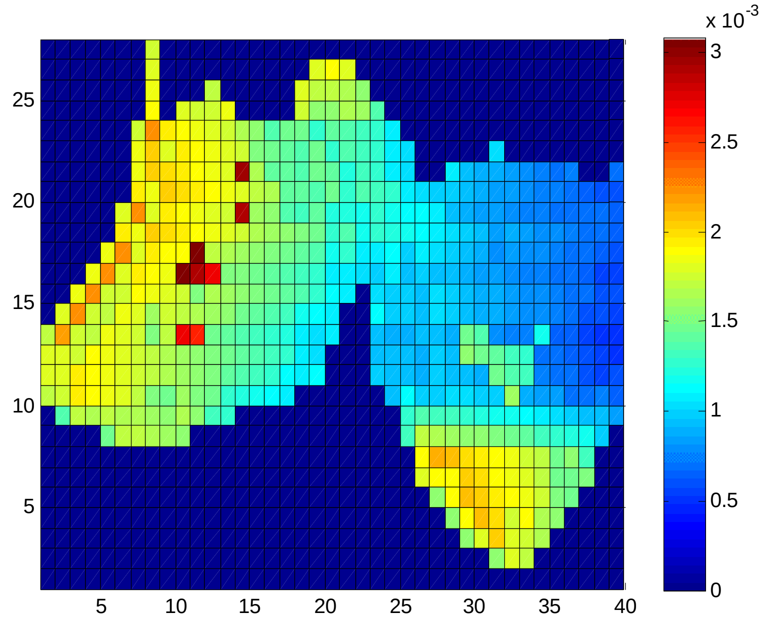


Figure 6.4.4: Energy Deposition Map (MeV) for Beam Re-Entry Phantom with 1cm x 1cm Meshes with 2 MeV Incident Photon Beam

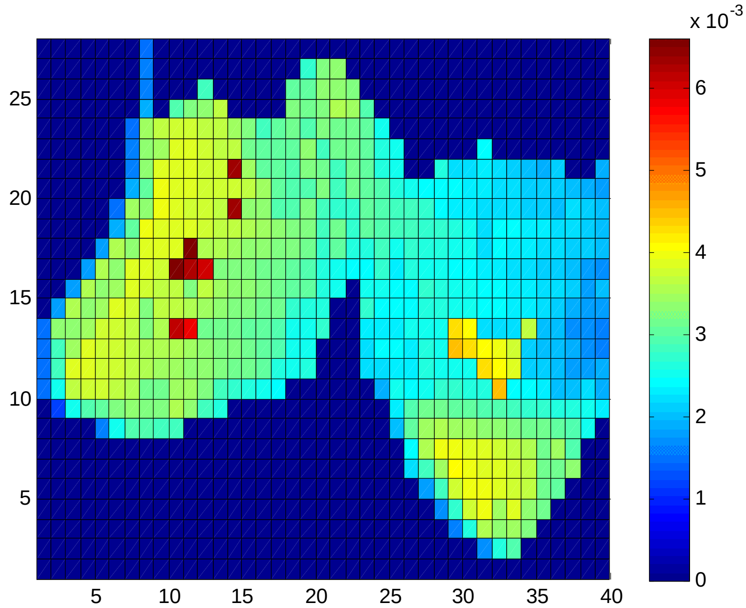


Figure 6.4.5: Energy Deposition Map (MeV) for Beam Re-Entry Phantom with 1cm x 1cm Meshes with 6 MeV Incident Photon Beam

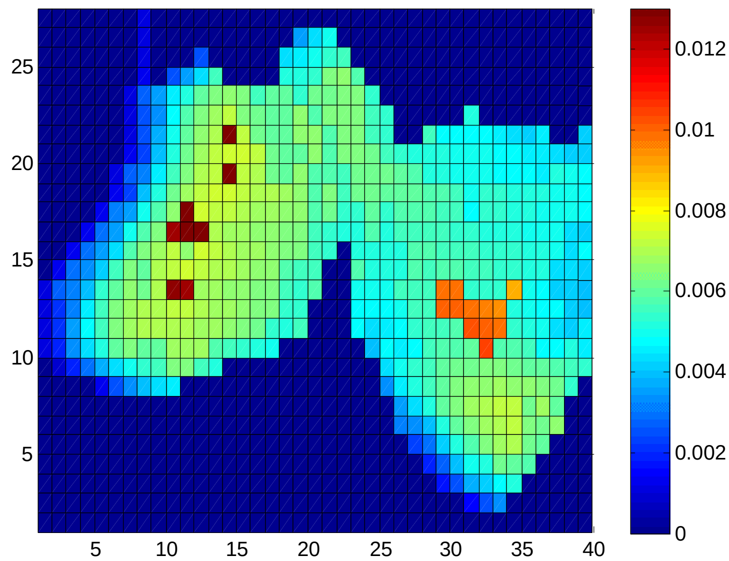


Figure 6.2.6: Energy Deposition Map (MeV) for Lung Phantom with 1cm x 1cm Meshes with 2 MeV Incident Photon Beam

Previously, comparison data was given for only benchmark problem excluding the air region.  In this case, results are given excluding the air and the Plexiglas regions since neither are parts of the human body.  In Table 6.4.1, it can be seen that the maximum percent error increases as the incident energy beam increases as well.  For the 2 MeV incident beam, the maximum percent difference is slightly high at 2.60%; however, the average is still low at 0.59%.  For the 6 MeV case, the maximum percent difference is even higher at 9.13%, but the average percent difference is slightly lower than that for the 2 MeV case at 0.52%.  The maximum percent difference for the 18 MeV case is even larger at 19.22%, but the average once again stays fairly low at 1.17%.

Table 6.4.2 shows the statistical results for both the COMET and reference solutions as well as calculation timing information.  For each of the three incident energy beam cases, the time required to run the COMET solution was around 16.6 to 16.7 minutes.  The EGSnrc reference cases required much more computational time at 278 hours, 400 hours, and 450 hours for the 2 MeV, 6 MeV, and 18 MeV incident beam cases respectively.

Table 6.4.1:  Comparison of COMET and Reference Solutions for Beam Re-Entry Phantom with 1cm x 1cm Meshes

| | 2 MeV Beam | 6 MeV Beam | 18 MeV Beam |
|---|---|---|---|
| | Comparison without air or Plexiglas | Comparison without air or Plexiglas | Comparison without air or Plexiglas |
| Max % Difference | 2.60 % | 9.13 % | 19.22 % |
| St. Dev. Of Max % Diff. | 0.050 % | 0.07 % | 0.10 % |
| Avg % Difference | 0.59 % | 0.52 % | 1.17 % |
| St. Dev. Of Avg % Diff | 0.57 % | 0.77 % | 1.98 % |
| RMS | 0.82 % | 0.93 % | 2.30 % |

Table 6.4.2: Uncertainty Associated with COMET and Reference Solutions and Running Time Comparison for Beam Re-Entry Phantom with 1cm x 1cm Meshes

| | 2 MeV Beam | | 6 MeV Beam | | 18 MeV Beam | |
|---|---|---|---|---|---|---|
| | Ref Sol w/o air or Plexiglas | COMET Sol w/o air or Plexiglas | Ref Sol w/o air or Plexiglas | COMET Sol w/o air or Plexiglas | Ref Sol w/o air or Plexiglas | COMET Sol w/o air or Plexiglas |
| Max Rel Std. Dev. | 0.041 % | 0.058 % | 0.035 % | 0.072 % | 0.046 % | 0.13 % |
| Avg Re Std. Dev. | 0.028 % | 0.045 % | 0.025 % | 0.041 % | 0.020 % | 0.049% |
| Comp Time | 278 hrs | 16.7 min | 400 hrs | 16.6min | 450 hrs | 16.6 min |

In the next three figures, the percent difference is shown for each of the three energy cases. The results obtained are similar to those seen previously. For the 2 MeV case, maximal error occurs within the body furthest from the incident photon beam. For the 6 MeV, errors occur closer to the skin surface nearest the incident photon beam. These result due to the location of minimal energy deposition. The 18 MeV case still produces the largest percent difference between the COMET solution and the reference solution. Again, this is due to the inability of the energy and angle coefficients to accurately describe the tracks and energy deposition of the liberated electrons.

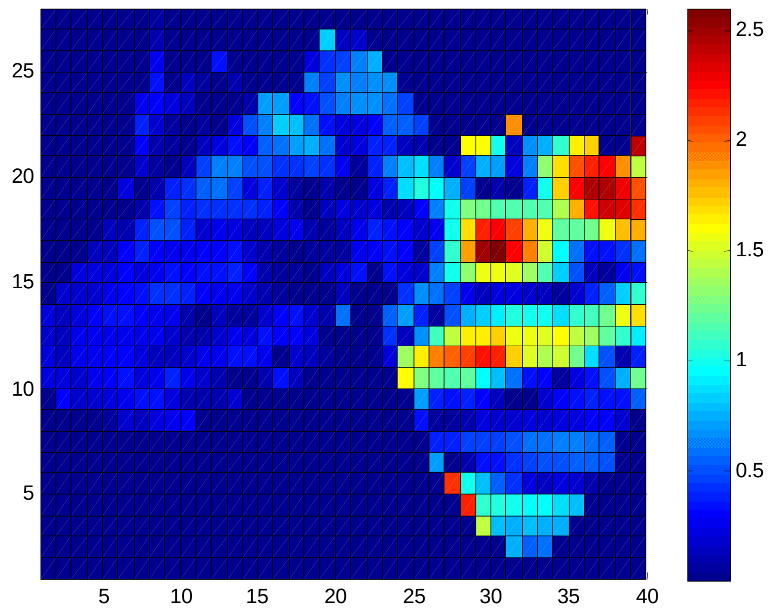


Figure 6.4.7: Percent Difference in Energy Deposition Estimate between COMET and Reference Calculations for Beam Re-Entry Phantom with 1cm x 1cm Meshes with 2 MeV Incident Photon Beam

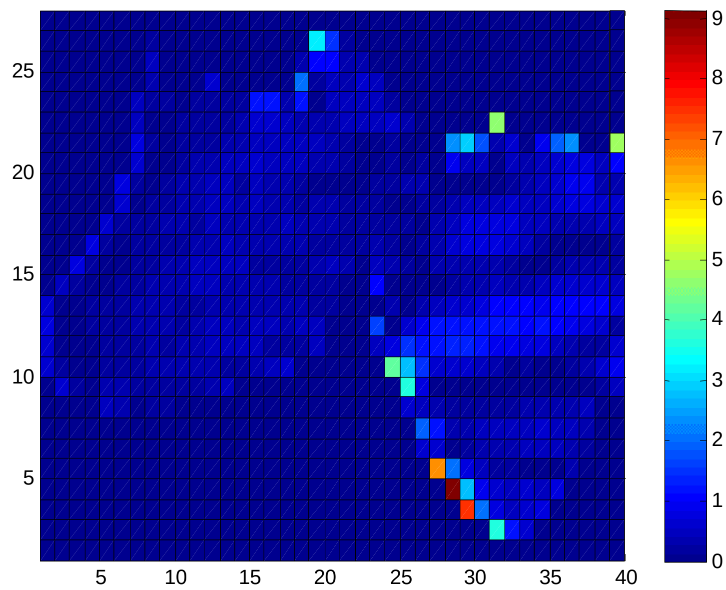


Figure 6.4.8: Percent Difference in Energy Deposition Estimate between COMET and Reference Calculations for Beam Re-Entry Phantom with 1cm x 1cm Meshes with 6 MeV Incident Photon Beam

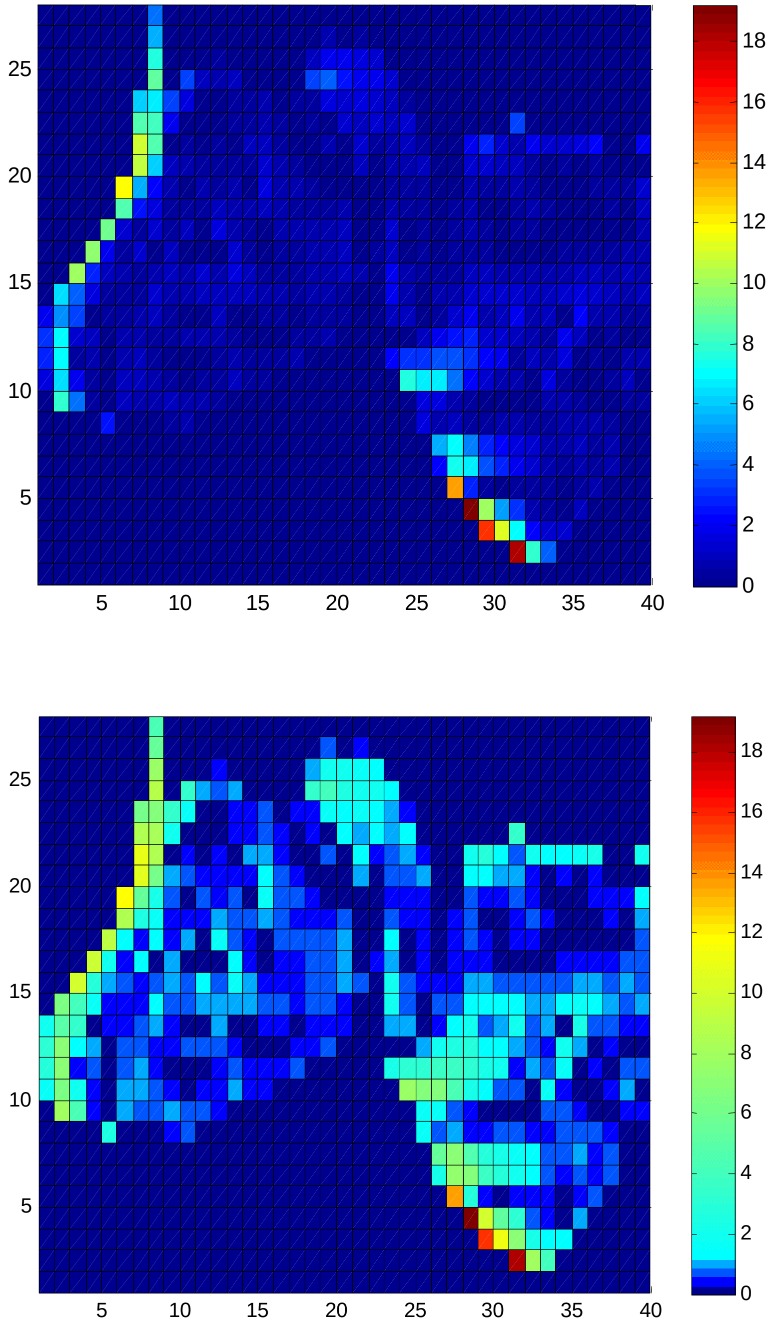


Figure 6.4.8: Percent Difference in Energy Deposition Estimate between COMET and Reference Calculations for Beam Re-Entry Phantom with 1cm x 1cm Meshes with 6 MeV Incident Photon Beam

**Mesh Size: 0.5 cm x 0.5 cm**

The second mesh size tested was 0.5cm x 0.5cm with total dimensions of 26 cm x 39 cm. Again, the third dimension extends to infinity in both directions. In this case, another material definition was used – bone marrow. Previously in the 1 cm x 1 cm case, no bone marrow was included. The benchmark can be seen below in Figure 6.2.10. Here six material definitions are defined. For each of the three incident energy beam cases, response function libraries are generated. For all six of the material definitions for one incident energy beam, 504 hours of pre-computational time was required.

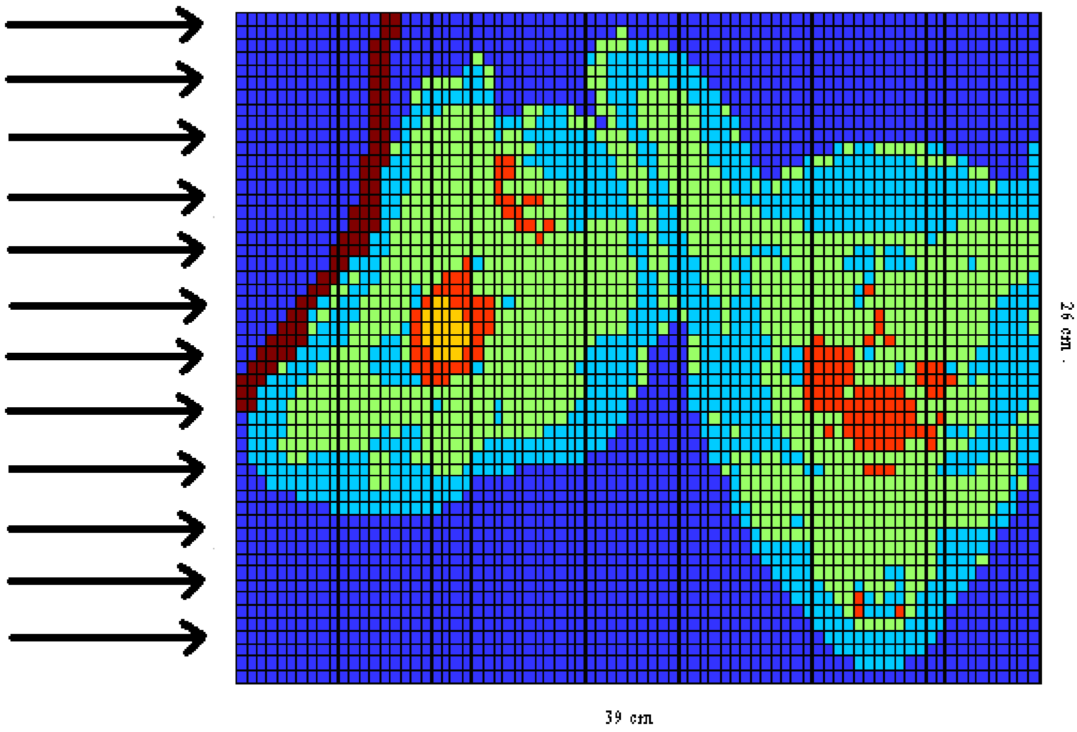


Figure 6.2.10: Beam Re-Entry Phantom Description with 0.5cm x 0.5cm Meshes
Dark Blue: Air
Light Blue: Adipose Tissue
Green: Muscle
Yellow: Bone Marrow
Orange: Skeleton
Dark Red: Plexiglas

Below in the following three figures, the energy deposition is plotted for each of the three incident beam energies. The patterns of energy deposition are what is to be expected. As the energy of the incident photon beam increases, the location of maximal energy deposition occurs deeper within the patient. The bony areas closer to the beam also receive more dose than the surrounding tissue.

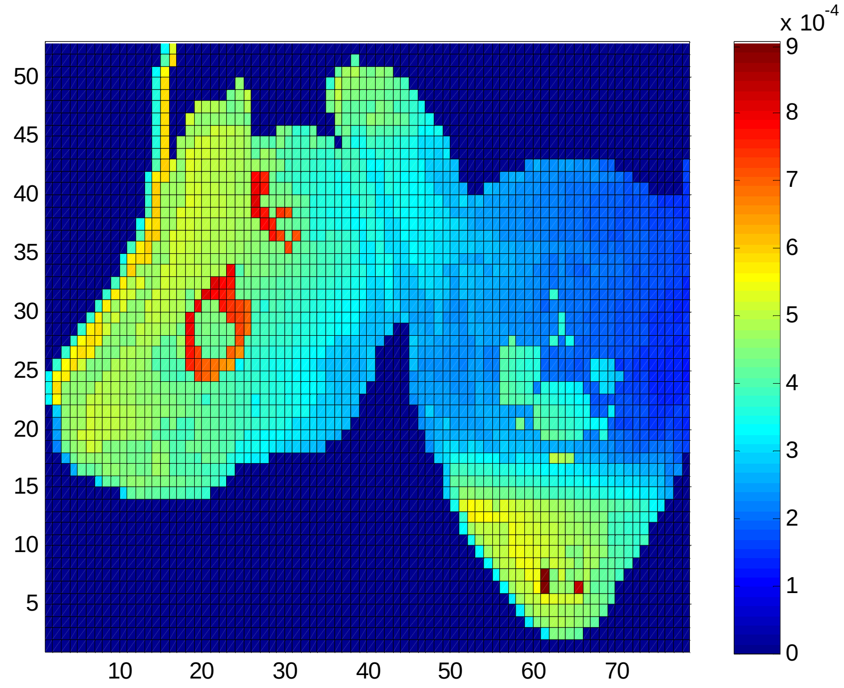


Figure 6.4.11: Energy Deposition Map (MeV) for Beam Re-Entry Phantom with 0.5cm x 0.5cm Meshes with 2 MeV Incdident Beam

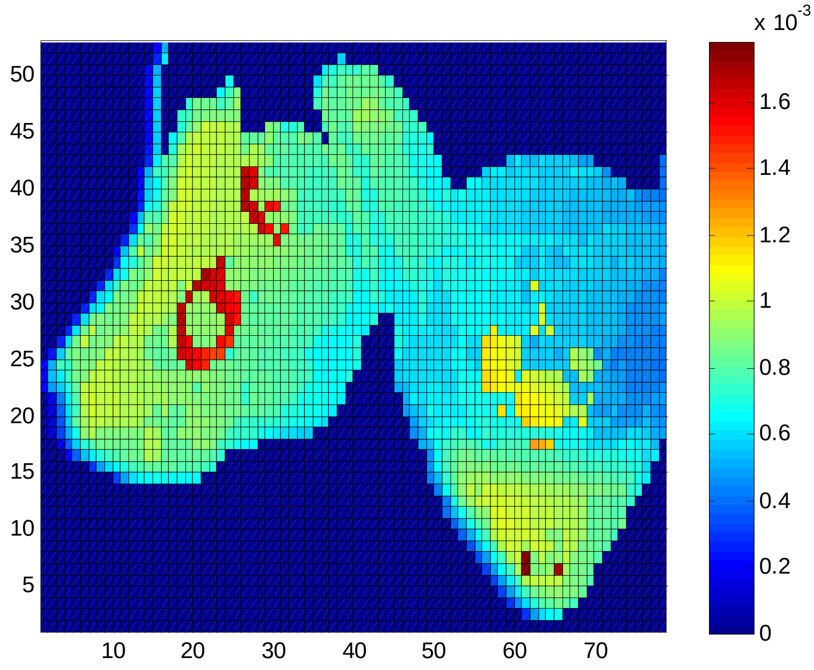


Figure 6.4.12: Energy Deposition Map (MeV) for Beam Re-Entry Phantom with 0.5cm x 0.5cm Meshes with 6 MeV Incident Beam

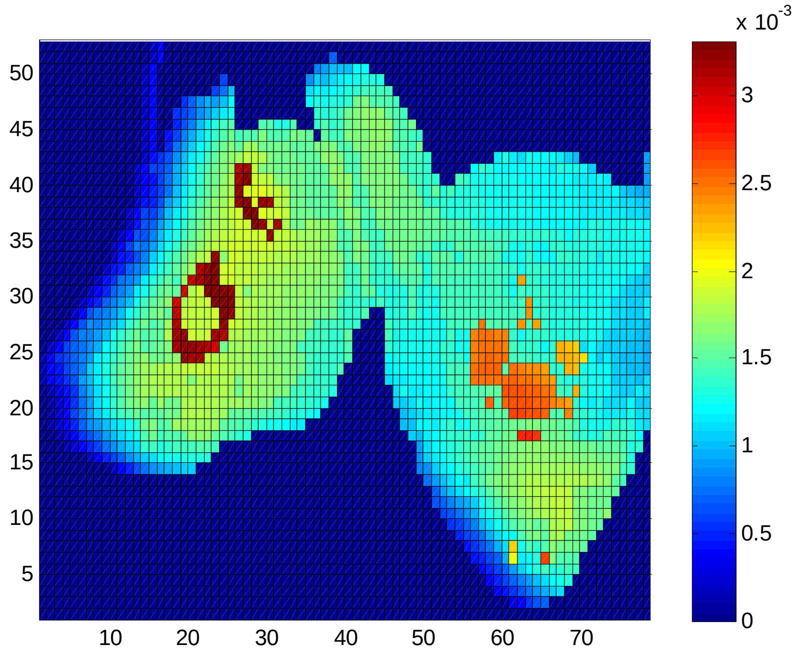


Figure 6.4.13: Energy Deposition Map (MeV) for Beam Re-Entry Phantom with 0.5cm x 0.5cm Meshes with 18 MeV Incident Beam

The data for comparison is shown below in Tables 6.4.3 and 6.4.4. As the incident beam energy increases, the maximum percent difference and average percent difference both increase. Here the percent differences are also higher than those obtained for the larger 1cm x 1cm mesh size. For the 2 MeV case, the maximum and average percent difference was found to be just under 4% and around 0.63 % respectively. The RMS value was found to be 0.87 %. For the 6 MeV, the maximum percent difference is much higher at 15.65 %, while the average percent difference is very similar to that obtained for the 2 MeV case at 0.65 % with an RMS value of 1.19 %. For the 18 MeV case, the maximum percent difference is 25.79 % with the average percent difference of 1.41 %. For this case, an RMS value of 2.99 % was obtained.Each of the COMET cases in this instance required around 76 minutes, while the reference solutions took much longer at 482 hours, 704 hours, and 1048 hours for the 2 MeV, 6 MeV, and 18 MeV incident beam cases respectively.

Table 6.4.3: Comparison of COMET and Reference Solutions for Beam Re-Entry Phantom with 0.5cm x 0.5cm Meshes

| | 2 MeV Beam | 6 MeV Beam | 18 MeV Beam |
|---|---|---|---|
| | Comparison without air or Plexiglas | Comparison without air or Plexiglas | Comparison without air or Plexiglas |
| Max % Difference | 3.95% | 15.65 % | 25.79 % |
| St. Dev. Of Max % Diff. | 0.077 % | 0.089 % | 0.096 % |
| Avg % Difference | 0.61 % | 0.65 % | 1.41 % |
| St. Dev. Of Avg % Diff | 0.62 % | 1.00 % | 2.64 % |
| RMS | 0.87 % | 1.19 % | 2.99 % |

Table 6.4.4: Uncertainty Associated with COMET and Reference Solutions and Running Time Comparison for Beam Re-Entry Phantom with 0.5cm x 0.5cm Meshes

| | 2 MeV Beam | | 6 MeV Beam | | 18 MeV Beam | |
|---|---|---|---|---|---|---|
| | Ref Sol w/o air or Plexiglas | COMET Sol w/o air or Plexiglas | Ref Sol w/o air or Plexiglas | COMET Sol w/o air or Plexiglas | Ref Sol w/o air or Plexiglas | COMET Sol w/o air or Plexiglas |
| Max Rel Std. Dev. | 0.074 % | 0.24 % | 0.077 % | 0.12 % | 0.98 % | 0.18 % |
| Avg Re Std. Dev. | 0.049 % | 0.056 % | 0.038 % | 0.041 % | 0.029 % | 0.05 % |
| Comp Time | 482 hrs | 75.7 min | 704 hrs | 76.0 min | 1048 hrs | 75.8min |

In the following three sets of figures, the percent difference is shown between the reference solutions and the COMET solutions. For the 2 MeV case, the maximum percent difference occurs at the end furthest from the incident photon beam in the areas of minimal energy deposition. For the 6 MeV case, maximum percent error occurs on the faces of the phantom closest to the incident beam. For the 18 MeV case, the maximum percent difference occurs in the region of the phantom closest to the beam. This error occurs here due to the inability of the expansion coefficients to accurately describe the electrons created from the interactions of the photons with the media. The results here are worse than those obtained for the 0.25 cm x 0.25 cm as has been seen with the lung and prostate benchmarks.

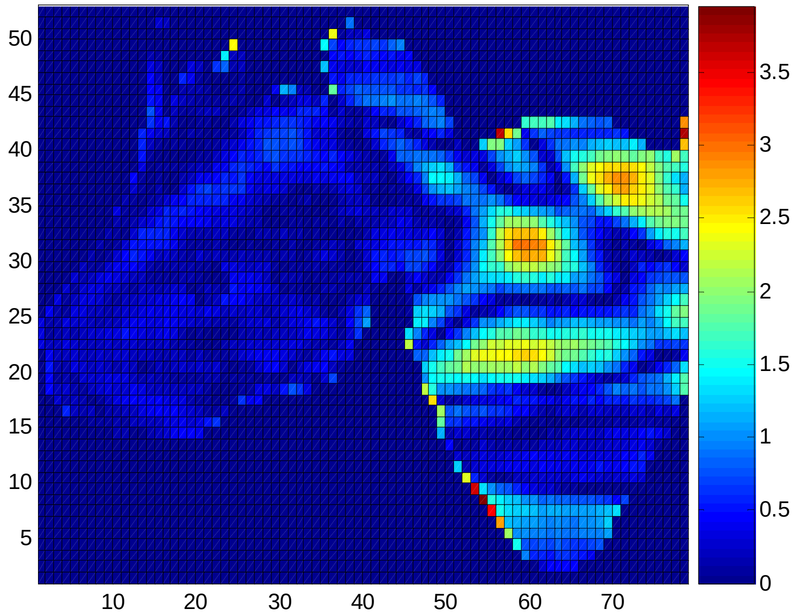


Figure 6.4.14: Percent Difference in Energy Deposition Estimate between COMET and Reference Calculations for Beam Re-Entry Phantom with 0.5cm x 0.5cm Meshes with 2 MeV Incident Photon Beam

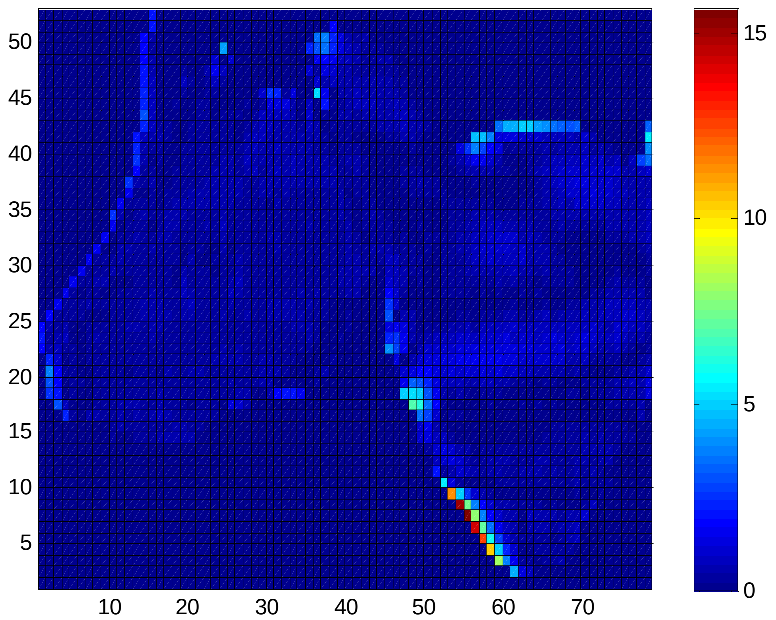


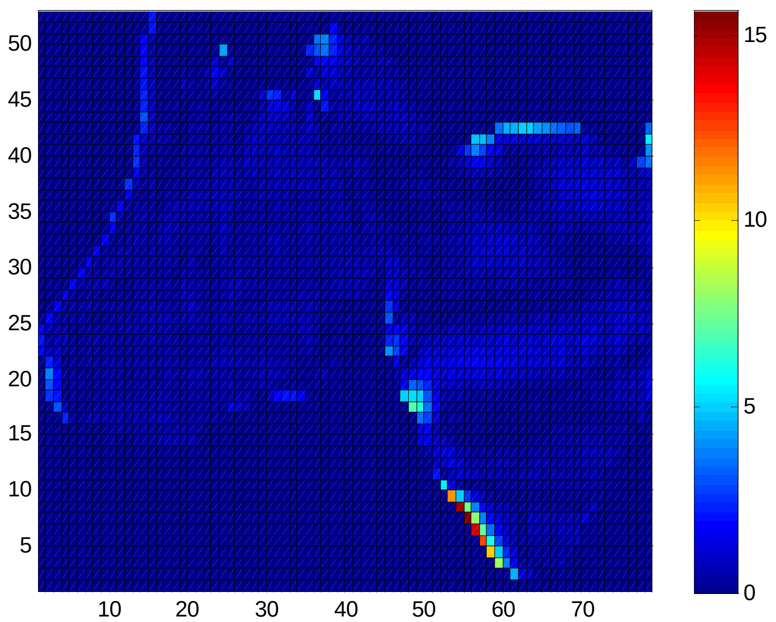


Figure 6.4.15: Percent Difference in Energy Deposition Estimate between COMET and Reference Calculations for Beam Re-Entry Phantom with 0.5cm x 0.5cm Meshes with 6 MeV Incident Photon Beam

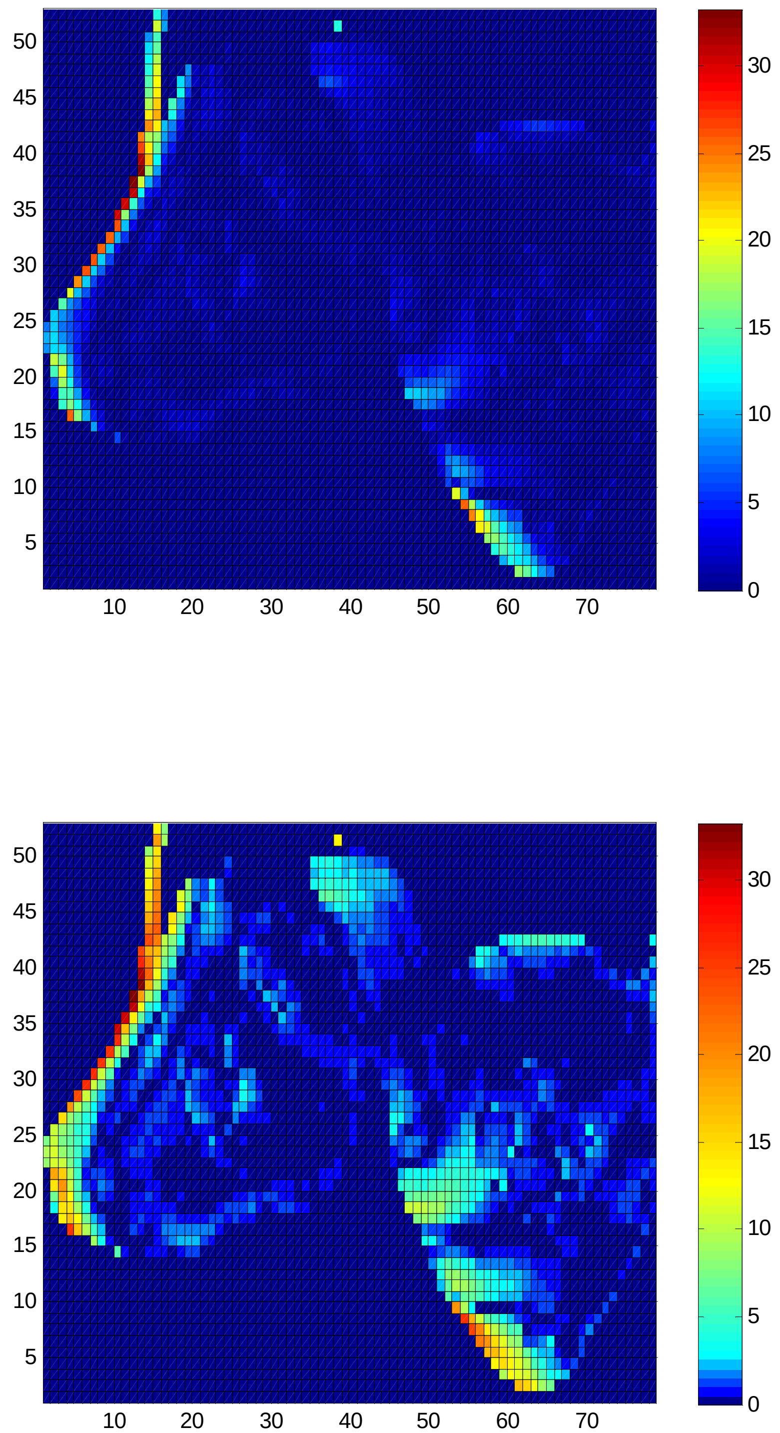


Figure 6.4.16: Percent Difference in Energy Deposition Estimate between COMET and Reference Calculations for Beam Re-Entry Phantom with 0.5cm x 0.5cm Meshes with 18 MeV Incident Photon Beam

**Mesh Size: 0.25 cm x 0.25 cm**

The final coarse mesh size tested here was 0.25 cm x 0.25 cm. The beam re-entry benchmark case is shown below in Figure 6.4.17. The benchmark is 26 cm x 39 cm with the third dimension once again extending to infinity. The figure also shows the location of the incident photon beam along the entire 26 cm face. Six material definitions are used in this case. For each incident beam, 504 hours of pre-computational time was required for the response function generation of all of the materials.

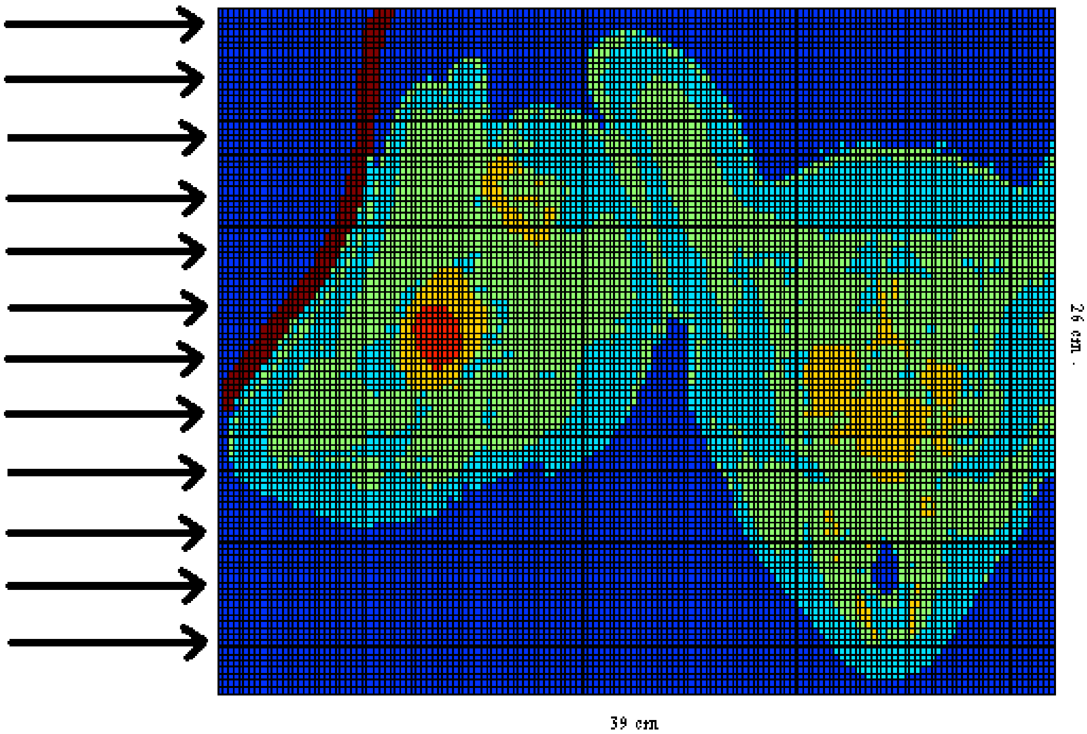


Figure 6.4.17: Beam Re-Entry Phantom Description with 0.25cm x 0.25cm Meshes
Dark Blue: Air
Green: Muscle
Light Blue: Adipose Tissue
Yellow: Skeleton
Orange: Bone Marrow
Dark Red: Plexiglas

The energy deposition plots for each of the incident photon beams is shown below in the following three figures. The energy deposition maps follow the expected patterns.

As the incident beam energy increases, the location of maximal dose deposition increases within the patient.

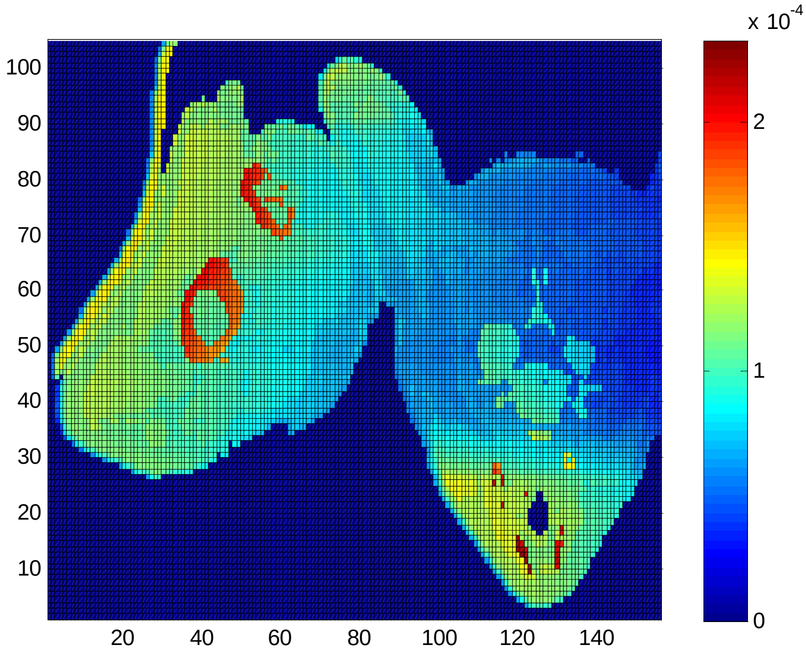


Figure 6.4.18: Energy Deposition Map (MeV) for Beam Re-Entry Phantom with 0.25cm x 0.25cm Meshes with 2 MeV Incident Photon Beam

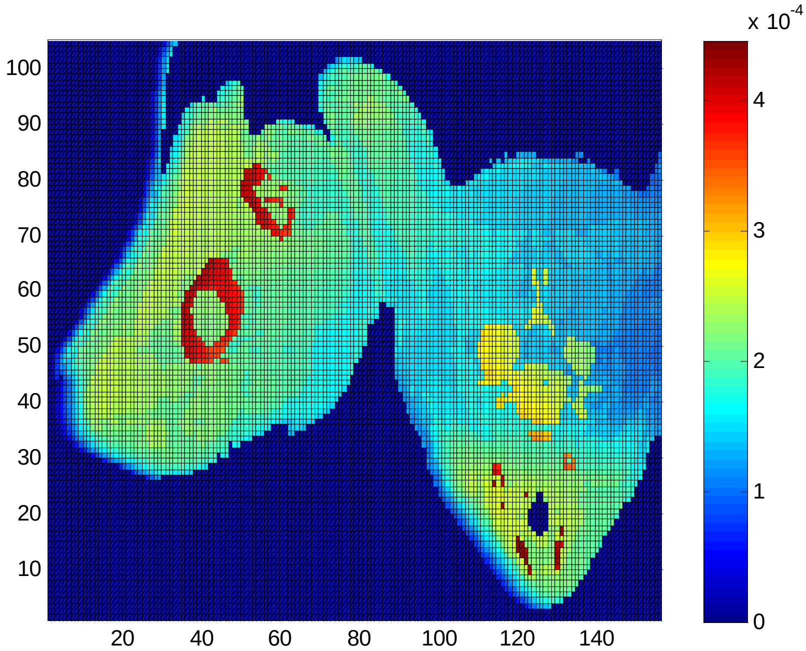


Figure 6.4.19: Energy Deposition Map (MeV) for Beam Re-Entry Phantom with 0.25cm x 0.25cm Meshes with 6 MeV Incident Photon Beam

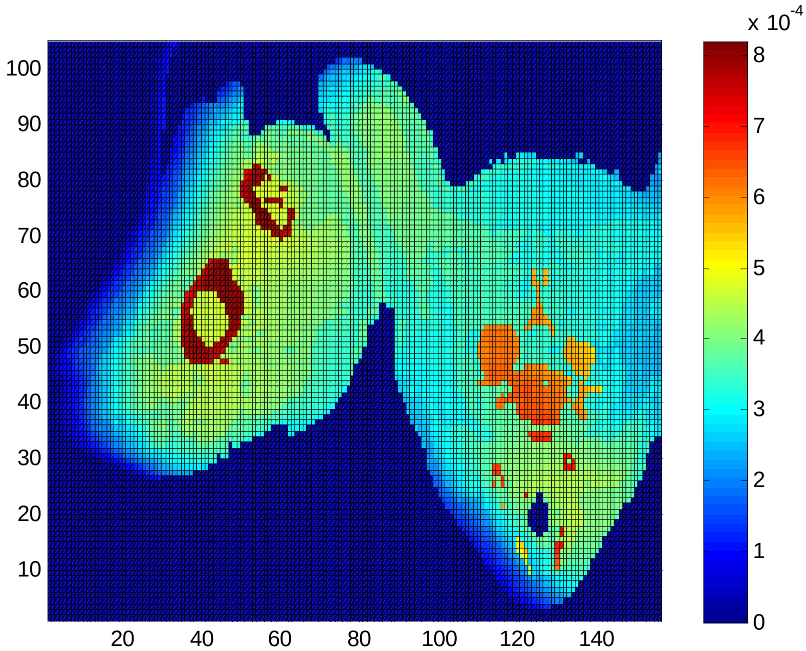


Figure 6.4.20: Energy Deposition Map (MeV) for Beam Re-Entry Phantom with 0.25cm x 0.25cm Meshes with 18 MeV Incident Photon Beam

The maximum percent difference for the 2 MeV case was quite large at 7.06%, but the average percent difference is still quite an acceptable value at 0.70% with an RMS value of 1.02 %. For the 6 MeV case, the maximal energy deposition value is just under 19%. This value is quite large; however, the average percent difference still lies under one percent at 0.72%. The RMS value found for this case is 1.37 %. The 18 MeV incident beam case produces a very high percent difference between the reference solution and the COMET solution at 43.42%. The average value of 1.62 % is not optimal in this case; however, it is not near the maximum value. The RMS value obtained for this situation is 1.62 %. The 6 MeV results were obtained in 2366 hours for the reference solution and 349 minutes for the COMET solution. For the 18 MeV incident beam case, the reference solution required around 2621 hours of computational time and 351 minutes for the COMET calculation. The COMET calculations in all cases produce results much faster than the EGSnrc reference case.

Table 6.4.5: Comparison of COMET and Reference Solutions for Beam Re-Entry Phantom with 0.25cm x 0.25cm Meshes

| | 2 MeV Beam | 6 MeV Beam | 18 MeV Beam |
|---|---|---|---|
| | Comparison without air or Plexiglas | Comparison without air or Plexiglas | Comparison without air or Plexiglas |
| Max % Difference | 7.06 % | 18.85 % | 43.42 % |
| St. Dev. Of Max % Diff. | 0.11 % | 0.11 % | 0.26 % |
| Avg % Difference | 0.70 % | 0.72 % | 1.62 % |
| St. Dev. Of Avg % Diff | 0.75 % | 1.16 % | 3.24 % |
| RMS | 1.02 % | 1.37 % | 3.62 % |

Table 6.4.6: Uncertainty Associated with COMET and Reference Solutions and Running Time Comparison for Beam Re-Entry Phantom with 0.25cm x 0.25cm Meshes

| | 2 MeV Beam | | 6 MeV Beam | | 18 MeV Beam | |
|---|---|---|---|---|---|---|
| | Ref Sol w/o air or Plexiglas | COMET Sol w/o air or Plexiglas | Ref Sol w/o air or Plexiglas | COMET Sol w/o air or Plexiglas | Ref Sol w/o air or Plexiglas | COMET Sol w/o air or Plexiglas |
| Max Rel Std. Dev. | 0.12 % | 0.24 % | 0.15 % | 0.16 % | 0.19 % | 0.25 % |
| Avg Re Std. Dev. | 0.080 % | 0.056 % | 0.057 % | 0.037 % | 0.042 % | 0.051 % |
| Comp Time | 2332 hrs | 388 min | 2366 hrs | 349min | 2621 hrs | 351 min |

In the following figures, the percent difference is shown between the reference solutions and the COMET solutions. For the 2 MeV case, the maximum percent difference occurs at the end furthest from the incident photon beam in the areas of minimal energy deposition. For the 6 MeV case, maximum percent error occurs on the faces of the phantom closest to the incident beam due to minimal energy deposition in this area. For the 18 MeV case, the maximum percent difference occurs in the region of the phantom closest to the beam. This pattern of error has been seen in all of the other cases. This error occurs here due to the inability of the expansion coefficients to accurately describe the electrons created from the interactions of the photons with the media. The results here are worse than those obtained for the 0.5 cm x 0.5 cm. Higher expansion coefficients are necessary to obtain better results for the smaller mesh sizes.

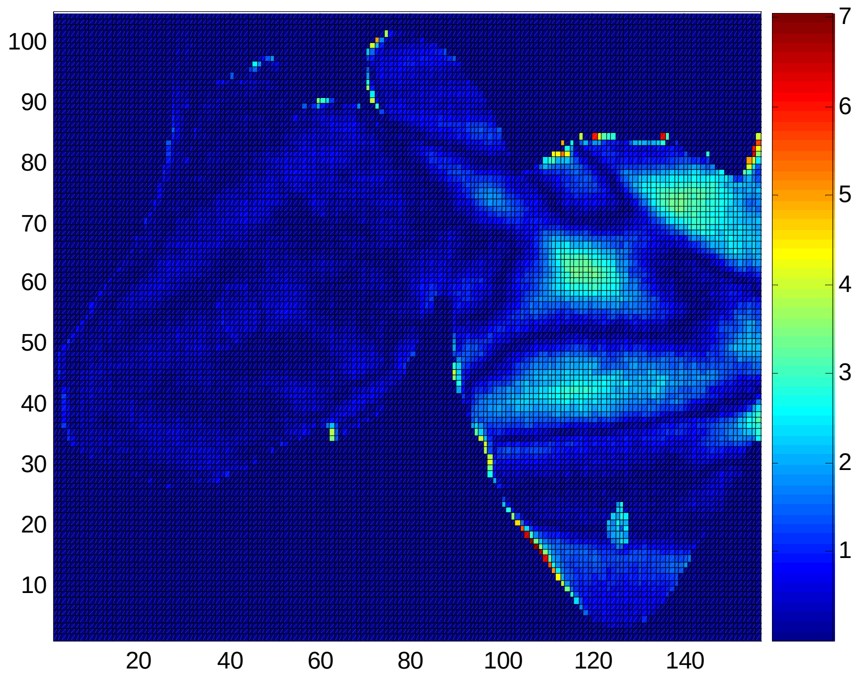


Figure 6.4.21: Percent Difference in Energy Deposition Estimate between COMET and Reference Calculations for Beam Re-Entry Phantom with 0.25cm x 0.25cm Meshes with 2 MeV Incident Photon Beam

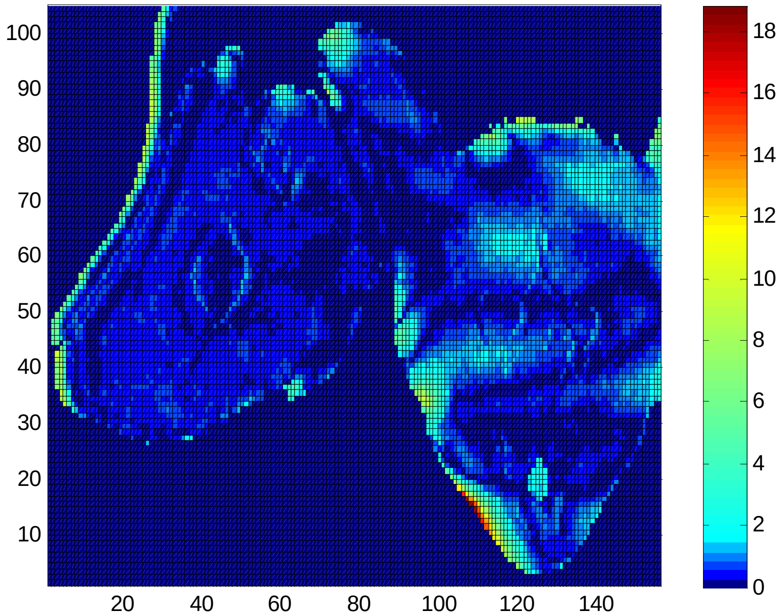


Figure 6.4.22: Percent Difference in Energy Deposition Estimate between COMET and Reference Calculations for Beam Re-Entry Phantom with 0.25cm x 0.25cm Meshes with 6 MeV Incident Photon Beam

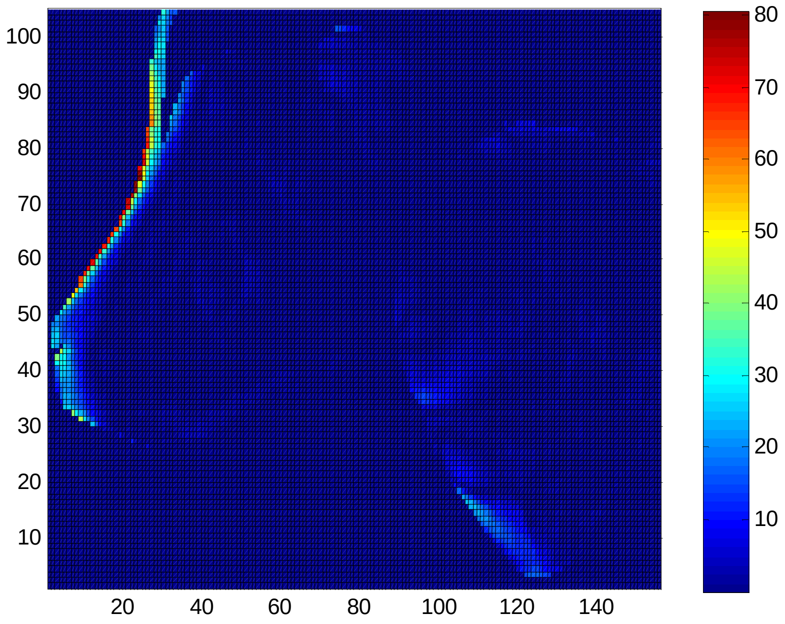


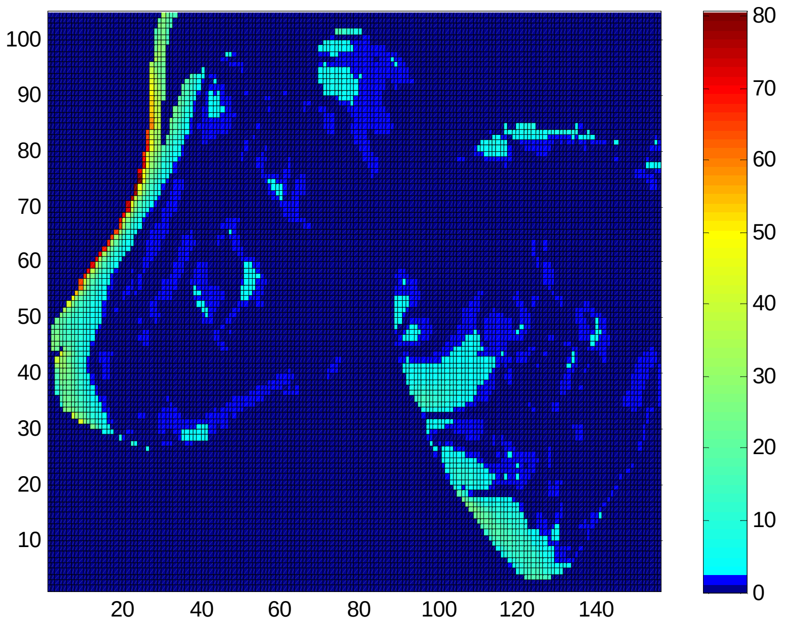


Figure 6.4.23: Percent Difference in Energy Deposition Estimate between COMET and Reference Calculations for Beam Re-Entry Phantom with 0.25cm x 0.25cm Meshes with 18 MeV Incident Photon Beam

## 6.5 CT Benchmark Conclusions

The results obtained for the benchmark problems presented in this chapter were quite good in some instances, while others were in need some improvement. Several patterns resulted from each of these cases. As the incident photon beam energy increased, the maximum and average percent differences also increased. The same expansion orders were used for each incident energy beam such that comparisons could be made easier between all of the cases. For the 18 MeV incident beam, higher energy and angular expansions may be needed to better model the liberated electrons crossing the mesh boundaries due to the high correlation between electron energy and angle.

The smaller mesh sizes produced worse results than those for the larger mesh sizes. This again was due to the expansion orders not accurately describing the situation. Smaller mesh sizes allow for more contours to be depicted within each phantom; however, with the smaller mesh sizes, liberated electrons can deposit a small portion of their energy and continue on to the next mesh. The expansion orders chosen here did not accurately depict this situation. Higher orders in energy may improve upon this situation.

The lung benchmark, prostate benchmark, and beam re-entry benchmark were all chosen because they represented very different clinical situations. For the lung benchmark, large areas of lower density inflated lung tissue were included to determine how well the COMET methodology handled heterogeneity. The prostate benchmark included quite a bit of bone and tissue in one large mass. The third benchmark of the beam re-entry case included regions of bone as well as a unique body surface that was not a smooth oval. The results did show that the COMET methodology can handle heterogeneity as well as unique body borders. The COMET solutions were also produced in minutes to hours as compared to the reference solutions that required weeks up to months to calculate.

# CHAPTER 7

# SECONDARY SENSITIVITY STUDY

Previously in Chapter 4, a sensitivity study was performed to determine the Legendre polynomial expansions to be used for energy, space, polar angle, and azimuthal angle. The same polynomial expansion was used for each incident beam energy such that comparisons could be made easier between the three cases. The previous sensitivity study was performed on simple phantoms: a water phantom and a simplified lung phantom. The coarse mesh used in each of these cases was also 1 cm x 1 cm. It was found that an expansion order of fourth in energy, second in space, fourth in polar angle, and third in azimuthal angle would be applied to the CT based benchmark problems. Good results were obtained when using these expansion orders. Some situations produced better results than others, and there is much room for improvement. A secondary sensitivity study was performed in order to determine if better results could be obtained if different expansion orders were chosen for each incident energy beam. In this case, a CT based phantom was used to test each of the expansion orders. Also, the coarse mesh size used was 0.5 cm x 0.5 cm. For more detailed information regarding this benchmark and the parameters used in EGSnrc, see Appendix B.

## 7.1 Sensitivity Study Problem Definitions

One benchmark problem was defined for this problem. It is a phantom description of a lung patient seen below in Figure 8.1.1. The phantom is 27.5 cm x 55 cm. As stated earlier, each coarse mesh was 0.5 cm x 0.5 cm in size. Each coarse mesh was homogeneous and was composed of one of five materials: air, adipose tissue, muscle, skeleton, or inflated lung tissue. The incident photon beam runs the entire length of the 30 cm face. Currently COMET can only handle incident beams that are composed of mono-energetic and mon-directional photons. As with each of the other benchmarks, the three incident beam energies were tested:  2 MeV, 6 MeV, and 18 MeV.  Reference calculations were performed using EGSnrc for comparison with our COMET Solutions. Additional information regarding this problem is found in Appendix B, and definitions for the statistics are in Appendix A.

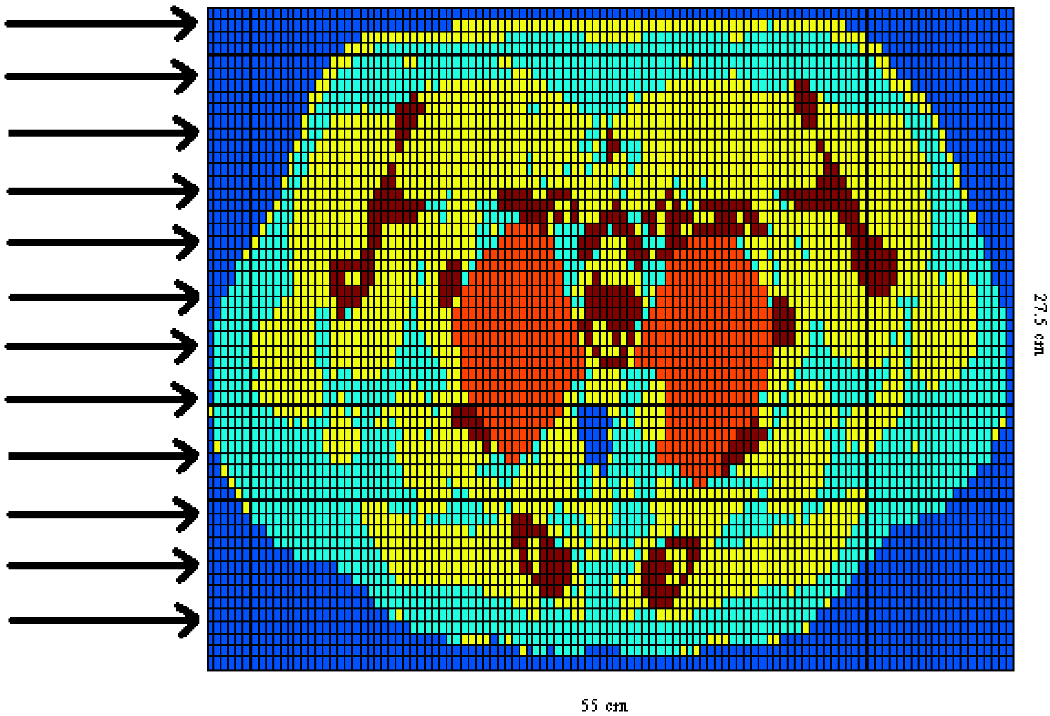


Figure 7.1.1:  Lung Phantom with 0.5cm x 0.5cm Coarse Meshes
Dark Blue:  Air
Light Blue:  Adipose Tissue
Dark Red:  Skeleton
Orange:  Inflated Lung Tissue
Yellow:  Muscle

Response function libraries were obtained using EGSnrc to determine the best expansion order for each variable (energy, space, polar and azimuthal angle).  Response functions were obtained for 5$^{th}$ order in each variable.  Using this one response function, every combination up to the 5$^{th}$ order can be obtained for COMET calculations.  As with the previous sensitivity study, three of the variables were set to 5$^{th}$ order while the fourth variable was altered from 1$^{st}$ to 5$^{th}$ order.  For each of these combinations, a COMET solution was obtained. These COMET solutions were then compared to the EGSnrc reference solution. Using these comparisons and the timing data, these comparisons could then be used to determine the best expansion to be used for future COMET calculations.

For each of these cases in the sensitivity study, twenty million particle histories were followed for each response function library that was generated. A new response function must be generated for each new energy, material definition, and size of the coarse mesh. For each reference calculation in EGSnrc, ten billion particles were used. Three reference calculations were performed – one for each incident energy beam.

**Secondary Sensitivity Study Benchmark Problem Results**

A single response function library with 5$^{th}$ order in energy, space, and angle was produced for each energy and material definition. For this lung benchmark, fifteen libraries were created. For each of the five material definitions, three libraries were created to account for each incident energy. The results for this benchmark problem are shown below for each of the three energies in Table 7.1.1. For each expansion order and beam energy, the maximum percent difference and average percent difference between the COMET solution and the reference solution is shown.

Table 7.1.1: Sensitivity Study Results for Lung Phantom with 0.5cm x 0.5cm Coarse-Meshes

| | 2 MeV Incident Beam | | | 6 MeV Incident Beam | | | 18 MeV Incident Beam | | |
|---|---|---|---|---|---|---|---|---|---|
| **Exp Order** | **Max % Diff** | **Avg % Diff** | **Calc Time (hr)** | **Max % Diff** | **Avg % Diff** | **Calc Time (hr)** | **Max % Diff** | **Avg % Diff** | **Calc Time (hr)** |
| **1555** | 8.03 % | 2.05 % | 3.0 | 13.68 % | 5.19 % | 4.2 | 43.31 % | 16.29 % | 5.0 |
| **2555** | 1.76 % | 0.27 % | 10.3 | 5.06 % | 1.01 % | 10.3 | 22.41 % | 3.74 % | 10.3 |
| **3555** | 1.81 % | 0.28 % | 33.4 | 4.30 % | 0.42 % | 33.4 | 22.52 % | 1.82 % | 28.7 |
| **4555** | 1.86 % | 0.30 % | 52.1 | 3.65 % | 0.40 % | 51.9 | 18.62 % | 1.04 % | 44.5 |
| **5555** | 1.89 % | 0.29 % | 84.9 | 4.11 % | 0.36 % | 85.1 | 16.03 % | 0.91 % | 98.3 |
| | | | | | | | | | |
| **5155** | 1.94 % | 0.30 % | 3.0 | 4.72 % | 0.38 % | 3.1 | 16.38 % | 0.93 % | 3.9 |
| **5255** | 1.96 % | 0.29 % | 10.4 | 4.12 % | 0.37 % | 10.5 | 16.08 % | 0.91 % | 11.9 |
| **5355** | 1.95 % | 0.29 % | 33.1 | 4.11 % | 0.37 % | 37.9 | 16.11 % | 0.91 % | 43.4 |
| **5455** | 1.91 % | 0.29 % | 51.8 | 4.11 % | 0.36 % | 51.9 | 16.08 % | 0.91 % | 59.5 |
| **5555** | 1.89 % | 0.29 % | 84.9 | 4.11 % | 0.36 % | 85.1 | 16.03 % | 0.91 % | 98.3 |
| | | | | | | | | | |
| **5515** | 32.50% | 5.08 % | 3.0 | 28.57 % | 5.46 % | 3.0 | 59.77 % | 6.41 % | 3.9 |
| **5525** | 4.04 % | 0.72 % | 32.9 | 8.85 % | 1.19 % | 32.7 | 36.70 % | 2.69 % | 66.4 |
| **5535** | 4.04 % | 0.72% | 33.2 | 8.85 % | 1.19 % | 33.3 | 36.70 % | 2.69 % | 67.2 |
| **5545** | 1.89 % | 0.29 % | 84.7 | 4.11 % | 0.36 % | 84.7 | 16.03 % | 0.91 % | 97.0 |
| **5555** | 1.89 % | 0.29 % | 84.9 | 4.11 % | 0.36 % | 85.1 | 16.03 % | 0.91 % | 98.3 |
| | | | | | | | | | |
| **5551** | 6.29 % | 1.11 % | 3.1 | 25.15 % | 1.14 % | 5.7 | 108.36 % | 3.18 % | 4.8 |
| **5552** | 3.86 % | 0.55 % | 10.2 | 11.25 % | 0.47 % | 10.2 | 97.82 % | 1.55 % | 16.4 |
| **5553** | 4.23 % | 0.41 % | 33.8 | 3.86 % | 0.41 % | 34.5 | 34.02 % | 1.18 % | 52.1 |
| **5554** | 2.30 % | 0.31 % | 52.0 | 5.93 % | 0.39 % | 51.9 | 28.16 % | 1.01 % | 59.4 |
| **5555** | 1.89 % | 0.29 % | 84.9 | 4.11 % | 0.36 % | 85.1 | 16.03 % | 0.91 % | 98.3 |

Each response function library required around 240 hours of computational time to run. For each energy case, 1200 hours were required to compute all the response functions necessary to calculate the solution. It should be once again noted that this is completely pre-computational, and these response functions can be re-used. The reference calculations for this lung benchmark required 712 hours for a 2 MeV beam, 1140 hours for a 6 MeV beam, and 1832 hours for an 18 MeV beam.

The highlighted values represent those that provided the best results. For the 2 MeV incident beam, the optimal expansion order was found to be 2$^{nd}$ in Energy, 1$^{st}$ in space, and 4$^{th}$ in both angles. For the 6 MeV beam, an expansion of 4$^{th}$ in energy, 1$^{st}$ in space, 4$^{th}$ in polar angle, and 3$^{rd}$ in azimuthal angle was found to produce the best results. Lastly, for the 18 MeV case, an expansion order of 4$^{th}$ in energy, 1$^{st}$ in space, and 4$^{th}$ in both angles was chosen. In this case, the expansion order of 5$^{th}$ in energy, 1$^{st}$ in space, 4$^{th}$

in polar angle, and $5^{th}$ in azimuthal angle was also considered for tested to see if much could be gained from this higher expansion order. For some cases, the chosen expansion order may produce a maximal percent difference that higher than other expansion orders; however, the average percent difference is similar with a greatly reduced calculation time.

## 7.2 Conclusions

Based on the sensitivity study, different expansion orders were tested for each incident photon beam. Each of these are tested and shown below in Table 7.2.1. For the 2 MeV incident beam, a maximum percent difference of 2.65 % and an average percent difference of 0.32 % was found using the 2144 expansion order. This calculation was done quickly in 25.6 minutes. The maximum percent difference is slightly higher than some of the better values obtained during the sensitivity study; however, the average value is comparable to those obtained earlier. The time required for this COMET solution was much shorter than any of those found during the sensitivity study or for the reference solution, which required 712 minutes. The 6 MeV situation was much like that of the 2 MeV case, the maximum percent error for the 4143 expansion orders was around 4.51%, which is higher than some of the previously calculated solutions from the sensitivity study. Again, the average percent difference of 0.42 % is similar to the best results obtained previously. Again, the timing difference is quite different. For the COMET situation with the optimized expansion orders, a time of 38.8 minutes was required. Again, this is much lower than the reference calculation that required 1140 minutes and even the other COMET solutions in the sensitivity study which all required hours to obtain.

For the 18 MeV case, two expansion orders were tested – 4144 and 5145. The 4144 expansion produced a maximum percent difference of 31.17 % and an average percent difference of 1.10 %. Much better maximum percent differences were obtained in the sensitivity study; however, the average percent difference is once again quite similar to those found earlier. This COMET solution required 1.4 hours compared to the 30.5 hours for the reference calculation. For the expansion orders of 5145, a maximum percent difference of 16.38 % and an average percent difference of 0.93 % were found in 3.33 hours.  These values are similar to the best values obtained for this incident energy beam during the sensitivity study.  This timing requirement was more than twice as long as that found for the 5145 case, but still much shorter than the 30.5 hours for the reference solution.

Table 7.2.1: Optimized Expansion Order Results for Secondary Sensitivity Study

| Exp Order | Max % Diff | Avg % Diff | COMET Calc Time | Ref Calc Time |
|---|---|---|---|---|
| 2 MeV Beam - 2144 | 2.65 % | 0.32 % | 25.6 minutes | 712 minutes |
| 6 MeV Beam - 4143 | 4.51 % | 0.42 % | 38.8 minutes | 1140 minutes |
| 18 MeV Beam - 4144 | 31.17 % | 1.10 % | 1.40 hours | 30.5 hours |
| 18 MeV Beam - 5145 | 16.38 % | 0.93 % | 3.33 hours | 30.5 hours |

From this sensitivity study, it can be seen that different orders are necessary based on the incident photon energy.  A case where a lower energy incident photon beam is impinging requires a lower expansion order compared to that of a higher energy incident photon beam.  The spatial variable expansion for all the cases was found to not really impact the results at all, thus a very low expansion order can be used here.  The angular expansions also prove to be quite important.  For all three cases, higher angular expansions seem to produce better results.  These angular expansions are more important as the incident photon energy increases.  For the 18 MeV cases, much higher expansion orders may be necessary to obtain adequate results for the maximum percent difference value.  The maximum percent difference is still a little high though, and additional sensitivity studies may need to be performed.

# CHAPTER 9

# CONCLUSIONS

## 9.1 Final Remarks

**Development of Benchmarks**

In this work, a large portion of the time and effort has been developing new benchmarks to be used to test dose calculation algorithms for medical physics applications. A very simple lung phantom was developed to test initially how well a system handles the introduction of heterogeneity. More complex, clinical benchmarks were also developed to test dose calculation algorithms. Three different situations were modeled: lung case, prostate case, and a beam re-entry case. The lung case was developed to determine how well algorithms handle the lower density lung region. This heterogeneity is extremely important because over-dosing to this region can occur at low doses. The prostate case included a large amount of bone. This was developed to determine how well an algorithm would handle a higher density heterogeneity. Bone accounts for the largest single heterogeneity within the body, so it was thought to be important to develop a benchmark that included a large amount of bone. The third benchmark was a beam re-entry phantom that included a region where two areas of skin are adjacent to each other. Thus, it is important that the algorithm correctly calculates the dose in the region where the skin touches in order to reduce the possibility of radiation burns. This benchmark also did not have a symmetric, regular border as the others did. This benchmark tested how well the algorithm handled situations with irregular borders.

Two benchmarks were also studied, but were not developed in this work. One was a simple water phantom, which is used throughout the medical physics community for both numerical and experimental work. The other benchmark tested was developed by Rogers and Mohan.[33] It was composed of water, lung tissue, and aluminum. It had been introduced to place stress on dose calculation algorithms, and it was included here for completeness of testing.

## Testing of COMET Methodology

In order to test the COMET methodology, a large response function library was generated for this work. Each library was based on the coarse-mesh size, incident photon beam energy, and the material definition within the coarse-mesh. A Legendre polynomial expansion was also chosen for each library for energy, space, azimuthal, and polar angle. Any combination of these expansions can be chosen for COMET calculations up to the highest order for which the library was generated.

Libraries were generated for water, non-inflated lung tissue, and aluminum with expansion orders of $5^{th}$ in every category for each incident energy case (2 MeV, 6 MeV, 18 MeV) and for coarse-meshes of size 1cm x 1cm and 0.5cm x 0.5cm. For skeletal muscle, inflated lung tissue, cortical bone, adipose tissue, and air, response function libraries were generated with expansion orders of $5^{th}$ order for each category for each incident energy and for coarse-meshes of size 1cm x 1cm, 0.5cm x 0.5cm, and 0.25cm x 0.25cm. For Plexiglas and red skeletal marrow, libraries were generated for expansion orders of $4^{th}$ in energy, $2^{nd}$ in space, $4^{th}$ in polar angle, and $3^{rd}$ in azimuthal angle for each incident energy and for coarse-meshes of size 1cm x 1cm, 0.5cm x 0.5cm, and 0.25cm x 0.25cm. These last two material response function libraries were not generated up to $5^{th}$ order in each case because they were not necessary for the secondary sensitivity study. Reference solutions were also calculated for each benchmark case and stored for further comparison.

## Conclusions

From the study of simple benchmark problems, quite a few conclusions can be determined about the COMET methodology. The water phantom may be quite a simple problem; however, it is very useful in determining how well the methodology works. For lower energy cases such as 2 MeV, maximal energy deposition occurs furthest from the incident beam in the region of lowest energy deposition. The error plot also showed that the error was highest at the corners furthest from the incident beam. This error pattern results due to the small amount of energy deposited and error propagation. For the 6 MeV case, the maximal error occurs in the region closest to the incident photon beam.

This results because along this strip, energy deposition is lower because the photons travel deeper within the tissue before interacting with the media and ejecting electrons. The 18 MeV cases produce some unusual results. With this higher energy case, the photons travel even further into the tissue before interactions occur. Thus, maximal energy deposition does occur even deeper within the tissue than the previous two incident beam cases. Based upon the results obtained for the 2 MeV and 6 MeV cases, it would be expected that the maximal error would occur closest to the incident beam since this is the location of smallest energy deposition. This however is not the case. The region directly adjacent to the incident beam is accurately calculated. The maximum error occurs slightly further inside the phantom.

Two other simple problems were tested – a simplified lung model and a non-clinical slab problem. Once again, only the simplified lung model was developed in this work. Both were used to test the methodology in a heterogeneous situation. The same results were obtained for each energy case with these heterogeneous phantoms as with the previous water phantom. The 2 MeV and 6 MeV incident photon beams produced errors that were due to locations of minimal energy deposition. The 18 MeV case produced errors in the same location and with the same magnitude as with the water phantom. Heterogeneity proved no problem for the COMET methodology in that similar results were obtained for the homogeneous and heterogeneous cases.

The results obtained from the more clinically relevant CT benchmarks produced good results overall. As before, smaller mesh sizes and lower incident energies produced better results. The same problems resulted as with the smaller, simpler benchmark problems. These problems showed that the COMET methodology is not sensitive (in terms of accuracy) to added heterogeneity of 5 or 6 different material definitions.

Looking at these benchmarks, it is obvious that as the incident photon energy increases, the maximal and average percent difference increases as well. A higher energy incident photon produces electrons whose energy and angle are very highly correlated. The current low expansion orders are not modeling this situation correctly. A higher expansion order in energy and angle may help to produce better agreement between our COMET and reference cases. The COMET methodology can better handle a lower energy incident photon beam.

It should be emphasized that the mono-energetic energies that were tested are not typical of radiation therapy treatment situations. Two typical treatment beams used at Emory University are 6 MV, which has an average photon energy of 2 MeV and a maximum photon energy of 6 MeV, and 18 MV, which has an average photon energy of 6 MeV and a maximum photon energy of 18 MeV. Even though high errors did occur for the 18 MeV incident beam, a typical clinical radiation therapy beam will be composed of many different energies with 18 MeV being the maximum. The COMET methodology handled the 6 MeV cases very well, which would be the average energy within the 18 MV beam.

The coarse-mesh size chosen also affected the maximum and average percent errors between the reference and COMET calculations. As the coarse-mesh size decreases, the maximum and average percent difference increases. The smaller mesh size better captures the shape of the internal organs and structures and is a more clinically relevant size. This smaller size however provides some problems for the COMET methodology. With the smaller size, the secondary electrons could travel through one mesh depositing its energy along the way. This occurs more with higher energy electrons. Because of this, a higher expansion order may be needed for the energy variable. For each of these cases, the COMET methodology best handles the 1cm x 1cm mesh with a 2 MeV incident beam, while the worst senario is the 0.25 cm x 0.25 cm mesh with an 18 MeV incident beam.

The secondary sensitivity study showed similar results to those obtained for the original sensitivity study performed. For these cases, the expansion of the spatial variable was acceptable at 1st order. As the energy of the incident photon beam increases, the need for a higher expansion order for the energy variable is necessary. Also with the increase of incident photon energy, the angular expansion orders become much more important due to the liberated secondary photons. With the higher energy photon, higher energy electrons must travel through the coarse mesh. These electrons have a very strong correlation between energy and angle. It became obvious that different expansion orders are necessary for each specific incident beam energy in order to obtain the best results.

One of the benefits of the COMET methodology is its timing. The COMET solutions were obtained much faster than the pure Monte Carlo reference solutions. COMET solutions typically required minutes to hours whereas the reference cases ran in weeks or months. The pre-computational time required for the response function library generation was large in some instances; however, these response functions must only be run once, and they may all be re-used.

## 9.2 Future Recommendations

**Numerical Benchmarks**

The obvious progression for the numerical benchmarks should be their extension to three dimensions since the obvious goal of COMET is its extension to three dimensions as well. A dose calculation algorithm is not clinically relevant unless it can handle a three dimensional situation. Currently the benchmarks also only deal with a beam incident on one entire surface of the benchmark. The benchmarks should be adapted for smaller incident beams that do not cover the entire surface since this would better mimic a clinical situation.

**COMET**

The largest problem found from this work has been the inaccuracies associated with a higher energy photon beam as well as smaller coarse mesh sizes. It is possible that one solution may be the use of higher expansion orders for energy and angle to better model the situation. Alternatively, developers may consider improving the electron transport method in COMET in order to keep the expansion order manageable in regards to file size, response function calculation time, and COMET calculation time.

COMET has shown it can handle extremely heterogeneous systems, so the next steps must be taken to make it more clinically relevant. In order for COMET to become more clinically applicable, many alterations must be made to the current state of the code. The source definition must be altered in order to handle a divergent incident photon beam with a poly-energetic spectrum. Also, the current methodology must be extended handle three dimensional problems.

# APPENDIX A

# STATISTICS DEFINITIONS

Maximum Percent Difference =

$$100\% * \left[ Maximum\left( \frac{|\text{reference solution of region i - COMET solution of region i}|}{\text{reference solution of region i}} \right) \right]$$

Average Percent Difference =

$$100\% * \left[ \frac{\sum_{i=1}^{\max region} \left( \frac{|\text{reference solution of region i - COMET solution of region i}|}{\text{reference solution of region i}} \right)}{\text{total number or regions}} \right]$$

Root Mean Square (%) =

$$100\% * \sqrt{\frac{\sum_{i=1}^{\max region} \left( \frac{|\text{reference solution of region i - COMET solution of region i}|}{\text{reference solution of region i}} \right)^2}{\text{total number or regions}}}$$

Standard Deviation of Average Percent Difference =

$$100\% * \sqrt{\frac{\sum_{i=1}^{\max region} \left( \left( \frac{|\text{ref sol of region i - COMET sol of region i}|}{\text{ref sol of region i}} \right) - \text{Average Percent Difference} \right)^2}{\text{total number or regions}}}$$

Standard Deviation of Maximum Percent Difference =

$$100\% * \sqrt{\left( (\text{std dev of ref sol region of max \% diff})^2 + (\text{std dev of COMET sol of region of max \% diff})^2 \right)}$$

# APPENDIX B

# BENCHMARK PROBLEM DEFINITIONS

Below in the first section, the material definitions are given that were used throughout this work. The composition is given as a list of each element composing the material and a corresponding weight fraction. The mass density of each material is also given. This data was obtained from the EGSnrc library.[27] Each benchmark problem is also given in this appendix describing the incident beam, phantom size, and material definition. For the cross-sectional library generation in EGS, the energy range associated with the photons was set to a minimum of 0.05 MeV and a maximum of 20 MeV. For the electrons, the minimum value was set to 0.52 MeV, while the maximum was set to 20 MeV. When running EGSnrc to obtain our reference and response function solutions, a minimum value of 0.56 MeV was set for the electron transport. Thus, if the electron's energy falls below this value, it deposits its energy locally. The minimum value for photon transport was set to 0.05 MeV. The maximum transport value for photon transport was set to the same value as the incident energy.

## Material Definitions

### Air – Dry, Near Sea Level

Table B.1: Air Composition

| Material | Fraction By Weight |
|---|---|
| C | 0.000124 |
| N | 0.755267 |
| O | 0.231781 |
| Ar | 0.012827 |

**Mass Density –** 0.00120479 g/cm^3

**Adipose Tissue – ICRP Definition**

Table B.2: Adipose Tissue Composition

| Material | Fraction By Weight |
|---|---|
| H | 0.119477 |
| C | 0.63724 |
| N | 0.00797 |
| O | 0.232333 |
| Na | 0.0005 |
| Mg | 0.00002 |
| P | 0.00016 |
| S | 0.00073 |
| Cl | 0.00119 |
| K | 0.00032 |
| Ca | 0.00002 |
| Fe | 0.00002 |
| Zn | 0.00002 |

**Mass Density –** 0.92 g/cm^3

**Aluminum**

Table B.3: Aluminum Composition

| Material | Fraction By Weight |
|---|---|
| Al | 1 |

**Mass Density –** 2.6989 g/cm^3

**Bone (Cortical) – ICRP Definition**

Table B.4: Cortical Bone Composition

| Material | Fraction By Weight |
|---|---|
| H | 0.63984 |
| C | 0.278 |
| N | 0.027 |
| O | 0.410016 |
| Mg | 0.002 |
| P | 0.07 |
| S | 0.002 |
| Ca | 0.147 |

**Mass Density** - 1.85 g/cm^3

## Lung Tissue (Inflated) – ICRU 1986

### Definition

Table B.5: Inflated Lung Tissue Composition

| Material | Fraction By Weight |
|---|---|
| H | 0.103 |
| C | 0.105 |
| N | 0.031 |
| O | 0.749 |
| Na | 0.002 |
| P | 0.002 |
| S | 0.003 |
| Cl | 0.003 |
| K | 0.002 |

**Mass Density –** 0.26 g/cm^3

## Lung Tissue (Non-Inflated) – ICRP Definition

Table B.6: Non-Inflated Lung Tissue Composition

| Material | Fraction By Weight |
|---|---|
| H | 0.101278 |
| C | 0.10231 |
| N | 0.02865 |
| O | 0.757072 |
| Na | 0.00184 |
| Mg | 0.00073 |
| P | 0.0008 |
| S | 0.00225 |
| Cl | 0.00266 |
| K | 0.00194 |
| Ca | 0.00009 |
| Fe | 0.00037 |
| Zn | 0.00001 |

**Mass Density -** 1.05 g/cm^3

**Marrow (Red Skeletal) – ICRU 1986 Definition**

Table B.7: Red Skeletal Marrow Composition

| Material | Fraction By Weight |
|---|---|
| H | 0.105 |
| C | 0.414 |
| N | 0.034 |
| O | 0.439 |
| P | 0.001 |
| S | 0.002 |
| Cl | 0.002 |
| K | 0.002 |
| Fe | 0.001 |

**Mass Density –** 1.03 g/cm^3

**Muscle (Skeletal) – ICRP Definition**

Table B.8: Skeletal Muscle Composition

| Material | Fraction By Weight |
|---|---|
| H | 0.100637 |
| C | 0.10783 |
| N | 0.02768 |
| O | 0.754773 |
| Na | 0.00075 |
| Mg | 0.00019 |
| P | 0.0018 |
| S | 0.00241 |
| Cl | 0.00079 |
| K | 0.00302 |
| Ca | 0.00003 |
| Fe | 0.00004 |
| Zn | 0.00005 |

**Mass Density** - 1.04 g/cm^3

**Plexiglas /Polymethylmethacrylate**

Table B.9: Plexiglas Composition

| Material | Fraction By Weight |
|---|---|
| H | 0.080538 |
| C | 0.599848 |
| O | 0.319614 |

**Mass Density –** 1.19 g/cm^3

**Water**

Table B.10: Water Composition

| Material | Fraction By Weight |
|---|---|
| H | 0.111894 |
| O | 0.888106 |

**Mass Density -** 1.00 g/cm^3

**Water Phantom- 1cm x 1cm Coarse-Meshes**

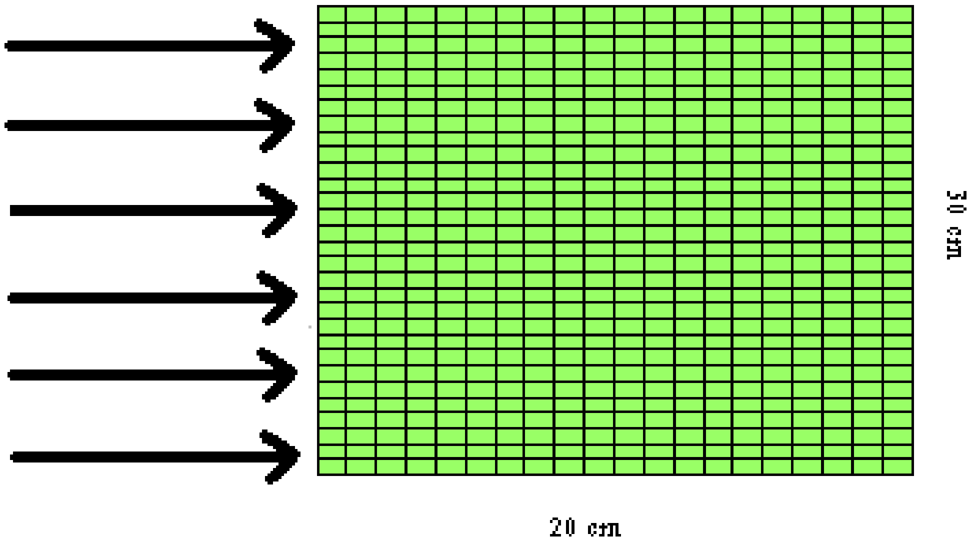


Figure B.1: Water Phantom with 1cm x 1cm Coarse-Meshes

**Material Definitions:**
Green - Water

**Beam Definition:**
Impinging on entire left face with mono-energetic, mono-directional photon beam

**Total Size:** 30 cm x 20 cm, third dimension extends to infinity in both directions
**Coarse-Mesh Size:** 1cm x 1cm
**Total Meshes:** 600

**Water Phantom- 0.5cm x 0.5cm Coarse-Meshes**

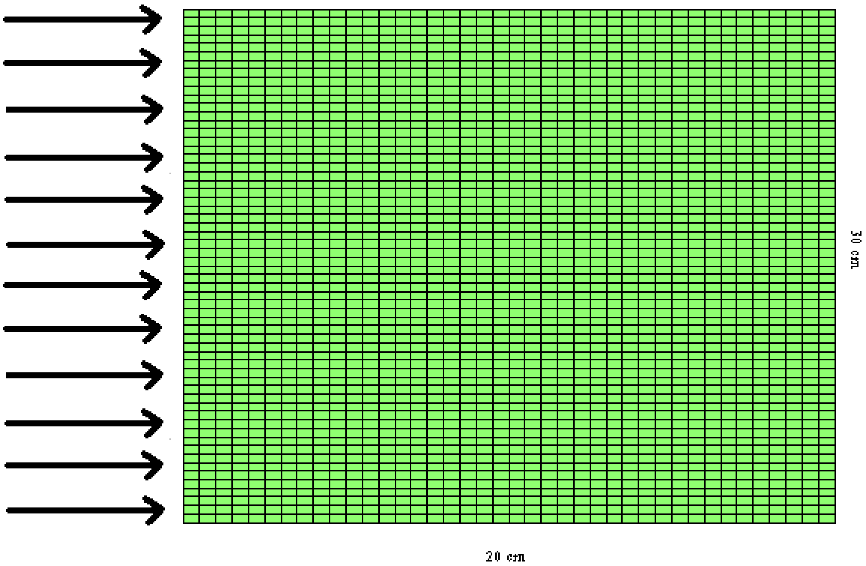


Figure B.2: Water Phantom with 0.5cm x 0.5cm Coarse-Meshes

**Material Definitions:**
Green - Water

**Beam Definition:**
Impinging on entire left face with mono-energetic, mono-directional photon beam

**Total Size:** 30 cm x 20 cm, third dimension extends to infinity in both directions
**Coarse-Mesh Size:** 0.5cm x 0.5cm
**Total Meshes:** 2400

**Simplified Lung Phantom- 1cm x 1cm Coarse-Meshes**

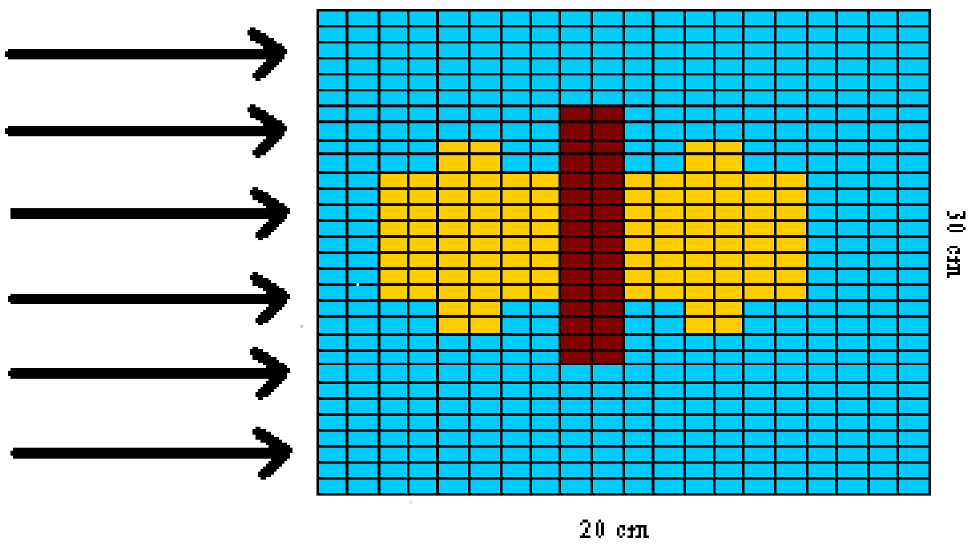


Figure B.3: Simplified Lung Phantom with 1cm x 1cm Coarse-Meshes

**Material Definitions:**
Blue - Water
Red - Bone (Cortical)
Yellow - Lung Tissue (Non-Inflated)

**Beam Definition:**
Impinging on entire left face with mono-energetic, mono-directional photon beam

**Total Size:** 30 cm x 20 cm, third dimension extends to infinity in both directions
**Coarse-Mesh Size:** 1cm x 1cm
**Total Meshes:** 600

**Simplified Lung Phantom- 0.5cm x 0.5cm Coarse-Meshes**

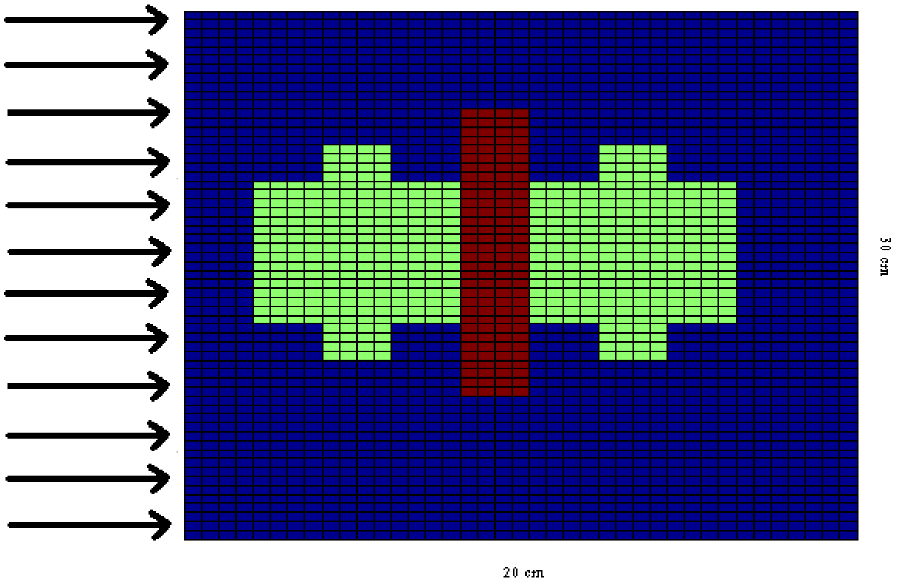


Figure B.4: Simplified Lung Phantom with 0.5cm x 0.5cm Coarse-Meshes

**Material Definitions:**
Blue – Water
Red – Bone (Cortical)
Green – Lung Tissue (Non-Inflated)

**Beam Definition:**
Impinging on entire left face with mono-energetic, mono-directional photon beam

**Total Size:** 30 cm x 20 cm, third dimension extends to infinity in both directions
**Coarse-Mesh Size:** 0.5cm x 0.5cm
**Total Meshes:** 2400

**Slab Phantom- 1cm x 1cm Coarse-Meshes**

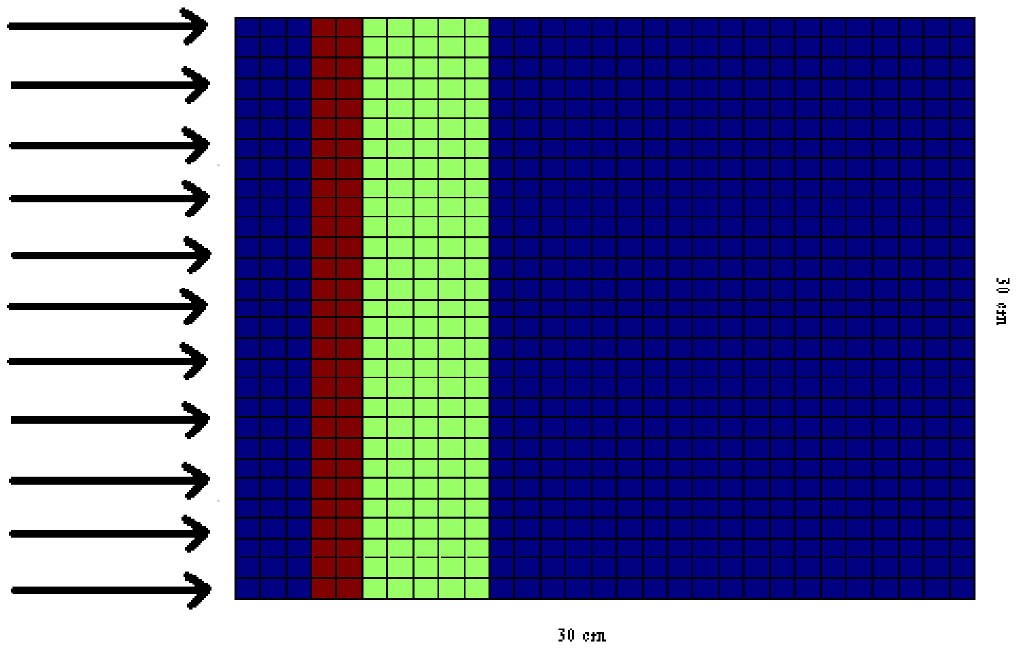


Figure B.5: Slab Phantom with 1cm x 1cm Coarse-Meshes

**Material Definitions:**
Blue - Water
Green - Lung Tissue (Non-Inflated)
Red - Aluminum

**Beam Definition:**
Impinging on entire left face with mono-energetic, mono-directional photon beam

**Total Size:** 30 cm x 30 cm, third dimension extends to infinity in both directions
**Coarse-Mesh Size:** 1cm x 1cm
**Total Meshes:** 900

**Slab Phantom- 0.5cm x 0.5cm Coarse-Meshes**

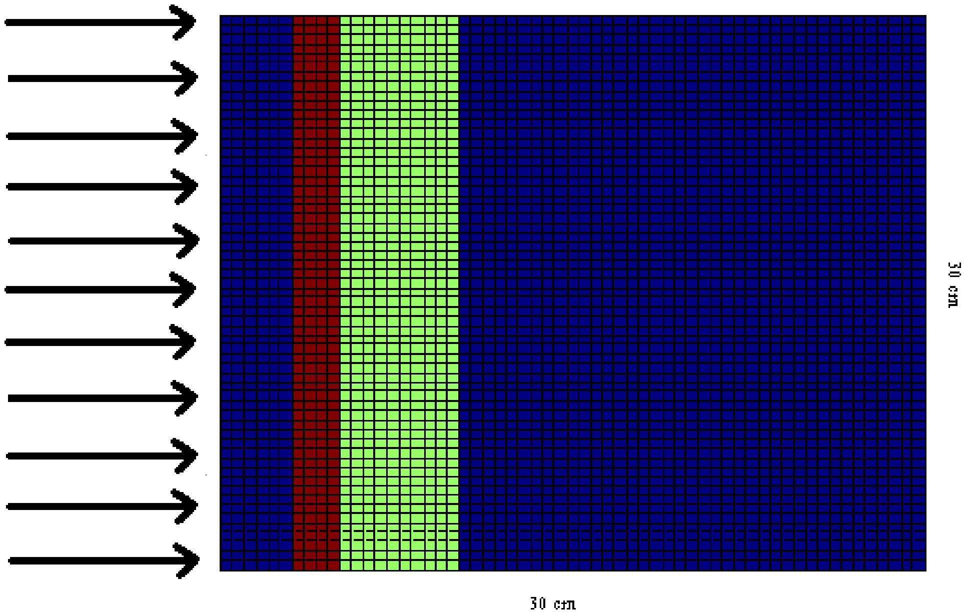


Figure B.6: Slab Phantom with 0.5cm x 0.5cm Coarse-Meshes

**Material Definitions:**
Blue - Water
Green - Lung Tissue (Non-Inflated)
Red - Aluminum

**Beam Definition:**
Impinging on entire left face with mono-energetic, mono-directional photon beam

**Total Size:** 30 cm x 30 cm, third dimension extends to infinity in both directions
**Coarse-Mesh Size:** 0.5cm x 0.5cm
**Total Meshes:** 3600

**Lung Phantom- 1cm x 1cm Coarse-Meshes**

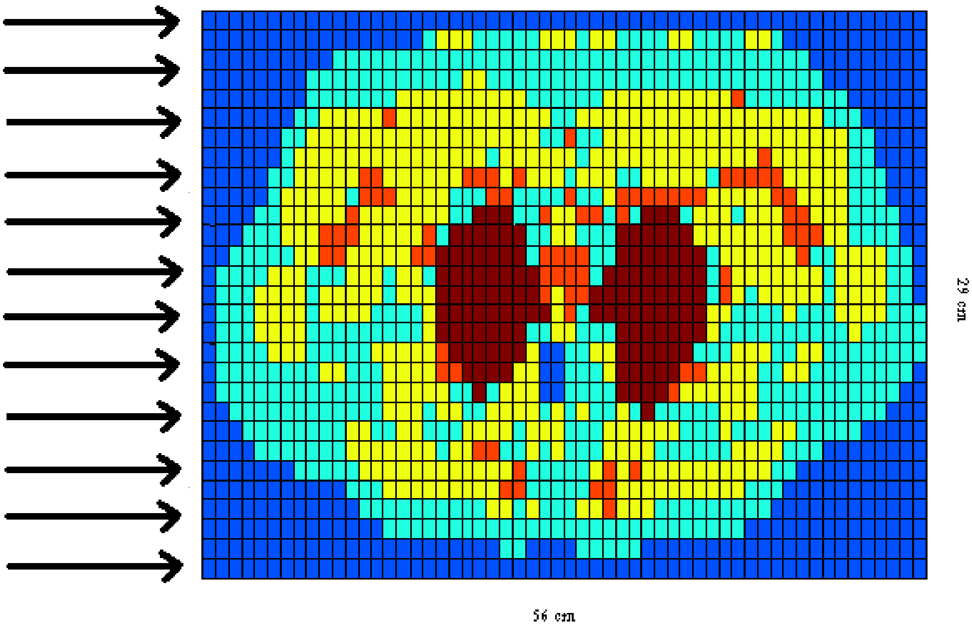


Figure B.7: CT Lung Phantom with 1cm x 1cm Coarse-Meshes

**Material Definitions:**
Dark Blue - Air (dry, near sea level)
Light Blue - Adipose Tissue
Yellow - Muscle (Skeletal)
Orange - Bone (Cortical)
Dark Red - Lung Tissue (Inflated)

**Beam Definition:**
Impinging on entire left face with mono-energetic, mono-directional photon beam

**Total Size:** 29 cm x 56 cm, third dimension extends to infinity in both directions
**Coarse-Mesh Size:** 1cm x 1cm
**Total Meshes:** 1624

**Lung Phantom- 0.5cm x 0.5cm Coarse-Meshes**

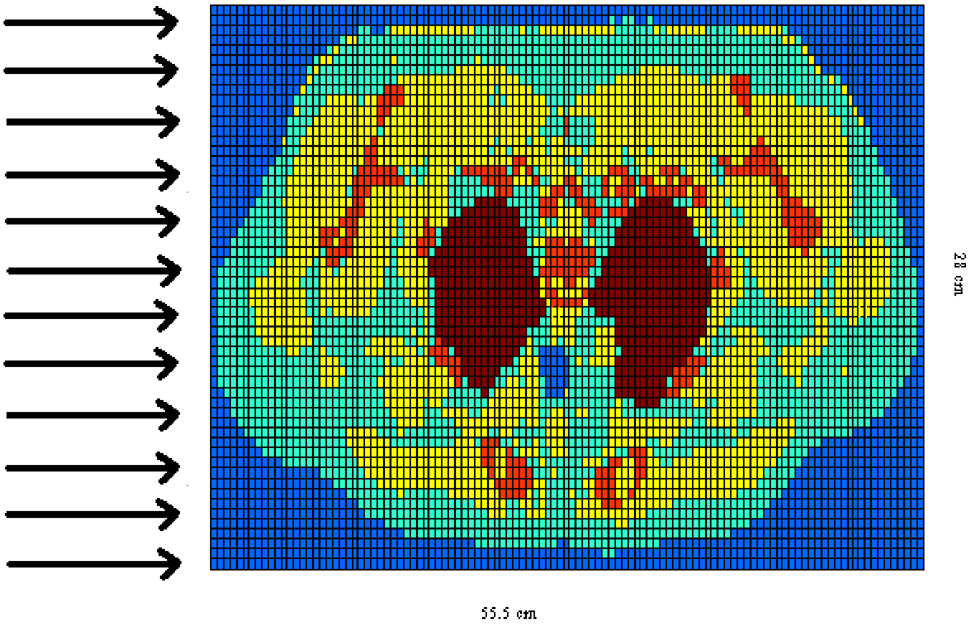


Figure B.8: CT Lung Phantom with 0.5cm x 0.5cm Coarse-Meshes

**Material Definitions:**
Dark Blue - Air (dry, near sea level)
Light Blue - Adipose Tissue
Yellow - Muscle (Skeletal)
Orange - Bone (Cortical)
Dark Red - Lung Tissue (Inflated)

**Beam Definition:**
Impinging on entire left face with mono-energetic, mono-directional photon beam

**Total Size:** 28 cm x 55.5 cm, third dimension extends to infinity in both directions
**Coarse-Mesh Size:** 0.5cm x 0.5cm
**Total Meshes:** 6216

**Lung Phantom- 0.25cm x 0.25cm Coarse-Meshes**

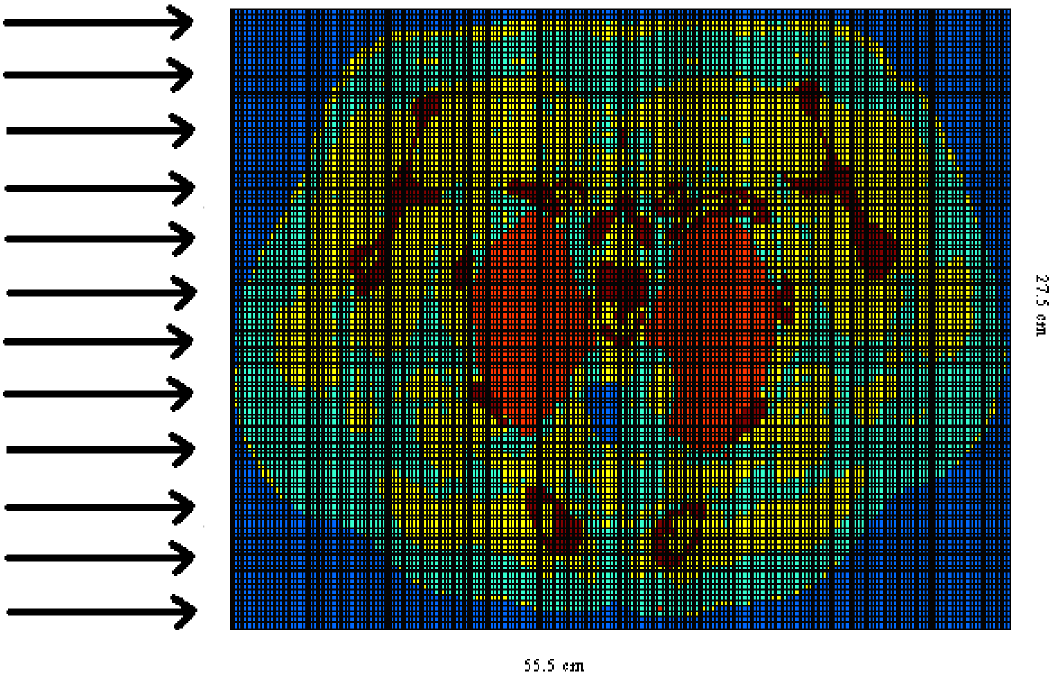


Figure B.9: CT Lung Phantom with 0.25cm x 0.25cm Coarse-Meshes

**Material Definitions:**
Dark Blue - Air (dry, near sea level)
Light Blue - Adipose Tissue
Yellow - Muscle (Skeletal)
Orange - Bone (Cortical)
Dark Red - Lung Tissue (Inflated)

**Beam Definition:**
Impinging on entire left face with mono-energetic, mono-directional photon beam

**Total Size:** 27.5 cm x 55.5 cm, third dimension extends to infinity in both directions
**Coarse-Mesh Size:** 0.25cm x 0.25cm
**Total Meshes:** 24420

**Prostate Phantom- 1cm x 1cm Coarse-Meshes**

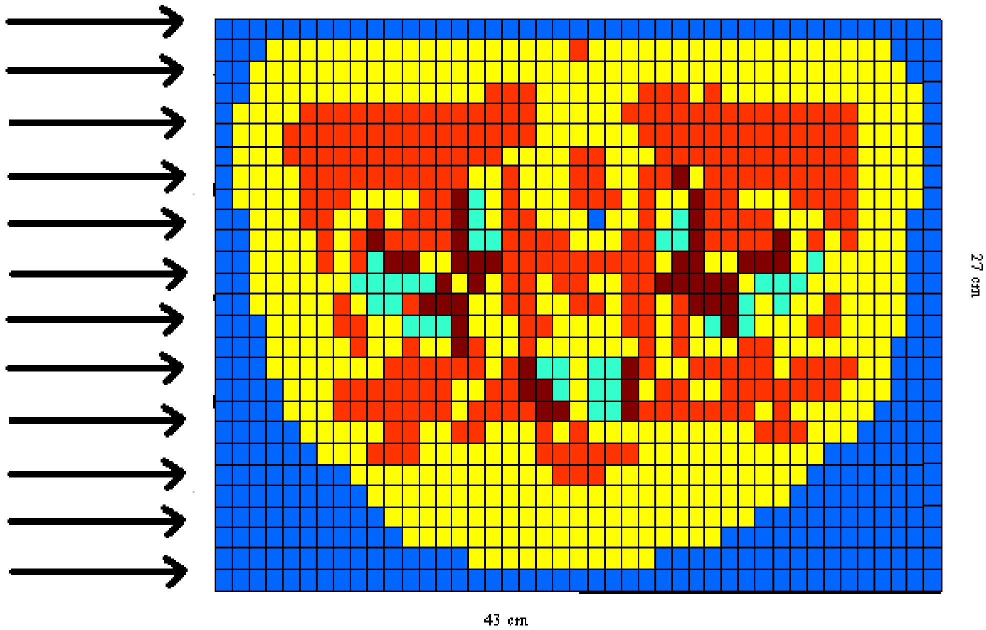


Figure B.10: CT Prostate Phantom with 1cm x 1cm Coarse-Meshes

**Material Definitions:**
Dark Blue - Air (dry, near sea level)
Yellow - Adipose Tissue
Orange - Muscle (Skeletal)
Dark Red - Bone (Cortical)
Light Blue - Marrow (Red Skeletal)

**Beam Definition:**
Impinging on entire left face with mono-energetic, mono-directional photon beam

**Total Size:** 27 cm x 43 cm, third dimension extends to infinity in both directions
**Coarse-Mesh Size:** 1cm x 1cm
**Total Meshes:** 1161

**Prostate Phantom- 0.5cm x 0.5cm Coarse-Meshes**

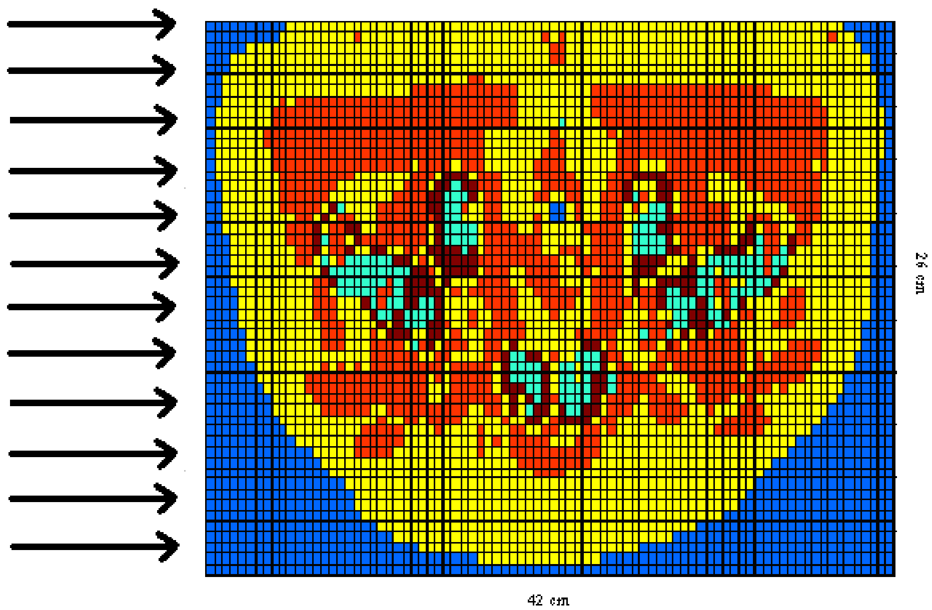


Figure B.11: CT Prostate Phantom with 0.5cm x 0.5cm Coarse-Meshes

**Material Definitions:**
Dark Blue - Air (dry, near sea level)
Yellow - Adipose Tissue
Orange - Muscle (Skeletal)
Dark Red - Bone (Cortical)
Light Blue - Marrow (Red Skeletal)

**Beam Definition:**
Impinging on entire left face with mono-energetic, mono-directional photon beam

**Total Size:** 26 cm x 41 cm, third dimension extends to infinity in both directions
**Coarse-Mesh Size:** 0.5cm x 0.5cm
**Total Meshes:** 4368

## Prostate Phantom- 0.25cm x 0.25cm Coarse-Meshes

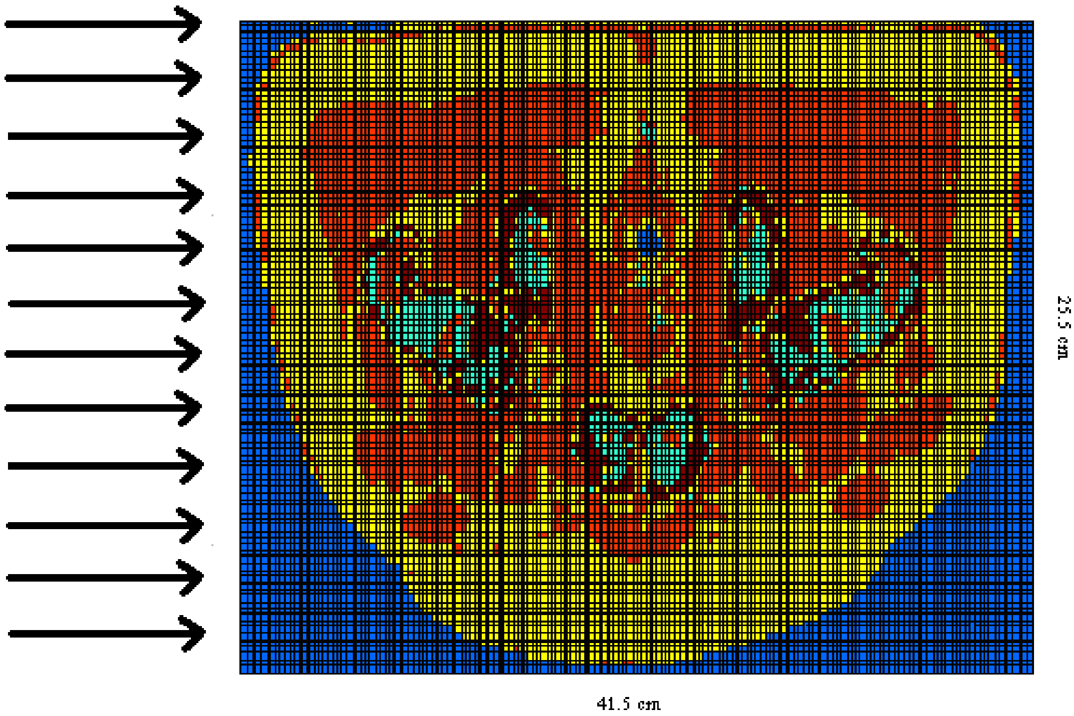


Figure B.12: CT Prostate Phantom with 0.25cm x 0.25cm Coarse-Meshes

**Material Definitions:**
Dark Blue - Air (dry, near sea level)
Yellow - Adipose Tissue
Orange - Muscle (Skeletal)
Dark Red - Bone (Cortical)
Light Blue - Marrow (Red Skeletal)

**Beam Definition:**
Impinging on entire left face with mono-energetic, mono-directional photon beam

**Total Size:** 25.5 cm x 41.5 cm, third dimension extends to infinity in both directions
**Coarse-Mesh Size:** 0.25cm x 0.25cm
**Total Meshes:** 16932

**Beam Re-Entry Phantom- 1cm x 1cm Coarse-Meshes**

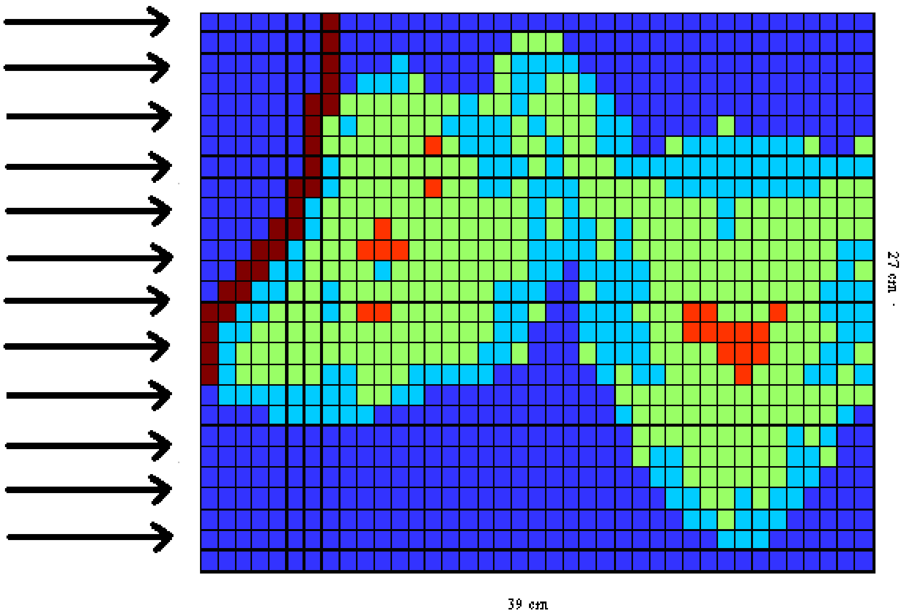


Figure B.13: CT Beam Re-Entry Phantom with 1cm x 1cm Coarse-Meshes

**Material Definitions:**
Dark Blue – Air (dry, near sea level)
Light Blue – Adipose Tissue
Green – Muscle (Skeletal)
Orange – Bone (Cortical)
Dark Red – Plexiglas/Polymethylmethacrylate

**Beam Definition:**
Impinging on entire left face with mono-energetic, mono-directional photon beam

**Total Size:** 27 cm x 39 cm, third dimension extends to infinity in both directions
**Coarse-Mesh Size:** 1cm x 1cm
**Total Meshes:** 1053

**Beam Re-Entry Phantom- 0.5cm x 0.5cm Coarse-Meshes**

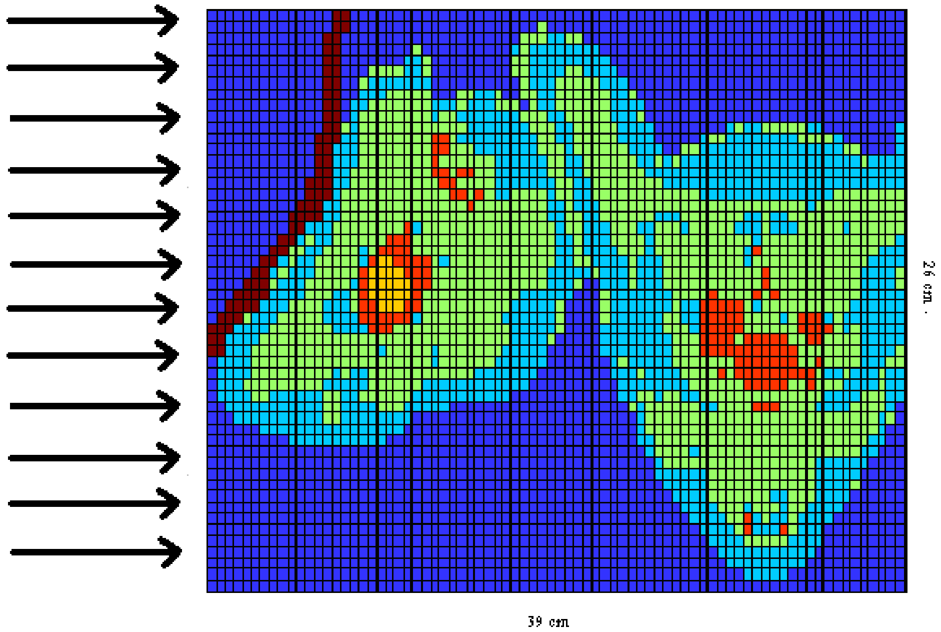


Figure B.14: CT Beam Re-Entry Phantom with 0.5cm x 0.5cm Coarse-Meshes

**Material Definitions:**
Dark Blue - Air (dry, near sea level)
Light Blue - Adipose Tissue
Green - Muscle (Skeletal)
Orange - Bone (Cortical)
Yellow - Marrow (Red Skeletal)
Dark Red – Plexiglas/Polymethylmethacrylate

**Beam Definition:**
Impinging on entire left face with mono-energetic, mono-directional photon beam

**Total Size:** 26 cm x 39 cm, third dimension extends to infinity in both directions
**Coarse-Mesh Size:** 0.5cm x 0.5cm
**Total Meshes:** 4056

**Beam Re-Entry Phantom- 0.25cm x 0.25cm Coarse-Meshes**

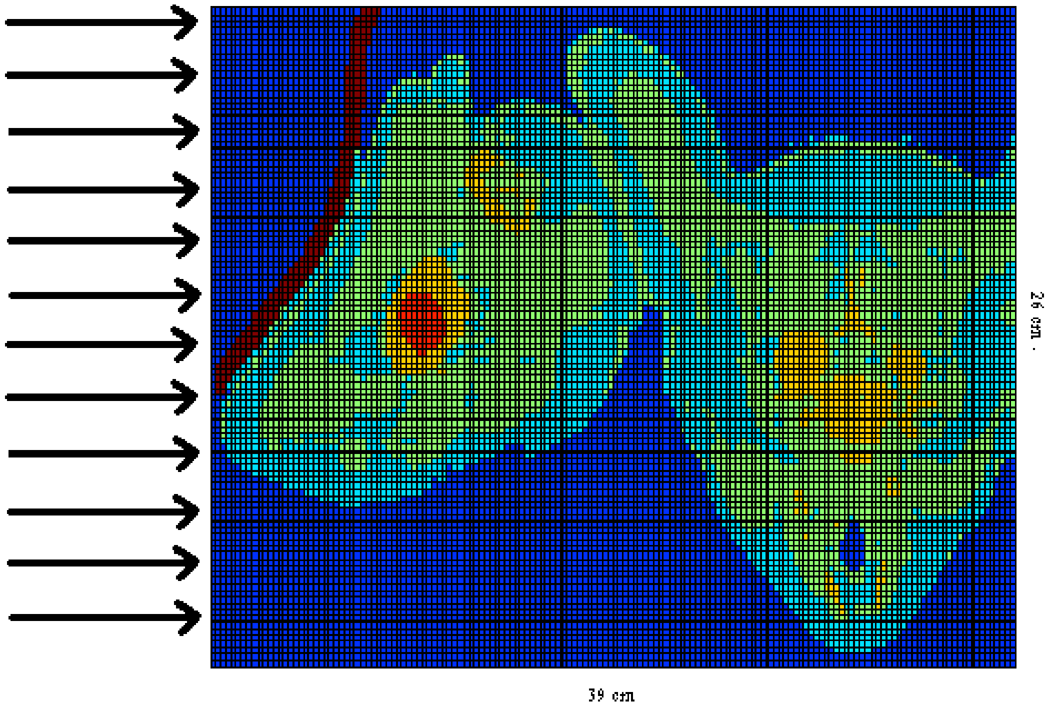


Figure B.15: CT Beam Re-Entry Phantom with 0.25cm x 0.25cm Coarse-Meshes

**Material Definitions:**
Dark Blue – Air (dry, near sea level)
Light Blue – Adipose Tissue
Green – Muscle (Skeletal)
Yellow – Bone (Cortical)
Orange – Marrow (Red Skeletal)
Dark Red – Plexiglas/Polymethylmethacrylate

**Beam Definition:**
Impinging on entire left face with mono-energetic, mono-directional photon beam

**Total Size:** 26 cm x 39 cm, third dimension extends to infinity in both directions
**Coarse-Mesh Size:** 0.25cm x 0.25cm
**Total Meshes:** 16224

**Lung Phantom (Secondary Sensitivity Study)- 0.5cm x 0.5cm Coarse-Meshes**

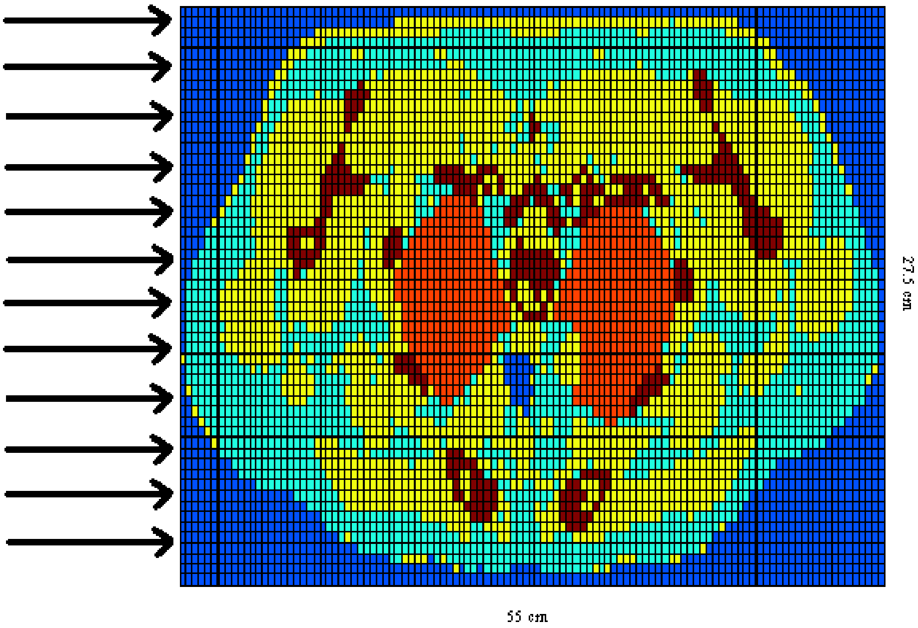


Figure B.16: CT Lung Phantom with 0.5cm x 0.5cm Coarse-Meshes for Secondary Sensitivity Study

**Material Definitions:**
Dark Blue - Air (dry, near sea level)
Light Blue - Adipose Tissue
Yellow - Muscle (Skeletal)
Dark Red - Bone (Cortical)
Orange - Lung Tissue (Inflated)

**Beam Definition:**
Impinging on entire left face with mono-energetic, mono-directional photon beam

**Total Size:** 27.5 cm x 55.5 cm, third dimension extends to infinity in both directions
**Coarse-Mesh Size:** 0.5cm x 0.5cm
**Total Meshes:** 6105

# APPENDIX C

# OVERESTIMATION AND UNDERESTIMATION OF DOSE PLOTS

Within the text of this work, dose deposition plots and percent difference plots are shown. It is also important to know how the COMET calculation compares to the reference EGS solution with regard to overestimation and underestimation of the dose. In each of the following figures, an expansion order of $4^{th}$ in energy, $2^{nd}$ in space, $4^{th}$ in polar angle, and $3^{rd}$ in azimuthal angle.

## Water Phantom

### 1cm x 1cm Coarse-Mesh

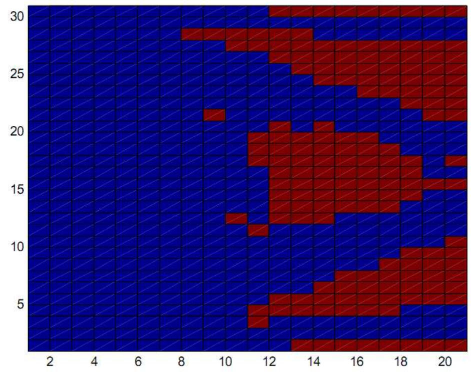


**(a)**

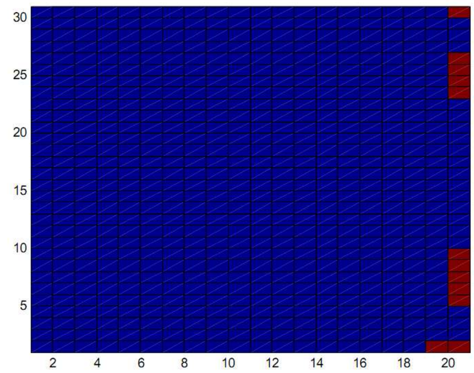


**(b)**

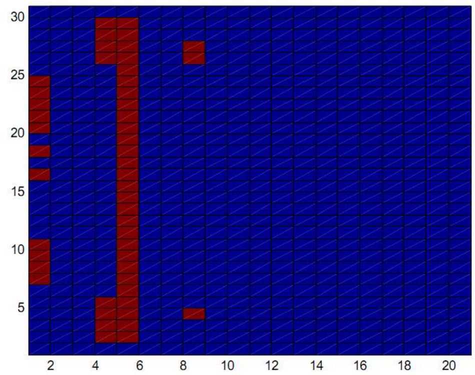


**(c)**

Figure C.1: Overestimation and Underestimation Dose Plot for Water Phantom with 1cm x 1cm Coarse-Meshes
Red – COMET Overestimates Dose, Blue: COMET Underestimates Dose
(a) 2 MeV Incident Beam (b) 6 MeV Incident Beam (c) 18 MeV Incident Beam

## 0.5cm x 0.5cm Coarse-Mesh

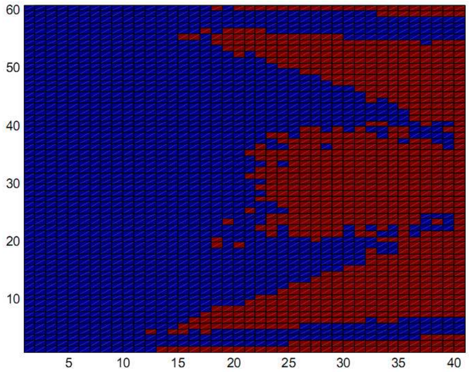


**(a)**

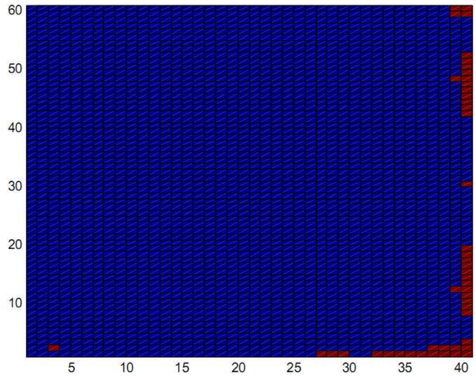


**(b)**

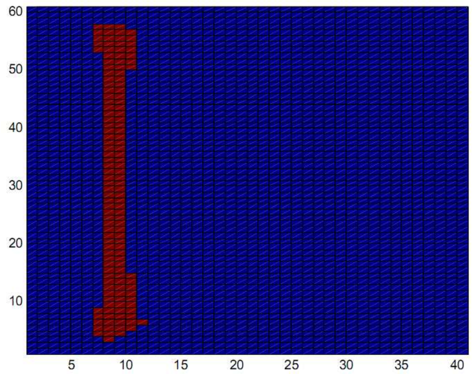


**(c)**

Figure C.2: Overestimation and Underestimation Dose Plot for Water Phantom with 0.5cm x 0.5cm Coarse-Meshes
Red – COMET Overestimates Dose, Blue: COMET Underestimates Dose
(a) 2 MeV Incident Beam (b) 6 MeV Incident Beam (c) 18 MeV Incident Beam

## Simplified Lung Phantom

### 1cm x 1cm Coarse-Mesh

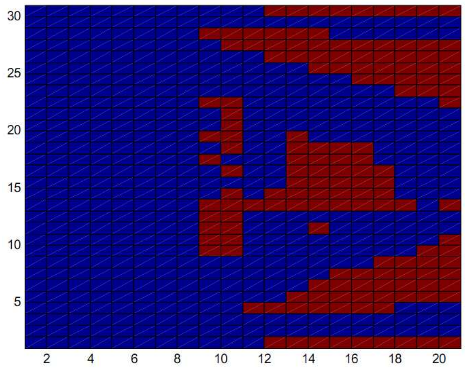


**(a)**

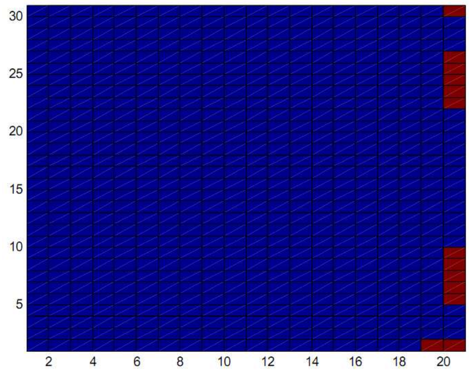


**(b)**

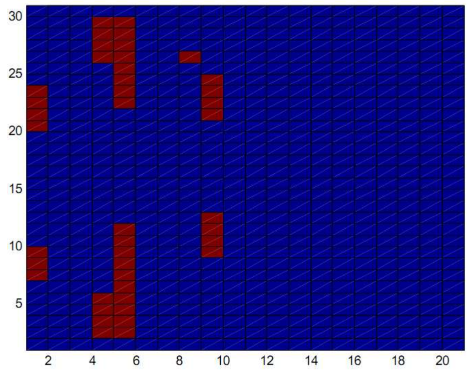


**(c)**

Figure C.3: Overestimation and Underestimation Dose Plot for Simplified Lung Phantom with 1cm x 1cm Coarse-Meshes
Red – COMET Overestimates Dose, Blue: COMET Underestimates Dose
(a) 2 MeV Incident Beam (b) 6 MeV Incident Beam (c) 18 MeV Incident Beam

**0.5cm x 0.5cm Coarse-Mesh**

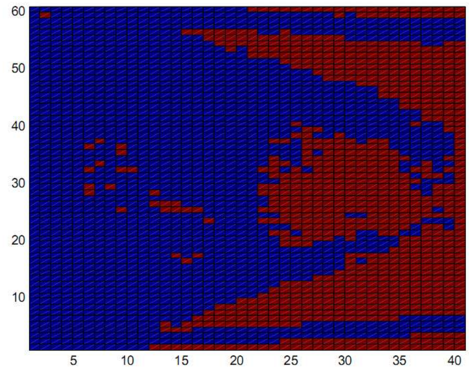


**(a)**

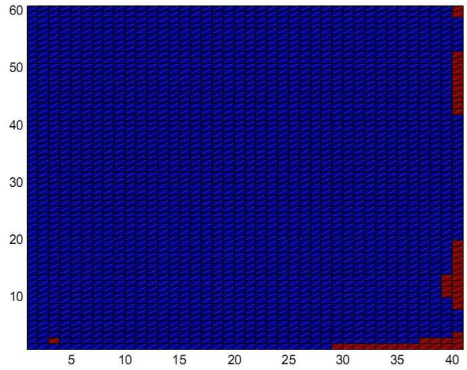


**(b)**

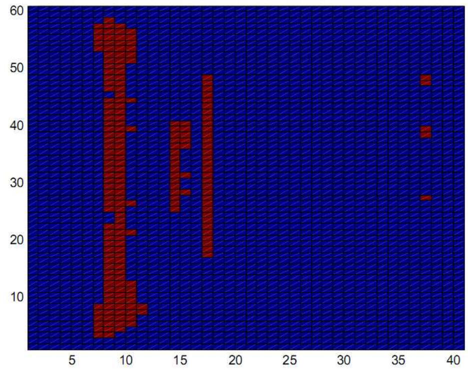


**(c)**

Figure C.4: Overestimation and Underestimation Dose Plot for Simplified Lung Phantom with 0.5cm x 0.5cm Coarse-Meshes
Red – COMET Overestimates Dose, Blue: COMET Underestimates Dose
(a) 2 MeV Incident Beam (b) 6 MeV Incident Beam (c) 18 MeV Incident Beam

## Slab Phantom

### 1cm x 1cm Coarse-Mesh

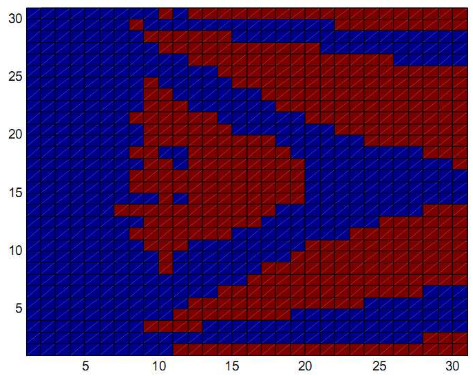


**(a)**

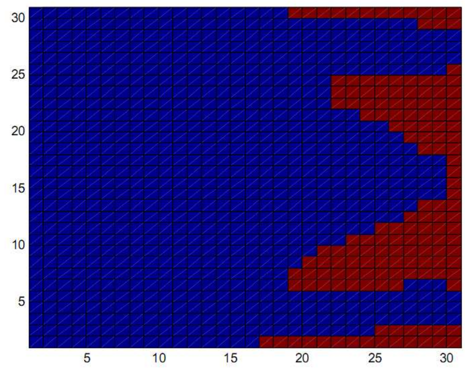


**(b)**

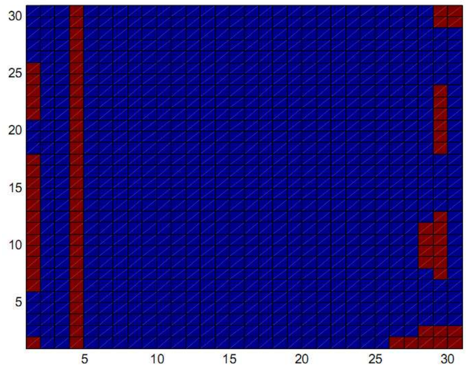


**(c)**

Figure C.5: Overestimation and Underestimation Dose Plot for Slab Phantom with 1cm x 1cm Coarse-Meshes
Red – COMET Overestimates Dose, Blue: COMET Underestimates Dose
(a) 2 MeV Incident Beam (b) 6 MeV Incident Beam (c) 18 MeV Incident Beam

**0.5cm x 0.5cm Coarse-Mesh**

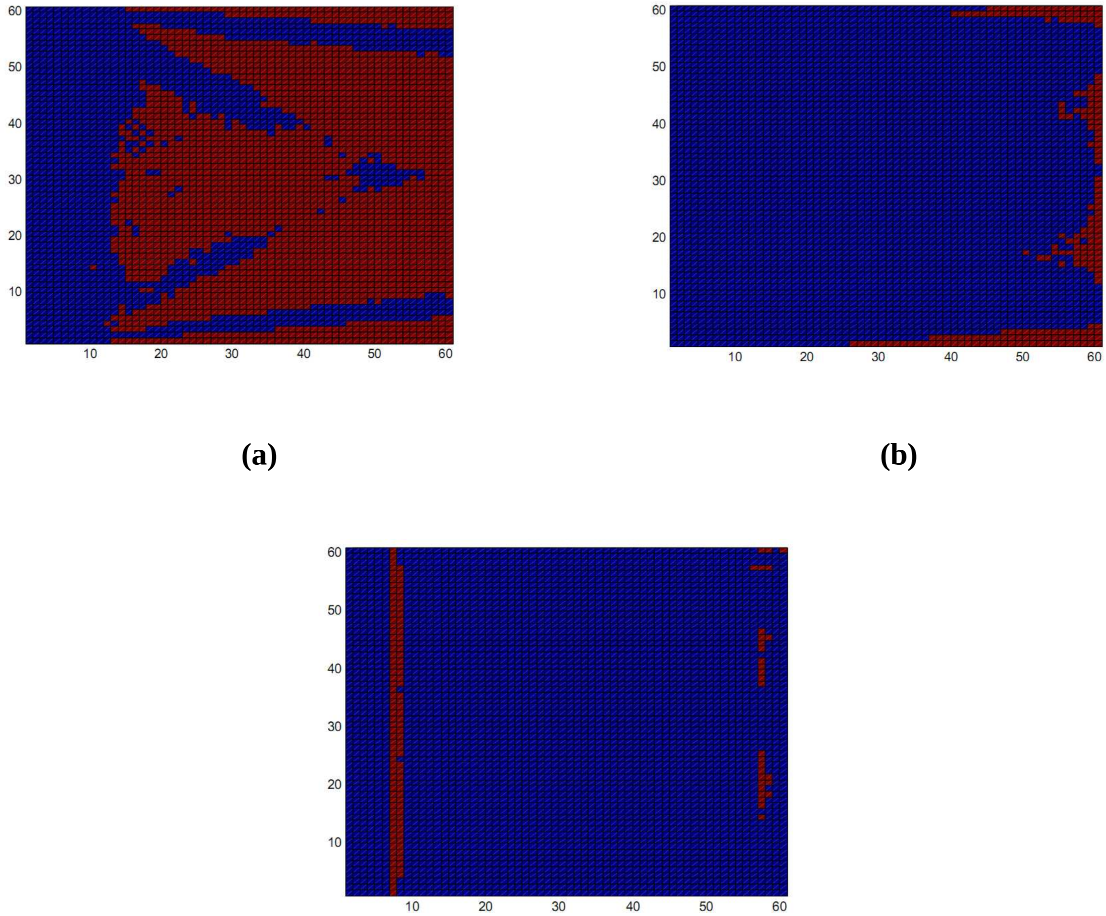


**(a)** **(b)**

**(c)**

Figure C.6: Overestimation and Underestimation Dose Plot for Slab Phantom with 0.5cm x 0.5cm Coarse-Meshes
Red – COMET Overestimates Dose, Blue: COMET Underestimates Dose
(a) 2 MeV Incident Beam (b) 6 MeV Incident Beam (c) 18 MeV Incident Beam

## CT Lung Phantom

### 1cm x 1cm Coarse-Mesh

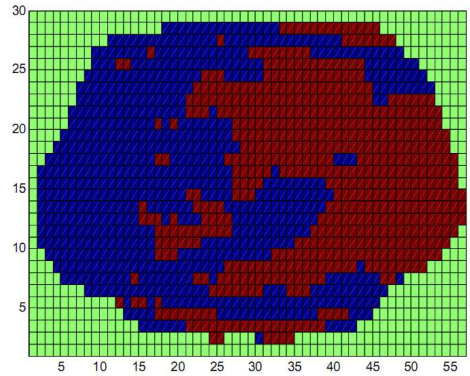


**(a)**

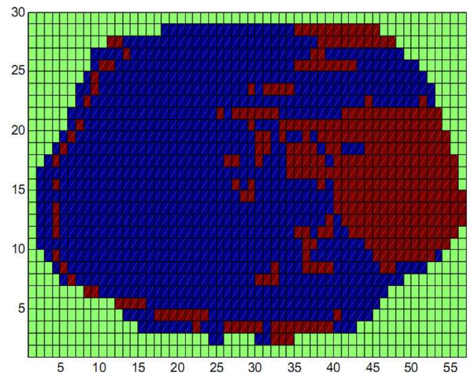


**(b)**

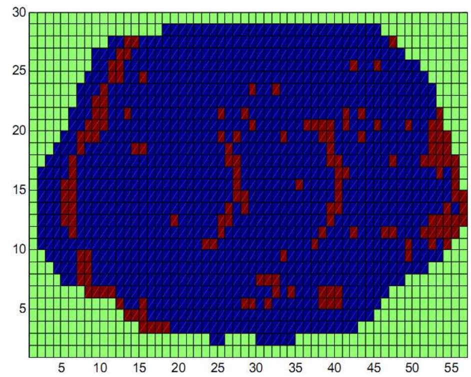


**(c)**

Figure C.7: Overestimation and Underestimation Dose Plot for CT Lung Phantom with 1cm x 1cm Coarse-Meshes
Red – COMET Overestimates Dose, Blue: COMET Underestimates Dose
(a) 2 MeV Incident Beam (b) 6 MeV Incident Beam (c) 18 MeV Incident Beam

**0.5cm x 0.5cm Coarse-Mesh**

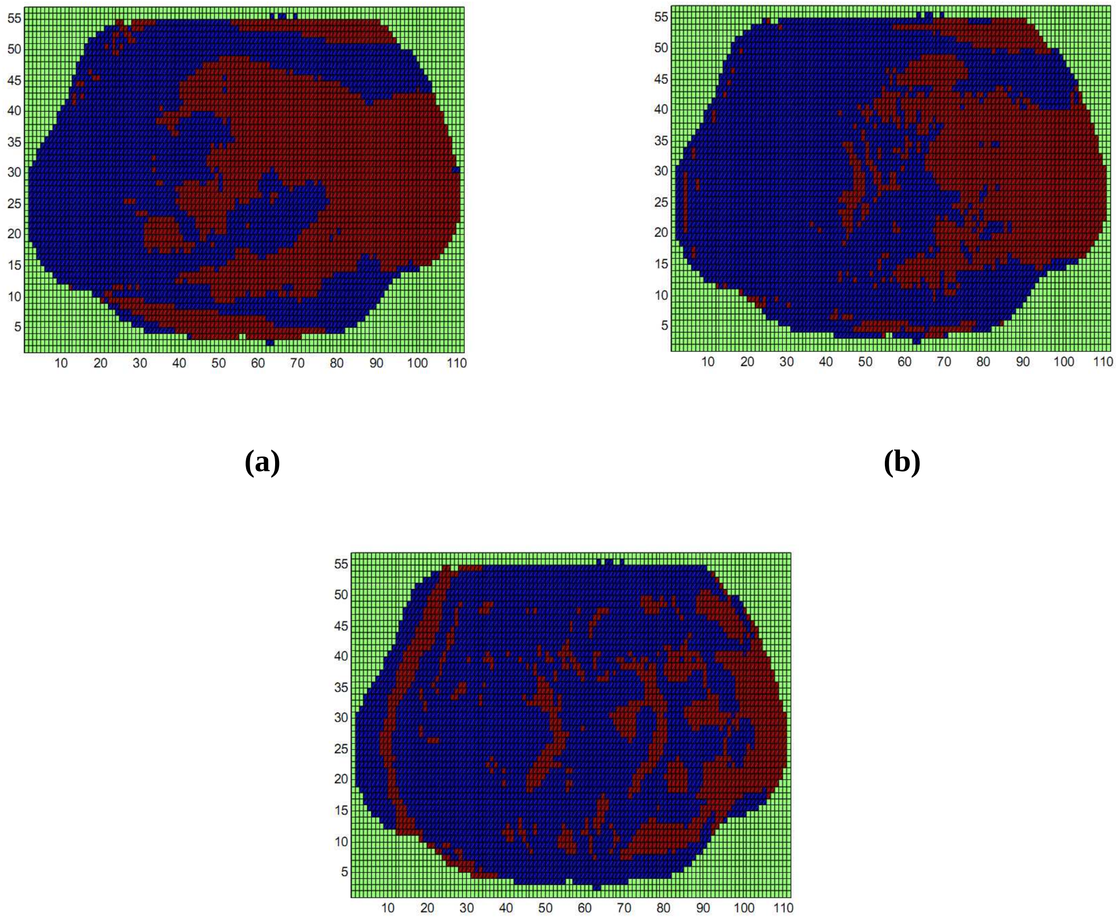


(a) (b)

(c)

Figure C.8: Overestimation and Underestimation Dose Plot for CT Lung Phantom with 0.5cm x 0.5cm Coarse-Meshes
Red – COMET Overestimates Dose, Blue: COMET Underestimates Dose
(a) 2 MeV Incident Beam (b) 6 MeV Incident Beam (c) 18 MeV Incident Beam

**0.25cm x 0.25cm Coarse-Mesh**

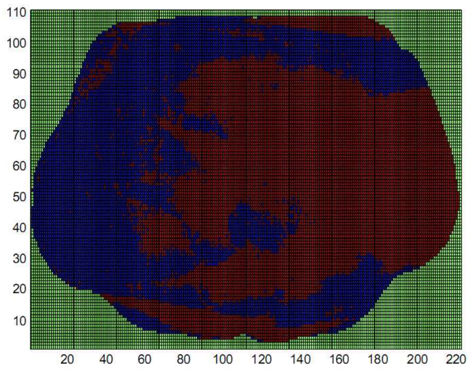


**(a)**

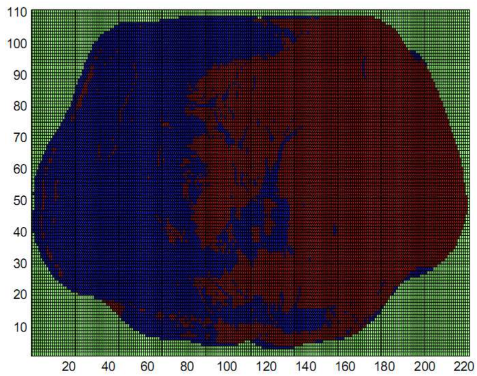


**(b)**

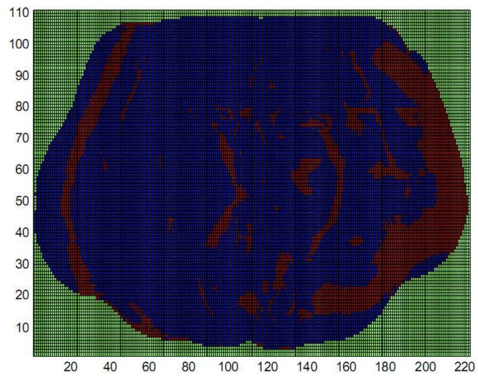


**(c)**

Figure C.9: Overestimation and Underestimation Dose Plot for CT Lung Phantom with 0.25cm x 0.25cm Coarse-Meshes
Red – COMET Overestimates Dose, Blue: COMET Underestimates Dose
(a) 2 MeV Incident Beam (b) 6 MeV Incident Beam (c) 18 MeV Incident Beam

## CT Prostate Phantom

### 1cm x 1cm Coarse-Mesh

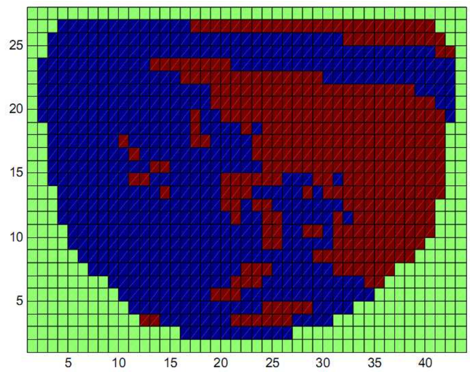


**(a)**

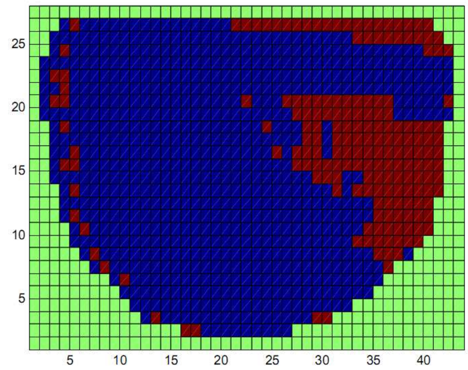


**(b)**

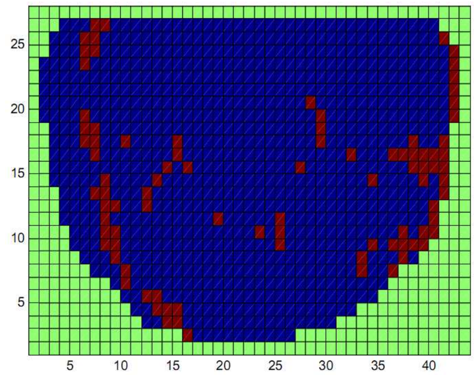


**(c)**

Figure C.10: Overestimation and Underestimation Dose Plot for CT Prostate Phantom with 1cm x 1cm Coarse-Meshes
Red – COMET Overestimates Dose, Blue: COMET Underestimates Dose
(a) 2 MeV Incident Beam (b) 6 MeV Incident Beam (c) 18 MeV Incident Beam

**0.5cm x 0.5cm Coarse-Mesh**

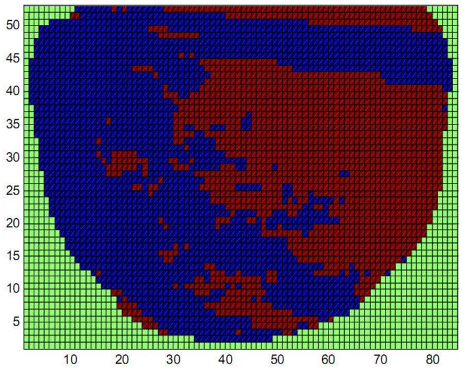


**(a)**

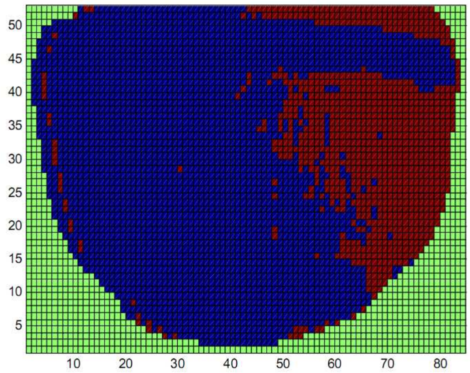


**(b)**

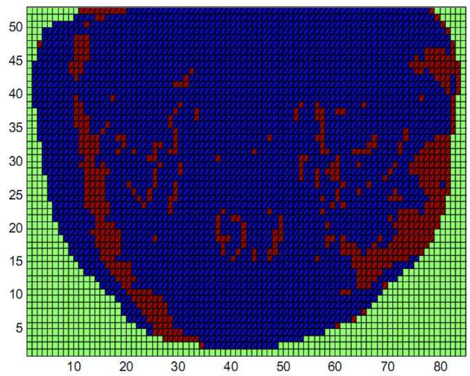


**(c)**

Figure C.11: Overestimation and Underestimation Dose Plot for CT Prostate Phantom with 0.5cm x 0.5cm Coarse-Meshes
Red – COMET Overestimates Dose, Blue: COMET Underestimates Dose
(a) 2 MeV Incident Beam (b) 6 MeV Incident Beam (c) 18 MeV Incident Beam

**0.25cm x 0.25cm Coarse-Mesh**

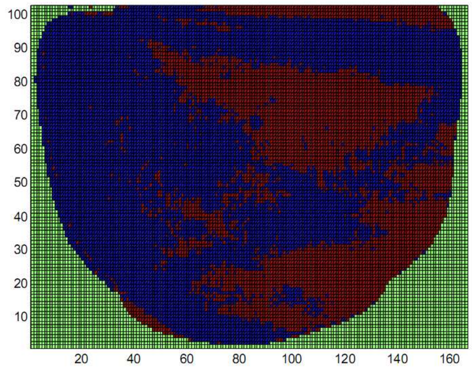


**(a)**

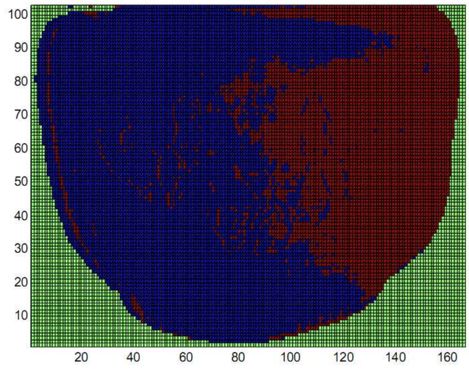


**(b)**

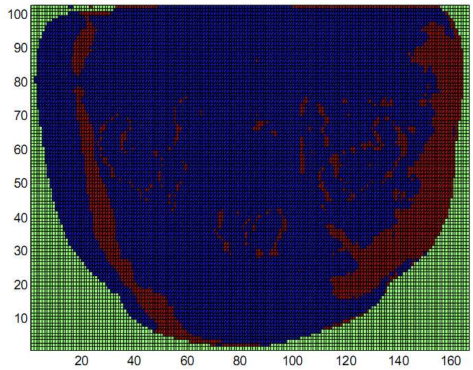


**(c)**

Figure C.12: Overestimation and Underestimation Dose Plot for CT Prostate Phantom with 0.25cm x 0.25cm Coarse-Meshes
Red – COMET Overestimates Dose, Blue: COMET Underestimates Dose
(a) 2 MeV Incident Beam (b) 6 MeV Incident Beam (c) 18 MeV Incident Beam

## CT Beam Re-Entry Phantom

### 1cm x 1cm Coarse-Mesh

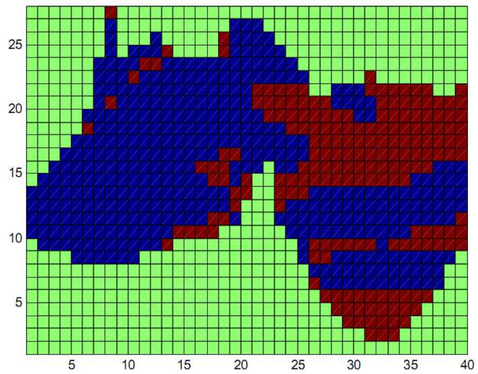


**(a)**

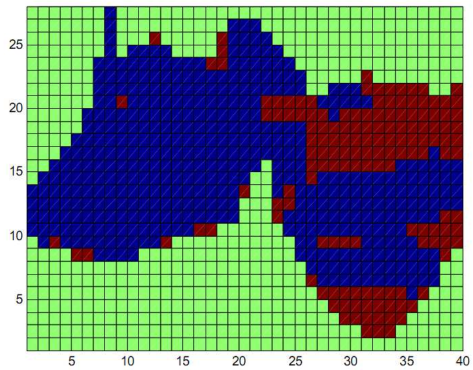


**(b)**

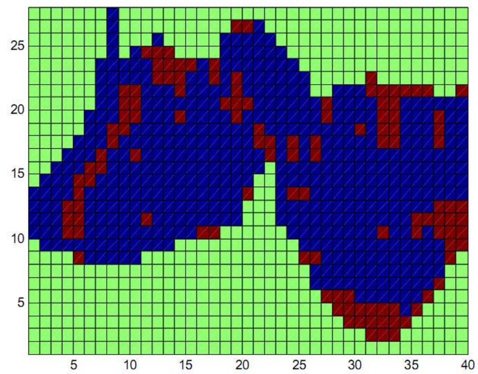


**(c)**

Figure C.13: Overestimation and Underestimation Dose Plot for CT Beam Re-Entry Phantom with 1cm x 1cm Coarse-Meshes
Red – COMET Overestimates Dose, Blue: COMET Underestimates Dose
(a) 2 MeV Incident Beam (b) 6 MeV Incident Beam (c) 18 MeV Incident Beam

**0.5cm x 0.5cm Coarse-Mesh**

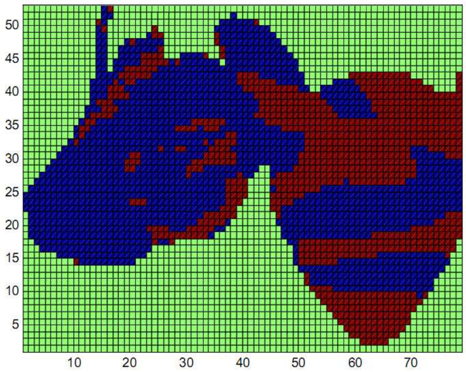


**(a)**

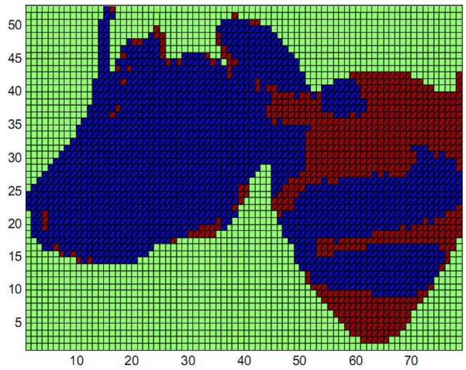


**(b)**

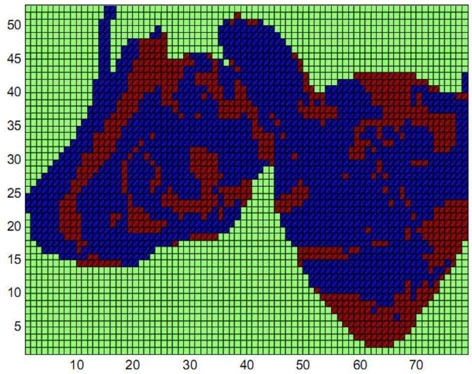


**(c)**

Figure C.14: Overestimation and Underestimation Dose Plot for CT Beam Re-Entry Phantom with 0.5cm x 0.5cm Coarse-Meshes
Red – COMET Overestimates Dose, Blue: COMET Underestimates Dose
(a) 2 MeV Incident Beam (b) 6 MeV Incident Beam (c) 18 MeV Incident Beam

### 0.25cm x 0.25cm Coarse-Mesh

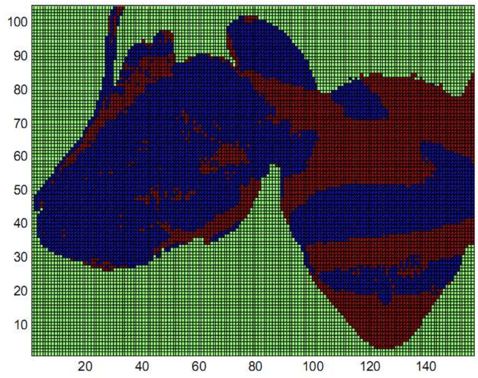

**(a)**

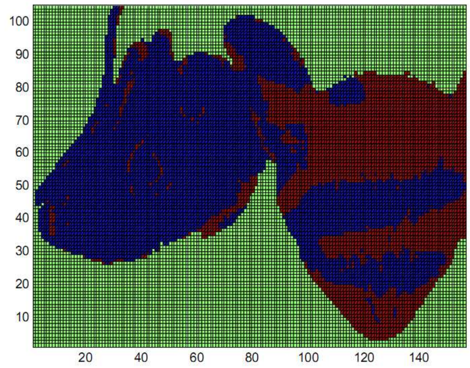

**(b)**

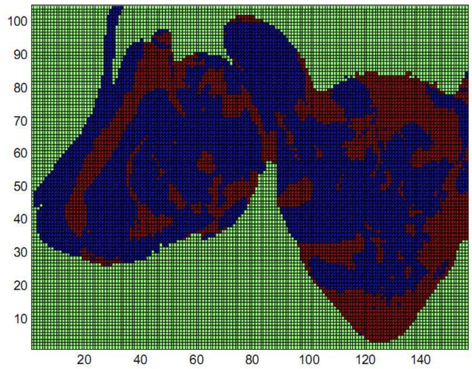

**(c)**

Figure C.15: Overestimation and Underestimation Dose Plot for CT Beam Re-Entry Phantom with 0.25cm x 0.25cm Coarse-Meshes
Red – COMET Overestimates Dose, Blue: COMET Underestimates Dose
(a) 2 MeV Incident Beam (b) 6 MeV Incident Beam (c) 18 MeV Incident Beam

# VITA
# MEGAN S. BLACKBURN

BLACKBURN was born in Marietta, Georgia and grew up in the neighboring town of Canton. In 2004 she received a B.S. with highest honors in Biomedical Engineering from the Georgia Institute of Technology in Atlanta, Georgia. She continued her graduate work at Georgia Tech and obtained a M.S. in Medical Physics 2006. She then continued her research while pursing a doctorate in Nuclear Engineering with a focus on Medical Physics. When he is not working on his research, Mrs. Blackburn enjoys spending time with her husband, David. They like searching for new restaurants in the Atlanta area and attending wine and beer tastings. Their two dogs, Toby and Yuri, also take them on hikes along the Chattahoochee River.

# REFERENCES


[1] Forget, B., Rahnema, F., and S. Mosher, "A Heterogeneous Coarse Mesh Solution for the 2-D NEA C5G7 MOX Benchmark Problem," *Progress in Nuclear Energy* **45**, 233-254 (2004).

[2] Mosher, S. and F. Rahnema, "The Incident Flux Response Expansion Method," *Trans. Th. Stat. Phys.* **34,** 1-26 (2006).

[3] Papanikolaou, N., et. al, "AAPM Report No. 85: Tissue Inhomogeneity Corrections for Megavoltage Photon Beams," Report of Task Group No. 65, Madison (2004).

[4] Khan, F., "The Physics of Radiation Therapy", 3rd Edition, *Lippincott Williams and Wilkins*, Philadelphia, 2003.

[5] ICRU Report No. 24, "Determination of Absorbed Dose in a Patient Irradiated by Beam of X or Gamma Rays in Radiotherapy Procedures" Washington, D.C. (1976).

[6] Wang, L., Chui, C., and M. Lovelock. "A Patient-Specific Monte Carlo Dose-Calculation Method for Photon Beams," *Medical Physics* **25**, 867-878 (1998).

[7] F. Verhaegen and J. Seuntjens, "Monte Carlo modeling of external radiotherapy photon beams," Phs. Med. Biol. **4**, R107-R164 (2003).

[8] N. Reynaert, S. C. van der Marck, D. R. Schaart, W. Van der Zee, C. Van Vliet-Vroegindeweij, M. Tomsej, J. Jansen, B. Heijmen, M. Coghe, and C. De Wagter, "Monte Carlo treatment planning for photon and electron beams," Radiat. Phys. Chem. **76**, 643-686 (2007).

[9] I. J. Chetty, B. Curran, J. E. Cygler, J. J. DeMarco, G. Ezzell, B. A. Faddegon, I. Kawrakow, P. J. Keall, H. Liu, C.-M. Ma, D. W. O. Rogers, J. Seuntjens, D. Sheikh-Bagheri, and J. V. Siebers, "Report of the AAPM Task Group No. 105: Issues associated with clinical implementation of Monte Carlo-based photon and electron external beam treatment planning," Med. Phys. 34, 4818-4853 (2007).

[10] Batho, H.F., "Lung Corrections in Cobalt 60 Beam Therapy," *J. Can. Assoc. Radiol.* **15**, 79-83 (1964).

[11] Young, M.E.J. and J.D. Gaylord, "Experimental Tests of Corrections for Tissue Inhomogeneities in Radiotherapy," *Br. J. Radiol.* **43**, 349-355 (1970).

[12] Sontag, M.R. and J.R. Cunningham, "Corrections to Absorbed Dose Calculations for Tissue Inhomogeneities," *Medical Physics* **4**, 431-436 (1977).

[13] Sontag, M.R. and J.R. Cunningham, "The Equivalent Tissue-Air Ratio Method for Making Absorbed Dose Calculations in a Heterogeneous Media," *Radiology* **129**, 787-794 (1978).

[14] Cunningham, J.R., "Scatter-Air Ratios," *Physics in Medicine and Biology* **17**, 42-51 (1972).

[15] Mackie, T., Scrimger, J., and J. Battista, "A Convolution Method of Calculating Dose for 15-MV X Rays," *Medical Physics* **12**, 188-196 (1985).

[16] Ahnesjo, A., "Collapsed Cone Convolution of Radiant Energy for Photon Dose Calculation in Heterogeneous Media, " *Medical Physics* **16**, 577-592 (1989).

[17] Ahnesjo, A., Sanders, S., and A. Trepp, "A Pencil Beam Model for Photon Dose Calculation," *Medical Physics* **19**, 263-273 (1992).

[18] Van Esch, A. et. al, "Testing of the Analytical Anisotropic Algorithm for Photon Dose Calculation," *Medical Physics* **33**, 4130-4148 (2006).

[19] Fogliata, A., et. al, "Dosimetric Validation of the Anisotropic Analytical Algorithm for Photon Dose Calculation: Fundamental Characterization in Water," *Physics in Medicine and Biology* **51**, 1421-1438 (2006).

[20] Wong, J.W. and R.M Henkelman, "A New Approach to CT Pixel-Based Photon Dose Calculation in Heterogeneous Media," *Medical Physics* **10**, 199-208 (1983).

[21] Papanikolaou, N., et. al, "Investigation of the Convolution Method for Polyenergetic Spectra," *Medical Physics* **5**, 1327-1336 (1993).

[22] Mackie, T., et. al, "Clinical Implementation of the Convolution/Superposition Method," *Proceedings of the 10th International Conference on the Use of Computers in Radiation Therapy*, Bombay, India (1990).

[23] Boyer, A., and E. Mok, "Calculation of Photon Dose Distributions in an Inhomogeneous Medium Using Convolutions," *Medical Physics* **13,** 503-509 (1986).

[24] Ciangaru, G., et. al, "Benchmarking Analytical Calculations of Proton Doses in Heterogeneous Matter," *Medical Physics* **12**, 3511-3523 (2005).

[25] Carrasco, P., et. al, "Comparison of Dose Calculation Algorithms in Phantoms with Lung Equivalent Heterogeneities Under Conditions of Lateral Disequilibrium," *Medical Physics* **31**, 2899-2911 (2004).

[26] Carrasco, P., et. al, "Comparison of Dose Calculation Algorithms in Slab Phantoms with Cortical Bone Equivalent Heterogeneities," *Medical Physics* **34**, 3323-3333 (2007).

[27]Kawrakow, K., and Rogers, D., "The EGSnrc Code System" Monte Carlo Simulation of Electron and Photon Transport," *Technical Report PIRS-701*, National Research Council of Canada, Ottaway, Canada, (2000).

[28] Satterfield, M. "Application of a Heterogeneous Coarse-Mesh Transport Method (COMET) to Radiation Therapy Problems," Master's Thesis, Georgia Institute of Technology (2006).

[29]Elder, Eric. Personal interview. January 2009. Interview.

[30]Rogers, D. and Mohan, R., "Questions for Comparison of Clinical Monte Carlo Codes," *The Use of Computers in Radiotherapy, XIIIth International Conference,* Heidelberg, Germany, 120-122 (2000).

[31]Van Riper, K., "SCAN2MCNP", *White Rock Science,* (2004).

[32] Goorley,T., Bull, J., Brown F., et. Al., MCNP Monte Carlo Team, X-5, MCNP5.1.40 Code System, Los Alamos National Laboratory, (2005).

[33]Rodrigues, G., et al. "Prediction of Radiation Pneumontitis by Dose – Voume Histogram Parameters in Lung Cancer – a Systemic Review," Radioth. Oncol. **71**, 127-138 (2004).

[34]Tai, P., et al. "Pelvic Fractures Following Irradiation of Endometrial and Varinal Cancers – a Case Series and Review of the Literature," Radiother. Oncol. **56**, 23-28 (2000).

[35]Vissink, A.., et al. "Oral Sequelae of Head and Neck Radiotherapy," Crit. Rev. Oral Biol. Med. **14**, 199-212 (2003).